Regulation of longevity by an mTOR/steroid signaling axis in *C. elegans*

Inaugural-Dissertation

zur

Erlangung des Doktorgrades

der Mathematisch-Naturwissenschaftlichen Fakultät

der Universität zu Köln

vorgelegt von

Klara Schilling

aus Köln, Deutschland

Köln, 21. Februar 2025

Table of Contents

I. Abbreviations

AAV	adeno-associated virus
ABC	ATP-binding cassette
AID	auxin-inducible degron
AMPK	adenosin monophosphate-kinase
ANOVA	analysis of variance
ARD	adult reproductive diapause
BA	bile acid
BP	biological process
BR	biological replicate
CAA	chloroacetamide
CAN	excretory canal neurons
cGMP	cyclic guanosine monophosphate
ChIP	chromatin immunoprecipitation
CRISPR	clustered regularly interspaced short palindromic repeats
CYP	cytochrome P450
DA	dafachronic acid
Daf-c	dauer-constitutive
Daf-d	dauer-defective
DAVID	database for annotation, visualization, and integrated discovery
DIC	differential interference contrast
DNA	deoxyribonucleic acid
DR	dietary restriction
EE	early endosomes
eIF4E	initiation factor 4E
ER	endoplasmic reticulum
ERβ	estrogen receptor β
FC	fold change
FoxO	forkhead box O
FXR	farnesoid X Receptor
GC-MS	gas chromatography–mass spectrometry
GDP	guanosine diphosphate
GFP	green fluorescent protein
GO	gene ontology
GPCR	G protein couples receptor
GSEA	gene set enrichment analysis
GTP	guanosine triphosphate
HEK	human embryonic kidney
HESI	heated electrospray ionization
IGFR	insulin-like growth factor receptor
IgG	immunoglobulin G
IIS	insulin-like growth factor-1 signaling
IPTG	Isopropyl b-1-D-thiogalactopyranoside
KD	knockdown
KEGG	kyoto encyclopedia of genes and genomes
LBH	Luria-Bertani
LC-MS	liquid chromatography–mass spectrometry
LCA	lithocholic acid
LDL	low-density-lipoproteins
LDLR	low-density-lipoprotein receptor
LE	late endosomes
LED	light-emitting diode
LXR	liver X receptor
LysC	lysyl-endo-peptidase
MCD	methyl-β cyclodextrin
mig	gonad migration phenotype
MS	mass spectrometry
MSTFA	N-Methyl-N-trimethylsilyl-trifluoracetamid
mTOR	mechanistic target of rapamycin
N/A	not applicable
NG	neon green
NGM	nematode growth medium

Abbreviations

NHR	nuclear hormone receptor
NPC	Nieman-Pick Type C
ns	not significant
Nvd	neverland
OSBP	oxysterol binding protein
OXPHOS	oxidative phosphorylation
PBS	phosphate-buffered saline
PCA	principal component analysis
PCR	polymerase chain reaction
qPCR	quantitative polymerase chain reaction
ROMK	renal outer medullary K+ channel
RNA	ribonucleic acid
RNAi	RNA interference
RXR	retinoid X receptor
SD	standard deviation
SDR	dehydrogenase/ reductase
SDS PAGE	sodium dodecyl sulfate p olyacrylamide gel electro phoresis
SEM	standard error of the mean
Ser	serine
sgRNA	single guide RNA
siRNA	small interfering RNA
TBST	tris-buffered saline with Tween20
TCA cycle	tricarboxylic acid cycle
TCEP	tris(2-carboxyethyl) phosphine
TGF-β	tumor growth factor beta
Thr	threonine
TORC	target of rapamycin complex
UTR	untranslated region
VDR	vitamin D Receptor

II. Abstract

The mTOR pathway is a key central regulator of cellular growth and aging. A modest inhibition of mTOR slows organismal growth and promotes longevity across taxa, including *C. elegans*. Work in mammalian systems suggests that the steroid cholesterol is a positive regulator of mTOR and that mTOR in turn regulates bile acid homeostasis in mice.

Worms synthesize cholesterol-derived bile acid-like steroids called dafachronic acids (DAs), which bind to the steroid receptor transcription factor DAF-12, the *C. elegans* homolog of the mammalian vitamin D, liver X, and farnesoid X receptors. DAF-12 serves as a molecular switch regulating developmental timing, dauer formation, as well as gonad signaling mediated longevity. We therefore hypothesized that *daf-12*/DA signaling might interact with mTOR signaling, using *raga-1* mutants as a genetic model of reduced TORC1.

We found that null mutations of *daf-12* as well as mutations in DA biosynthetic enzymes abolished *raga-1* longevity, suggesting that reduced mTOR signaling acts through DA/DAF-12 signaling to extend life span. Consistently, with the idea of a regulatory cascade, we found that *raga-1* mutation resulted in dramatic upregulation of DA levels to promote DAF-12 transcriptional activity. Furthermore, *daf-12* mutation reverses a subset of the transcriptomic and metabolomic changes induced by *raga-1* loss.

Functional genomic screening of differentially expressed genes from the transcriptome revealed the dehydrogenase *dhs-26* (the *C. elegans* ortholog to the human short-chain dehydrogenase DHRS1), to be required for *raga-1* longevity. Our work suggests that *dhs-26* plays an integral role in steroid signaling to regulate life span: *dhs-26* levels are potently regulated by the positive regulatory arm of steroid/DAF-12 signaling, *dhs-26* mutants exhibit decreased Δ7-DA levels, and *raga-1;dhs-26* lifespan can be rescued by Δ7-DA supplementation. Using single worm proteomics, we identified downstream pathways of DHS-26, including peroxisome and lysosome function, lipid transport, ribosomal biogenesis and oxidative phosphorylation as possible mediators of life span regulation.

These findings demonstrate that mTOR and DAF-12 steroid signaling act in a unified pathway to regulate animal longevity through a cell non-autonomous, hormonal mechanism. This

cascade engages DHS-26 as a novel regulator of DA levels and DAF-12 activity required for longevity downstream of mTOR signaling. These studies open the possibility that mTOR signaling might act systemically in higher animals through regulation of bile acid-like hormones and nuclear receptor signal transduction.

III. Introduction and Background

Aging is the main risk factor for the major debilitating diseases that afflict humanity, including heart disease, cancer and neurodegeneration. Fortunately, in recent years, scientists have begun to discover resilience mechanisms that can potentially oppose aging and age-related diseases. In particular, genetic models have given us essential insights into molecular signaling pathways that can promote healthy aging. Major longevity pathways, whose manipulation can improve organismal resilience in age include insulin signaling (Kenyon, Chang et al. 1993), germline signaling (Berman and Kenyon 2006), as well as mTOR signaling (Vellai, Takacs-Vellai et al. 2003). Interestingly, these longevity pathways (partially) work through cell non-autonomous hormonal signaling to coordinate organismal benefits. Insulin/IGF signaling acts through a hormonal mechanism, secreting IGF and insulin in response to appropriate cues. Similarly, germline signaling was shown to be dependent on bile acid-like signaling to coordinate cell non-autonomous organismal benefits (Gerisch, Rottiers et al. 2007).

The cell autonomous role of mTOR signaling has been intensively studied in the last decades (Mannick and Lamming 2023), but cell non-autonomous mechanisms remain elusive. However, recent evidence suggests that when downregulated in the nervous system, mTOR can induce lifespan benefits without major growth defects (Smith, Lanjuin et al. 2023), suggesting it can work through the nervous system to affect downstream processes throughout the body. This study is in line with the finding of hypothalamic mTOR signaling regulating feeding behavior (Cota, Proulx et al. 2006). These reports imply a possible cell non-autonomous mechanism downstream of mTOR signaling that remains little explored. **Our work provides a critical connection between mTOR and bile acid-like hormonal signaling that acts throughout a systemic mechanism to regulate animal life span**. In the following chapters I will elaborate on these two pathways working in tandem and underline the importance of bile acid-like hormones in organismal health.

1. Aging and aging research

1.1. The potential of aging research for humankind

Aging entails the gradual decline in cellular and organismal function over time that affects all living things. The question of why and how we age has intrigued humankind for centuries, and the pursuit of interventions that could improve health with age is as old as civilization itself. In the last decades research of the aging process and mechanisms that oppose it have helped illuminate core mechanisms of aging. Major breakthroughs in the understanding of metazoan aging have emerged from the study of simple model organisms. One such breakthrough was the discovery that mutations in the *C. elegans* gene *age-1*, extend worm life span over 80% (Friedman and Johnson 1988). This groundbreaking work showed that longevity is malleable and can be regulated by single gene mutations. Further, *age-1* and related molecules identified the insulin/IGF pathway as a central regulator of life span (Kenyon, Chang et al. 1993). Since then, this pathway and others have been shown to remarkably regulate life span.

Aging is thought to originate from the accumulation of cellular damage over time. This damage is widely accepted to be a primary driver of aging related pathology and disease (Gems and Partridge 2013). Many age-related conditions, such as cancer, atherosclerosis and chronic inflammation, are also linked to dysregulated cellular activity and run-on programs stemming from developmental or reproductive processes (Blagosklonny 2008, Gems and Partridge 2013). These shared roots have inspired key questions about the sources of damage, the mechanisms that attempt to maintain balance, and the potential to slow or even reverse the effects of aging. Anti-aging interventions strive to maintain health. Health was classically described as the absence of pathology, but more recently scientists have attempted to portray health as more than just the absence of disease. For example Lopez-Otin and Kroemer defined health in terms of three main parameters that are essential to maintain physiology: functioning spatial compartmentalization, maintenance of homeostasis, and adequate response to stressors (Lopez-Otin and Kroemer 2021). These definitions are important because they allow us to begin thinking about preventative medicine and interventions to maintain health before the explicit manifestation of disease.

1.2. Hallmarks of aging help categorize its essence

Researchers proposed a framework of hallmarks to explain the molecular, cellular, and systemic mechanisms underlying aging (Lopez-Otin, Blasco et al. 2013, Lopez-Otin, Blasco et al. 2023). This categorization helps to conceptualize the essence of aging and its underlying mechanisms. These hallmarks were chosen based on three key criteria: (1) they emerge as part of the normal aging process, (2) their worsening accelerates aging, and (3) interventions targeting them can slow aging and extend healthspan. Based on these criteria, researchers propose twelve biological functions that are particularly important to unravel the mysteries of aging: genomic instability, telomere attrition, epigenetic alterations, loss of proteostasis, disabled macroautophagy, deregulated nutrient-sensing, mitochondrial dysfunction, cellular senescence, stem cell exhaustion, altered intercellular communication, chronic inflammation, and dysbiosis (Lopez-Otin, Blasco et al. 2023). It is important to note that these hallmarks can be interconnected. Therefore, it can be difficult to study only one dissected hallmark.

All this work was done to achieve a detailed understanding of the human aging on a molecular level. This understanding is fundamental to allow us to effectively fight aging and in turn aging dependent diseases, and many groups are using these hallmarks as proxies to test if interventions will have an age-related benefit.

In recent years, the technology and systems biology have led to the discovery of biomarkers of aging that have the potential to revolutionize the field. Transcriptomics, epigenomics, proteomics, and metabolomics allow researchers to analyze aging at the single organism and even single cell level, and uncover its complex patterns over time (Franzosa, Hsu et al. 2015, Aldridge and Teichmann 2020, Mehrmohamadi, Sepehri et al. 2021). The development of so-called aging clocks (Horvath 2013), combined with physiological and functional assessments, enable the precise measurement of biological aging, beyond the simple measurement of chronological age. In particular, they enable investigators to assess whether interventions can impact aging in an abbreviated time frame, and help evaluate the effectiveness of anti-aging strategies. Unraveling cellular functions on a molecular level will continue to pave the way for interventions that may slow aging, improve healthspan, and reduce the burden of age-related diseases, bringing us closer to deciphering the mysteries of aging.

2. Steroid metabolism

One group of biomolecules that has been shown to regulate a variety of physiological and developmental functions are steroids (Beato and Klug 2000). Typically steroids bind and thereby act through their respective nuclear hormone receptors (NHR) that can alter gene transcription and thereby cellular activity. Steroid hormones are of particular relevance for development and aging throughout taxa. This is exemplified by the steroid hormone dafachronic acid (DA), which is a key player in developmental decision making in *C. elegans* and was also shown to be required for germline induced longevity. The precursor of DA and other steroids which is especially relevant for this work is cholesterol.

2.1. Cholesterol as a multi purpose molecule

Cholesterol molecules display a cyclopentanophenanthrene four-ring molecular structure, characteristic of the sterol family (Cole, Short et al. 2019). It is a vital component of cell membranes and serves as an indirect signaling molecule by modulating membrane fluidity and thereby regulating membrane permeability to water and ions (Rog, Pasenkiewicz-Gierula et al. 2009).

Cholesterol can be obtained from the diet or made by *de novo* synthesis in mammals. The discovery of the major reactions of the mammalian cholesterol biosynthesis pathway was a breakthrough by Bloch and Lynen, who were awarded the Nobel Price in Medicine and Physiology in 1964 (Kennedy and Westheimer 1964). Notably, lower organisms such as nematodes are cholesterol auxotrophs and therefore require cholesterol provided in their food source to ensure proper growth (Hieb and Rothstein 1968).

Adipose tissue is a major site of cholesterol storage that is strongly regulated by animals' age, the volume of the adipose tissue, and early nutritional deficits (Angel and Farkas 1974). Additionally, the liver is the main site for cholesterol homeostasis including biosynthesis and degradation, uptake through low-density lipoprotein receptors (LDLR) (Brown and Goldstein 1986), storage, and esterification (Weber, Boll et al. 2004). Cholesteryl esters are formed when a cholesterol molecule is attached to a fatty acid. Once cholesterol is available, it can

directly or as a derivate activate downstream pathways or be stored in form of cholesteryl esters.

Cholesteryl esters are hydrophobic molecules that in mammals are bound to lipoproteins to allow regulated travel through the blood stream (Ginsberg 1998). From the blood stream, lipid loaded LDL particles are taken up by the target tissue via the LDL receptor via clathrin-coated vesicle mediated endocytosis (**Figure III-1**). Lipoproteins are then transported to early endosomes (EE). Throughout the maturation of endosomes, the acidic environment promotes the lipoproteins to dissociate from the LDLR. The receptors return to the cell surface, whereas the lipoproteins are degraded in the lysosomes to release free cholesterol. Lysosomal cholesterol levels regulate the transcription of the LDLR gene and genes involved in cholesterol biosynthesis, providing a regulatory feedback loop to ensure proper cholesterol homeostasis, marking the lysosome as a key regulatory hub for cholesterol maintenance

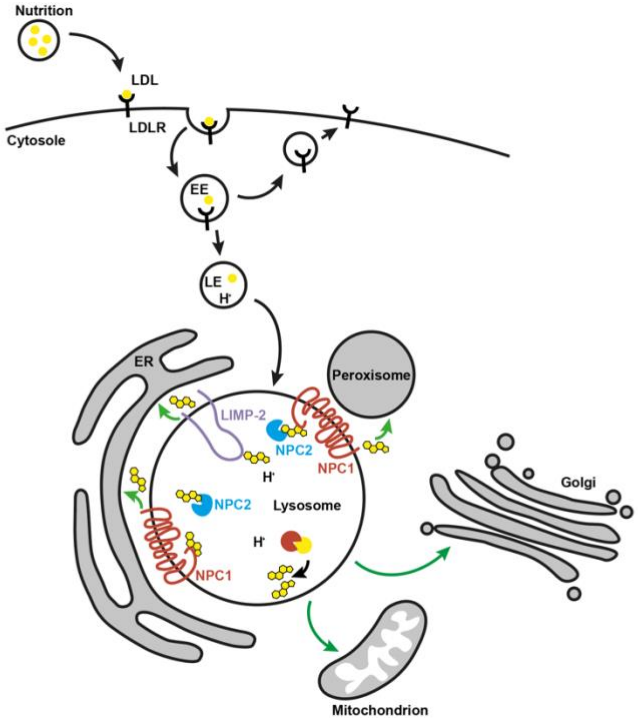

Figure III-1: The lysosome is the key regulatory hub of cholesterol homeostasis. Dietary low-density lipoproteins (LDLs) (yellow circle) are recognized by LDL receptors (LDLRs). LDLR binding triggers the formation of early endosomes (EE). During EE maturation LDLRs release LDL and are shuttled back to the cellular surface. Matured late endosomes (LE) further acidify and form lysosomes in which LDLs are degraded to cholesteryl esters which are hydrolized to free cholesterol (yellow four-ring structure). Free cholesterol molecules are bound by Nieman-Pick Type C2 (NPC2), which transfers them to the membrane bound cholesterol transporters Nieman-Pick Type C1 (NPC1). Free cholesteorl can also bind to the lysosomal integral membrane protein 2 (LIMP2) for transport. NPC1 as well as LIMP2 allow cholesterol transport through the lysosomal membrane, allowing accessability to other organelles such as mitochondria, ER, Golgi, and peroxisomes (indicated by green arrows). Modified from (Meng, Heybrock et al. 2020).

(Meng, Heybrock et al. 2020). From the lysosomes, cholesterol is transported to the endoplasmic reticulum, Golgi, mitochondria, and peroxisomes via physical interaction with the respective organelle (Chu, Liao et al. 2015, Hoglinger, Burgoyne et al. 2019).

Two proteins that mediate the transport of cholesterol out of the lysosome are Niemann-Pick Type C (NPC) protein 1 and lysosomal integral membrane protein 2 (LIMP2). The cholesterol binding proteins NPC1 and NPC2 allow redistribution of lysosomal cholesterol to other cellular membranes (Carstea, Morris et al. 1997). Crystallography and cryo-electron approaches identified membrane bound NPC1 and soluble intra-lysosomal NPC2 to harbor hydrophobic pockets that bind cholesterol (Winkler, Kidmose et al. 2019). NPC2 binds sterols and transfers them to the N-terminal domain of NPC1, which in turn shuttles sterols to the cytoplasm via a proton-driven mechanism. The mechanisms by which organelles take up lysosomal cholesterol are still not fully understood. Crystallography of LIMP2 revealed its binding to cholesterol, indicating a function in sterol delivery (Conrad, Cheng et al. 2017). Follow-up work identified LIMP2 as a yet unknown cholesterol transporter that shuttles LDL-derived free cholesterol molecules through its ectodomain tunnel to membranes in close proximity to the lysosome (Heybrock, Kanerva et al. 2019). The transport functions of NPC1 and LIMP2 are believed to be independently regulated as the two proteins do not show endogenous interaction.

The importance of cholesterol for organismal health is displayed by the variety of human diseases caused by a dysregulation of cholesterol homeostasis, including neurological and neurodegenerative disorders such as Alzheimer's, Huntington's, and Parkinson's disease (Vance 2012, Segatto, Leboffe et al. 2014). A dysregulation of lysosomal cholesterol storage by mutation of the cholesterol transporter NPC1 can result in the neurological cholesterol-storage disorder NPC syndrome (Baudry, Yao et al. 2003). Furthermore, the *de novo* synthesis of cholesterol is essential for brain function, since the molecule can not penetrate the blood brain barrier (Jurevics and Morell 1995). Patients suffering from Smith-Lemli-Opitz syndrome have a mutation in the last step of cholesterol biosynthesis, characterized by severe mental and growth impairments (Waterham, Wijburg et al. 1998). Finally, perturbation of cholesterol homeostasis is a major contributor to cardiovascular disease (Daniels, Killinger et al. 2009).

2.2. Bile acids and their function in mammals

Besides its direct bioactivity, cholesterol is also required as a precursor for the biosynthesis of various steroidal hormones including sex sterols, corticosteroids, oxysterols, vitamin D, and bile acids. Here, we focus in particular on bile acids and related molecules. Primary bile acids are synthesized predominantly in the liver, the main endocrine organ of mammals (Miller and Auchus 2011, Hofmann and Hagey 2014).

Primary bile acid biosynthesis in mammals requires 16 different enzymes to convert cholesterol to bile acids and can be divided into four general processes. The initiating process is the ATP-dependent 7α-hydroxylation of cholesterol by CYP7A1, which is only expressed in the liver (Russell 2003). This first step is considered rate-controlling (Elliott and Hyde 1971). It is not yet understood in which order the downstream steps occur, since some biosynthetic enzymes fulfill multiple functions within the biosynthesis pathway (Russell 2009). Bile acid biosynthesis additionally requires the further modification of the sterol precursors' ring structure, the oxidation and shortening of the side chain initiated by the sterol hydroxylase CYP27A1, and the conjugation of the bile acid with an amino acid, usually glycine or taurine. Bile acid biosynthesis is subcellular divided into reactions catalyzed in the cytosol, peroxisomes, and mitochondria (Solaas, Ulvestad et al. 2000).

Bile acids were previously believed to act exclusively as emulsifiers for dietary lipids, cholesterol, and fat-soluble vitamins in the small intestine (Russell 2003). Later they were discovered to act as signaling molecules that regulate metabolism, growth, and homeostasis (Wollam and Antebi 2011) by functioning as ligands for NHRs; however, bile acids can also act as signaling molecules transcription-independently. Reports of bile acid dependent activation of intracellular protein kinases, modulation of ion fluxes, but also activation of TGR5, a G-protein coupled bile acid receptor was reported (Keitel, Kubitz et al. 2008).

The lipophilic character of steroid hormones allows them to pass through the target cells' membrane by simple diffusion. However, the detergent-like properties of bile acids also make them cytotoxic (Morita, Ikeda et al. 2019). They disrupt cell membranes, promote reactive oxygen species formation, and ultimately can lead to apoptosis. To protect hepatocytes from damage, the last step of bile acid biosynthesis entails the conjugation of bile acids to taurine

or glycine, forming bile acid conjugates (Ferdinandusse, Denis et al. 2009). These conjugates are secreted from hepatocytes into the bile canalicular lumen by the ATP-binding cassette (ABC) transporter family member ABCB11 (Strautnieks, Bull et al. 1998). From the bile canalicular lumen, bile travels through the biliary tract to the intestine and can get reabsorbed in the terminal ileum, allowing active reabsorption by hepatocytes during enterohepatic circulation. Via the blood stream bile acids can reach target cells throughout the organism such as the liver, brown and white adipose tissue (Kiriyama and Nochi 2019). Once bile acids enter their target cells, they can bind to bile acid binding steroid hormone receptors, which are intracellular transcription factors that regulate their target gene expression in response to lipophilic hormones. These target genes in turn regulate system wide growth, development, and reproduction (Beato and Klug 2000).

Primary bile acids are modified by bacterial enzymes in the distal intestine to produce secondary bile acids (Hofmann and Hagey 2014). Secondary bile acids can return to the liver to undergo further metabolism and join the pool of primary bile acids.

2.3. Bile acids are ligands of the nuclear hormone receptor superfamily in humans

Ligand inducible transcription factors that are activated by steroid hormone binding are clustered in the NHR superfamily. Members of this superfamily, which all use cholesterol derived compounds as ligands are the liver X receptors (LXR) A and B (Janowski, Grogan et al. 1999), the vitamin D receptor (VDR) (Haussler and Norman 1969, Mizwicki, Keidel et al. 2004), and the farnesoid X receptor (FXR) (Makishima, Okamoto et al. 1999). The two isoforms of LXRs, A and B, form heterodimers with either of the two isoforms of the retinoid X receptor (RXR), A and B, to facilitate the activation of their target gene expression (Zhao and Dahlman-Wright 2010). The function of the three NHRs (LXR, VDR, and FXR) are closely connected as they all play a role in bile acid homeostasis and signaling (**Figure III-2**). LXRs are cholesterol sensors that regulate the expression of genes involved in intracellular cholesterol transport, cholesterol biosynthesis, but also cholesterol absorption and excretion on an organismal level. LXRs further control bile acid anabolism (Janowski, Willy et al. 1996). Bile acids are additionally ligands for the orphan nuclear receptor FXR, which is expressed in the liver, intestine, and kidneys, all tissues with high levels of bile acid activity (Makishima, Okamoto et

al. 1999). Activation of FXR induces a variety of genes involved in lipid, carbohydrate, protein, autophagic turnover and inflammation (Panzitt and Wagner 2021). One of the major known functions of FXR remains the protection of the liver from bile acid toxicity by regulating the transcription of genes involved in bile acid homeostasis. The activation of FXR by bile acid binding leads to the downregulation of CYP7A1 expression, the rate limiting enzyme of bile acid biosynthesis, thus reducing overall bile acid levels (Makishima, Okamoto et al. 1999, Parks, Blanchard et al. 1999). This endocrine negative feedback loop allows FXR to control its own physiological ligand availability.

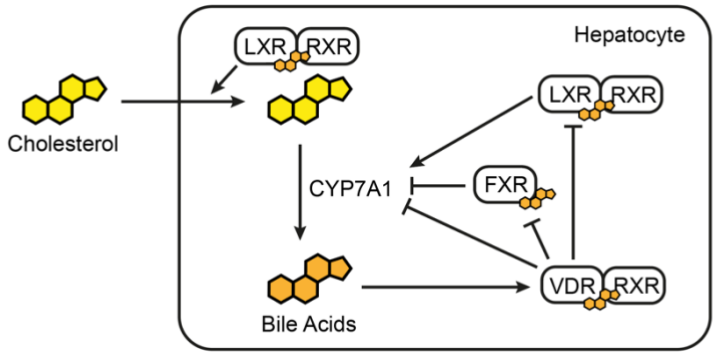

Figure III-2: Simplified illustration of the NHR regulatory network. The Liver X receptor (LXR) modulates cholesterol absorption and transport by hepatocytes. In hepatocytes, the key enzyme CYPA1 initiates the biosynthesis of cholesterol derived bile acids. CYP7A1 transcription is regulated by NHRs that utilize bile acids as ligands. CYP7A1 is positively regulated by LXR, but negatively regulated by the farnesoid X receptor (FXR) and vitamin D receptor (VDR). To be transcriptionally active, LXR and VDR need to dimerize with the retinoid X receptor (RXR). Bile acid activation of VDR prevents excessive accumulation of bile acids through feedback regulation of bile acid biosynthesis.

In human hepatocytes, bile acids activate VDR signaling, which feedback inhibits bile acid synthesis during cholestasis, and thereby protects liver cells (Han and Chiang 2009, Han, Li et al. 2010). Active VDR signaling inhibits LXR function by inhibiting bile acid biosynthesis and therefore bile acid binding to LXRs (Jiang, Miyamoto et al. 2006). VDR interacts with FXR, inhibiting FXR target gene expression, which would be required for bile salt export and bile acid binding (Honjo, Sasaki et al. 2006).

This complex functional entanglement in the function of the described NHRs is perhaps not surprising, since they are evolutionarily derived from the same ancestral protein. All three receptors were found to be the mammalian orthologues of the *C. elegans* NHR DAF-12 (Mooijaart, Brandt et al. 2005). Potentially, they evolved to form a more specialized and complex regulatory network linked to bile acid homeostasis essential for human health.

2.4. Bile acid-like hormones in nematodes – dafachronic acids

C. elegans are cholesterol auxotrophs, requiring dietary cholesterol intake for development (Hieb and Rothstein 1968, Chitwood 1999). It is hypothesized that many nematodes share the cholesterol auxotrophic characteristic due to the loss of the first three enzymes of cholesterol biosynthesis, which are highly oxygen consuming chemical reactions (Shamsuzzama, Lebedev et al. 2020). Nematodes are exposed to long periods of low oxygen, making oxygen a limited resource that was potentially prioritized for respiration rather than cholesterol biosynthesis. *C. elegans* utilize dietary cholesterol for the biosynthesis of bile acid-like steroids called dafachronic acids (DAs).

Details of the DA biosynthesis pathway were identified by utilizing a developmental arrested stage of *C. elegans* known as dauer diapause. Dauer diapause decisions are dependent on hormone biosynthetic genes and DAF-12 activity. This connection was utilized as a tool to identify so far uncharacterized genes involved in hormone biosynthesis as these mutants would display altered dauer phenotypes.

The biosynthesis of steroidal ligands is tightly controlled by a neuroendocrine network, in which environmental cues are integrated to produce endocrine signals by the amphid neurons ADF, ASG, ASI, and ASJ located in the nerve ring of the *C. elegans* head region (Bargmann and Horvitz 1991).

DA biosynthesis requires multiple enzymatic steps (**Figure III-3**). Our lab dissected key aspects of DA biosynthesis, which primarily results in the formation of Δ7-DA. This cascade of reactions starts with the Rieske oxygenase DAF-36/Neverland (Nvd) which functions as a cholesterol 7-desaturase, catalyzing the formation of 7-dehydrocholesterol (Wollam, Magomedova et al. 2011). This initial step is followed by a so far unknown enzyme that forms lathosterol. The next two steps of steroid biosynthesis require the short-chain dehydrogenase DHS-16 (Wollam, Magner et al. 2012), and the cytochrome P450 DAF-9 (Gerisch, Weitzel et al. 2001), resulting in the formation of lathosterone and ultimately Δ7-DA. More recently, the DA oxidoreductase activity of the cytochrome P450 family member DAF-40 was suggested to be involved in DA biosynthesis (Wollam 2011), as *daf-40* mutants displayed phenotypes

typical for steroid biosynthesis genes. Further characterization of DAF-40 function revealed that it can utilize known DAs such as Δ7-DA and transform them into alternative DA variants including 2α-OH-Δ7-DA and Δ1,7-DA (Gudibanda 2019). Therefore, it was concluded that DAF-40 functions as a DA interchanger required to synthesize biologically potent, but labile DA variants.

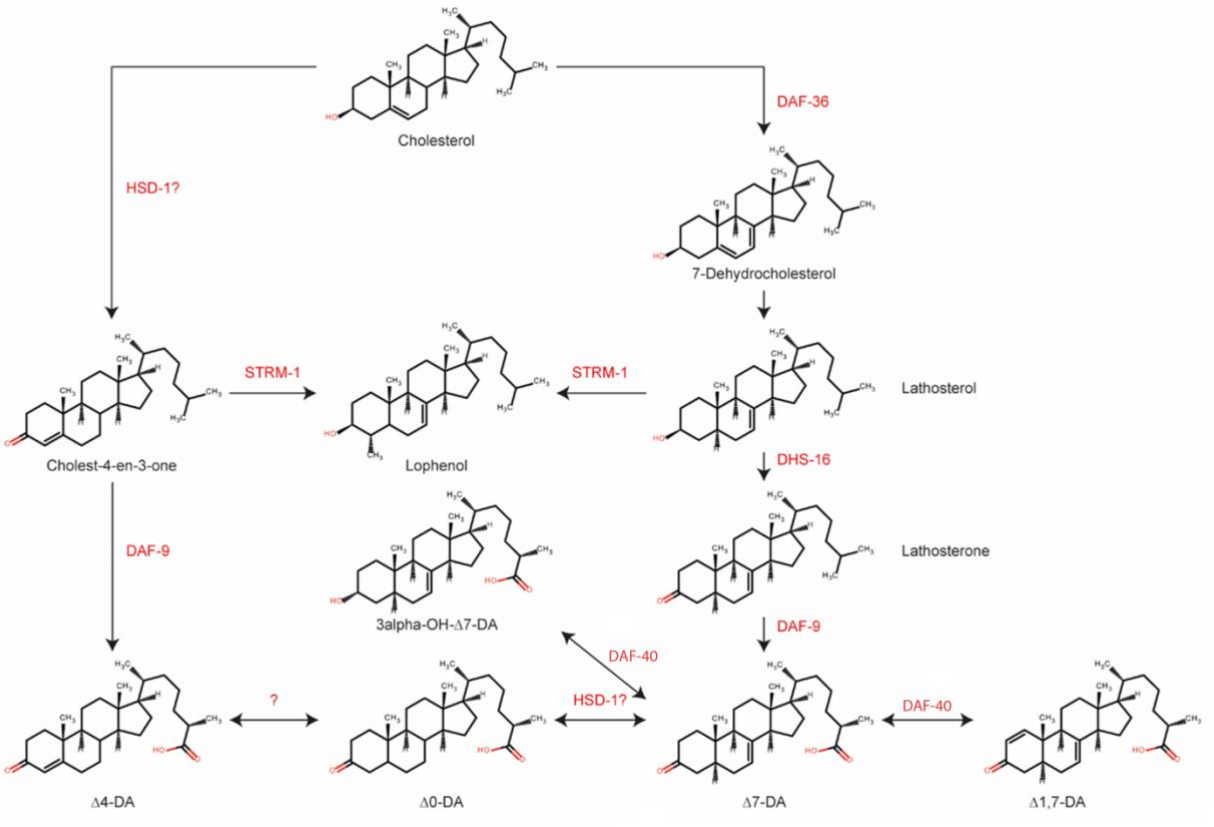

Figure III-3: Overview of dafachronic acid biosynthesis pathways. The dafachronic acid biosynthesis pathway in *C. elegans* is well described, but still harbors some open questions. Cholesterol is utilized in a cascade of bioenzymatic steps to result in the synthesis of various dafachronic acid variants. Δ4-DA synthesis (displayed on the left) is not well understood. The biosynthesis of Δ7-DA is well characterized. The image was adapted from Witting *et al.* (Aguilaniu, Fabrizio et al. 2016) who adapted it from Schroeder *et al.* (Mahanti, Bose et al. 2014).

Alternative DA biosynthesis pathways are less well studied. Cholest-4-en-3-one was suggested as a DAF-9 substrate, since, in the presence of DAF-9, it was able to induce DAF-12 activity by 109-fold compared to conditions with absent DAF-9 (Motola, Cummins et al. 2006). HSD-1, the worm orthologue to the vertebrate 3beta-HSDs, was suggested as a steroidogenic enzyme. Cholest-4-en-3-one is able to rescue *hsd-1* mutant associated defects, indicating Cholest-4-en-3-one being downstream of HSD-1 in steroid biosynthesis (Patel, Fang et al. 2008). However, the physiological HSD-1 substrate remains unknown.

The HSD-1 branch has also been suggested to give rise to the production of Δ4-DA, which is a somewhat less potent ligand for DAF-12. Other studies indicate that endogenous Δ4-DA is not detectable (Mahanti, Bose et al. 2014), suggesting that the Δ4-DA isoform is rapidly converted to the more potent Δ7-DA or only made in small amounts. Cholest-4-en-3-one and the Δ7-DA precursor lathosterol can be utilized by the methyltransferase STRM-1 (sterol A-ring methylase-1) to produce lophenol (Hannich, Entchev et al. 2009).

Bile acid biosynthesis in mammals and the synthesis of bile acid-like molecules in *C. elegans* are analogous, highlighting strong evolutionary conservation (**Figure III-4**). Though DAF-36/Rieske and CYP7A1 are very biochemically and structurally different enzymes, they carry out the analogous first committed step in bile acid synthesis in worms and mammals, respectively, in modifying the 7-position of the cholesterol backbone. The cholesterol sensing nuclear hormone receptor NHR-8 analogously regulates DAF-36 expression in worms (Magner, Wollam et al. 2013) similar to how LXR regulates CYP7A1 in mammals (Chiang, Kimmel et al. 2001). Further, DAF-9 is a conserved biochemical orthologue of CYP27A1 (Motola, Cummins et al. 2006), both of which carry out 26-oxidation of the cholesterol side chain, and display inhibition by the chemical moiety dafadine, underlining their structural similarities (Luciani, Magomedova et al. 2011). DAF-12 and FXR are also structural and functionally orthologues: DAs regulate DAF-12, while various bile acids regulate FXR. DAF-12 works within a steroid-regulated microRNA switch to regulate development and aging (Bethke, Fielenbach et al. 2009, McCormick, Chen et al. 2012), transcriptionally regulating the micro RNAs of the *let-7* family *mir-48*, *mir-84*, and *mir-241* that were previously studied in the context of heterochronic circuits (Abbott, Alvarez-Saavedra et al. 2005). Northern blot and qPCR analyses of the *let-7* family members *mir-48*, *mir-84*, and *mir-241* reveals strong regulation in *daf-12* mutants, placing DAF-12 upstream of microRNA expression (Esquela-Kerscher, Johnson et al. 2005, Bethke, Fielenbach et al. 2009). In a landmark paper, our lab elucidated the molecular mechanisms by which DAF-12 and DAs activate *mir-84* and *mir-241* promotors *in vivo* within worms as well as *in vitro* in mammalian cell culture (Bethke, Fielenbach et al. 2009).

Interestingly, the *C. elegans* DA biosynthesis pathway is spatially distributed to many tissues. DAF-36 is mainly expressed in the intestine, the organ that absorbs dietary cholesterol

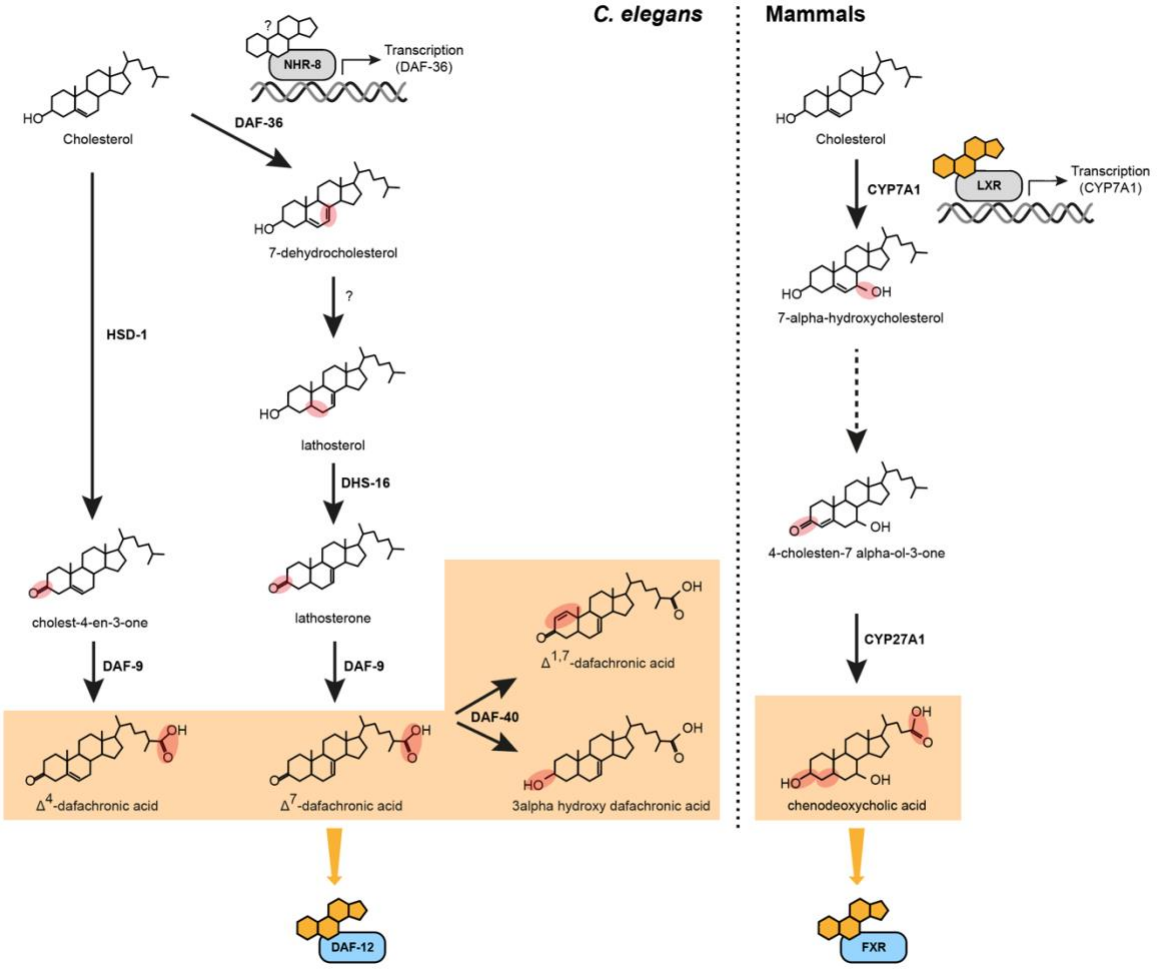

Figure III-4: Parallels between bile acid biosynthesis pathways in *C. elegans* and mammals. In *C. elegans* as well as mammals, cholesterol is utilized by a cascade of enzymes that iare required for the biosynthesis of bile acid and several bile acid like hormones dafachronic acids. The biosynthesis pathways are initiated by DAF-36 and its mammalian orthologue CYP7A1, which are both regulated by the respective nuclear hormone receptors NHR-8 and LXR. The last step in *C. elegans* DA biosynthesis is performed by DAF-9, resulting in the synthesis of Δ4-DA and Δ7-DA. Analogously, the mammalian DAF-9 orthologue CYP27A1 is responsible for the initiation of sterol side chain shortening and oxidation, required to progress in bile acid production. In *C. elegans*, synthesized DAs bind to the nuclear hormone receptor DAF-12, which shows strong parallells to how bile acids are ligands of the DAF-12 orthologue FXR to modulate FXR transcriptional activity upon binding. Both, *C. elegans* and mammalian bile acid biosynthesis pathways are well characterized, but nevertheless still present open questions. Molecule modifications are highlighted in red.

(Rottiers, Motola et al. 2006, Magner, Wollam et al. 2013). DHS-16, which carries out the next known step, is expressed in the hypodermis, neurons, and terminal pharyngeal bulb (Wollam, Magner et al. 2012). The alternative DA pathway enzyme HSD-1 is exclusively expressed in XXX neuroendocrine cells (Patel, Fang et al. 2008). DAF-9, synthesizing the last step of DA biosynthesis, is expressed in the hypodermis, XXX cells, as well as the spermatheca, potentially allowing a quick transition from lathosterol to DAs (Gerisch and Antebi 2004). DA synthesized in the XXX cells travels to its target tissue where it binds to DAF-12. DAF-12 is

widely expressed throughout different tissues and depends on the worm's developmental stage. L1 animals display strong DAF-12 expression in the epidermal seam cells as well as in various head neurons, which is diminished in the time course of development and is lost in L4 larvae and adults (Antebi, Yeh et al. 2000). Adult animals show DAF-12 expression in the intestine and the somatic gonadal tissue.

2.5. Dafachronic acids are required for germline dependent longevity in *C. elegans*

Ablation of the germline through laser microsurgery, or genetically in the germline-less mutant, *glp-1,* potently extends *C. elegans* longevity (Hsin and Kenyon 1999, Arantes-Oliveira, Apfeld et al. 2002). Longevity in germline-less mutants is not due to sterility per se since lifespan of animals in which the entire gonad was ablated with a laser microbeam at hatching, was unaffected. Whereas laser ablation of the germline precursor cells without damaging the somatic-gonad, resulted in animals that lived approximately 60% longer (Hsin and Kenyon 1999, Arantes-Oliveira, Apfeld et al. 2002). Lifespan extension upon germline loss due to laser ablation or *glp-1* mutation requires functional steroid signaling as both was abolished upon loss of DAF-12 or DA biosynthesis pathway genes (Hsin and Kenyon 1999, Gerisch, Weitzel et al. 2001, Gerisch, Rottiers et al. 2007). Evidently these signals originate from the somatic gonad (Yamawaki, Berman et al. 2010). These studies indicates that germline signaling acts through a cell non-autonomous hormonal mechanism to promote lifespan extension via DAF-12 steroidal signaling.

It was long believed that *glp-1* mutants might have increased DA production as one of the mechanisms leading to increased lifespan. In support of this hypothesis, long lived *glp-1* mutants were shown to have elevated Δ7-DA levels (Shen, Wollam et al. 2012). On the other hand, another study could not detect changes in DA levels compared to *wt* animals (Li, Liu et al. 2015). These discrepancies could result from the sensitivity of hormone measurements to sample size and handling. Altogether, these findings provided seminal evidence for steroid hormones in general, and bile acid steroids in particular in regulating lifespan-extending mechanisms in metazoans.

3. Dauer diapause regulation by upstream pathways

The steroid signaling patwhay has been shown to be involved in *C. elegans* aging through ligand binding to DAF-12 and downstream signaling. However, DAF-12 function is best characterized as a molecular switch orchestrating developmental decision making and dauer diapause transition. This underlines the intimate connection between lifespan and developmental timing as both pathways converge on DAF-12 ligand binding and activity.

During the life cycle, *C. elegans* progresses through developmental stages that are separated by molting. Under favorable environmental conditions, hatched embryos develop continuously and transit through four distinct larval stages, L1, L2, L3, and L4, before reaching adulthood (**Figure III-5**). Animals typically molt to adults after 35 h (25°C), 48 h (20°C), or 74 h (16°C) dependent on the culture temperature (Wormbook). Under stressful conditions, such as lack of food, overcrowding or elevated temperature, *C. elegans* larvae can alter their trajectory of continuous reproductive growth and arrest at various diapause stages. Known diapause stages include L1, dauer, L3, and L4 arrests, as well as adult reproductive diapause (ARD) (Baugh and Hu 2020). The best described developmental arrest in *C. elegans* is the

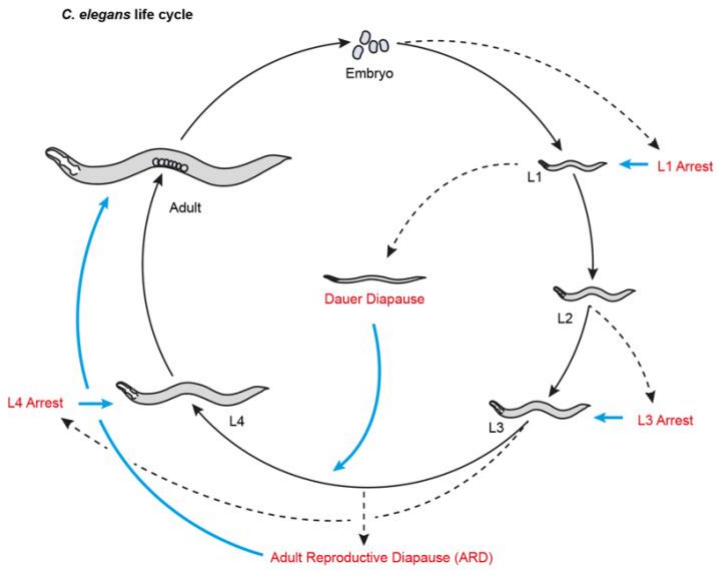

Figure III-5: *C. elegans* life cycle allows developmental arrests as responses to unfavorable environmental conditions. Under optimal growth conditions, newly hatched C. elegans undergo various larval stages until they develop into a reproductive adult (solid black arrows). As a response to unfavourable environmental conditions such as starvation, overcrowding or temperature stress, *C. elegans* are able to stall growth at different stages of their development (dotted black arrows). Once growth conditions improve, worms recover from the arrested stage amd resume development (blue arrows). Image adapted from Wormbook.

dauer diapause first characterized in 1975 (Cassada and Russell 1975). Pioneering genetic studies led to the first isolation of dauer-constitutive (Daf-c) and dauer-defective (Daf-d) mutants in the forthcoming years (Albert, Brown et al. 1981, Riddle, Swanson et al. 1981). Late L1 animals that encounter unfavorable environmental conditions such as too high or low temperatures, starvation, or overcrowding alter their regular developmental trajectory and instead form dauer larvae (Cassada and Russell 1975). Dauer larvae have defined morphological phenotypes: The worms are thinner, possess a thicker protective striated cuticle, cease pharyngeal pumping, exhibit a developmental arrest of the germline, and display shrinkage of muscle, hypodermal and intestinal cells. Dauer larvae are extremely resistant to stressors and can endure several months until environmental conditions improve. Dauer larvae are considered non-aging as the animals exit dauer to resume their development to reproductive adults with a normal life span of about two weeks (Klass and Hirsh 1976).

On a molecular level, dauer is known to be regulated by four distinct signaling pathways (**Figure III-6**): Guanylyl cyclase activity, insulin signaling, transforming growth factor (TGF)-β signaling, and steroid signaling. Favorable environmental conditions induce the secretion of a distinct combination of ascarosides, also known as dauer pheromone (Ludewig and Schroeder 2013). Under high nutrient conditions and low population density, ascarosides fall below a critical threshold, resulting in the production of the signaling molecule cyclic guanosine monophosphate (cGMP) and in turn the secretion of insulin-like peptides and the transforming growth factor DAF-7/TGF-β molecules. Downstream of this, the conserved type 1 and 2 receptors for TGF-β signaling, DAF-1 and DAF-4 as well as the receptor for insulin-like/IGF peptides, DAF-2, respond to the secretion of their ligands and inhibit the respective transcription factor activities of their downstream targets (Hu 2007, Fielenbach and Antebi 2008). This negative regulation of transcription factors is the essence that bypasses dauer development. TGF-β and insulin/IGF signaling ultimately converge on DA hormone signaling,

the fourth regulatory pathway of dauer diapause. Synthesized DA is the ligand of the NHR DAF-12 which drives the transcriptional program to develop into reproductive adults.

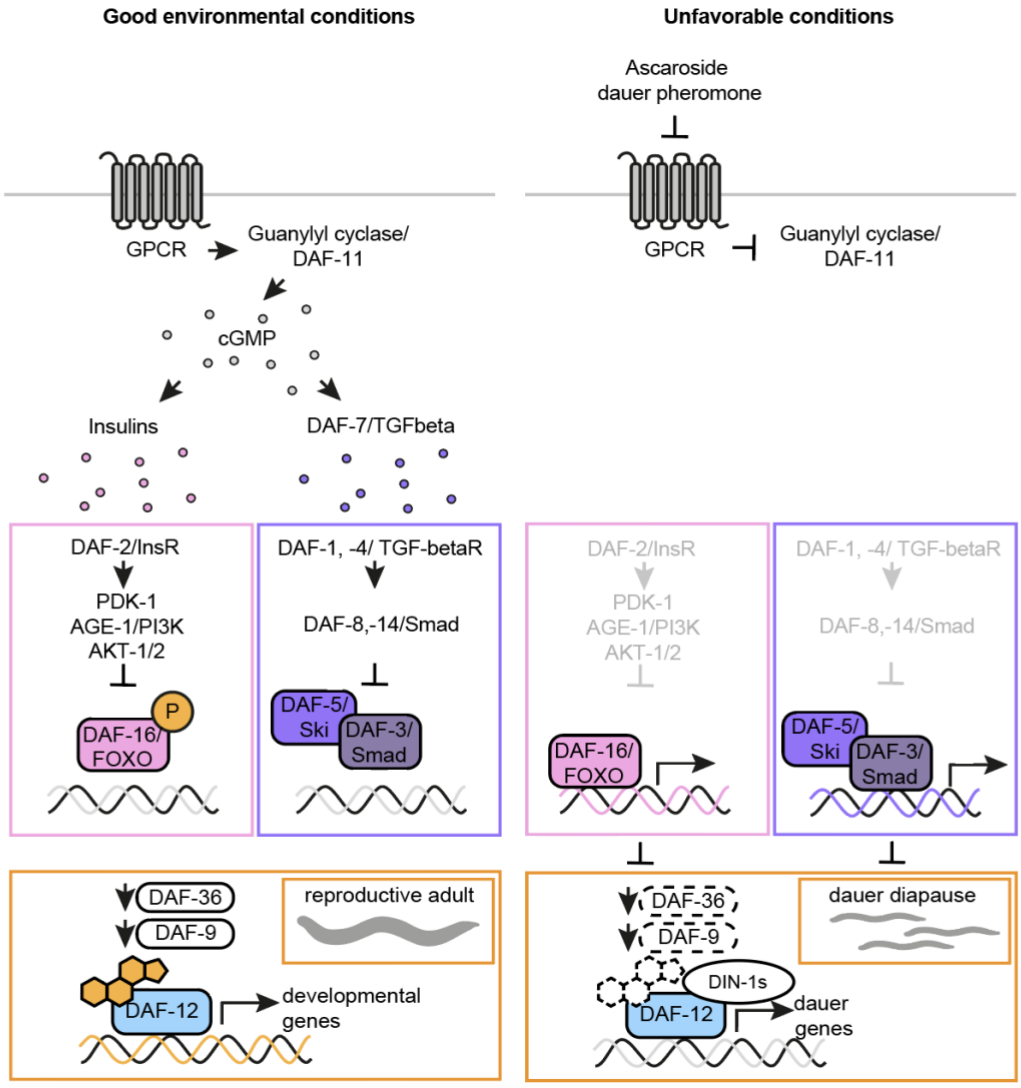

Figure III-6: Scematic overview of the regulation of *C. elegans* dauer development by cellular signaling pathways. Dauer formation is regulated by four signaling pathways, the guanylyl cyclase pathway, insulin/IGF-1 signaling, TGF-β signaling, and the steroid hormone pathway. Under good environmental conditions, G protein couples receptors located in the membrane of chemosensory neurons drive guanylyl cyclase/DAF-11 activity, synthesizing the signaling molecule cGMP. cGMP triggers the release of insulin and TGFβ, which activate the respective signaling pathways in the endocrine tissues: Insulin binds to the insulin receptor DAF-2 which drives the phosporylation of DAF-16/FOXO by AKT-1 and AKT-2. Phosphorylated DAF-16 is retained in the cytosol and can not translocate into the nucleus. TGFβ binds to the TGFβ receptor/DAF-1 and DAF-4 heterodimer, inhibiting Smad transcriptional complexes. Under insulin and TGFβ secretion target tissues have active dafachronic acid biosynthesis which bind to the nuclear hormone receptor DAF-12 to promote growth. Under unfavorable conditions with high ascaroside dauer pheromone levels inhibit GPCR and guanylyl cyclase activity in chemosensory neurons. DAF-16 and Smad complexes are transcriptionally acive, supressing the biosynthesis of dafachronic acids. Unligated DAF-12 binds to its cosupressor DIN-1S, inducing the transcriprion of dauer promoting genes. The illustration was adapted from (Butcher 2017).

Under low nutrient conditions and high population density, this signaling cascade is reversed: high levels of ascarosides bind to their cognate GPCRs, resulting in downregulation of cGMP, TGF-β, insulin/IGF and DA signaling, resulting in dauer development.

The nature of ascarosides, insulin/IGF signaling, TGF-β signaling, and steroid signaling will be described in more detail below.

3.1. Ascarosides trigger dauer formation by inhibiting guanylyl cyclase activity

Dauer pheromones was discovered in 1982 when it was observed that extracts from cultured media supernatants can prevent dauer larvae from resuming development despite the presence of food signals. This observation highlighted the antagonistic effects between dauer pheromone and food cues (Golden and Riddle 1982). Dauer pheromone represents population density and is a harbinger of food scarcity. It allows other individuals of the same population to prepare for changes in environmental quality to ultimately improve the survival of the whole population. Neural cues reflecting overcrowding, high temperatures, and the absence of food are then integrated to influence dauer commitment at the late L1 larval stage.

The dauer pheromone is comprised of a group of small-molecule signals, called ascarosides, that are involved in dauer entry and exit (Ludewig and Schroeder 2013). There are many known classes of ascarosides; the three best characterized differ in their conjugation of the central dideoxy-sugar ascarylose to either a saturated fatty acid, an unsaturated fatty acid, or a ketone (Jeong, Jung et al. 2005, Butcher, Fujita et al. 2007). DAF-22 is a peroxisomal enzyme required for the biosynthesis of such short-chain fatty acid-derived side chains (Izrayelit, Robinette et al. 2013) that was first described in 1985 (Golden and Riddle 1985). Loss of *daf-22* results in the lack of certain ascarosides that regulate development and behavior. Under physiological conditions, different ascaroside classes are present and contribute to the biological activity. Dissecting the activity of individual ascarosides has shown that conjugates with unsaturated fatty acids and ketones are the most potent variants regulating dauer formation (Butcher, Fujita et al. 2007).

Molecular genetic analysis has placed ascarosides upstream of conserved signaling pathways such as insulin/IGF signaling and the TGF-β pathway. Ascarosides function as ligands for the

ascaroside-sensing GPCRs. GPCR receptor binding seems to be highly specific for different ascarosides and regulates various biological functions including dauer formation, developmental timing and mate attraction (Srinivasan, Kaplan et al. 2008).

It is thought that each ascaroside is sensed by one or multiple receptors and receptors specific for single ascarosides have been identified. A receptor specific to ascr#2 is DAF-37, which can form homodimers or can function in a DAF-37/DAF-38 heterodimer (Park, O'Doherty et al. 2012). Further, the ascr#5-specific receptors SRG-36 and SRG-37 have been found (McGrath, Xu et al. 2011). These two provide examples for highly structure-specific ascaroside receptors, potentially resulting in particular physiological responses. But not only receptor and ligand identity define the resulting biological effect. The expression and binding of the same ascaroside/GPCR combination expressed in two different chemosensory neurons can mediate different physiological outputs. This is best exemplified by ascr#2 binding to DAF-37. Binding in the ASI neurons induces dauer formation, whereas binding in the ASK neurons results in hermaphrodite repulsion (Park, O'Doherty et al. 2012). There are four classes of chemosensory neurons that have been identified to play a role in *C. elegans* dauer formation: ADF, ASG, ASI, and ASJ. Ablation of all these neurons results in constitutive dauer formation regardless of the environmental conditions (Bargmann and Horvitz 1991).

GPCRs activate the downstream receptor guanylyl cyclase that catalyzes the turnover of guanosine triphosphate (GTP) to the second messenger molecule cGMP. One member of the large family of guanylyl cyclases in *C. elegans* is encoded by *daf-11* (Birnby, Link et al. 2000). During unfavorable environmental conditions, ascaroside levels increase and GPCRs in chemosensory neurons are inactive. This results in the inhibition of DAF-11 by GPA-2 and GPA-3, leading to the decrease of cGMP levels (Kim, Sato et al. 2009). This pathway is essential to enable proper dauer induction. Over-activation of GPA-2 and GPA-3 results in pheromone-independent constitutive dauer formation, whereas loss of GPA-2 and GPA-3 function results in dauer defective animals (Zwaal, Mendel et al. 1997).

cGMP functions as a second messenger upstream of insulin/IGF signaling (IIS) and TGF-β signaling. The dauer phenotype of dauer pathway mutants was utilized to map the epistasis relationship between the different pathways. The Daf-c phenotype of *daf-11* mutants was suppressed by mutation *daf-5 and daf-16*, which are negatively regulated by TGF-β and IIS

signaling respectively (Vowels and Thomas 1992, Thomas, Birnby et al. 1993). Additionally, the *daf-11* induced Daf-c phenotype can be rescued by exogenous cGMP (Birnby, Link et al. 2000).

3.2. Insulin signaling pathway

The insulin pathway has been shown to be evolutionarily conserved from worms to mammals as a controller of metabolism, development, and lifespan. The Daf-c mutant, *daf-2*, was first described to be twice as long lived *C. elegans* as wild type by Cynthia Kenyon in 1993 (Kenyon, Chang et al. 1993). Later it was shown to encode the ancestral insulin/IGF receptor (Kimura, Tissenbaum et al. 1997). Since then, the importance of IIS on *C. elegans* aging was further solidified. The insulin pathway is activated by the secretion of insulin-like peptides, which bind to DAF-2, the *C. elegans* orthologue of the mammalian insulin receptor (Hua, Nakagawa et al. 2003). The activation of DAF-2 recruits the phosphoinositide 3-kinase AGE-1/PI3K, in turn activating the downstream components PDK-1, AKT-1 and AKT-2. This signaling cascade results in the phosphorylation of the forkhead box O (FoxO) protein DAF-16 which prevents its translocation into the nucleus, thereby inhibiting the activation of DAF-16 target genes. Conversely, when insulin signaling is downregulated, DAF-16 enters the nucleus to turn on genes involved in metabolism, stress resistance, and longevity.

The insulin pathway has been shown to be evolutionarily conserved from worms to mammals as a central regulator of metabolism, stress, development, and lifespan. Neuronal and intestinal IIS signaling, but not muscular IS, is able to regulate longevity, since *daf-2* inhibition in these tissues can extend life span (Zhang, Zhang et al. 2022). The FoxO transcription factor DAF-16 is the main downstream effector of IIS (Lin, Dorman et al. 1997, Ogg, Paradis et al. 1997), its function is not limited to IIS; instead, it integrates signals from various signaling pathways such as germline and mechanistic target of rapamycin (mTOR) signaling (Sun, Chen et al. 2017). Besides its involvement in organismal lifespan, insulin-like signaling also plays a crucial role in regulating *C. elegans*' dauer diapause (Kimura, Tissenbaum et al. 1997). Upon unfavorable environmental conditions IIS signaling is decreased, resulting in loss of DAF-16 phosphorylation, DAF-16 nuclear localization and thereby the transcription of DAF-16 target genes (Lee, Kennedy et al. 2003).

The tissue specificity of IIS and localization of the insulin receptor DAF-2 was determined by utilizing green fluorescent protein (GFP) expression under the *daf-2* promotor, reporting fluorescence signals in the intestine and nervous system (Hunt-Newbury, Viveiros et al. 2007). We now know that DAF-2 is expressed mostly in neurons, including the XXX secretory cells (Zhang, Zhang et al. 2022), the hub for dafachronic acid biosynthesis, with only little expression in non-neuronal tissue such as the hypodermis and the intestine (Kimura, Riddle et al. 2011). To regulate dauer, IIS signaling functions cell non-autonomously. Experiments with tissue specific expression of DAF-2 in *daf-2* mutants showed that rescue of longevity and dauer phenotypes was only achieved when *daf-2* was expressed in neurons and intestinal cells. Expression in muscle cells did not show rescue effects in lifespan or dauer; instead, muscular *daf-2* rescued metabolic defects (Apfeld and Kenyon 1998, Wolkow, Kimura et al. 2000). The tissue specificity of DAF-16/FoxO was also investigated utilizing tissue specific *daf-16* rescue. DAF-16 expression only in the intestine, not other tissues of *daf-16;daf-2* mutants was able to increase life span up to 60% (Libina, Berman et al. 2003). To induce dauer formation, neuronal DAF-16 expression was sufficient (Libina, Berman et al. 2003), which is in line with reports of high *daf-16::gfp* expression in the nervous system of dauer larvae (Lin, Hsin et al. 2001).

Interactions between IIS signaling and the highly conserved mTOR pathway have been investigated in mammals. mTOR acts through two complexes, target of rapamycin complex (TORC)1 and TORC2, both composed of the core protein *let-363*/TOR bound to distinct additional components. In mammals, insulin was shown to phosphorylate and thereby activate TORC1 (Avruch, Hara et al. 2006). Possible connections in *C. elegans* are not as well understood. There is evidence that mTOR might be downstream or independent of insulin signaling since *let-363* RNA interference (RNAi) induced longevity was not influenced by mutations in *daf-16* alone (Vellai, Takacs-Vellai et al. 2003). However, other studies show that mutation of daf-16/FoxO causes a complete loss of longevity induced by decreased TORC1 signaling in *ragc-1* mutants, but not in rapamycin treated worms (Robida-Stubbs, Glover-Cutter et al. 2012), suggesting that TORC1 might act through DAF-16/FoxO whereas TORC2 might regulate life span DAF-16/FoxO independently. The connection to dauer is further strengthened by *let-363*/TOR and *daf-15*/Raptor (a component of the TORC1 complex) mutants showing dauer-like phenotypes that lack the cuticular and intestinal characteristics

of full dauers (Jia, Chen et al. 2004). The formation of dauer-like larvae by mutating mTOR components implies a regulation of dauer by TOR signaling that requires further investigation.

The rigorous study of insulin signaling in model organisms has provided insights that were utilized to develop disease interventions for IIS dependent diseases such as diabetes and related disorders (Graham and Pick 2017). The insulin IIS signaling pathway is an example of the importance of hormonal and tissue non-autonomous signaling to regulate lifespan, metabolism and developmental decisions, ultimately promoting organismal health.

3.3. TGF-β signaling pathway

A dauer regulating pathway working downstream of guanylyl cyclases and in parallel to IIS signaling is the TGF-β pathway. More recently, it has been found that mutation of *daf-7*/TGF-β results in a 2-fold increase in *C. elegans* lifespan (Shaw, Luo et al. 2007). The TGF-β signaling pathway was shown to regulate lifespan by interacting with the IIS pathway and regulating DAF-16 localization (Shaw, Luo et al. 2007).

DAF-7/TGF-β is expressed in the ASI amphid neurons (Ren, Lim et al. 1996, Schackwitz, Inoue et al. 1996). It is secreted and acts cell non-autonomously by binding to the ubiquitously expressed DAF-1 (type I) (Georgi, Albert et al. 1990) and DAF-4 (type II) (Estevez, Attisano et al. 1993) serine/threonine kinase TGF-β receptors. Upon TGF-β receptor activation, the downstream components DAF-8 and DAF-14 are phosphorylated (Narasimhan, Yen et al. 2011), causing translocation to the nucleus where they prevent dauer formation. DAF-8 and DAF-14 have a similar role to the corresponding mammalian SMADs. Another SMAD-like transcription factor, DAF-3, is a positive regulator of dauer diapause induction (Patterson, Koweek et al. 1997). In particular, in favorable environmental conditions, nuclear DAF-8/DAF-14 (Inoue and Thomas 2000) inhibits the DAF-3/SMAD and DAF-5 (homolog of mammalian oncoprotein SNO/SKI (da Graca, Zimmerman et al. 2004)) heterodimer to prevent dauer. Upon unfavorable environmental conditions, there is no expression of DAF-7/TGF-β in the ASI amphid neurons, no TGF-β receptor activation, and no activation of DAF-8/DAF-14 in target tissues. Hence, the DAF-3/DAF-5 dimer is transcriptionally active and drives gene expression of a dauer inducing program.

Mutations of various TGF-β pathway components lead to strong dauer phenotypes. Worms with a loss of *daf-1, -4, -7, -8, or -14* display a Daf-c phenotype, whereas mutations in the *daf-3* or *daf-5* genes cause Daf-d (Patterson and Padgett 2000). Studies investigating the effects of high temperatures on dauer development showed that growing worms at 27°C was sufficient to induce dauer in *wt* animals despite the availability of food (Ailion and Thomas 2000). This study also showed that *daf-3*/SMAD mutants, which display a Daf-d phenotype at temperatures below 25°C, form dauer constitutively at 27°C. Previously it has been hypothesized that neuronal DAF-7/TGF-β signals to non-neuronal tissue to prevent dauer diapause. Recent work using an auxin-inducible degron (AID) system showed that loss of DAF-3/SMAD in the ciliated sensory neurons bypasses the dauer arrest induced by *daf-7* mutation, indicating that neuronal DAF-3 is essential for animal-wide tissue remodeling necessary for dauer induction (Aghayeva, Bhattacharya et al. 2021). This indicates a not yet fully understood complexity of the TGF-β dependent induction of dauer.

3.4. Steroid signaling pathway

The most downstream regulatory pathway for dauer bypass and entry is the steroid signaling pathway. Under good environmental conditions, DA biosynthetic pathway genes are expressed and DAs are formed. DAs bind to DAF-12 and assemble a putative co-activator complex to bypass *C. elegans* dauer formation (Antebi, Yeh et al. 2000), but the nature of this co-activator complex remains elusive.

In the presence of dauer pheromone, Insulin and DAF-7/TGF-β secretion is inhibited and DAF-16/FoxO and DAF-5/DAF-3 are transcriptionally active resulting in reduced DAF-9/cytochrome P450 expression (Gerisch and Antebi 2004). This inhibits DA biosynthesis. In the absence of DA, DAF-12 binds to DIN-1S/SPEN, more specifically the alternative splicing-isoform DIN-1S, shifting development to the dauer diapause (Ludewig, Kober-Eisermann et al. 2004). Dauer animals can resume reproductive development once the time of extreme stress has passed.

Similarly to mutants of the upstream dauer pathways IIS and TGF-β, also mutants of the steroid signaling pathway show altered dauer phenotypes. Mutations in DA biosynthetic enzymes such as DAF-36, catalyzing the first step and DAF-9/cytochrome P450, catalyzing the

last step of Δ7-DA biosynthesis also trigger dauer formation (Gerisch, Weitzel et al. 2001, Gerisch and Antebi 2004, Wollam, Magomedova et al. 2011). Whereas mutants of the NHR *daf-12* are Daf-d (Albert and Riddle 1988, Thomas, Birnby et al. 1993, Gerisch, Weitzel et al. 2001, Jia, Albert et al. 2002). Interestingly, *daf-9* mutant phenotypes of gonadal Mig and Daf-c can be phenocopied by cholesterol deprivation (Gerisch, Weitzel et al. 2001). The cholesterol transporter Niemann-Pick homologs, *ncr-1* and *ncr-2,* important to maintain cholesterol homeostasis in the lysosome (Sym, Basson et al. 2000), also show altered dauer phenotypes as cholesterol availability is essential for DA biosynthesis. While *ncr-1* and *ncr-2* single mutants are weakly Daf-c, *ncr-1;ncr-2* double mutant display a strong Daf-c phenotype (Li, Brown et al. 2004).

Several different isoforms of DA can activate DAF-12 including Δ7-DA, Δ4-DA, and 3α-hydroxy derivatives. The roles of different DA hormone isoforms in dauer formation remain obscure. It is known that DA variants can vary in potency and stability to act as DAF-12 ligands. The DA-oxidoreductase DAF-40 was previously hypothesized to synthesize highly unstable but potent ligands (e.g. Δ1,4,7-DA) (Wollam 2011, Gudibanda 2019), but such ligands have yet to be identified *in vivo* because of their instability. It was initially hypothesized that steroids exhibit their biological effects by binding to specific NHRs and inducing conformational changes of their binding partners (Ojasoo, Dore et al. 1988). Nowadays, it is understood that NHR-ligand signaling is more complex than initially assumed and that different ligands binding to the same NHR can assert alternative biological functions. This is exemplified by binding of the estrogen receptor to either its high affinity ligand estradiol or a low affinity ligand 27-hydroxycholesterol to regulate vasculature function (Umetani and Shaul 2011, Lathe and Kotelevtsev 2014). Similar effects can be observed looking at physiological but also synthetically designed DAF-12 ligands showing a large range of structural variation, potencies and biological functions such as effects on fecundity, body size and survival (Sharma, Wang et al. 2009, Wang, Zhou et al. 2009, Galilea, Santillan et al. 2024). There is potential to utilize a repertoire of synthetic NHR ligands to specifically modulate the steroid endocrine system for pharmacological use. Work in this direction has recently been conducted in the simple model *C. elegans* looking at synthetic DAF-12 ligands (Wang, Zhou et al. 2009, Galilea, Santillan et al. 2024).

4. The mTOR pathway is a conserved regulator of lifespan

4.1. Pleiotropic functions of the mTOR pathway

The mTOR pathway is a key regulator of organismal growth and metabolism, and a major regulator of longevity conserved across taxa (Saxton and Sabatini 2017). Downregulation of the mTOR pathway increases lifespan significantly in model organisms as diverse as yeast, worms, flies, and mice, and drugs that inhibit mTOR are considered promising anti-aging interventions (Heitman, Movva et al. 1991, Vellai, Takacs-Vellai et al. 2003, Kapahi, Zid et al. 2004, Kaeberlein, Powers et al. 2005, Harrison, Strong et al. 2009). mTOR is regulated by growth, energy, and stress signaling pathways, as well as by various metabolites such as amino acids, s-adenosyl methionine, and fatty acids (Bar-Peled, Chantranupong et al. 2013, Yasuda, Tanaka et al. 2014, Gu, Orozco et al. 2017). The mTOR signaling pathway acts as a central control hub integrating external cues to translate those into downstream activities such as metabolism, development, growth and aging (Saxton and Sabatini 2017). Overall, mTOR drives organismal growth by regulating downstream pathways including protein synthesis and autophagy as well as transcription factors that control metabolism (**Figure III-7**). Loss of nutrient sensing can result in uncontrolled mTOR activity and thus trigger cancer (Menon and Manning 2013). Downregulation of the mTOR signaling consistently extends lifespan in *C. elegans* (Vellai, Takacs-Vellai et al. 2003, Johnson, Rabinovitch et al. 2013), *Drosophila* (Kapahi, Zid et al. 2004), and mice (Miller, Harrison et al. 2014).

The core component of the mTOR pathway is the serine/threonine kinase *let-363*/*TOR*, named after its lethal mutant phenotype in *C. elegans*. mTOR was first discovered through a screen of rapamycin resistant mutants in yeast, hence the name target of rapamycin (Kunz, Henriquez et al. 1993). *let-363*/*TOR* is a member of the PI3K-kinase family and serves as the catalytic subunit of two mutually exclusive complexes formed either with DAF-15/Raptor (Hara, Maruki et al. 2002) or with RICT-1/Rictor and SINH-1/Sin1 (Sarbassov, Ali et al. 2004, Yang, Inoki et al. 2006), which are called TOR complex (TORC)1 and TORC2, respectively. These two complexes differ in their upstream inputs as well as in their cellular outputs (Liu and Sabatini 2020). TORC1 controls cell growth and metabolism, TORC2 instead regulates proliferation and survival. Rapamycin can directly inhibit TORC1, while TORC2 shows

insensitivity to acute rapamycin treatment. However, prolonged rapamycin treatment can reduce TORC2 activity by hindering rapamycin-bound mTOR to form new TORC2 complexes (Sarbassov, Ali et al. 2006).

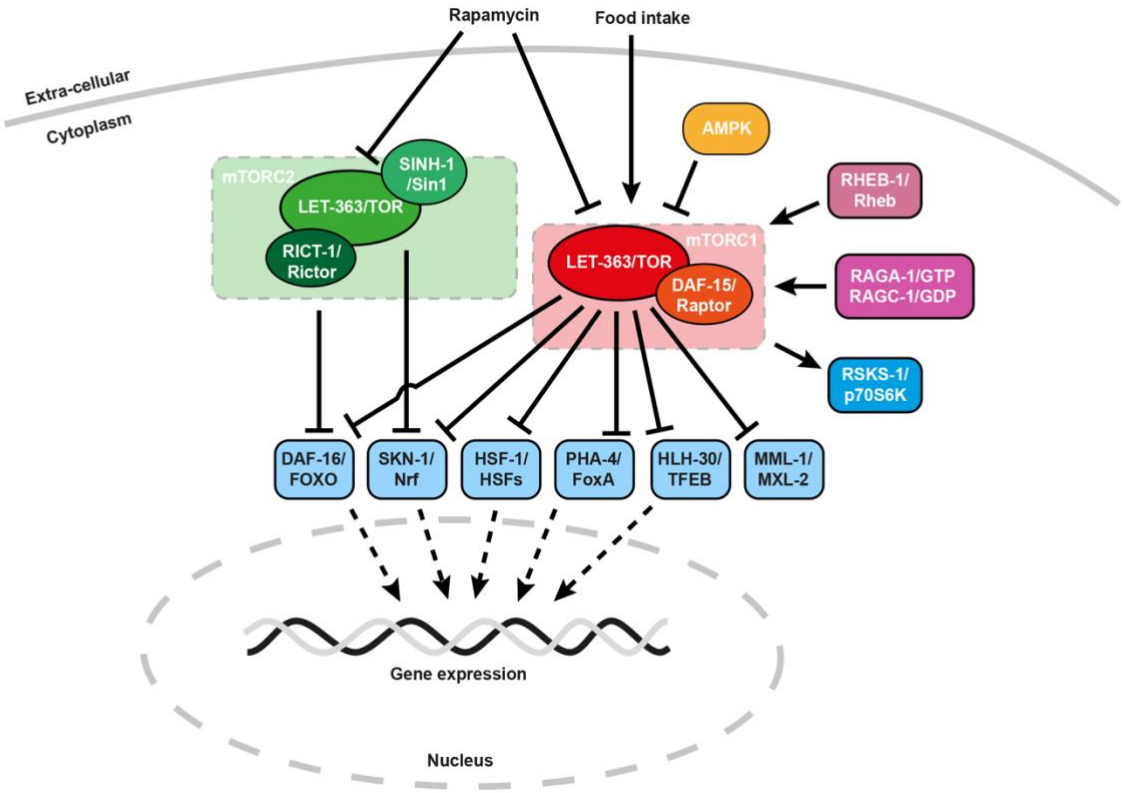

Figure III-7: Simplified scheme of the regulatory mechanisms of the mTOR complexes mTORC1 and mTORC2 in *C. elegans*. *C. elegans'* mTOR pathway can be separated into two sub-pathways, surrounding the mTOR Complexes 1 (red) and 2 (green). Both harbor the central *let-363*/TOR as their catalytic subunit but require binding to other proteins to build the respective functional complexes. mTORC1 can be regulated by various upstream modulators such as AMPK, RHEB-1/Rheb, and the Rag GTPases RAGA-1 and RAGC-1. mTORC1 in turn activates its downstrem target RSKS-1/p70S6K. Both, mTORC1 as well as mTORC2 regulate the nuclear translocation and thereby activation of transcriptions factors required to regulate different aspects of cellular growth. While both complexes are targeted by rapamycin, only mTORC1 is activated upon food intake. Modified from Blackwell *et al.* (Blackwell, Sewell et al. 2019).

TORC1 is a core regulator of cell growth that promotes anabolic functions such as the synthesis of proteins, lipids, and nucleotides while suppressing catabolic functions such as autophagy. Downregulation of TORC1 activates the downstream transcription factors DAF-16, SKN-1, HSF-1, and MML-1 to induce longevity (Robida-Stubbs, Glover-Cutter et al. 2012, Seo, Choi et al. 2013, Raymond Laboy 2023). TORC2 mediated longevity seems to act through SKN-1, but not DAF-16 (Robida-Stubbs, Glover-Cutter et al. 2012). To regulate protein synthesis TORC1 phosphorylates and thereby regulates two key effectors; the p70S6 Kinase 1 RSKS-1/S6K (Holz, Ballif et al. 2005) and the eukaryotic initiation factor 4E (eIF4E) binding

protein *ifet-1*/4E-BP (Li, DeBella et al. 2009). *rsks-1* inactivation can prolong *C. elegans* lifespan in a *pha-4*/FoxA dependent manner (Sheaffer, Updike et al. 2008). TORC1 affects *de novo* lipid synthesis through regulation of the phosphatidic acid phosphatase lipin 1 (Peterson, Sengupta et al. 2011). When phosphorylated by mTORC1, lipin 1 remains in the cytoplasm. Upon decrease of mTOR activity, lipin 1 is catalytically active and translocates to the nucleus, inhibiting SREBP (sterol responsive element binding protein) transcription factor promotor activity and protein abundance (Porstmann, Santos et al. 2008, Peterson, Sengupta et al. 2011). SREBP transcription factors regulate the expression of enzymes required for fatty acid and cholesterol biosynthesis (Lewis, Griffiths et al. 2011). In *C. elegans* a direct regulation of *de novo* lipid biosynthesis by TORC1 has not been shown, however there is evidence of a lipid/TORC1 signaling pathway that coordinates nutrient and metabolic signals to regulate growth and development (Zhu, Shen et al. 2013). Another target of TORC1 is the hypoxia inducible factor HIF1α. TORC1 increases HIF1α expression, shifting glucose metabolism from oxidative phosphorylation to glycolysis (Duvel, Yecies et al. 2010).

One way that TORC1 inhibits catabolic pathways is through HLH-30/TFEB, a master regulator of autophagy and lysosomal biogenesis. Autophagy is a conserved cellular mechanism mediating the turnover of cytosolic and organellar components to maintain energy homeostasis. HLH-30/TFEB is a transcription factor that is required to transition into the nucleus to be transcriptionally active. This nuclear translocation is blocked by TORC1-mediated phosphorylation of HLH-30/TFEB (Martina, Chen et al. 2012). Upon loss of phosphorylation, HLH-30 can be transported to the nucleus to activate expression of lysosome biogenesis and autophagy genes (Roczniak-Ferguson, Petit et al. 2012). The lifespan prolonging effects of rapamycin treatment in flies require functional TORC1-mediated inhibition of the autophagy machinery (Bjedov, Toivonen et al. 2010). In *C. elegans,* long life was reported in animals with increased *lipl-4* expression, which was induced upon inhibition of TOR, providing a link between autophagy, mTOR and lifespan extension (Lapierre, Gelino et al. 2011).

4.2. Nutrient sensing mTOR and AMPK pathways affect lifespan

A pathway antagonistic to TORC1 is the serine/threonine kinase AMPK. AMPK is a heterotrimer composed of the α, β, and γ subunits. It functions as a metabolic and energy sensor regulating proteins involved in carbohydrate and fat metabolism via phosphorylation. Overactivation of AMPK has been shown to induce lifespan extension in *C. elegans* and *Drosophila.* This overactivation can be achieved through various means such as overexpression of the AAK-2 (*C. elegans)* or AMPK-α (*Drosophila*) subunit (Apfeld, O'Connor et al. 2004, Stenesen, Suh et al. 2013), or expression of only the catalytic *aak-2* subunit of a gain-of-function mutant (Mair, Morantte et al. 2011). There are AMPK substrates that are also regulated by TORC1 such as ULK1 (Kim, Kundu et al. 2011), a rate limiting component of autophagy. Under glucose starvation ULK1 is directly phosphorylated and thereby activated by AMPK. Under conditions of sufficient nutrient availability and high mTOR activity, ULK1 activation is prevented by phosphorylation of Ser757 blocking the phosphorylation of the AMPK target sites Ser317 and Ser777. Furthermore, AMPK was reported to directly inhibit TORC1 by phosphorylation of raptor (Gwinn, Shackelford et al. 2008). The regulation of AMPK by TORC1 has also been shown. In this case the TORC1 target p70S6 kinase phosphorylates AMPK, inhibiting its function (Dagon, Hur et al. 2012). The maintenance of balance between mTOR and AMPK activity is required to promote cell growth in response to nutrient cues.

An alternative pathway to robustly induce lifespan extension across taxa is by dietary restriction (DR) without malnutrition (Green, Lamming et al. 2022). There are different methods to induce DR. A *C. elegans* genetic model caused by a mutation in the pharyngeal gene *eat-2* displays reduced pharyngeal pumping rates resulting in lower bacterial intake (Avery 1993). Alternatively, decreasing the bacterial concentration on worm culture plates or in liquid cultures can also be utilized to induce DR (Greer and Brunet 2009). In mice, DR can be induced by reducing the total amount of food received every day (Weindruch, Walford et al. 1986) or alternating periods of feeding and fasting (Goodrick, Ingram et al. 1990), both of which cause extended lifespan. DR studies in rhesus monkeys showed increased physical activity, and maintained muscle and immune function with age in contrast to the control group (Mattison, Roth et al. 2012). Overall, DR has been reported to increase lifespan by delaying the onset of age-related decline.

On a molecular level, DR regulates nutrient signaling to induce physiological benefits such as maintained health and lifespan extension. Studies in *C. elegans* have shown that DR is independent of DAF-16/FoxO, but requires mTOR to extend lifespan (Hansen, Taubert et al. 2007). Similar effects were reported in *Drosophila* (Kapahi, Zid et al. 2004). However, there is evidence that at least parts of the DR effects mediated by AMPK act through the FoxO transcription factor DAF-16 to increase lifespan (Greer, Dowlatshahi et al. 2007). DR caused by glucose restriction acts through *aak-2* in *C. elegans* to result in lifespan extension (Schulz, Zarse et al. 2007). It is likely that contradictory data is caused by DR induction via different means, suggesting that DR regimes vary in their molecular mechanism that induces beneficial effects. Regardless of its positive effects, DR is not considered a feasible anti-aging strategy in humans due to its decrease in life quality. Therefore, understanding the complex regulation of DR-related molecular mechanisms could be a more realistic strategy for healthy aging.

4.3. Lysosomal regulation of mTOR

Positive upstream regulators of TORC1 activity are the Rag GTPases (RAS-related GTP-binding protein) consisting of two families in mammals, RagA/B and RagC/D, which form heterodimers. *C. elegans* harbor only one respective homolog, RAGA-1 and RAGC-1 (Schreiber, Pierce-Shimomura et al. 2010). The Rag GTPases were described to interact with TORC1 in an amino acid sensitive manner in mammalian cells (Sancak, Peterson et al. 2008). A *C. elegans* RNAi screen looking for mutants with improved locomotion behavior in later life identified RAGA-1/RagA (Schreiber, Pierce-Shimomura et al. 2010). *raga-1* null mutants are not only protected from loss of motility, but were also found to be robustly long lived. Besides the desired beneficial effects, *raga-1* null mutation also induces negative effects such as slowed development and reduction in brood size. However, these effects are not as severe as observed with *let-363*/TOR mutants, indicating that there is remaining residual TORC1 function in *raga-1* mutants (Schreiber, Pierce-Shimomura et al. 2010). Hyperactivation of TORC1 can be induced by utilizing a gain of function *raga-1* transgene with constitutive GTP-binding, causing a decrease in lifespan (Schreiber, Pierce-Shimomura et al. 2010). Today, different alleles of *raga-1* null mutants are utilized as well-established genetic models to decrease mTOR activity and to induce longevity.

The importance of spatiotemporal regulation of TORC1 has become clearer in recent years. Nutrient cues can trigger the recruitment of TORC1 to the lysosomal surface (**Figure III-8**) (Menon, Dibble et al. 2014). In mammals this recruitment is mediated by the RagA/B heterodimer with RagC/D and the ragulator protein complex (Sancak, Bar-Peled et al. 2010). The presence of amino acids drives the conversion of RagA/B into its GTP-bound form, whereas RagC/D must be GDP bound for the interaction with TORC1 to occur (Tsun, Bar-Peled et al. 2013). Subsequently, the ragulator-Rag complex directly interacts with TORC1 to anchor it at the lysosomal surface (Kim, Goraksha-Hicks et al. 2008, Sancak, Bar-Peled et al. 2010). To induce TORC1 activity, lysosomal TORC1 localization has to be stabilized by membrane bound Rheb (Buerger, DeVries et al. 2006). Rheb exists in two states, GTP and GDP-loaded, which is controlled by the presence of secreted growth factors. To enable TORC1 binding, Rheb is required to be GTP-bound (Dibble and Manning 2013).

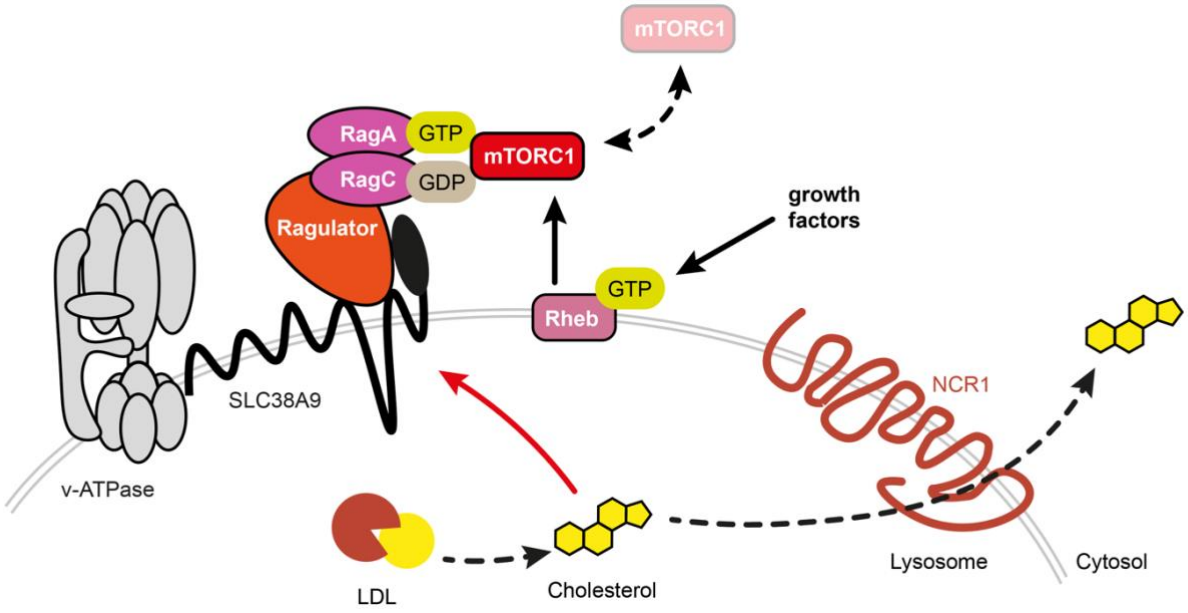

Figure III-8: Lysosomal recruitment of mTORC1 drives specific activities in mammals. Lysosomal cholesterol is transported into the lysosomal lumen via low-density lipoproteins (LDL) which are degraded to cholesteryl esters and further hydrolized to cholesterol. Cholesterol levels are regulated by shutteling lysosomal cholesterol into the cytosol via the cholesterol transporter Niemann-Pick Type C Receptor 1 (NCR1). Lysosomal cholesterol induces a conformational change in the transmembrane protein SLC38A9, stabilizing the rescruitment of mTORC1 to the RagA and C/Rag complex. This recruitment is further stabilized by Rheb which is localized in the lysosomal membrane.

More recently it was shown that TORC1 recruitment to the lysosome is more complex than initially hypothesized. Besides amino acids, experiments in mammalian cell culture have identified lysosomal cholesterol as an essential nutrient input that drives TORC1 recruitment

and activation at the lysosomal surface independent of amino acid availability (Castellano, Thelen et al. 2017). The cholesterol dependent recruitment was mediated by the lysosomal transmembrane protein SLC38A9. In response to high lysosomal cholesterol levels SLC38A9 undergoes conformational changes leading to the activation of TORC1. Follow-up studies identified the role of NPC1 as the key cholesterol exporter balancing lysosomal TORC1 recruitment, allowing mTORC1 dissociation from the lysosome, and thereby deactivation (Davis, Shin et al. 2021). Loss of NPC1 caused cholesterol accumulation and TORC1 hyperactivation. Physiological cholesterol levels in the lysosome have been shown to be regulated by endoplasmic reticulum (ER)-lysosome contact sites allowing cholesterol trafficking (Lim, Davis et al. 2019). This trafficking is mediated by the oxysterol binding protein (OSBP) which is anchored at the ER surface and is able to deliver cholesterol to the lysosome. Studies further investigating OSBP showed that autophagic dysregulation caused by a loss of NPC1 could be restored by inactivation of OSBP (Lim, Davis et al. 2019).

Recently, the hypothesis that the recruitment of TORC1 to the lysosomal surface is the only way for TORC1 activation and thereby regulation of cellular processes has been questioned. It rather seems that lysosomal and non-lysosomal TORC1 phosphorylate distinct substrates in response to different amino acid sources (Fernandes, Angelidaki et al. 2024). Cytoplasmic TORC1 was shown to be regulated by exogenous amino acids, whereas lysosomes provide a local amino acids supply by lysosomal proteolysis that is recognized by lysosomal TORC1. This finding is essential to identify function-specific TORC1 regulators.

4.4. Implications between mTOR and steroid signaling

The relationship of DA/DAF-12 signaling to mTOR signaling is not well understood. Aguilaniu and colleagues suggest that DR elevates *daf-9*/CYP450 expression, increases DA production and curiously acts through *nhr-8* (but not *daf-12*) to promote longevity, but many questions remain unclear about this model (Thondamal, Witting et al. 2014). A more recent study suggests a mechanistic connection between steroid and mTOR signaling via the release of ascarosides by intestinal peroxisomes as a response to reduced TORC1 signaling (Li, Hua et al. 2022). Simultaneously, phosphoproteome data of TORC1 identified DIN-1 as a direct target of TORC1 phosphorylation (Sewell, Poss et al. 2022). However, the DAF-12 binding isoform DIN-

1S does not harbor the sequence reported in the TORC1 phosphoproteome. It is possible that the phosphorylation of other DIN-1 isoforms regulates *din-1* expression or alternative splicing events and therefore DIN-1S levels. The effects of a potential TORC1-steroid crosstalk on lifespan are not described.

The regulation of dauer larvae in mTOR mutants is further evidence that mTOR and steroid signaling might be interconnected. The TORC2 complex component *sinh-1* was found as a regulator of dauer formation in *C. elegans.* An RNAi screen performed to find positive regulators of *C. elegans* lifespan identified reduced *sinh-1* levels to extend mean life span, to increase thermotolerance and stress resistance, but interestingly also to enhance dauer formation (Hansen et al.2005). The presence of an mTOR/steroid signaling axis is additionally supported by reports of TORC2 activity being required for food-dependent dauer entry. This study shows that the essential TORC2 component *rict*-1 acts in the intestine to promote neuronal expression of *daf-7*/TGF-β (O'Donnell, Chao et al. 2018).

Further evidence that supports the hypothesis of a hormonal mechanism regulating dietary signaling pathways such as mTOR and AMPK is the effect of lithocholic acid (LCA) on AMPK activity. LCA is a bile acid that was shown to have anti-aging effects in *C. elegans* and *Drosophila* by activating AMPK through a lysosomal glucose-sensing pathway (Qu, Chen et al. 2024). In this report, proteomics analysis of SIRT1 co-immunoprecipitated proteins identified TUB-like protein 3 (TULP3) to be an LCA receptor regulating vacuolar H^+-ATPase (v-ATPase) to drive AMPK activation at the lysosome. A possible connection to *daf-12* signaling in *C. elegans*, however, was not explicitly tested. Additional evidence that steroid/DAF-12 signaling is a central regulator of life span was shown recently. It was found that the FXR agonist obeticholic acid (OCA) extends lifespan in *C. elegans* (Lijun Zhang 2025). This lifespan extension was shown to be dependent on the FXR homologs in *C. elegans, nhr-8* and *daf-12,* highlighting the importance of NHR signaling for organismal aging (Lijun Zhang 2025). **These findings associate endocrine, metabolic, and dietary regulation to regulate lifespan in *C. elegans,* but the relationships remain obscure.**

The essential role of mTOR on organismal health has been extensively investigated and described. Mild loss of mTOR activity, such as in *raga-1* mutants, is able to prolong lifespan and protect from muscular decline in age. However, it is known to disrupt several anabolic

processes resulting in reduced growth, reduced fertility, and slowed development. Studies examining the effects of tissue specific reduction of RAGA-1 revealed that neuron-specific AID induced knockdown of RAGA-1 is sufficient to extend lifespan without impairing effects (Smith, Lanjuin et al. 2023). This study challenges previous ideas and suggests a mechanism in which **neuronal mTOR regulation is required to enable cell non-autonomous signaling to induce its benefits, potentially through a hormonal mechanism.** Indeed, preliminary data shows that knockout of mTOR components via adeno-associated viruses (AAV) regulates bile acid homeostasis in mice (Zaufel 2022), suggesting a yet understudied role of TORC1 in regulating cholesterol and bile acid metabolism.

There are hints of an emergent mTOR/steroid signaling axis; however, the underlying mechanisms for the coupling of these two pathways remain elusive.

IV. Research Aims

To date, convergent mechanisms of health- and lifespan are incompletely understood and thus aging-associated phenotypes are still difficult to manipulate. Gaining better understanding of conserved mechanisms could potentially provide pharmacologically accessible targets to address aging.

Hormonal, cell non-autonomous mechanisms for lifespan extension have been described for the major longevity pathways IIS and *glp-1.* Furthermore, studies have revealed that germ line longevity was dependent on functional DA biosynthesis. Recently it was shown that longevity effects by decreased mTOR signaling only require neuronal reduction of mTOR activity. **We thus hypothesize that mTOR longevity is regulated cell non-autonomously via a hormonal mechanism, potentially involving steroid signaling.** There is first evidence that mTOR affects bile acid levels and composition in mice.

Further work suggests that mTOR and DAF-12 signaling might act in a unified pathway since both regulate dauer formation, longevity, and depend on cholesterol availability. Therefore, **we suggest a mechanistic connection between mTOR and steroid signaling that we aim to further characterize.** Utilizing the simplified model *C. elegans* offers a tractable model to investigate the mTOR/steroid signaling axis and its effects on longevity *in vivo*. Indeed, our initial data demonstrates that null mutations of *daf-12* as well as mutations in DA biosynthetic enzymes abolish *raga-1* longevity, suggesting that reduced mTOR signaling acts through DA/DAF-12 signaling to increase lifespan.

The presented work will focus on two aims to characterize the mTOR/steroid axis in detail:

1. What are the **upstream** mechanisms linking *raga-1* to steroid signaling?
2. What are the **downstream** mechanisms mediating steroid gene-dependent *raga-1* longevity?

If mTOR signaling does indeed act through steroid signaling in *C. elegans* and higher organisms, this would open the door to a pharmacologically accessible pathway through the provision of downstream bile acids. In addition, better understanding of how steroid/NHR

signaling and mTOR are intertwined may have important implications for ameliorating cholesterol induced inflammatory processes, cardiovascular diseases, and neurodegeneration in general and in the context of aging.

V. Results

1. Steroid signaling is essential for mTOR mediated longevity

Previous studies have reported a connection between mTOR and steroid signaling (Li, Hua et al. 2022), but not in the context of aging. To address whether DAF-12 and other steroid signaling genes are required for mTOR-dependent longevity, we constructed mTOR/steroid double mutants. We used a mutation in the RAS-related GTPase RAGA, *raga-1(ok701)*, as a genetic model for reduced mTOR signaling. We used null mutants of the *daf-12*/VDR as well as various mutants in DA biosynthetic enzymes as genetic models for perturbed steroid signaling.

As seen previously, *raga-1* mutants showed a strong increase in lifespan compared to N2 (wt) animals (**Figure V-1**) (Schreiber, Pierce-Shimomura et al. 2010). Interestingly, *raga-1* longevity was fully dependent on the ability to synthesize dafachronic acid (**Figure V-1 Aa-d**). Mutations of the dafachronic biosynthesis enzymes DAF-36/Rieske, and DAF-9/CYP27A1, and DAF-40 completely abolished *raga-1* longevity. So did the null mutation of the nuclear hormone receptor transcription factor DAF-12/VDR. Thus, genes directly involved in steroid synthesis and DA-dependent transcription were epistatic to *raga-1* for life span. By contrast, mutation of *nhr-8*, a nuclear receptor closely related to *daf-12* (Magner, Wollam et al. 2013) did not alter *raga-1* lifespan (**Figure V-1 Ae**).

Class II nuclear hormone receptors, like DAF-12 typically act as transcriptional activators in the presence of ligand, and transcriptional repressors in the absence of ligand. To evaluate the importance of the repressor arm of DAF-12 activity, we tested a mutation of the DAF-12 co-suppressor DIN-1S but saw no effect on of *raga-1* longevity (**Figure V-1 Af**). Further, we assessed the contribution of DA to mTOR-induced longevity by provisioning Δ7-DA to short lived *raga-1;daf-9* mutants. Supplementing Δ7-DA was sufficient to rescue the Daf-c phenotype of *daf-9(dh6)* mutants (**Figure IX-1**) and rescued the lifespan effects induced by a lack of dafachronic acid biosynthesis in *raga-1;daf-9(rh50)* mutants (**Figure V-1 C-D**). Notably, animals supplemented with D7-DA showed lifespan benefits in the second half of the population's lifespan. This rescue was dosage and time dependent: 0.05 µM Δ7-DA was

sufficient to induce slight beneficial effects, but the rescue was greatest at the highest tested dosage of 1 µM Δ7-DA. Possibly even higher dosages might be able to further increase lifespan of *raga-1;daf-9* animals. Altogether, these results indicate that *raga-1* longevity depends on DA signaling to drive the functional positive arm, but not the negative regulatory arm of DAF-12 activity.

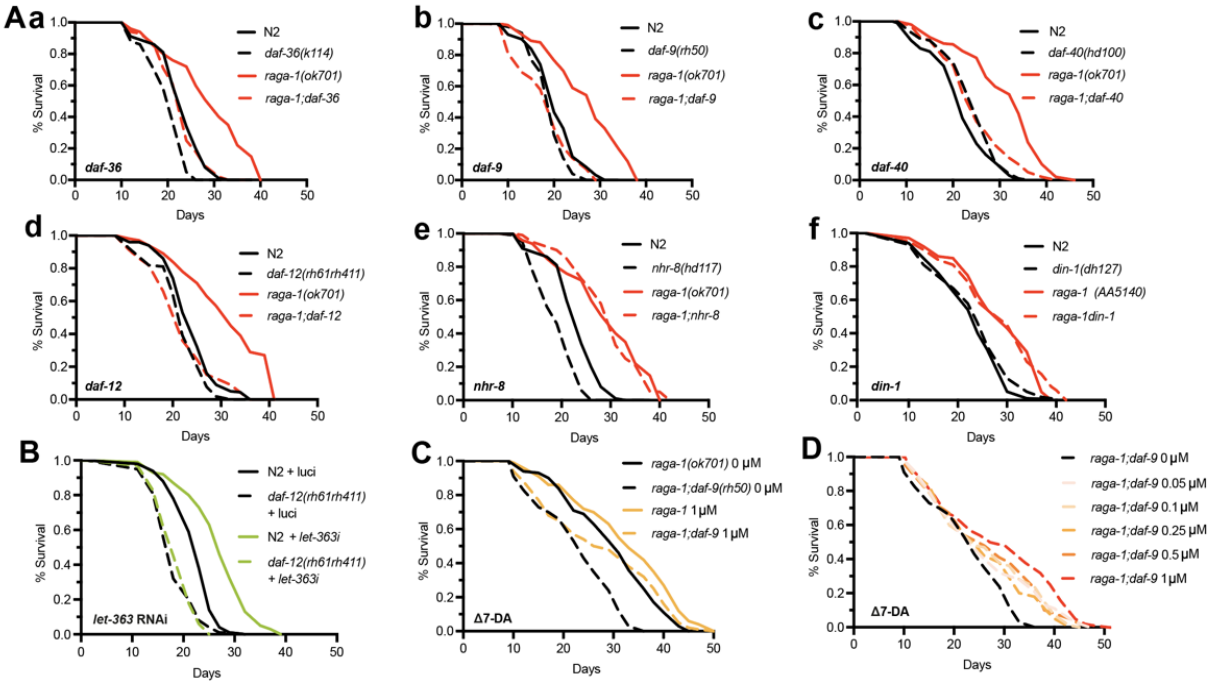

Figure V-1: mTOR mediated longevity is dependent on functional steroid signaling. (A) Lifespan analysis of various steroid mutants in the *raga-1(ok701)* mutant background. (a) *daf-36(k114)*, (b) *daf-9(rh50)*, (c) *daf-40(hd100)*, and (d) *daf-12(rh61rh411)* are required for *raga-1(ok701)* longevity. (e) *nhr-8(hd117)* and (f) *din-1(dh127)* mutation does not abolish *raga-1* longevity (>100 worms per lifespan, 3 biological replicates, Mantel-Cox Log rank test). (B) *daf-12 (rh61rh411)* worms on *let-363* RNAi and luciferase RNAi as positive control showed comparable effects to *raga-1(ok701)* lifespan (>100 worms per lifespan, RNAi treatment day 1 of adulthood on, 3 biological replicates, Mantel-Cox Log rank test). (C-D) Supplementing D7-dafachronic acid rescues *raga-1;daf-9* mutant lifespan in a dosage dependent manner, 1 µM supplementation showing the strongest tested effect compared to EtOH vehicle control (>100 worms per lifespan, supplementation treatment egg on, 1 biological replicate, Mantel-Cox Log rank test).

To investigate if the observed effects on life span were *raga-1* specific or more generally mTOR pathway dependent, we knocked down the mTOR kinase itself LET-363 by RNAi feeding (**Figure V-1 B**). In this case, too, mutation of *daf-12* abolished *let-363* RNAi mediated lifespan increase, confirming that suppression is mTOR pathway, not gene specific.

Our lab had previously shown that small nucleoli are a cellular hallmark of longevity and that mutations that extend life span exhibit smaller nucleolar size (Tiku, Jain et al. 2017). In particular, longevity models such as reduced mTOR signaling, insulin-like signaling, and dietary restriction cause nucleolar contraction and prolong life in a manner dependent on the cytosolic zinc-finger protein NCL-1. NCL-1 mutation causes nucleolar expansion and results in partial or complete loss of longevity in various long lived strains. To assess if *raga-1;daf-12* mutant interactions involve nucleolar function, we measured the nucleolar size of

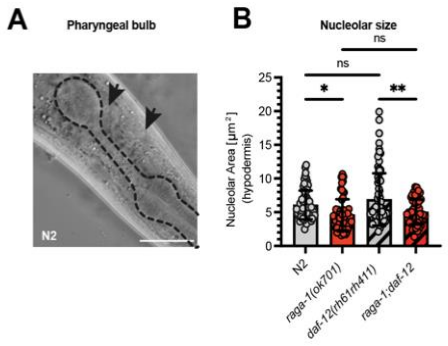

Figure V-2: Steroid signaling dependent mTOR longevity is uncoupled from nucleolar size. (A) Assessment of nucleolar size by measuring head hypodermal cells (black arrowheads) located in the space between the pharyngeal bulbs (dotted outline). Representative image of N2 worms. (B) Quantification of a representative replicate showing decreased nucleolar size in long-lived *raga-1(ok701)* mutants, but no further change in short-lived *raga-1;daf-12* mutants (3 biological replicates, L4 larvea, 30 worms tested per condition and biological replicate, bars represent mean ± SD, One-way ANOVA, ns p>0.05, * p< 0.05, ** p<0.01).

hypodermal cells (**Figure V-2A**) located between the two pharyngeal bulbs for consistency. As previously described (Tiku, Jain et al. 2017), long-lived *raga-1* mutants show reduced nucleolar size. Mutation of *daf-12*, however, did not alter nucleolar size of *raga-1* animals (**Figure V-2 B**), indicating that steroid signaling acts through mechanisms independent of the nucleolus to regulate life span.

2. Steroid signaling acts downstream of mTOR

To understand the hierarchy of regulation between mTOR and steroid signaling, we first asked if mTOR acts upstream or downstream of the steroid signaling pathway. To test this idea, we measured the expression of steroid genes on mRNA and protein levels. The global transcriptomics measurements shown below (**Figure V-8**) revealed that mRNA of multiple genes in the steroid pathway were slightly or significantly elevated in *raga-1* compared to N2 (**Figure V-3 A**). Specifically, *nhr-8, dhs-16, daf-40*, and *daf-12* showed significant elevation of

mRNA levels. The increased mRNA levels suggest that *raga-1* mutants might elevate steroid pathway activity.

It is known that dafachronic acid biosynthesis is particularly important for developmental decision making in *C. elegans'* larval development. Accordingly, the biosynthetic genes are strongly regulated throughout the different larval stages. We wondered if *raga-1* mutants might display altered expression of DA biosynthetic enzymes during development. Additionally, we aimed to understand if the transcriptional changes of steroid genes' mRNA also translated to similarly elevated protein levels of the respective gene. To measure protein levels, the fluorescence intensities of GFP fusion reporter proteins were quantified over the course of development (**Figure V-3**). The *daf-36::GFP* was expressed from an extrachromosomal array, whereas the reporters for DHS-16, DAF-9, DAF-40, and DAF-12 were integrated into the genome. The different steps of dafachronic acid biosynthesis are distributed to different tissues to coordinate hormone biosynthesis throughout the body. DAF-36 is primarily expressed in the intestine (Rottiers, Motola et al. 2006). DAF-9 is expressed in XXX cells, and, together with DHS-16 and DAF-40, is also present in the hypodermis (Mak and Ruvkun 2004, Wollam, Magner et al. 2012). The hormone receptor DAF-12 is widely expressed, including the nervous system and somatic gonad (Antebi, Yeh et al. 2000). Based on the expression patterns, the protein expression was assessed in the full body for reporters of the steroid genes *daf-36, daf-9, dhs-16*, and *daf-40*. To assess the neuronal expression of DAF-12, only the head neurons were assessed to avoid oversaturation by intestinal background fluorescence.

Comparing *raga-1* and N2 background animals, DAF-36, DAF-9, and DAF-12 levels were mainly consistent throughout development and did not show significant differences. DAF-40 as well as DHS-16 showed decreased protein levels, and thereby opposite regulation compared to the measured mRNA. The opposing regulation of mRNA and protein levels might reflect a feedback loop of decreased protein levels triggering higher mRNA production.

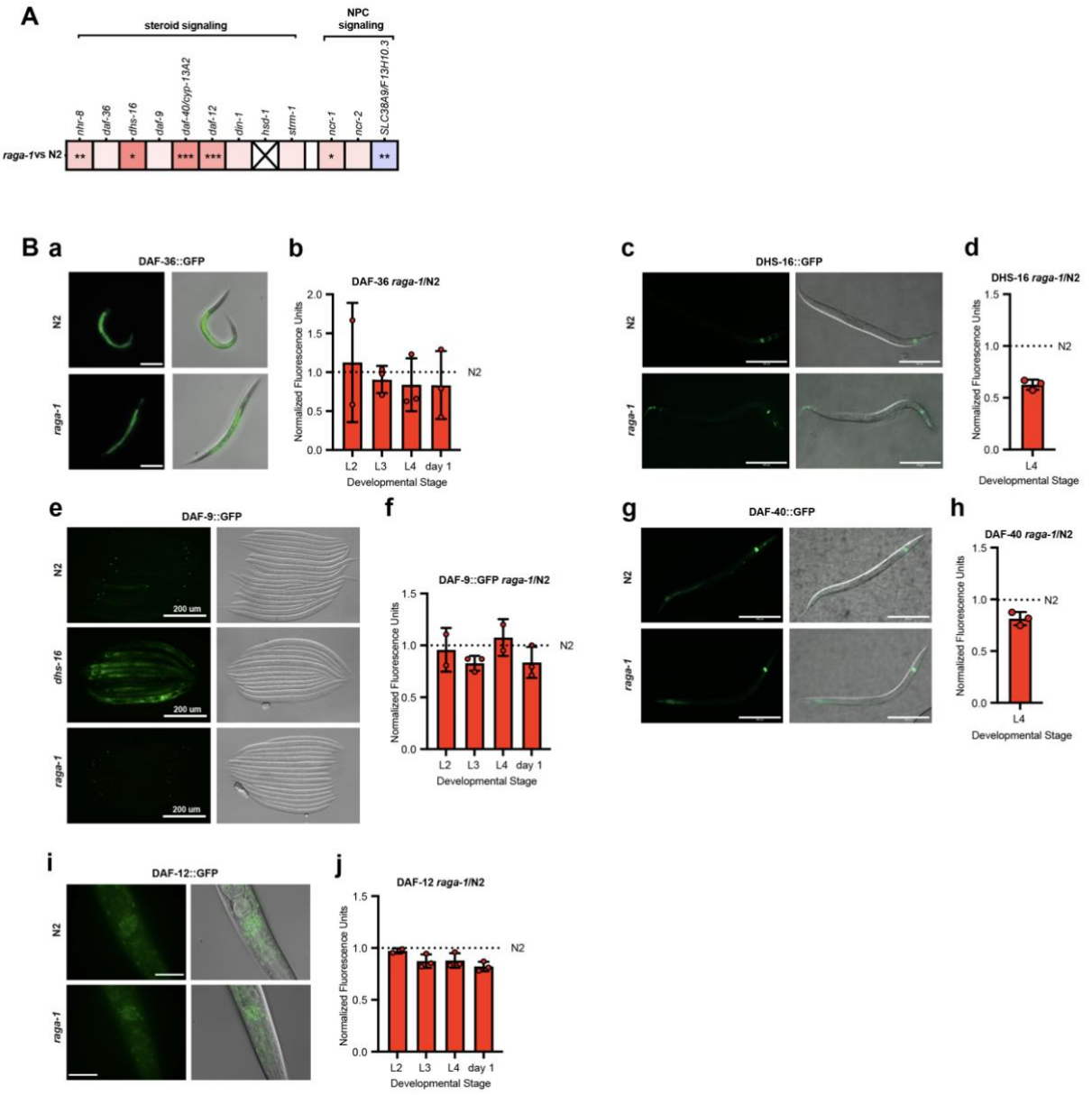

Figure V-3: Steroid gene and protein levels are inconsistently regulated in mutants with decreased mTOR signaling. (A) Heat map of read counts of RNA sequencing data comparing *raga-1(ok701)*/N2. Known steroid signaling genes show significant increase of mRNA levels for *nhr-8, dhs-16, daf-40*, and *daf-12* as well as significantly altered levels of the NPC signaling pathway genes *ncr-1*, and SLC38A9 (statistical significance was calculated using *t*-test, ns p>0.05, * p<0.05, ** p<0.01, *** p<0.001). (B) Images and quantification of the expression of reporter protein constructs of steroid signaling genes throughout development. Protein expression is unchanged comparing *raga-1(ok701)*/N2 for (a-b) DAF-36 or (e-f) DAF-9 but decreased for (c-d) DHS-16, (g-h) DAF-40, and (i-j) DAF-12 (imaged developmental stages: L2, L3, L4, and day 1, graphs display mean ± SD of 2-3 biological replicates, fluorescence intensity was normalized to the background. (a-b) image of L2 animals, full body quantification, scale bar 100 µm, (c-d) image of L4 animals, full body quantification, scale bar 200 µm, (e-f) image of L3 animals, full body quantification, scale bar 200 µm, (g-h) image of L4 animals, full body quantification, scale bar 200 µm, (i-j) imag of day 1 adults, quantification of head fluorescence, scale bar 20 µm)

Since protein levels do not necessarily correlate with enzyme activity, we aimed to directly measure steroid levels of the dafachronic acid synthesis pathway compounds via mass spectrometry (**Figure V-4**). Interestingly, even though expression of steroid biosynthesis enzymes was unaltered or decreased in *raga-1* animals, we observed a significant upregulation of Δ7-dafachronic acid and its precursor lathosterol. Thus, the strong changes in sterol levels seem to reflect increases in DA production or decreases in DA breakdown. Even though we did not observe elevated steady-state levels of cholesterol and other DA intermediates, it is possible that *raga-1* animals have elevated flux through the pathway, including increased cholesterol uptake. Therefore, DA levels might be elevated regardless of biosynthetic enzyme levels.

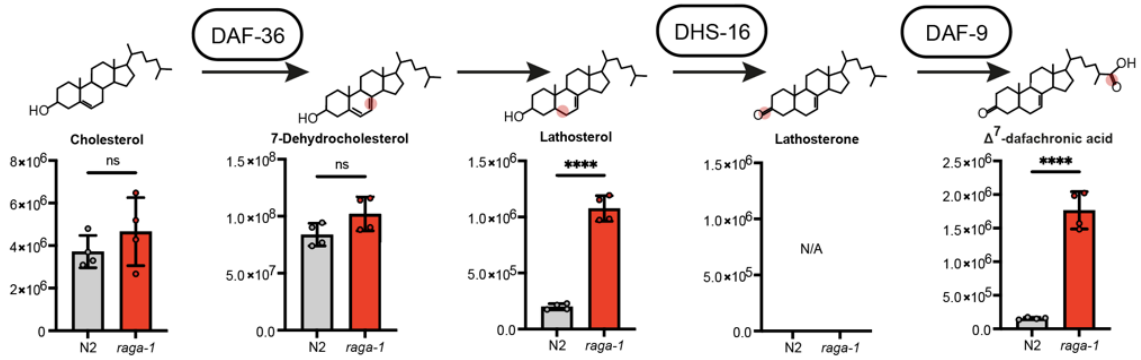

Figure V-4: mTOR regulates dafachronic acid synthesis. Simplified overview of the D7-dafachronic acid synthesis pathway. Steroidomics reveals no changes in cholesterol or 7-Dehydrocholesterol, but significant increase of Lathosterol and D7-dafachronic acid levels in *raga-1*/N2 (4 biological replicates, bars represent mean ± SD, statistical significance was calculated with *t*-test, ns $p<0.05$, **** $p<0.0001$)

In sum, mTOR and steroid signaling act in a regulatory cascade: *raga-1* elevates levels of Δ7-DA and works through a hormonal mechanism. By inference, elevated levels of DA activate DAF-12 transcriptional activity in target tissues throughout the body to mediate organismal longevity.

3. mTOR activity is unchanged in steroid mutants

We next wondered if DA/DAF-12 signaling could in turn regulate mTOR signaling. Decreased mTOR activity induces longevity, while increased mTOR activity shortens life span (Schreiber, Pierce-Shimomura et al. 2010, Robida-Stubbs, Glover-Cutter et al. 2012). This led us to hypothesize that steroid mutants might upregulate mTOR activity and counteract the lifespan

benefits in *raga-1* mutants. To test this idea, we first analyzed mRNA expression levels of known mTOR pathway components, using our RNA-seq data (see **Figure V-8**).

The transcriptomics data revealed minimal changes of mTOR pathway gene expression. The TORC1 core protein complex, comprised of *let-363*/TOR and *daf-15*/raptor, was slightly but significantly downregulated in *daf-12* mutants. For components of the TORC2 pathways only *sinh-1* showed modest but significant decrease in transcript levels. The transcript levels of the mTOR pathway genes *rheb-1, raga-1, ragc-1, rsks-1,* and *rict-1* were unchanged. The observed transcriptional changes might suggest a decrease, rather than an increase, of mTOR pathway activity in steroid mutants (**Figure V-5**).

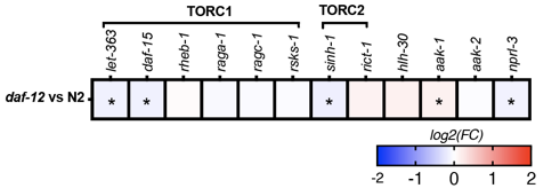

Figure V-5: Steroid mutants show no or only small changes in mTOR gene mRNA levels. Heat map of differential expression of RNA sequencing data comparing *daf-12(rh61rh411)*/N2. Known TORC1 and TORC2 signaling genes show small to no changes on mRNA levels. *let-363*, *daf-15*, *sinh-1*, and *nprl-3* show slight but significant decrease of mRNA, *aak-1* shows slight but significant increase in mRNA levels (statistical significance was calculated using *t*-test, ns $p>0.05$, * $p<0.05$)

Next, we asked if steroid signaling regulates mTOR pathway activity. To do so, we investigated mTOR activity in various steroid signaling mutants by two independent mTOR signaling outputs, nuclear localization of HLH-30 and AMPK phosphorylation. The first readout examines the nuclear localization of the transcription factor HLH-30. HLH-30/TFEB is a transcription factor modulating the expression of autophagy-related and lysosomal genes (Settembre, Di Malta et al. 2011). HLH-30/TFEB activity can be measured by its nuclear localization, which is controlled by mTOR (Lapierre, De Magalhaes Filho et al. 2013) and can be visualized via an HLH-30::NeonGreen reporter fusion protein (**Figure V-6 B**). Active TORC1 inhibits HLH-30 by phosphorylation (**Figure V-6 A**). Phosphorylated HLH-30 cannot enter the nucleus and therefore cannot activate its target genes' expression. The percentage of seam cells showing nuclear HLH-30::Neongreen localization was measured (**Figure V-6 C-D**). As expected, *raga-1* mutants showed increased levels of HLH-30 nuclear localization. HLH-30 nuclear localization was unchanged in steroid single mutants such as *daf-12, daf-9, nhr-8*, and *daf-36* compared to wt, and in the *daf-36*;*raga-1* background compared to *raga-1* conditions.

This suggests that mTOR function through its target gene *hlh-30* is independent of the tested steroid pathway genes.

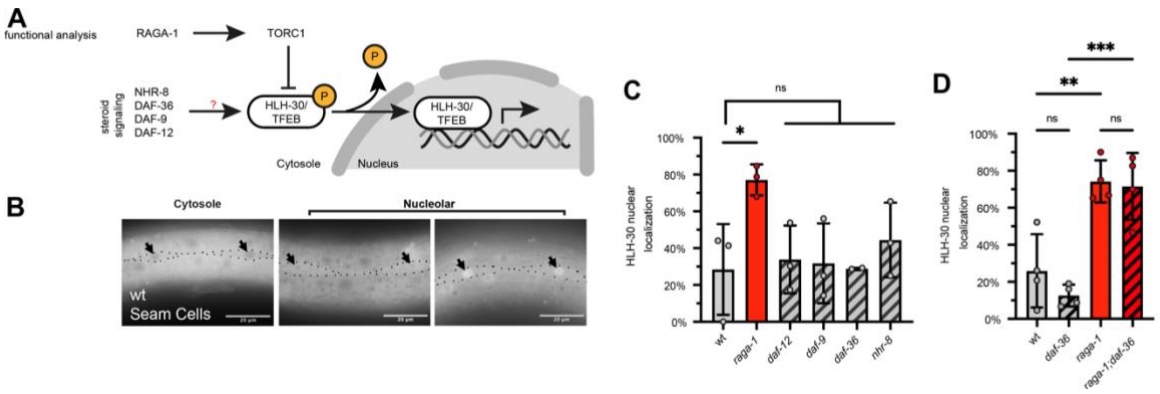

Figure V-6: Steroid mutants have regular mTOR activity looking at HLH-30 nuclear localization. (A) Schematic overview of HLH-30/TFEB inhibition by TORC1. Dephosphorylation and thereby activation of HLH-30/TFEB allows it to translocate into the nucleus. (B) Representative images of wt worms with cytosolic, and nuclear HLH-30 reporter localization in the seam cells (outlined and marked with arrow heads). Scale bar represents 20 µm. (C-D) Steroid mutants have unchanged HLH-30 nuclear localization in *wt* as well as in *raga-1* background animals (day 1 adults, 3-4 biological replicates, bars represent mean ± SD, statistical significance was calculated using One-way ANOVA, ns p>0.05, *, p<0.05, ** p<0.01, *** p<0.001)

As a second, independent readout, we also examined phospho-AMPK corresponding with mTOR activity. TORC1 and AMPK are antagonistic players regarding metabolism and longevity and are mechanistically linked. AMPK functions as an upstream inhibitor of TORC1, whereas downregulation of TORC1 enhances levels of AAK-2/AMPK phosphorylation via the TORC1 target p70S6 kinase (Gwinn, Shackelford et al. 2008, Dagon, Hur et al. 2012, Zhang, Lanjuin et al. 2019). Measuring AAK-2/AMPK phosphorylation is an indirect readout of mTOR activity

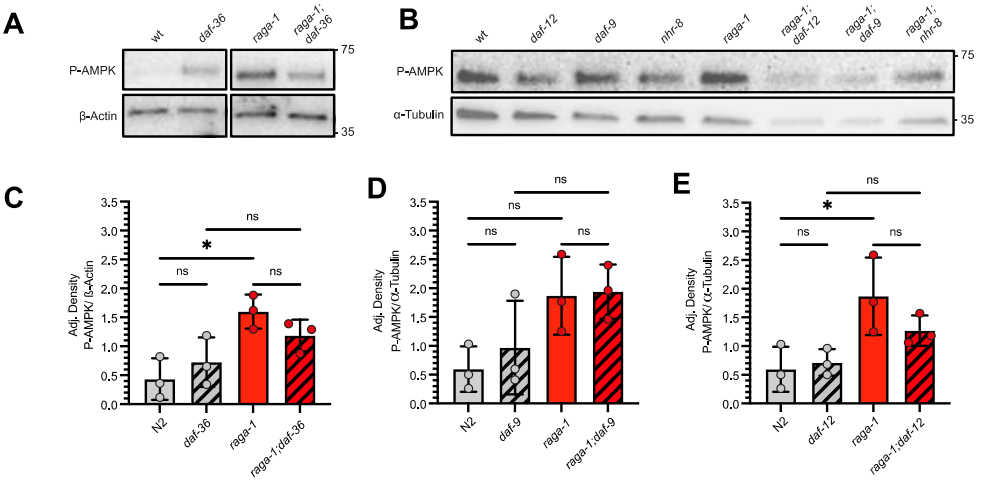

Figure V-7: Steroid mutants did not show altered mTOR levels looking at P-AMPK levels. (A-B) Representative immunoblots of AMPKα phosphorylation at position Thr172 in day 1 adults. (C-E) Quantification shows no changes of AMPKα phosphorylation upon steroid gene mutation (3 biological replicates, bars represent mean ± SD, statistical significance was calculated using One-way ANOVA, ns p>0.05, *, p<0.05)

(**Figure V-7**) (Zhang, Lanjuin et al. 2019). As expected, *raga-1* mutants displayed increased levels of AMPK phosphorylation when normalizing p-AMPK to β-Actin or α-Tubulin controls. Steroid/mTOR double mutants did not significantly affect P-AMPK ratios compared to *raga-1*.

In sum, our work shows a close regulation between mTOR and steroid signaling pathways. Our data indicate that mTOR mutants elevate dafachronic acid levels and act through DAF-12 to promote longevity. This regulation is one-directional, with steroid signaling downstream of mTOR signaling, whereas changes in steroid signaling do not affect mTOR pathway activity in this context.

4. Transcriptomic and metabolomic analysis of mTOR/steroid signaling

To elucidate the mechanism by which *raga-1* longevity acts through DA/DAF-12 signaling, we conducted global transcriptomics and metabolomics measurements comparing N2, *raga-1*, *daf-12* and *raga-1;daf-12* animals. We sought to identify single genes, pathways, and compounds that are differentially regulated in a *daf-12* dependent manner (**Figure V-8A**), which could give us insight into downstream regulatory mechanisms involved in mediating the observed lifespan effects.

To assess sample quality and reproducibility I utilized principal component analysis (PCA). Samples for transcriptomics as well as metabolomics clustered according to their genotypes, indicating good, reproducible quality. The transcriptomics set showed a strong separation of *raga-1* from the other 3 genotypes along PC1 (**Figure V-8B**), consistent with the idea that *daf-12;raga-1* suppresses *raga-1* and brings it closer to WT. PC2 showed a separation of *raga-1* and *raga-1;daf-12* from the other genotypes, likely reflecting changes induced by *raga-1* not dependent on *daf-12*. Mutation of *daf-12* also separated along component 1, albeit to a lesser extent. Principle component analysis of the metabolomics displayed a similar separation of genotypes; PC1 showed a separation of *raga-1* genotypes from others, while PC2 displayed a separation of *daf-12* genotypes from the others (**Figure V-8 C**). The clear separation between wt and *raga-1*, as well as wt and *daf-12* in transcriptomics and metabolomics data indicated phenotypical differences that might shed light into downstream regulated mechanisms.

Volcano plots of differentially regulated genes revealed that *raga-1;daf-12* double mutants show a high number of transcriptional changes compared to *raga-1* as well as *daf-12* single mutants (**Figure V-8 D**). The total set of up-regulated genes in *raga-1;daf-12/raga-1* was analyzed for enriched KEGG pathways displayed below (**Figure V-10**, highlighted in red). We observed a significant enrichment of genes involved in axon regeneration, lysosome, hippo signaling, and longevity regulating pathways. Notably *aak-1* and *ncr-1* were identified in the lysosomal gene cluster, which are already implicated in mTOR signaling, providing proof of principle to my method (Lawrence and Zoncu 2019). KEGG enrichments of genes down-regulated in *raga-1;daf-12/raga-1* were most strongly enriched in lysine degradation, and arginine and proline metabolism (**Figure V-10**, highlighted in blue), but also showed genes involved in TCA cycle, one carbon pool, glutathione metabolism, and the biosynthesis of cofactors to be differentially regulated. The role of peroxisomes in the context of mTORC1 regulation was published previously (Li, Hua et al. 2022) and it is encouraging that our method was able to detect known gene sets.

This indicates that *raga-1* and *daf-12* are regulators of various downstream pathways potentially one or multiple of which could be causing the observed lifespan effects. Below, I will describe a functional genomics screen I performed to unravel the downstream mechanism that mediates the mTOR/steroid signaling longevity. For that screen genes that were differentially regulated in *raga-1;daf-12/raga-1* were taken into consideration as potential candidate genes.

In contrast to the transcriptomics changes, metabolomic alterations in *raga-1;daf-12/raga-1* were less pronounced. Of the 119 metabolites detected, most metabolites were not significantly changed, but those that did were mostly elevated. Nineteen metabolites were

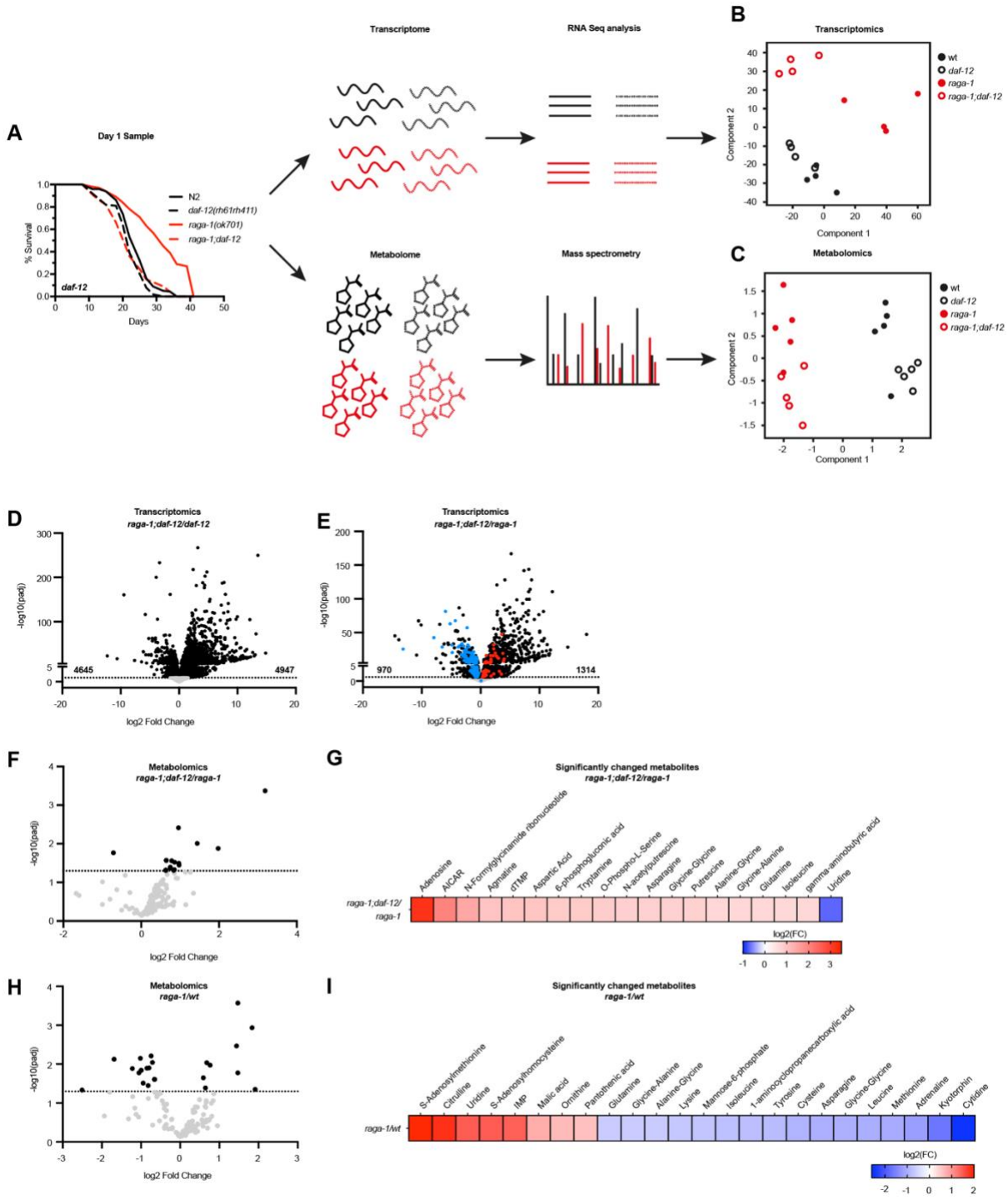

Figure V-8: Transcriptomics and metabolomics samples cluster strongly regarding their *raga-1* and *daf-12* background. (A) Schematic overview of RNA sequencing and metabolomics sample preparation. (B-C) PCA plots show clear clustering of samples accoring to genotypes and genetic background. (D) Volcano pot displays strong transcriptional changes in the comparison *raga-1;daf-12/daf-12*, as well as (E) comparing *raga-1;daf-12/raga-1.* Red and blue data points represent up- and down-regulated genes used for the functional genomic screen (4 biological replicates, day 1 adults). (F) Volcano plot displays only few significant changes of metabolite levels comparing *raga-1;daf-12/raga-1*. (G) Heat map of significantly regulated metabolites in *raga-1;daf-12/raga-1.* (H) Volcano plot displays only few significant changes of metabolite levels comparing *raga-1/wt*. (I) Heat map of significantly regulated metabolites in *raga-1/wt* (5 biological replicates, day 1 adults).

significantly changed when comparing short-lived *raga-1;daf-12* mutants to long-lived *raga-*

1 (**Figure V-8 F-G**). Eighteen of these regulated metabolites were elevated in *raga-1;daf-12*, with adenosine, AICAR, N-formylglycinamide ribonucleotide, agmatine, and dTMP showing the strongest changes. Only uridine levels were significantly decreased in *raga-1;daf-12* mutants compared to *raga-1*. Despite the impact of altered mTOR metabolism on lifespan, only a handful of metabolites were significantly changed when comparing long-lived *raga-1* mutants to wt (**Figure V-8 H**). The strongest altered compounds were S-adenosylmethionine (involved in methionine metabolism), citrulline, S-adenosylhomocystein, as well as the nucleoside/nucleotide uridine and inosine monophosphate (IMP) (**Figure V-8 I**). Interestingly, the enrichment of uridine in *raga-1/wt* is reversed in the short lived *raga-1;daf-12* mutant compared to *raga-1*. Additionally, a number of metabolites downregulated in *raga-1* were upregulated in *raga-1 daf-12*, including amino acids and their conjugates glutamine, glycine-alanine, alanine-glycine, isoleucine, asparagine, and glycine-glycine. Conceivably some of these differential metabolites could reflect alterations in TCA cycle or 1-carbon metabolism.

5. A functional genomics screen reveals genes mediating longevity through the mTOR/steroid signaling axis

To unravel the mechanisms acting downstream of DAF-12 mediating the observed longevity effects, we performed a functional genomics screen (**Figure V-9**). The transcriptomics data (**Figure V-8**) was analyzed to generate a list of candidate genes. The selection of candidate genes was approached by two angles: Unbiased and targeted candidate selection (**Figure V-10**).

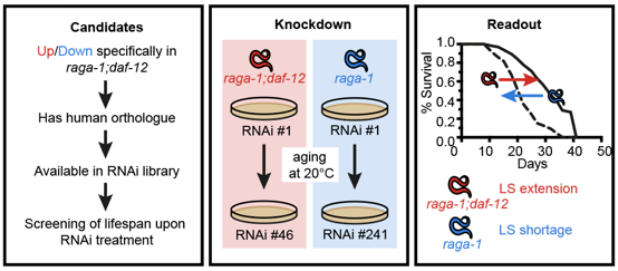

Figure V-9: Schematic outline of the functional genomics screen. The RNAi knockdown screen was approached by selecting candidate genes that are specifically regulated in *raga-1;daf-12* mutants, conserved, and available in the RNAi library. These genes would be used for RNAi mediated knckdown egg on throughout the whole life. As a readout, worm lifespan was assessed.

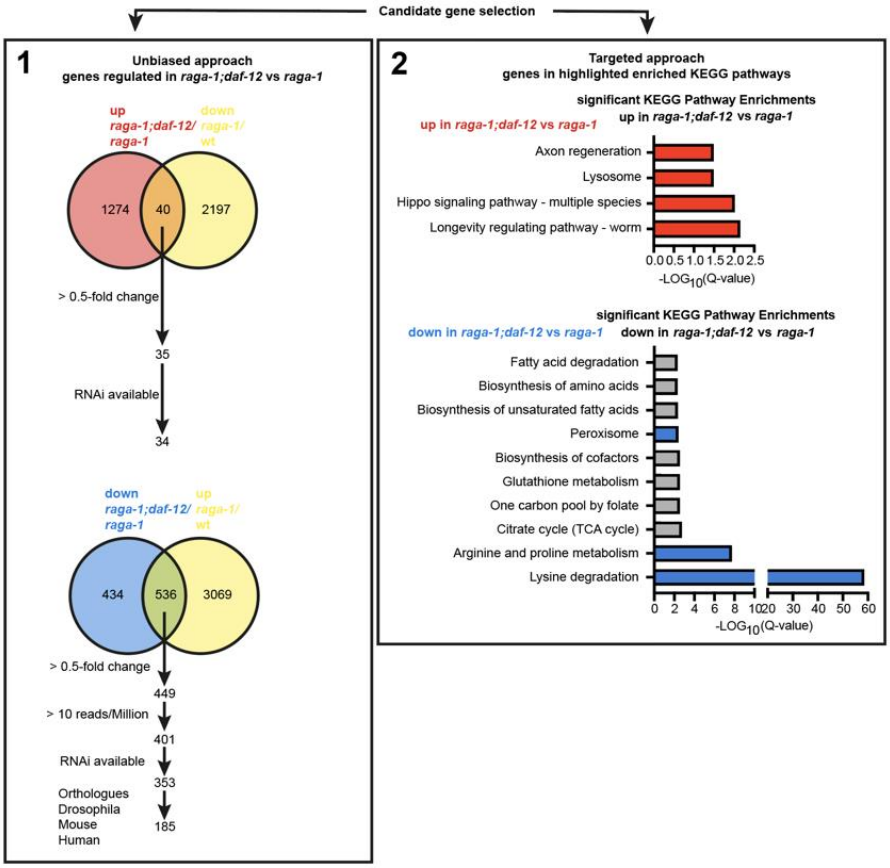

Figure V-10: Candidate gene selection for the functional genomics screen was based on differential gene regulation in transcriptomics. Candidate genes were selected from the transcriptomics data set according to two criteria (1) Unbiased approach of differentially expressed genes. In red are genes selected for knockdown in *raga-1;daf-12* mutants to prolong their lifespan. Genes up-regulated in *raga-1;daf-12/raga-1* and additionally down-regulated in *raga-1*/N2, resulting in 34 genes. In blue are genes that were screened for abolishing *raga-1* lifespan upon RNAi mediated knockdwn. These genes are down-regulated in *raga-1;daf-12/raga-1* and additionally up-regulated in *raga-1*/N2, resulting in 185 genes. (2) The targeted approach is based on KEGG pathway enrichments of genes up-regulated in *raga-1;daf-12/raga-1* (in red) and down-regulated in *raga-1;daf-12/raga-1* (in blue). Hypergeometric test (total of 18547 detected genes) reveals p=1.0 comparing genes up in *raga-1;daf-12/raga-1* with down in *raga-1*/wt (red), and p<0.0001 for genes down in *raga-1;daf-12/raga-1* and up in *raga-1/*wt (blue).

Unbiased candidate selection: Genes were considered that showed a reversal of differential expression comparing *raga-1;daf-12/raga-1* and *raga-1/wt*. Targeted candidate selection: Genes of enriched pathways were included as candidates to pick up on specifically regulated pathways that might be essential for mTOR mediated longevity. All genes involved in the KEGG pathway enrichments longevity regulating pathway, hippo signaling, lysosome, and axon regeneration for enriched genes, as well as genes listed under lysine degradation, arginine and proline metabolism, and peroxisomes for genes decreased in *raga-1;daf-12/raga-1* were included into the list of candidate genes for the screen.

The total list of genes from the unbiased candidate selection was further narrowed down. Thirty four of the genes up-regulated in *raga-1;daf-12/raga-1* and down-regulated in *raga-1/wt* matched a cut-off of a 0.5-fold change expression and were available in our laboratory's RNAi library. From 536 genes down-regulated in *raga-1;daf-12/raga-1* and up-regulated in *raga-1/wt* only 353 genes remained after applying cutoffs of a fold change above 0.5, more than 10 read-counts per million, and the availability of RNAi clones for candidate genes. To further narrow down the number of candidates, only genes were considered that are conserved in higher organisms, resulting in a final list of 185 genes.

Genes that were screened for rescue of *raga-1;daf-12* lifespan upon knockdown are displayed in red. These genes are up-regulated in the short-lived *raga-1;daf-12* compared to *raga-1* and down-regulated in long-lived *raga-1/wt*. Genes that were screened for decreasing *raga-1* lifespan upon knockdown are displayed in blue. These genes were down-regulated in the short-lived *raga-1;daf-12/raga-1* and additionally up-regulated in *raga-1*/wt and are therefore potentially required for mTOR mediated longevity.

The total set of candidate genes, combined from the unbiased and targeted candidate selection, was knocked down egg on and was tested for their ability to affect organismal lifespan. To compare the results of the various lifespans, the relative mean lifespan for each RNAi condition was calculated and plotted. Each lifespan experiment included *raga-1* and *raga-1;daf-12* fed with RNAi targeting luciferase as a control condition. Genes were considered a hit when they induced significant lifespan changes compared to the control conditions. Some genes' knockdown induced developmental arrests; these RNAi conditions were not further pursued.

Most candidate gene knockdowns in *raga-1;daf-12* generally increased *raga-1;daf-12* lifespan. Out of 46 tested RNAi clones, 7 showed significant increase in lifespan, with one condition showing the most drastic improvement of *raga-1;daf-12* lifespan, *rom-1* (**Figure V-11 A, Table** IX-3). In follow-up experiments *rom-1* lifespan effects could not be reproduced (data not shown). Thus, *rom-1* was not further pursued in this work.

raga-1 lifespan was decreased by the knockdown of most candidate genes. Out of 180 genes 83 genes were able to significantly decrease *raga-1* lifespan (**Figure V-11 B, Table** IX-2). The 40 genes with the strongest regulatory effects were enriched in genes involved in lysine degradation (green), peroxisomal genes (purple), as well as arginine and proline metabolism (orange), suggesting the importance of these pathways for *raga-1* longevity (**Figure V-11 C**). These enrichments are in line with the earlier observed KEGG pathway enrichments of down-regulated gene sets in *raga-1;daf-12/raga-1*. Knockdown of some genes further prolonged

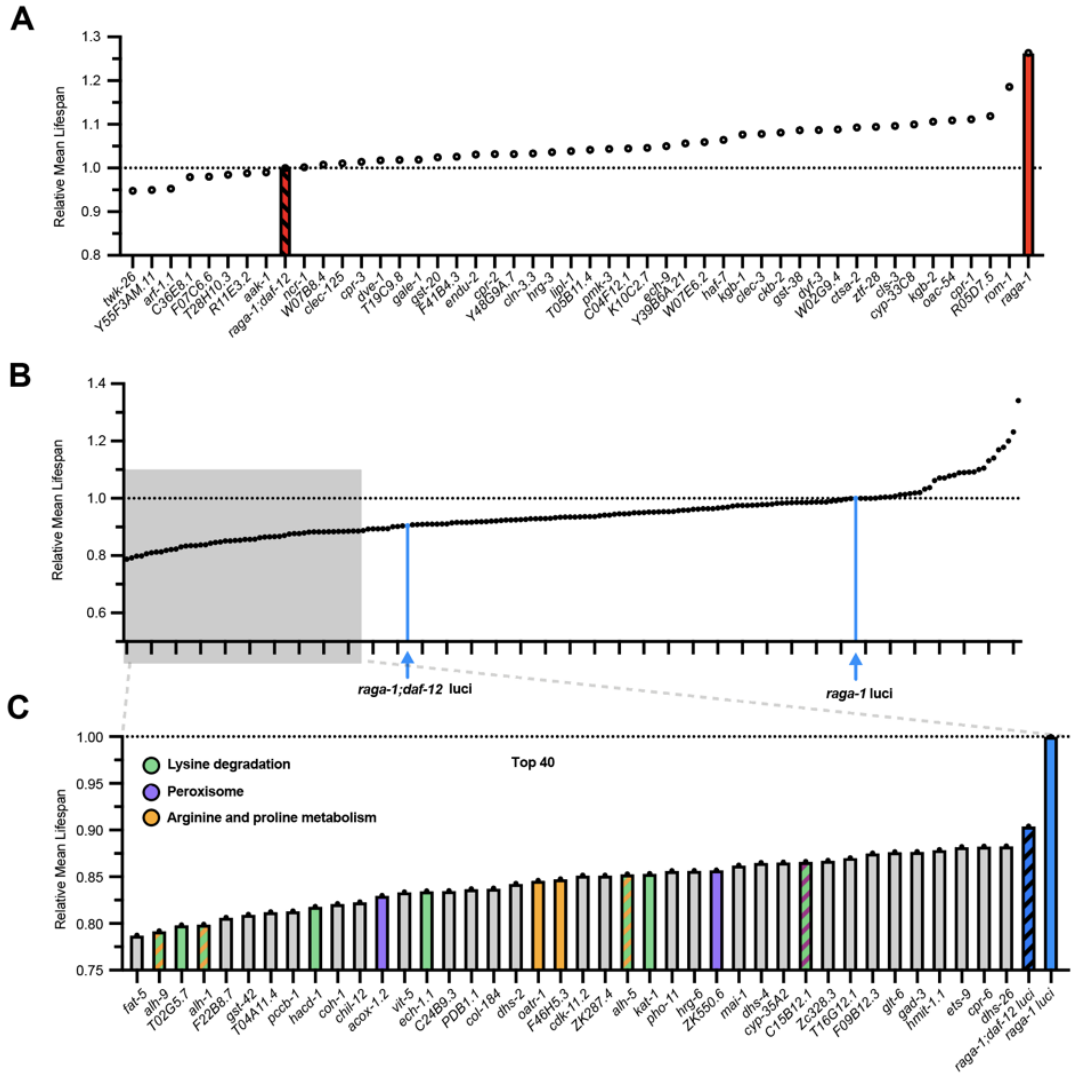

Figure V-11: Functional genomics screen results. (A) The results of the functional genomics screen of 46 candidates potentially rescuing *raga-1;daf-12* lifespan. (B) The results of the functional genomics screen with 180 candidates potentially abolishing *raga-1* longevity. (C) Zoom in on the 40 strongest RNAi effects on *raga-1* lifespan. The top 40 genes show enrichment in genes involved in lysine degradation, peroxisome function, and arginine and proline metabolism. (*raga-1* and *raga-1;daf-12* grown on luciferase RNAi were included as controls in every aging experiment, RNAi conditions inducing larveal arrests were not included, bars represent relative mean lifespan, 1 biological replicate, RNAi treatment egg on.)

raga-1 longevity, the top 3 genes being F38B6.4/GART, *sams-1*/MAT1;2A, and H41C03.1. The aim of this screen was to identify mediators that act in the steroid/mTOR signaling axis focusing on genes diminishing *raga-1* lifespan. Therefore, F38B6.4, *sams-1*, and H41C03.1 were not further pursued. Two genes, *C15B12.1* and *dhs-26*, were selected to be further tested for reproducibility. *C15B12.1* and *dhs-26* were able to significantly decrease *raga-1* lifespan without showing strong changes compared to *raga-1;daf-12*. Literature review and predicted biological functions of *C15B12.1* and *dhs-26* did not yet describe links to mTOR function and therefore offer scientific novelty to this project. *dhs-26* RNAi lifespan effects were significant and reproducible in contrast to results from *C15B12.1*; therefore, *dhs-26* was selected for further characterization (**Figure V-12 A**).

6. DHS-26 is required for mTOR mediated longevity

Literature research suggested that *dhs-26* might be a missing link in steroid signaling: (1) it is predicted to function as a dehydrogenase. (2) DHS-26 has a sequence identity of 41% with the human orthologue DHRS1, which is reported to be able to catalyze the *in vitro* reduction of steroids such as estrone, androstene-3,17-dione, and cortisone (Zemanova, Navratilova et al. 2019). To investigate *dhs-26* further, we obtained a complete knockout allele deleting all 6 exons, termed *dhs-26(syb8968)*, using CRISPR genome engineering (**Figure V-12 C**). Lifespan experiments validated that RNAi mediated knockdown of *dhs-26* and the *dhs-26* mutant similarly suppress *raga-1* lifespan (**Figure V-12 B**). We noticed that *raga-1;dhs-26* mutant lifespan was dependent on the purity of the cholesterol used to prepare agar plates. Of note,

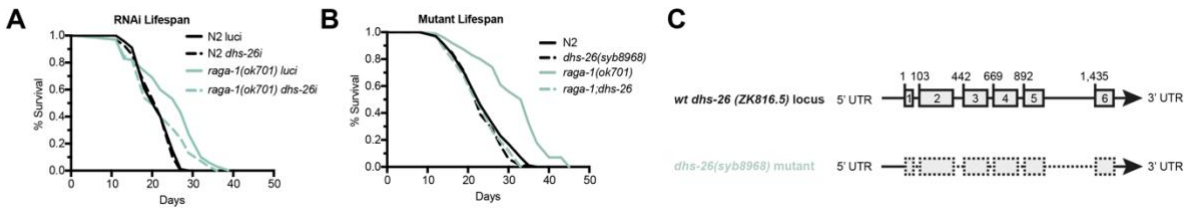

Figure V-12: *dhs-26* is required for *raga-1* longevity. (A) Lifespan analysis of *raga-1* worms on *dhs-26* and control (*luci*) RNAi. Egg on treatment of worms with *dhs-26* RNAi showed consistent decrease in *raga-1* lifespan without effects on N2 animals, making it the strongest hit of the functional genomic screen. (B) Lifespan analysis of *dhs-26(syb8968)* full knockout mutants shows complete abolishment of *raga-1* longevity (C) Scematic of *dhs-26(syb8968)* mutant design. (3 biological replicates, >100 worms per lifespan).

whereas I observed a partial reduction of *raga-1* longevity in *raga-1;dhs-26* animals when supplementing agar plates using 95% pure cholesterol (**Figure IX-3**), I observed a complete suppression of life span back to wt levels when *raga-1;dhs-26* mutants were supplemented with ≥99% pure cholesterol (**Figure V-12 B**). Presumably impurities of other steroid intermediates in the 95% pure cholesterol stock mask *raga-1;dhs-26* mutants' phenotypes. All experiments performed henceforth were executed using plates containing ≥99% pure cholesterol.

7. Dhs-26 is a novel DAF-12 target gene

To characterize DHS-26 expression *in vivo*, I designed an endogenously tagged *dhs-26::FLAG::mScarlet* reporter strain using CRISPR technology (referred to as DHS-26::Scarlet). Available single cell sequencing data suggests that *dhs-26* is expressed in the canal associated neurons, amphid sheath cells, cephalic socket cells, and NA sheath glia (Lorenzo, Onizuka et al. 2020). All these cells are neuron or glia-like cells involved in neuronal development and function. As suggested by the single cell sequencing data, *in vivo* expression of the generated DHS-26::Scarlet reporter was most pronounced in the excretory canal neurons (CAN) (**Figure V-13 A**, highlighted in red). Less pronounced reporter expression was found in the head, in the cephalic sheath cells and glial cells **(Figure IX-2**).

Since our transcriptomics data showed that *dhs-26* mRNA levels were increased in *raga-1* mutant animals, we asked if reporter expression was differentially regulated in the *raga-1* background. We focussed on the CAN since this cell gave the clearest, albeit low expression. Surprisingly, the DHS-26::Scarlet reporter expression levels were unchanged in the CAN (**Figure V-13 B and D**). It is possible that the low expression levels of DHS-26 did not allow us to capture small changes in reporter levels. Furthermore, we only assessed reporter expression in the CAN, not in glia or sheath cells; potentially DHS-26 levels in these other tissues would show regulation.

The effect of cholesterol purity on *raga-1;dhs-26* mutant lifespan suggests that DHS-26 might be regulated by cholesterol or derivates. We therefore quantified the DHS-26::Scarlet reporter expression under cholesterol deprivation. DHS-26 levels were significantly down-

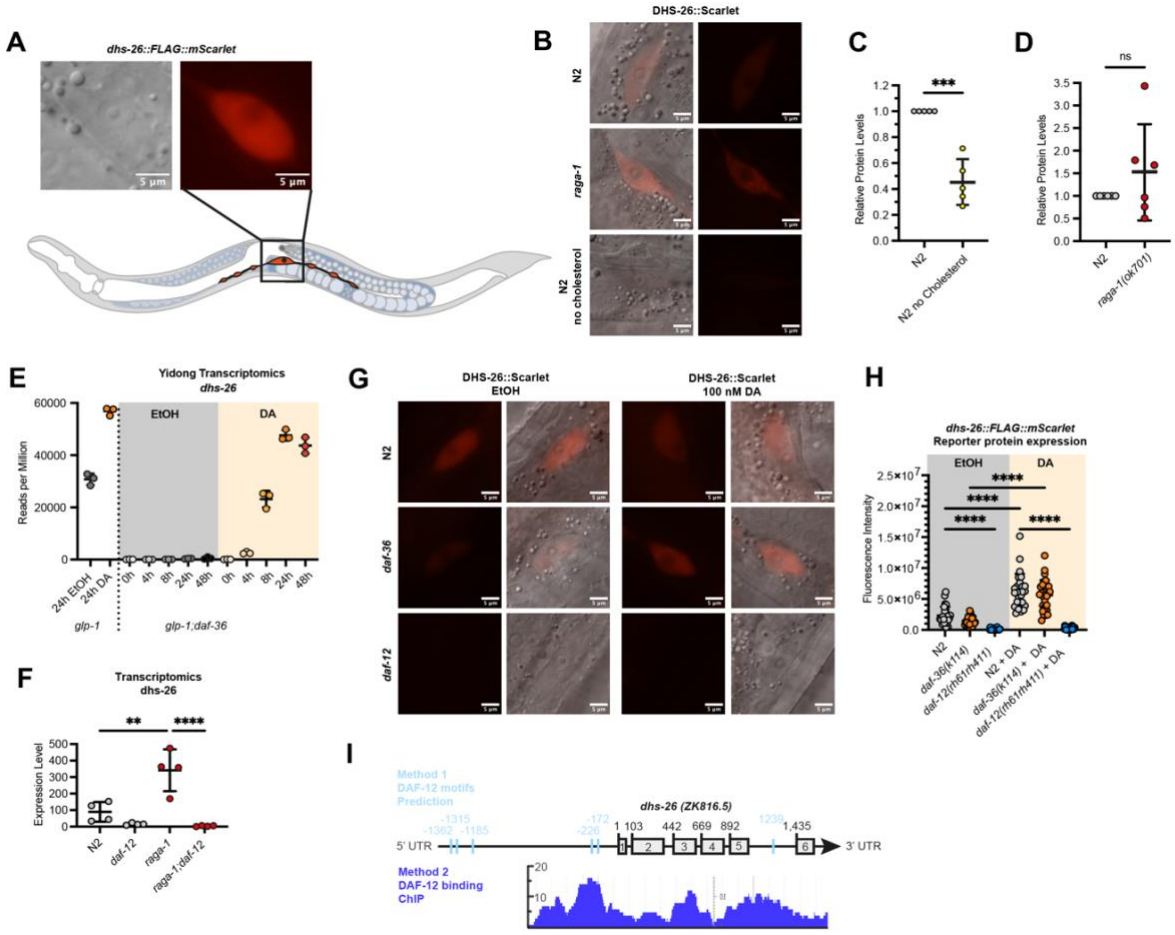

Figure V-13: *dhs-26* is a DAF-12 target gene, expressed in the CAN. (A) Microscopy imaging of the *dhs-26::FLAG::Scarlet* reporter reveals strongest expression in the canal associated neurons. The scematic image shows CAN localization (in red) in a day 1 animal. (B) Representative images of *dhs-26::FLAG::Scarlet* reporter expression in *raga-1* animals and upon cholesterol deprivation. (C-D) Quantification of fluorescence intensitie shows downregulation of *dhs-26::Scarlet* upon cholesterol deprvation and no change in *raga-1* background animals. (E) Yidong's Transcriptomics analysis shows a dramatic reduction of *dhs-26* mRNA in *daf-36* mutants and a time dependent rescue upon D7-dafachronic acid supplementation but not upon treatment with EtOH vehicle control. Additionally, basal *dhs-26* levels were elevated upon D7-dafachronic acid supplementation (3 biological replicates, treatment with D7-dafachronic acid day 1 on). (F) *dhs-26* mRNA levels in transcriptomics data shows decreased levels in *daf-12(rh61rh411)* mutants. (G) Representative images of *dhs-26::FLAG::Scarlet* in *daf-36(k114)* and *daf-12(rh61rh411)* mutants with and without 100 nM D7-dafachronic acid supplementation or treatment with EtOH vehicle control. Treatment egg on. (H) Quantification of fluorescence intensities of one representative replicate shows reduction of *dhs-26::Scarlet* expression in *daf-36* and *daf-12*, and rescue upon D7-dafachronic acid supplementation in *daf-36*, but not *daf-12* mutants (day 1 animals, scale bars represent 5 µm, fluorescence intensity was normalized to the background, graphs display mean ± SD of 3-6 biological replicates, statistical significance was calculated using (C-D) *t*- test, or (H) One-way ANOVA, ns $p>0.05$, *** $p<0.001$, **** $p<0.0001$). (I) Depiction of the genomic *dhs-26* locus with exons represented by numbered boxes. Predicted DAF-12 binding motifs are highlighted in light blue. Potential binding sites suggested by DAF-12 ChIP read counts are highlighted in dark blue.

regulated upon a lack of cholesterol (**Figure V-13 B-C**). Since cholesterol is the precursor of DAs, we wondered if DHS-26 levels could be directly regulated by DAs. Indeed, existent transcriptomics data from our laboratory showed significant Δ7-DA-dependent regulation of *dhs-26* mRNA levels (**Figure V-13 E**). In detail, *daf-36* mutants deficient in dafachronic acid

biosynthesis were supplemented with Δ7-DA or the vehicle control EtOH over a time course of 48 hours (Yidong Shen, unpublished). These experiments were carried out in the germline-less *glp-1(e2141)* mutant background, allowing the observation of somatic changes without confounding effects of germ cells and embryos. *dhs-26* mRNA was completely absent in *daf-36* mutants treated with EtOH, and mRNA levels were rescued by Δ7-DA supplementation.

To understand if *dhs-26* mRNA is directly regulated by DA or by DA ligand binding to DAF-12, we inspected *dhs-26* expression in our transcriptomics data. *wt* animals showed low *dhs-26* expression with an average read count of 89 per million (**Figure V-13 F**). This expression was further reduced below 16 reads/million in *daf-12* mutants. This supports our hypothesis that a functional steroid signaling - Δ7-DA ligand as well as DAF-12 nuclear hormone receptor activity - is required for *dhs-26* expression.

To validate these findings, I analyzed DHS-26::Scarlet reporter levels in animals deficient in dafachronic acid synthesis (*daf-36(k114)*) or in DAF-12 null mutants (*daf-12(rh61rh411)*) with and without additional dafachronic acid supplementation (**Figure V-13 G-H**). Egg on supplementation of 100 nM D7-dafachronic acid was sufficient to increase DHS-26::Scarlet levels in *wt* background animals. As Yidong's RNA sequencing suggested, *daf-36* and *daf-12* mutants showed decreased levels of DHS-26 expression which could be rescued by Δ7-DA supplementation in *daf-36* mutants, but not in DAF-12 receptor mutants, supporting our hypothesis that *dhs-26* is a DA/DAF-12 regulated gene.

DA/DAF-12 regulation of *dhs-26* could be direct or indirect. If *dhs-26* is indeed a direct DAF-12 target gene we would expect the genomic *dhs-26* region to harbour DAF-12 binding motifs. DAF-12 binding was assessed via two independent methods: (1) via a bioinformatic prediction of DAF-12 motifs (see **Figure VIII-1**) on the *dhs-26* locus and (2) via assessing the binding of DAF-12 reported in publicly available DAF-12 ChIP sequencing data from Wormbase (**Figure V-13 I**). The bioinformatic approach predicted six potential binding sites of DAF-12 in proximity of the *dhs-26* genomic sequence. Three of these predicted binding sites are localized further than 1000 bp upstream of the *dhs-26* start codon. Generally, DAF-12 binds its targets most frequently within 500 bp upstream of the start codon (Hochbaum, Zhang et al. 2011), making two of the predicted binding sites localized 226 bp and 172 bp upstream the

most likely. Furthermore, one predicted binding site is localized between exons 5 and 6. These three binding loci (-226, -172, +1239) show a trend, but no significant binding peak in the DAF-12 ChIP sequencing data. It is possible that the insignificant DAF-12 binding is due to too low *dhs-26* expression. To validate if the observed binding sites are utilized by DAF-12 to regulate *dhs-26* expression, it would be required to repeat the ChIP sequencing. Doing so together with supplementing DA could potentially increase *dhs-26* expression.

As described above, *raga-1* mutants displayed strongly elevated D7-dafachronic acid levels measured by mass spectrometry (**Figure V-4**). DAF-12 is a dafachronic acid receptor that activates upon ligand binding and drives the expression of its target genes such as possibly *dhs-26*. The significantly elevated *dhs-26* mRNA levels in *raga-1*, but no change of DHS-26 protein in *raga-1* is possibly due to the analysis of a suboptimal cell type, suggest that DAF-12 activity is increased in *raga-1* mutants. This leads us to hypothesize that elevated DAF-12 activity and resulting target gene expression are required to induce the lifespan benefits observed by decreased mTOR activity. Validation experiments to determine whether *dhs-26* is actually a DAF-12 target gene will be addressed in the future.

8. DHS-26 is a missing link in the steroid signaling pathway

Our findings highlight the importance of *dhs-26* in mediating mTOR dependent longevity. Additionally, our data suggests that *dhs-26* is a target gene of ligand bound DAF-12. The strong sequence homology to the mammalian DHRS1 suggests a potential role of DHS-26 as a missing link in the dafachronic acid biosynthesis.

To investigate dafachronic acid biosynthesis in *dhs-26* mutants, we directly measured steroid levels via mass spectrometry. We observed that *dhs-26* mutants displayed a significant reduction of Δ7-DA levels compared to *wt* (**Figure V-14**). However, cholesterol and lathosterol levels remained unchanged. This evidence supports the role of DHS-26 as a novel missing link of the steroid signaling pathway or as a factor that can indirectly impact levels of DA. However, the precise mechanism remains unknown. As a player in steroid biosynthesis, the tight regulation of *dhs-26* expression by DAF-12 could allow for a positive or negative

feedback loop to quickly react to environmental or signaling cues by regulating dafachronic acid biosynthesis.

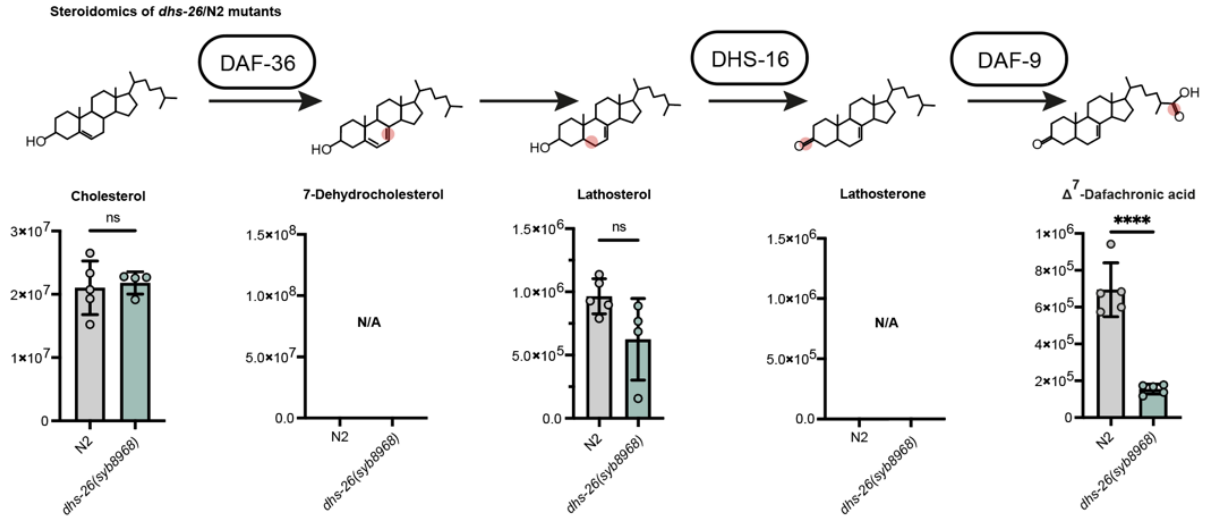

Figure V-14: DHS-26 is required for Δ7-DA biosynthesis. Depiction of the simplified D7-dafachronic acid synthesis pathway. Steroidomic measurements show a significant reduction of D7-dafachronic acid levels in *dhs-26(syb8968)* knockout mutants compared to N2, but no changes in cholesterol or lathosterol levels (5 biological replicates, statistical significance was calculated using *t*-test, ns p>0.05, **** p<0.0001).

The reduction of Δ7-DA levels in *dhs-26(syb8968)* mutants suggests that animals require dafachronic acid to benefit from mTOR mediated lifespan benefits. We hypothesized that re-supplementing Δ7-DA to DA deficient, short lived *raga-1;dhs-26* animals might rescue their lifespan. To test this, I supplemented 0.5 µM Δ7-DA and EtOH vehicle control egg on and measured lifespan. Indeed, supplementation of Δ7-DA did not increase *raga-1* longevity, but significantly prolonged *raga-1;dhs-26* lifespan compared to EtOH control (**Figure V-15**). This demonstrates that the observed lifespan effects of *raga-1;dhs-26* mutants act through the Δ7-DA pathway, supporting the role of DHS-26 in steroid signaling.

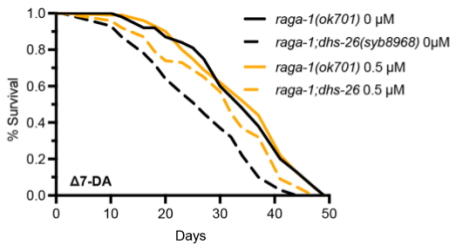

Figure V-15: Dafachronic acid supplementation rescues *raga-1;dhs-26* lifespan. Lifespan analysis of the *dhs-26(syb8968)* mutant in the *raga-1(ok701)* mutant background. Supplementing Δ7-dafachronic acid rescues *raga-1;dhs-26* mutant lifespan. 0.5 µM Δ7-DA supplementation compared to EtOH vehicle control (>100 worms per lifespan, supplementation treatment egg on, 1 biological replicate, Mantel-Cox Log rank test).

Reduced Δ7-DA levels in *dhs-26* mutants suggest that it could affect dauer formation. In *C. elegans* dauer diapause formation is tightly linked with dafachronic acid levels. The Daf-c phenotype is induced by reduced DA levels and is characteristic for loss of function mutants of genes involved in DA synthesis. Further, dauer can be induced by starvation, and increased growth temperatures up to 27°C, and via genetic means by mutating dauer pathways genes. DAF-12 functions as a molecular switch regulating the developmental decision between dauer diapause (ligand-free DAF-12) and the development to reproductive adults (ligand-bound DAF-12). Dafachronic acid synthesis is regulated by upstream pathways to be able to assess environmental cues, based on which the animal makes developmental decisions (Fielenbach and Antebi 2008). Upon favorable environmental conditions GPCRs in amphid neurons get activated, leading to the secretion of insulin and TGF-β/DAF-7. Insulin binds to the insulin receptor/DAF-2, and TGF-β/DAF-7 to the TGF-β receptor/DAF-1,4 which activate downstream signaling cascades resulting in the regulation of *daf-9* expression and therefore dafachronic acid biosynthesis to promote continuous development. Downregulation of these pathways leads to dauer diapause (see **Figure III-6**).

Counterintuitively, *dhs-26* mutant animals that have reduced Δ7-DA levels did not show increased levels of dauer formation (**Figure V-16 A**). On the contrary, *dhs-26* animals displayed significantly reduced dauer formation compared to *wt* when inducing dauer by growing animals at 27°C. To investigate which arms of the known upstream dauer pathways are required for the reduced *dhs-26* mutant's dauer levels, double mutants with insulin/IGF-1 and TBF-β signaling mutants, *daf-2(e1368)* and *daf-7(e1372)* respectively, were created. To investigate the role of steroid signaling in the *dhs-26* dauer phenotype, *dhs-26;daf-36(k114)* double mutants were tested for their dauer formation. As expected, *daf-36(k114), daf-2(e1368),* as well as *daf-7(e1372)* mutants displayed dauer formation with increased temperatures (**Figure V-16 A-C**). However, none of the tested pathways' dauer formation was altered either up or down upon additional mutation of *dhs-26*, indicating that *dhs-26* might function downstream of these pathways or in a yet unknown way to regulate dauer diapause. How *dhs-26* regulates dauer development and why the common rules for dauer formation do not apply for *dhs-26* mutants remains elusive. We speculate that *dhs-26* mutants might

regulate the formation of a DA isoform that can rescue dauer diapause formation, but not lifespan.

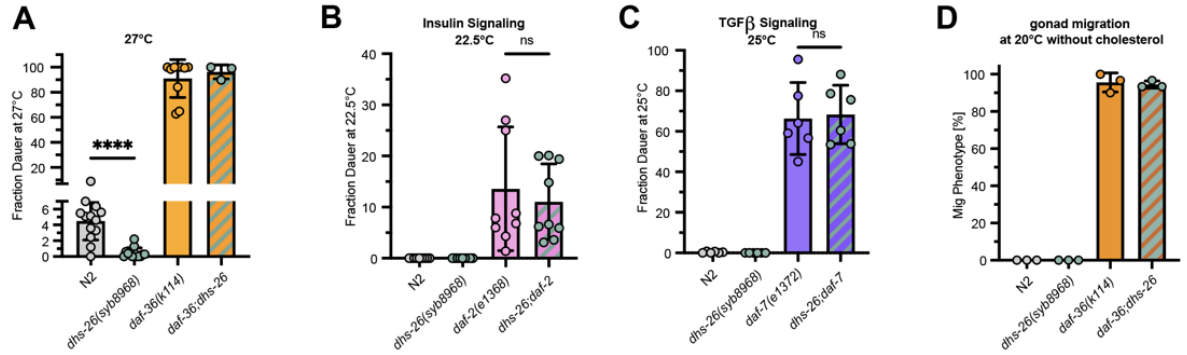

Figure V-16: Dauer formation is regulated by *dhs-26*, but how remains unclear. (A) Dauer assay shows decreased dauer formation of *dhs-26(syb8968)* induced by egg on growth at 27°C for 48h. *daf-36(k114)* mutants show strong dauer formation, which is unchanged in *daf-36;dhs-26* mutants. (B) Dauer assessment of mutants of the insulin receptor *daf-2(e1368)* showed dauer induction at 22.5 °C, which was unchanged in *daf-2;dhs-26* animals. (C) Dauer assessment of mutants of the TGFβ pathway *daf-7(e1372)* showed dauer induction at 25 °C, which was unchanged in *daf-7;dhs-26* mutants. (D) Distal tip cell migration defects were induced by egg on cholesterol deprivation. *daf-36(k114)* mutants show strong migration defects, which were unchanged in *daf-36;dhs-26* double mutants. (3-13 biological replicates, bars represent mean ± SD, statistical significance was calculated using One-way ANOVA, ns $p>0.05$, **** $p<0.0001$)

An alternative signature of changes in steroid signaling and DA production is the penetrance of gonadal migration defects (Mig), caused by the gonadal distal tip cell's continued migration along the ventral body wall (Gerisch, Weitzel et al. 2001). Upon cholesterol deprivation, dafachronic acid biosynthesis deficient *daf-36* mutants typically fail the scheduled turn of the gonad during mid L3 development and therefore display strong defects (**Figure V-16 D**). We observed the expected Mig phenotype penetrance in *daf-36* mutants, but not *dhs-26* single mutants despite the decrease in Δ7-DA levels. *dhs-26* mutants showed similar Mig phenotype to N2 indicating that *dhs-26* is not involved in distal tip cell migration.

My results suggest a novel role of DHS-26 as a positive regulator of Δ7-DA levels. The question if *dhs-26* has a role is as a direct biosynthetic enzyme or rather an indirect regulator of steroid signaling remains open. For the first time we were able to uncouple low Δ7-DA levels from dauer and distal tip migration defects; *dhs-26* mutants did not display the expected phenotypes, suggesting yet unknown means of regulation of these pathways.

9. DHS-26 acts via downstream pathways to regulate mTOR mediated longevity

My work strongly suggests an important yet unknown role of DHS-26 in the context of steroid signaling as well as mTOR dependent longevity. It remains elusive how DHS-26 mediates mTOR longevity. To further characterize the role of DHS-26 in general biological processes, and also in the context of aging, we aimed to understand the underlying downstream pathways that are regulated by DHS-26. To do so, single worm proteomics data was generated (**Figure V-17**). PCA revealed a high sample quality and reproducibility within the measured genotypes reflected by closely clustered biological replicates. Additionally, there was a strong separation of *raga-1* backgrounds from N2, *dhs-26* and *daf-12*. The number of detected proteins ranged between 5999 and 6219 indicating a good range of comparability between the samples.

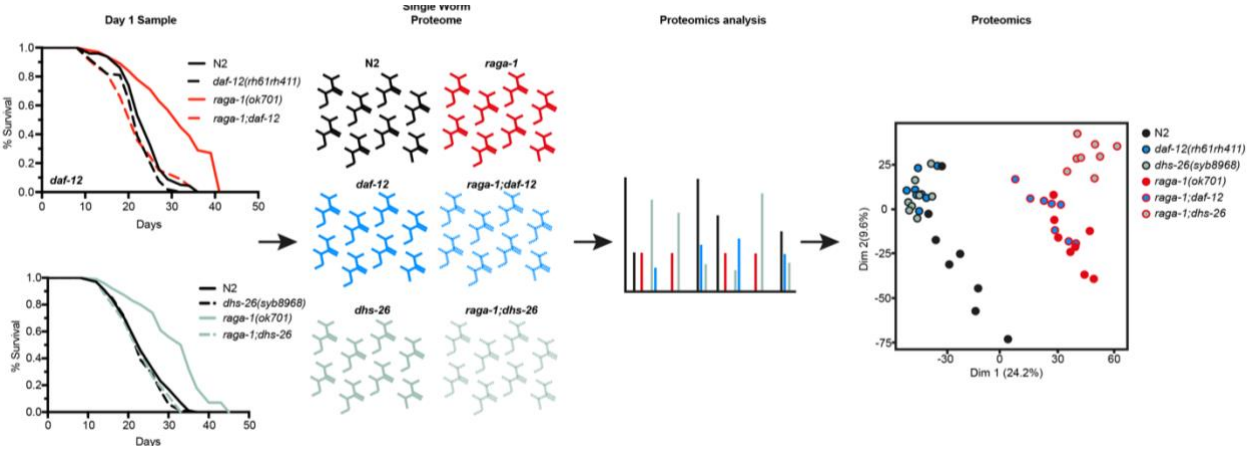

Figure V-17: Proteomics analysis reveal a strong cluster separation of *wt* and *raga-1* background samples. Schematic overview of proteomics sample set preparation. PCA plot analysis shows a strong clustering of the biological replicates within one genotype. Samples also clustered strongly according to their genetic background, N2 or *raga-1(ok701)*.

To get a detailed understanding of DHS-26 function, we first compared *dhs-26* single mutants with wt animals. Volcano plot analysis displayed strong proteomic changes of 515 proteins up-regulated proteins as well as 745 down-regulated proteins in *dhs-26* mutants compared to wt animals (**Figure V-18 A**). KEGG pathway enrichments of differentially regulated proteins (**Figure V-18 B-C**) revealed a strong up-regulation of proteins involved in oxidative phosphorylation, proteasome function, and multiple aspects of nucleic acid homeostasis (including DNA replication and repair mechanisms, splicing, and degradation). Proteins that

were down regulated in *dhs-26* mutants were enriched in metabolic pathways, amino acid biosynthesis and energy homeostasis (TCA cycle and Glycolysis/Gluconeogenesis).

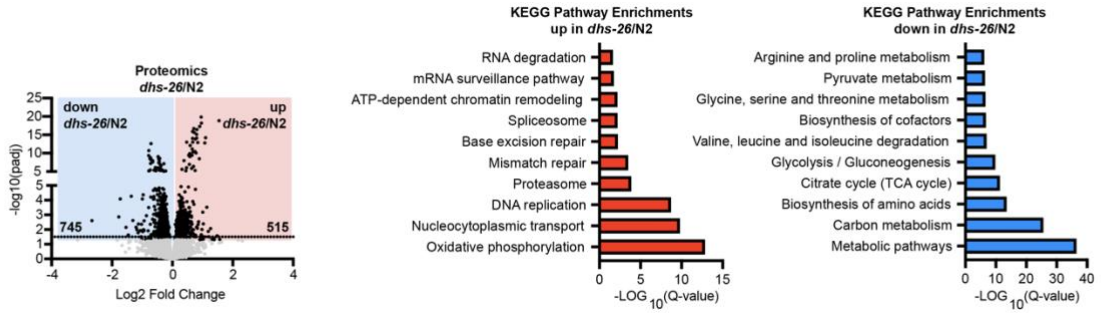

Figure V-18: DHS-26 regulates various downstream pathways. (A) Volcano plot analysis of the proteomics data shows a strong differential regulation of protein expression by *dhs-26*. (B) KEGG pathways enrichment of positively regulated proteins reveals oxidative phosphorylation, and pathways connected to DNA and RNA mainenace and function. (C) Negatively regulated proteins in *dhs-26(syb8968)* mutants were enriched in metabolic pathway proteins, carbon metabolism, amino acid biosynthesis and TCA cycle proteins.

The KEGG pathway enrichments indicate a variety of DHS-26 functions. Since we observed a strong regulation of *dhs-26* expression through components of the steroid signaling pathway it is likely that observed KEGG enrichments display known pathways regulated by steroid signaling. However, we might also uncover novel pathways in which steroid hormone signaling acts on a molecular level. This underlines the importance of a fine tuned balance of steroid hormones to maintain a huge diversity of biological functions.

Next, we utilized the single worm proteomics data set (**Figure V-17**) to narrow down the role of DHS-26 in the context of aging. To do so, we inversely correlated the protein expression between the short-lived *raga-1;dhs-26* and the long-lived *raga-1* animals to identify genes that might be required or detrimental in longevity but are oppositely regulated in the short-lived *raga-1;dhs-26* mutants (**Figure V-19**). The volcano plot comparing protein expression between *raga-1;dhs-26* and *raga-1* displayed 1093 up- and 515 down-regulated proteins, respectively. 254 proteins were negatively regulated in *raga-1;dhs-26/raga-1* and additionally positively regulated in *raga-1*/N2. Within these 254 proteins, the strongest KEGG pathway enrichments included proteins related to metabolic pathways, oxidative phosphorylation, lysosome, and phagosome formation. Additional pathway analysis of GO biological processes revealed proteins connected with proteolysis, lipid transport, and ascaroside biosynthesis to be enriched (**Figure V-19**). KEGG pathway enrichment analysis of the proteins up-regulated in

raga-1;dhs-26/raga-1 and additionally down-regulated in *raga-1*/N2 revealed 205 proteins involved in ribosomal biogenesis, cysteine and methionine metabolism, cofactor biosynthesis, and RNA degradation (Figure V-19 C). The functional characterization of DHS-26 in the context of aging opened many so far unknown angles in which steroid biosynthesis might induce organismal health benefits and how it might regulate cellular organization.

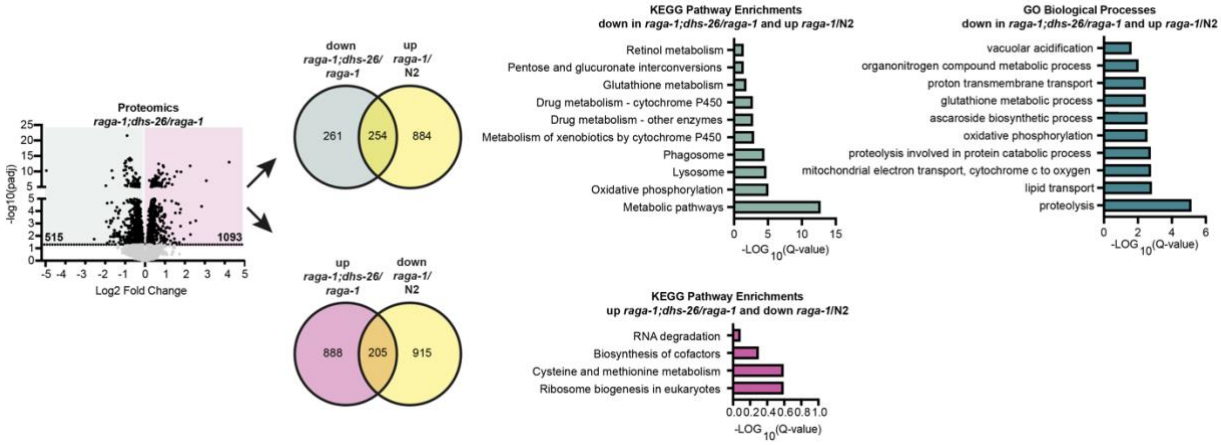

Figure V-19: The role of DHS-26 in the context of aging. (A) Volcano plot of differentially regulated proteins in proteomics comparing *raga-1;dhs-26/raga-1* reveals strong changes. (B) Top 10 KEGG pathway and GO enrichments of proteins down in *raga-1;dhs-26/raga-1* and additionally up in *raga-1*/N2. (C) KEGG pathway enrichment of proteins up in *raga-1;dhs-26/raga-1* and additionally down in *raga-1*/N2. Hypergeometric test (average of 6154 detected proteins) reveals p<0.0001 comparing proteins down in *raga-1;dhs-26/raga-1* with up in *raga-1*/wt (green), and p=0.313 for proteins up in *raga-1;dh-26/raga-1* and down in *raga-1/*wt (purple).

We next investigated how much of DHS-26 function in aging overlaps with DAF-12. Identifying unique DHS-26 regulated pathways would allow us to unravel novel pathways influenced by steroid signaling to maintain organismal health in aging. A comparison of *raga-1;daf-12* with *raga-1* showed only mild proteome changes, with 104 proteins up-regulated and 112 proteins down-regulated. Overall, *raga-1;daf-12/raga-1* showed fewer significantly regulated proteins than seen in *raga-1;dhs-26/raga-1* (**Figure V-19** and **Figure V-20 A**).

raga-1;daf-12 and *raga-1;dhs-26* mutants showed an overlap of positively and negatively regulated proteins (**Figure V-20 B** and **C**). 20 proteins up-regulated in the long-lived *raga-1* mutant were inversely regulated in short-lived *raga-1;daf-12* and *raga-1;dhs-26* mutants. Conceivably, these proteins play an important role in mediating the benefits of decreased mTOR signaling in the context of aging. These 20 proteins are involved in peroxisome formation, lysosome metabolism, lipid transport, and other functions.

DHS-26 also showed unique protein down-regulation in the context of aging. Mainly proteins involved in metabolic pathways as well as oxidative phosphorylation were uniquely regulated by DHS-26, and not by DAF-12. Interestingly, DHS-26 and DAF-12 down-regulated a shared set of lysosomal proteins, while DHS-26 alone additionally regulated a specific set of lysosomal proteins.

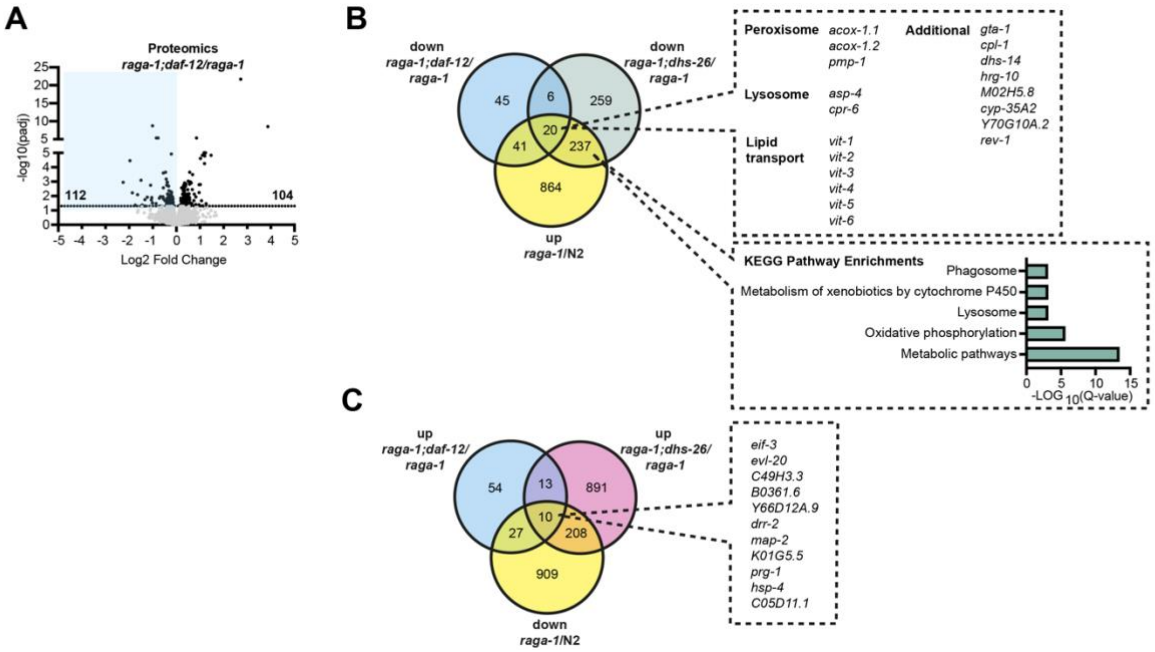

Figure V-20: DHS-26 regulates unique pathways and pathways shared with DAF-12. (A) Volcano plot of proteins differentially regulated in proteomics data reveals changes between *raga-1;daf-12* and *raga-1*. (B) Venn diagram overlapping proteins negatively regulated in *raga-1;daf-12* and *raga-1;dhs-26* compared to *raga-1*, as well as positively regulated comparing *raga-1*/N2, reveals 20 proteins. These proteins are involved in peroxisomal and lysosomal function, lipid transport, and other pathways. Genes that were not regulated in *raga-1;daf-12*, but showed negative regulation in *raga-1;dhs-26/raga-1* are enriched in proteins connected to metabolic processes, oxidative phosphorylation, lysosome and phagosome function, and metabolism of xenobiotics. Hypergeometric test (average of 6154 detected proteins) reveals p<0.0001 comparing proteins between all three conditions. (C) Venn diagram overlapping proteins positively regulated in *raga-1;daf-12* and *raga-1;dhs-26* compared to *raga-1*, as well as negatively regulated comparing *raga-1*/N2, reveals 10 proteins. These proteins do not cluster regarding their physiological function. Genes that were not regulated in *raga-1;daf-12*, but showed positive regulation in *raga-1;dhs-26/raga-1* did not show significant KEGG patwhay enrichments.

10 proteins down-regulated in the long-lived *raga-1* mutant were reversed in *raga-1;daf-12* and *raga-1;dhs-26* (**Figure V-20 C**). These genes did not show enrichment of particularly pathways. These include proteins involved in ER trafficking and proteins involved in proteasome activity. Also in this data set *dhs-26* mutants showed unique up-regulation of 208 protein in the context of aging. KEGG pathway enrichment of these genes did not reveal any significant pathway enrichments.

My data reveals a tight connection of regulated pathways downstream of *dhs-26* as well as the established steroid pathway gene *daf-12*, supporting our hypothesis of *dhs-26* as a missing link in steroid signaling. Notably, loss of *dhs-26* showed more regulated targets than *daf-12*. This could be explained by loss of *dhs-26* only affecting the positive regulatory arm of DAF-12 signaling. By contrast, loss of DAF-12 function completely abolished DAF-12 expression of target genes included in the positive as well as negative regulatory arm.

10. Summary

Although the mTOR as well as the steroid signaling pathways are both well studied, it is poorly understood how they might interact with each other and function in a singular pathway. In this work, I found that there is a unified regulatory mechanism connecting mTOR and steroid signaling through DA production, which can modulate lifespan in *C. elegans*.

The described data suggest that the mTOR pathway is not regulated by genes of the steroid signaling pathway. However, *raga-1* appears to regulate the synthesis of DAs and the activity of DAF-12. Indeed, the generated metabolomics data show that mTOR-deficient mutants display strongly increased Δ7-DA levels, though the mechanism behind this observation remains unclear. Consistently, longevity of *raga-1;daf-9* mutants can be rescued by Δ7-DA supplementation, showing that the availability of Δ7-DA is required for mTOR mediated longevity. The influence of mTOR activity on DA synthesis seems in turn to up-regulate DAF-12 activity reflected by elevated mRNA levels of its newly characterized target gene DHS-26.

From a functional genomics screen, I identified *dhs-26* to suppress mTOR-dependent longevity. Further characterization of *dhs-26* reveals its expression to be almost exclusively in CAN cells, as well as strongly regulated by the availability of Δ7-DA and activity of DAF-12. My work suggests DHS-26 as a novel regulator of dafachronic acid levels, showing decreased Δ7-DA levels upon DHS-26 loss. The role of DHS-26 in canonical steroid signaling is further solidified by rescue of *raga-1;dhs-26* lifespan by Δ7-DA supplementation. Proteomics analyses suggest that DHS-26 regulates mTOR mediated lifespan by regulating downstream pathways such as ribosomal biogenesis, mitochondrial function, lysosome and peroxisome maintenance, and ascaroside biosynthesis.

Collectively, our findings support a regulatory cascade connecting mTOR and steroid signaling which is crucial for lifespan in *C. elegans*. These findings help us understand the underlying biological mechanism of the interaction between mTOR and steroid signaling and downstream factors that are required to maintain *raga-1* lifespan extension in a DAF-12-dependent manner. My work gives novel insight into the understudied dehydrogenase DHS-26 and its downstream pathways in the context of aging. Understanding the nature of the mTOR/signaling axis can help us understand aging and age-related diseases on a molecular level.

VI. Discussion

Nutrient sensing and downstream pathways adapting metabolism play an important role in aging. In the past two decades the role of the mTOR pathway as a core driver of longevity has been established. However, recent work has shown that the mTOR pathway might act in a cell non-autonomous manner, revealing a new angle of mTOR signaling.

Here I present insight into a yet unknown, hormonal mechanism that might be involved in lifespan benefits resulting from a decrease in mTOR activity. I show that mTOR mediated longevity requires functional dafachronic acid biosynthesis and that mTOR is a regulator of dafachronic acid levels. Interestingly, I only observed minor and inconsistent changes in the mRNA and protein levels of steroid biosynthetic genes upon mTOR inhibition. Changes observed in the transcriptome of long-lived *raga-1* mutants were reversed upon *daf-12* mutation, such as genes involved in lysosomal function, peroxisome homeostasis, lysine degradation and arginine and proline metabolism. A similar reversing effect of metabolites was displayed for adenosine and uridine.

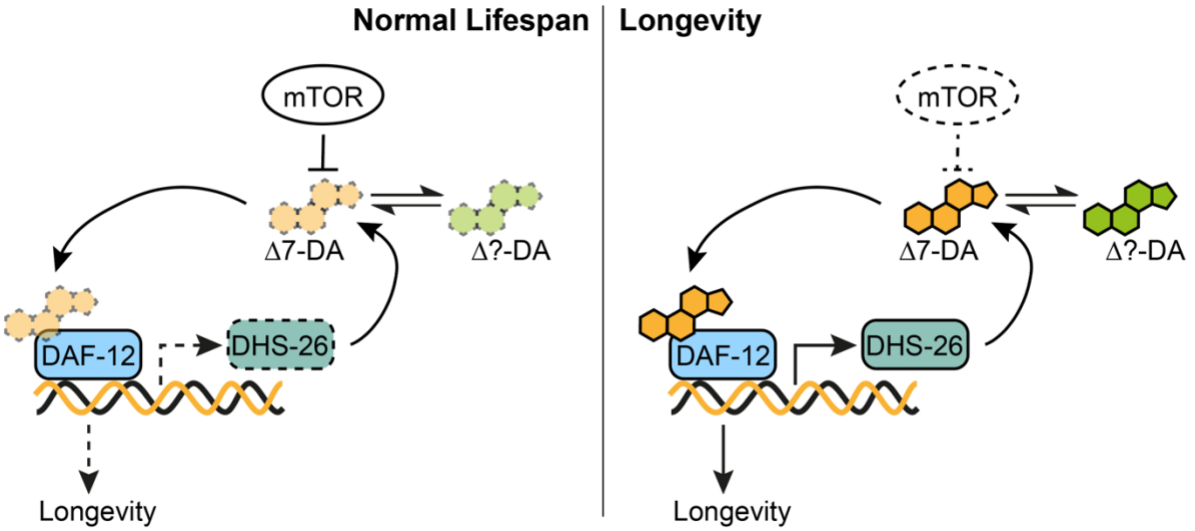

Figure VI-1: Working model of mTOR working through DAF-12/steroid signaling to induce longevity. My results suggest a model in which mTOR negatively regulates the Δ7-dafachronic acid (DA) pool. Upon Δ7-DA binding to the nuclear hormone receptor DAF-12, DAF-12 drives the expression of the dehydrogenase DHS-26. DHS-26 in turn is required to increase Δ7-DA levels. DAs exist in several variants. The right balance between different DAs might be required for mTOR dependent lifespan extension. Under *wt* conditions, the mTOR pathway inhibits Δ7-DA production and thereby downstream pathways.

Through an RNAi knockdown screen, I identified the dehydrogenase DHS-26 to be essential for longevity induced by a decrease in mTOR activity. Further characterization showed DHS-26 to be a potential DAF-12 target that might act as a missing link in dafachronic acid biosynthesis. Null mutants of *dhs-26* display a dramatic decline of Δ7-DA levels and preliminary data suggests that *raga-1;dhs-26* lifespan is rescued by supplementation of Δ7-DA. Due to DHS-26 expression predominantly in neurons, we suspect a neuronal mechanism in which mTOR might act.

1. mTOR longevity acts through a cell non-autonomous steroid signaling pathway

Downregulation of mTOR signaling is a consistent driver of longevity. This has been reported in organisms such as *C. elegans*, *Drosophila*, and mice (Saxton and Sabatini 2017). This downregulation can be achieved via genetic alterations, but also pharmacological approaches have been shown to induce similar effects. Recently, additional evidence showed that the downregulation of mTOR pathway activity is not required throughout the whole organism, but that decrease in neurons is sufficient to result in lifespan benefits (Smith, Lanjuin et al. 2023). **This suggests that the beneficial effects of decreased mTOR may be signaled through the body via a cell non-autonomous, potentially endocrine hormonal signaling mechanism.**

Indeed, we find our hypothesis supported by our results showing the complete abolishment of longevity mediated by mTOR inhibition by loss of various steroid biosynthetic genes. DAF-12 and the DA biosynthesis enzymes DAF-36 and DAF-9 were required to allow *raga-1* induced longevity, and mutations in these genes reduced lifespan to the level of *wt* animals. We could show the same epistatic effects when treating *daf-12* mutants with *let-363* RNAi, suggesting that this is not a *raga-1* specific phenotype, but rather an mTOR wide mechanism. The lifespan of the biosynthetic gene mutants was rescued by supplementation of Δ7-DA indicating the canonical steroid pathway to play a role in mTOR longevity. These findings go in line with work conducted in germline less *glp-1* mutants. *glp-1* mutants' longevity was shown to be dependent on the steroid genes *daf-36, daf-9*, and *daf-12* and lifespan of *glp-1;daf-36*, and *glp-1;daf-9* animals could be rescued by supplementation of DA, more precisely the variant Δ4-DA (Gerisch, Rottiers et al. 2007). That steroid signaling is required not only in longevity induced by decreased mTOR, but also germline mediated longevity, suggests a role of steroid

signaling as a potential convergent mechanism of longevity. Further longevity models that seem to converge on steroid signaling will be discussed in more detail below.

It becomes apparent that not only the levels of the stabile and well characterized DA variant Δ7-DA is important to mediate *raga-1* longevity, but that also other DA variants are required, as mutation in the DA interchanger DAF-40 also abolished *raga-1* longevity. Previous work characterized the physiological effects of DA variants such as Δ1,7-DA, Δ4,7-DA, and Δ1,4,7-DA (Wollam 2011). *daf-40* null and *daf-40;daf-9* double mutants were less responsive to dauer rescue by Δ1,7-DA and Δ4,7-DA compared to *daf-9* mutants with the exception of rescue by 1,4,7-DA (Wollam 2011), suggesting a possibility in which DAF-40 produces Δ1,4,7-DA. Notably, dauer rescue by Δ1,4,7-DA required much lower concentration than Δ7-DA, supporting the hypothesis of high affinity ligands regulating dauer and possibly lifespan. The effect of *daf-40* on established longevity pathways is understudied; however, preliminary data suggests that *daf-40* is partially required for gonadal longevity as *daf-40* mutants did not benefit from lifespan extension after the ablation of germline precursor cells by laser microsurgery (Wollam 2011). Wollam's work reports *daf-40* mutants to have significantly reduced levels of Δ7-DA potentially being the cause for loss of *glp-1* longevity. Whether supplementation of Δ7-DA to short-lived *glp-1;daf-40* mutants is able to rescue longevity remains unknown.

There have been reports on the biological effects of different DA variants (Sharma, Wang et al. 2009), but there are still open questions on the biological processes that are specifically regulated by DA variants. It is known that ligand binding of different DAs to the NHR DAF-12 can induce various responses (Galilea, Santillan et al. 2024). My work focuses on the role of Δ7-DA as it is a stable DA variant that can be synthetically synthesized and can be detected via mass spectrometry. Considering the effects of *daf-40* mutants on *glp-1* and *raga-1* mutants' lifespan, it would be insightful to further explore the role of other DA variants in the context of aging. Assessing the crystal structures of ligand bound DAF-12 displayed diverse conformational changes in response to DA variants as well as synthetic ligands (Mancino, Ceccarelli et al. 2021, Galilea, Santillan et al. 2024). A set of different conformational changes could result in selective target gene expression and therefore activation of specific downstream programs required for healthy *C. elegans* aging. The physiological relevance for

transcription factors to affect distinct groups of target genes dependent on their ligand binding state is exemplified in the steroid receptor mineralocorticoid receptor (MR) (Fuller, Yao et al. 2012) and the estrogen receptor β (ERβ) (Vivar, Zhao et al. 2010). It was shown that MR can respond to two physiological ligands, aldosterone and cortisol which can each act as primary targets dependent on the targeted tissue. (Fuller, Yao et al. 2012). ERβ can regulate three distinct classes of target genes that were enriched dependent on ERβ being un-ligated or estradiol bound. The third set of genes were ligand-state independently enriched in the presence of ERβ.

While an increase in DAs and a functional DAF-12 receptor was required for longevity mediated by reduced mTOR activity, loss of the DAF-12 negative regulator DIN-1 did not affect longevity mediated by reduced mTOR activity. DIN-1 is a target of alternative splicing, resulting in the formation of different isoforms. Only the short isoform DIN-1S is a DAF-12 binding partner and *din-1* was shown to be required for *daf-9* longevity at 15°C (Ludewig, Kober-Eisermann et al. 2004). This goes in line with my work in which *din-1* mutants displayed normal lifespan compared to wt at 20°C. It would be interesting to investigate if the over expression of DIN-1S could influence mTOR induced longevity. Increase in DIN-1 levels might promote the DIN-1S bound state of DAF-12, driving the negative regulatory arm. I hypothesize that this could cause similar effects as visible in DA biosynthesis mutants, leading to a decrease of longevity mediated by reduced mTOR activity. Phosphoproteome data of TORC1 targets identified DIN-1 as a direct TORC1 target (Sewell, Poss et al. 2022). Further analysis of the precise phosphorylation site Serine1472 showed that the DAF-12 binding partner DIN-1S does not harbor this site and can therefore not be targeted by TORC1. Nevertheless, DIN-1 to be a direct TORC1 target highlights how closely the mTOR and steroid pathway are connected. Phosphorylation of other DIN-1 isoforms might influence the expression and thereby frequency of DIN-1S binding to DAF-12. There are studies demonstrating how insulin signaling in response to glucose levels can cause a physiologically meaningful switch of exon usage via reversible phosphorylation, linking nutritional signals to the spliceosome (Stamm 2008). Phosphorylation of other DIN-1 isoforms therefore might be able to regulate *din-1* mRNA splicing events in response to food cues. We speculate a scenario in which DAF-12 could potentially directly regulate splicing of DIN-1, adding a new mechanism of DAF-12 regulation. The role of transcription factors in regulating alternative splicing events has been shown

previously via a high throughput screen identifying factors that modulate alternative splicing (Han, Braunschweig et al. 2017). One-third of found factors were categorized as transcription factors (Han, Braunschweig et al. 2017).

DIN-1 protein levels upon inhibition of mTOR signaling have not yet been measured, but it would be interesting to further investigate the role of the steroid signaling negative regulatory arm in future studies.

Our results suggest an epistatic relationship between steroid signaling genes and *raga-1*. To fully understand the upstream mechanisms linking *raga-1* to steroid signaling we investigated the order of regulation.

2. Steroid signaling is downstream of mTOR

The mTOR pathway is a well-established regulator of a number of downstream pathways and overall protein synthesis (Fonseca, Smith et al. 2014, Saxton and Sabatini 2017). In line with this, our transcriptomics data displayed an increase in the mRNA levels of some steroid signaling pathway genes that would suggest increased steroid pathway activity under decreased mTOR conditions. Surprisingly, the detected mRNA levels did not reflect in protein levels measured by reporter protein expression. The expression of steroid biosynthetic genes is tightly controlled by negative feedback loops to ensure balanced steroid homeostasis and organism-wide commitment to developmental decisions based on DA levels. In line with this, my work shows a significant increase of DAF-9::GFP expression upon *dhs-16* mutation, suggesting that *daf-9* expression is elevated upon decrease of DA precursor levels, as was shown in previous works (Wollam, Magner et al. 2012). A similar feedback regulation for *daf-40* or *daf-12*, showing increased mRNA levels, has not yet been established.

Due to inconclusive results regarding steroid gene mRNA and protein levels, we decided to directly measure the levels of compounds involved in DA biosynthesis in *raga-1* mutants. Measurements of Δ7-DA and its precursors showed elevated levels of lathosterol and Δ7-DA, but no changes in cholesterol and 7-dehydrocholesterol, despite the unchanged levels of steroid biosynthetic enzymes. This could hint to two possible mechanisms: (1) mTOR deficiency increases steroid biosynthesis by regulating the catalytic activity of involved

biosynthetic enzymes without altering protein levels. Interestingly, the conversion of 7-dehydrocholesterol to lathosterol, for which the enzyme is yet unknown, seems to be most affected by the decrease in mTOR activity, suggesting that mTOR potentially regulates the activity or levels of this unknown enzyme. It is known that post-translational modifications can regulate enzyme activities. For example, insulin controls metabolic enzyme activity through changes of phosphorylation. Insulin binding to the insulin receptor induces the inhibition of AMPK, resulting in the dephosphorylation of glycogen synthase and the increase in glycogen synthase enzymatic activity (Saltiel 2021). A similar mechanism could be possible for the unknown enzyme involved in lathosterol formation. (2) Alternatively, mTOR could directly or indirectly block the degradation of lathosterol or Δ7-DA which would lead to an accumulation of newly synthesized compounds. Possible mTOR does so via post translational modifications of involved enzymes. A potential role of mTOR in steroid stability is not yet understood. Elevated levels of Δ7-DA could stop the continuous production of Δ7-DA via a feedback loop known to regulate DA biosynthesis (Lee and Schroeder 2012), leading to the accumulation of the precursor lathosterol. Whether elevated steroid levels are caused by increased biosynthesis or reduced degradation could be assessed by a flux analysis of the DA biosynthesis pathway. Metabolic flux analysis quantitatively describes cellular fluxes by feeding a tracer (de Falco, Giannino et al. 2022), potentially isotope C^{13} labeled cholesterol, for a defined period of time. Mass spectrometry analysis could be used to track C^{13} isotope incorporation into DA and its precursors. Elevated levels of C^{13} in Δ7-DA would suggest increased levels of *de novo* Δ7-DA biosynthesis, whereas lack of C^{13} labeled Δ7-DA or low C^{13}/ C^{12} ratios would hint towards decreased flux through the pathway and rather accumulation of Δ7-DA by inhibited Δ7-DA catabolism in decreased mTOR conditions.

Our results that mTOR regulates the bile acid pool in *C. elegans* are in line with previous studies that displayed altered bile acid pools in mTOR deficient mice. Mouse models with deficient TORC1 such as $Raptor^{-/-}$ mice showed a loss of 12-hydroxylated (12-OH) bile acids. Whereas $Tsc1^{-/-}$ mice exhibiting hyperactive TORC1 activity were found to have elevated 12-OH bile acid levels (Zaufel 2022). 12-OH bile acids are secondary bile acids that, when conjugated were found to promote liver fibrosis (Xie, Jiang et al. 2021). It remains unknown if animals with elevated 12-OH bile acids pools show effects on lifespan or other health

parameters. An additional link between mTORC1 and the regulation of BA metabolism was suggested by work showing that detrimental effects of SIRT1 overexpression were rescued by restoring mTORC1 activity (Garcia-Rodriguez, Barbier-Torres et al. 2014). In more detail, SIRT mice exhibit elevated levels of free bile acids as well as conjugated bile acids in the liver. These animals additionally showed reduced liver regeneration after partial hepatectomy. However, feeding SIRT mice with leucine, the most effective amino acid to induce mTORC1 activation through RagGTPases (Laplante and Sabatini 2009), significantly improved survival after partial hepatectomy by 20% and reduced total bile acid levels in the liver (Garcia-Rodriguez, Barbier-Torres et al. 2014). **This evidence shows that the mTOR/bile acid signaling axis is conserved from *C. elegans* to mice.**

Loss of steroid signaling genes did not alter mTOR activity, suggesting that the **steroid signaling/mTOR signaling axis is a one-directional regulation in which steroid signaling is biologically downstream of mTOR.**

3. Steroid signaling is a convergent point to regulate longevity

We could show that nuclear hormone signaling is required to induce mTOR mediated longevity. A similar hormonal mechanism was reported for the lifespan of germline less *glp-1* mutants (Gerisch, Rottiers et al. 2007), animals with reduced *daf-2*/InsR activity (Dumas, Guo et al. 2013), and the dietary restriction mimicking mutant *eat-2* (Thondamal, Witting et al. 2014).

In line with my results, the supplementation of Δ4-DA was able to rescue the lifespan effects in *glp-1;daf-9* mutants (Gerisch, Rottiers et al. 2007). Expectedly, supplementation in the NHR mutants *daf-12* did not show lifespan effects suggesting the role of canonical DA binding to DAF-12. In line with lifespan of *glp-1* animals being dependent on bile acid-like signaling in *C. elegans*, these animals have elevated Δ7-DA levels compared to *wt* (Shen, Wollam et al. 2012), which is in accord with our data also showing elevated Δ7-DA upon reduced TORC1 signaling. A similar regulation of DA in two independent longevity signaling pathways, induced by mutation of *glp-1* and a decrease in mTOR activity, suggests steroid signaling as a convergent point to mediate lifespan benefits.

Additionally to germline and mTOR longevity, steroid hormone signaling has also been linked to longevity induced by DR as also DR induced an increase of Δ7-DA levels in *C. elegans*, and longevity induced by DR mimicking mutants *eat-2* was dependent on *daf-9* (Thondamal, Witting et al. 2014). DR is known to extend longevity and generally improve health in age (Mattison, Roth et al. 2012). In *C. elegans*, DR can be induced by bacterial deprivation (Greer and Brunet 2009) or by utilizing a genetic model with decreased food intake by mutation of the *eat-2* gene (Avery 1993). Both variants to induce DR in *C. elegans* result in longevity that was found to be dependent on the steroid biosynthesis gene *daf-9* (Thondamal, Witting et al. 2014). In line with my data and the reports in *glp-1*, supplementation of Δ7-DA rescued the lifespan of dietary restricted *daf-9* mutants (Thondamal, Witting et al. 2014). However, this study did not report the same requirement of the upstream DA biosynthetic enzyme *daf-36*, which seemed to be dispensable for DR induced longevity in *C. elegans*. This could mean that the alternative, *daf-36* independent DA biosynthesis pathway is sufficient to provide required levels of DAs for DR animals but is not enough to maintain DA levels for mTOR mediated longevity. Long lived animals under bacterial deprivation displayed similarly strong elevation of Δ7-DA (Thondamal, Witting et al. 2014). This is similar to our results showing a dramatic increase of Δ7-DA in *raga-1* mutants. However, the finding by Witting *et al.* suggests that it is not the DA ligand binding to DAF-12 that is required to induce DR longevity, but rather DA binding to the non-canonical NHR-8. In contrast to this, my data suggests NHR-8 to be non-essential for mTOR longevity, as *nhr-8* mutants display unchanged longevity effects induced by *raga-1*. Even though it is reported that DR in *C. elegans* requires a functional downstream mTOR signaling pathway to extend life (Hansen, Taubert et al. 2007), there is evidence that DR might also act in an mTOR independent way through the DAF-16/FoxO transcription factor (Greer, Dowlatshahi et al. 2007).

The physiological impact of bile acids on organismal health is highlighted in the effects of the bile acid lithocholic acid (LCA). Recently it was shown that supplementation of LCA phenocopies anti-aging effects of caloric restriction in mice (Qu, Chen et al. 2024). LCA also induces longevity in *C. elegans* and *Drosophila* (Qu, Chen et al. 2024). It does so by activating AMPK, which is a regulator for age related signaling pathways. AMPK inhibits TORC1 and FoxO to induce beneficial lifespan effects (Apfeld, O'Connor et al. 2004, Burkewitz, Zhang et al. 2014). LCA is an endogenous bile acid that is found in humans and that is elevated after 36 h

of fasting (Fiamoncini, Rist et al. 2022). The question of the molecular mechanism activated by LCA remains unanswered. Nematodes and flies are not able to synthesize this particular bile acid; that LCA still induces longevity in these animals suggests that they possess LCA-sensing and downstream machineries, speculatively through DAF-12. This speculation goes in line with studies focusing on the finding of novel DAF-12 activators that previously identified 3-keto-lithocholic (3-keto-LCA) acid as a weak DAF-12 activator in a tissue culture-based compound screen (Motola, Cummins et al. 2006). Interestingly, LCA did not act as a DAF-12 activator directly, suggesting that a derivatization of LCA to 3-keto-LCA is required for DAF-12 binding. This idea would correlate with the observation that DAF-12 ligands are typically 3-keto sterols (Motola, Cummins et al. 2006). The well-established DAF-12 targets Δ4-DA and Δ7-DA are also 3-keto sterols, 3-keto-4-cholestenoic acid and 3-keto-7,(5α)-cholestenoic acid, respectively (Beckstead and Thummel 2006). Investigations have shown that DAF-12 can accommodate a large range of structural variations in ligand geometry (Galilea, Santillan et al. 2024). Structurally diverse ligands can vary in their binding affinity with EC50 values ranging from 23 nM (Δ7-DA) up to 1000 nM (Δ5-DA) *in vivo* (Sharma, Wang et al. 2009). To clearly connect DAF-12 as a mechanistic target of LCA, it would be required to assess *daf-12* mutants' lifespan with and without LCA treatment. Loss of the lifespan extending effects of LCA in *daf-12* mutants would hint to DAF-12 as the LCA binding partner to extend life.

The benefits induced by LCA are the latest reports of the physiological relevance of steroid signaling for organismal health. Less recently, steroid/DAF-12 signaling was also connected with the effects of Sirtuins. Sirtuins are a family of signaling proteins that can regulate cellular processes such as autophagy, proteostasis, and metabolism (Houtkooper, Pirinen et al. 2012). One isoform, SIRT1 is of particular interest since it was shown to protect from metabolic and aging-related diseases and offers a target for pharmacological approaches (Satoh, Imai et al. 2017). However, the underlying mechanism and SIRT1 downstream pathways remained elusive. DAF-12 was shown to be coregulated by SIRT1 suggesting a mechanism in which also sirtuin signaling acts through steroid signaling to induce health benefits (Bayele 2019). This

expands our understanding of the complex network in which steroid/DAF-12 signaling is functioning as a convergent point to mediate organismal health (**Figure VI-2**).

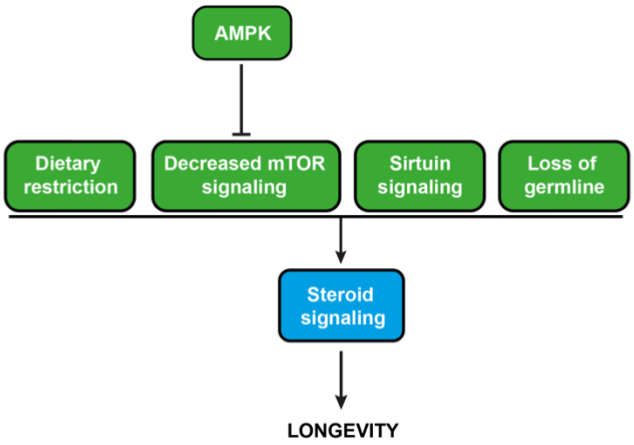

Figure VI-2: Steroid signaling as a converging point for longevity pathways. Several longevity pathways such as longevity induced by dietary restriction, sirtuin signaling, loss of germline and decreased mTOR signaling seem to be mediated by steroid signaling. AMPK is an upstream regulator of mTOR.

It is striking that many **longevity pathways, gonadal longevity, longevity induced by dietary restriction, and effects mediated by sirtuins, hinge on steroid NHR signaling.** Additionally, the dramatic longevity effect of LCA stresses the biological impact of bile acids on healthy aging. My presented work highlights the effects of steroid signaling on mTOR signaling. **mTOR is one of the most interconnected biological pathways potentially linking other longevity models into a singular complex network. Speculatively, endocrine NHR signaling might be a convergent mechanism to induce longevity benefits.**

4. DHS-26/DHRS1 is a novel and conserved regulator of steroid signaling

My work suggests that steroid signaling is downstream of mTOR signaling; however, how the mTOR/steroid signaling axis affects lifespan remains elusive. To investigate downstream targets that mediate the mTOR/steroid signaling axis dependent longevity, I performed a functional genomics RNAi screen. One candidate that gave us the most consistent longevity effects and was able to reduce *raga-1* mutants' longevity dramatically was the short-chain dehydrogenase *dhs-26*. DHS-26 is highly conserved and shares 41% homology with its mammalian homolog dehydrogenase/reductase (SDR family) member 1 (DHRS1) (Kishore, Arnaboldi et al. 2020). The cellular functions of DHS-26/DHRS1 are poorly characterized. DHS-

26 is characterized by *in silico* analysis and was predicted to have oxidoreductase activity (Kishore, Arnaboldi et al. 2020). DHRS1, also known as SDR19C1, was given its name in 2001 and was afterward shown to be a NADPH-dependent reductase that is able to catalyze the *in vitro* reductive conversion of steroids such as estrone, androstene-3,17-dione, and cortisone, as well as xenobiotics, suggesting a role in steroid and xenobiotic metabolism (Wu, Xu et al. 2001, Zemanova, Navratilova et al. 2019). This initial characterization of DHRS1 also reports DHRS1 subcellular localization to the ER of human liver and adrenals. Due to its suggested role in steroid signaling, we hypothesize that the effects of *C. elegans' dhs-26* knockdown on *raga-1* longevity might act through steroid signaling. Indeed, *dhs-26* mutants showed dramatic loss of Δ7-DA and supplementation of Δ7-DA was able to rescue *raga-1;dhs-26* lifespan, indicating that **DHS-26 acts through the canonical steroid signaling pathway to mediate mTOR longevity.** The supplementation experiment was performed once, further replicates showing similar rescue effects are required to solidify this conclusion.

Even though the characterization of the mammalian DHRS1 supports the idea that DHS-26 might be involved in *C. elegans* steroid biosynthesis, the precise enzymatic function of DHS-26 is not yet understood. My data shows DHS-26 as a potential positive regulator of Δ7-DA, but it remains elusive if this is directly through Δ7-DA biosynthesis, the regulation of an alternative potentially high affinity ligand produced from the Δ7-DA pool, or the regulation of dauer pheromone production. The dauer phenotypes of *dhs-26* mutants are still intriguing since the deficiency in DA did not drive these mutants into the dauer state as seen for *daf-36* mutants. Even the opposite effect was observed for *dhs-26* mutants as they show reduced dauer penetrance at 27°C. There has been evidence that high temperatures such as 27°C are sufficient to induce dauer independent of pheromone (Ailion and Thomas 2000) suggesting that the observed dauer penetrance at 27°C might be *dhs-26* independent. In case of reduced DAF-12 levels in *dhs-26* mutants this would be understandable, since the dauer program is induced by ligand-free DAF-12 together with its corepressor DIN-1S (Ludewig, Kober-Eisermann et al. 2004). In the absence of DAF-12, DIN-1 cannot induce dauer formation. DAF-12 protein levels in *dhs-26* mutants were not yet assessed, but doing so would give insight into possible causes for the surprising dauer formation phenotype. An alternative possibility is, that the DA levels measured in *dhs-26* mutants are not sufficiently low to induce dauer. It was observed that DA levels of Daf-c worms such as *daf-2(e1370)*, *daf-7(ok3125*), and *daf-*

11(ks67) showed levels below 15% of *wt* animals (Li, Chen et al. 2013). My work measured DA levels around 22% in *dhs-26* mutants compared to *wt* suggesting that the critical threshold of 15% was not reached and therefore DA concentration was not sufficiently low to drive dauer formation in *dhs-26* mutants. *dhs-26* mutation also did not influence dauer penetrance of steroid, insulin or TGF-β pathway mutants, suggesting *dhs-26* to be downstream or parallel to these pathways to induce dauer. Based on our observation of decreased Δ7-DA levels but *wt*-like dauer formation we hypothesize that DHS-26 loss might promote the synthesis of an alternative ligand that can rescue dauer phenotypes but not lifespan.

To further characterize the biological function of *dhs-26* mutants it would be important to map the levels of various ascarosides, as well as intermediates of the DA biosynthesis pathway and alternative DA variants in *dhs-26* mutants compared to *wt* animals. Measuring a wide range of DA variants as well as ascaroside levels in *dhs-26* mutants would also provide insight if DHS-26 as a short-chain dehydrogenase might be an enzyme involved in both DA formation and ascaroside biosynthesis. Both pathways require a lipid shortening step (Butcher, Ragains et al. 2009, Russell 2009) that could potentially be catalyzed by DHS-26. An example of a dehydrogenase that is involved in two crucial catalytic steps is the succinate dehydrogenase, involved in TCA cycle and OXPHOS (Martinez-Reyes and Chandel 2020). Other reports of an enzyme that can catalyze different reactions come from the methionine salvage pathway (Dai, Wensink et al. 1999). Both enzymes, E-2 and E-2' are expressed from the same gene and have the same inert apo-enzyme structure. However, metal binding into their catalytic centers, Ni^{2+} and Co^{2+} for E-2 and Fe^{2+} for E-2', dictates their distinct activities (Dai, Wensink et al. 1999). In both cases it allows a tight coordination between two metabolic pathways or within a pathway. DHS-26 could similarly coordinate ascaroside and DA biosynthesis in response to anabolic and catabolic organismal cues. Implications of DHS-26 in dauer pheromone production are further solidified, as *dhs-26* mutants display differential expression of proteins clustering withing the GO enrichment term "ascaroside biosynthetic process", listing *daf-22, acox-1.1* and *acox-1.2* to be significantly downregulated upon loss of *dhs-26*.

There is evidence that intestinal peroxisomes release ascarosides in response to reduced TORC1 signaling (Li, Hua et al. 2022). This study showed that mTOR signals to intestinal peroxisomes, which in turn release ascarosides targeting chemosensory neurons that further

downstream converge on DAF-12 to arrest animal development. But potential implications of an mTOR/peroxisome/steroid signaling regulatory pathway in aging have not yet been described. My functional genomics screen reveals the peroxisomal gene *acox-1.2* as a regulator for *raga-1* longevity. *acox-1.2* encodes for an acyl-coenzyme A oxidase (Kishore, Arnaboldi et al. 2020) that I showed to be regulated by DAF-12 as well as DHS-26. Alongside ACOX-1.2 also the peroxisomal protein ACOX-1.1 and the predicted peroxisomal protein PMP-1 (Kishore, Arnaboldi et al. 2020) showed regulation by DAF-12 and DHS-26 in my proteomics data set. However, these genes were not tested in the functional genomics screen for aging. It would be interesting to investigate these in future studies.

There is unpublished evidence that the supplementation of the ascarosides ascr#3 and ascr#10 to *wt C. elegans* induces the differential expression of *dhs-26* mRNA after 12 hours of treatment (A. Ludewig, unpublished). Further experiments revealed that *dhs-26* mutants are protected against lifespan shortening typically induced by ascr#10 supplementation in *wt* worms. Biologically, this places DHS-26 downstream of ascarosides, but upstream of the production of DAs. Potentially, DHS-26 regulates a so far unknown interplay between dauer diapause, DA production and ascaroside biosynthesis.

To further characterize the mode of DHS-26 action, we aimed to investigate its cellular localization. Single cell sequencing in *C. elegans* reports *dhs-26* expression in excretory canal neurons (CAN), amphid sheath cells, cephalic socket cells, and sheath glia, showing a clear tissue specificity of *dhs-26* expression exclusively in neuronal and glial tissue (Lorenzo, Onizuka et al. 2020). Imaging experiments with our *dhs-26::Scarlet* reporter strain could clearly recapitulate expression in the CAN as well as in the reported head neurons and glial cells. Glia cells were believed to only function to maintain homeostasis, and to provide support and protection to neurons (Temburni and Jacob 2001). Only in recent years has the signaling capability of glia cells been explored (Bar-Ziv, Dutta et al. 2023). It was shown that the activation of the mitochondrial unfolded protein response in glia cells improves neuronal protein homeostasis and prolongs lifespan in *C. elegans* (Bar-Ziv, Dutta et al. 2023). Mechanistically, they found that cephalic sheath glia secrete small clear vesicles as signaling molecules to surrounding neurons. This shows that glia are not passive bystanders in signal transduction but are rather active participators. The expression of *dhs-26* in sheath glia, the

cephalic sheath neurons, and other surrounding neurons of the *C. elegans* nerve ring as it was reported in single cell transcriptomics (Lorenzo, Onizuka et al. 2020) hints to a cell-overarching steroid signaling pathway. It is possible that DHS-26-mediated neuronal signals and signals through glia cells are required for the lifespan extension reported for neuronal knockdown of *raga-1* (Smith, Lanjuin et al. 2023).

The CAN specific expression of DHS-26 raises the question if these neurons are core drivers of *C. elegans* longevity mediated by a decrease in mTOR signaling. CANs are two bilaterally symmetric neurons (Forrester, Perens et al. 1998) with incompletely understood functions. It is known that *C. elegans* larval development requires the function of the two CANs. Killing CAN via laser ablation results in larval arrest (Forrester and Garriga 1997), but so far the underlying mechanism is unknown. Interestingly, it was found that the nematode *Pristionchus pacificus* expresses the dauerless gene (*dau-1*) exclusively in their CAN analogous cells (Mayer, Rodelsperger et al. 2015). CAN ablation or mutation of *dau-1* results in an increase in dauer formation. A screen looking for *P. pacificus* that shows Daf-c phenotypes that could be rescued by Δ7-DA revealed the hydroxysteroid dehydrogenase (HSD) to be involved in dauer decisions (Carstensen, Villalon et al. 2021). The *P. pacificus-hsd-2* gene encoding for the respective HSD is expressed in CANs, generating a strong link between dafachronic acid biosynthesis in *P. pacificus* to a tissue in *C. elegans* whose function had not yet been connected to dauer diapause. My work sheds light into the analogous function of CAN in *C. elegans* as a player in steroid signaling, highlighting the particular importance of a functioning neuronal signaling network for organismal wide effects.

Recent data suggests that particularly the neuronal signaling network is important to induce longevity in *raga-1* mutants by utilizing AID induced spatio-temporal knockdown of *raga-1* (Smith, Lanjuin et al. 2023). Neuronal knockdown of *raga-1* as well as *let-363* was able to promote longevity without the deleterious effects of decreased mTOR such as reduced body size, growth rate, and brood size that are typically found. The authors analyzed differentially regulated genes in the neuronal knockdown of *raga-1* to identify players that potentially mediate longevity. Curiously, they did not find *dhs-26* to be differentially regulated in worms carrying neuronal *raga-1::AID* treated with auxin compared to the control group. This is surprising since my data suggests *dhs-26*, with its endogenously neuronal expression, to be a

potential mediator for mTOR longevity. There are some experimental differences between my work and the published study. My transcriptomics measurements that showed elevated levels of *dhs-26* mRNA were performed in *raga-1* null mutants that were collected on day 1 of adulthood. In contrast to this, the presented study started auxin treatment on day 1, not egg on, and harvested *raga-1::AID* worms on day 3. It would be interesting to see if egg on auxin treatment of *raga-1::AID* and sample collection at the same timepoint as my work might result in more similar regulation of *dhs-26* mRNA. For other DA biosynthetic genes such as *daf-9*, expression is tightly regulated by development as it was shown in a systematic transcriptomics analysis of distinct developmental stages (Gerstein, Lu et al. 2010). This work also quantified *dhs-26* mRNA levels, reaching a peak around L4 and decreasing in young adulthood (Gerstein, Lu et al. 2010). It is possible that in the next few days of adulthood *dhs-26* levels further decrease in wt and *raga-1* mutants, explaining the discrepancy between my measurements of elevated *dhs-26* mRNA on day 1 and the published work which showed no significant changes of *dhs-26* levels at day 3 of adulthood (Smith, Lanjuin et al. 2023).

Besides *dhs-26* mRNA levels, my work suggests a regulation of DHS-26 on the translational level, as DHS-26 levels of my reporter protein was not significantly changed in the *raga-1* mutant background. To conclude if the presented study showing neuronal knockdown in *raga-1* might act through neuronal DHS-26 and thereby through an endocrine cell non-autonomous steroid signaling pathway it would be essential to further explore the four following aspects: (1) Does prolonged RAGA-1::AID mediated knockdown induce differential expression of *dhs-26*? (2) Are DHS-26 protein levels affected upon RAGA-1::AID knockdown? (3) Does knockdown of RAGA-1::AID induce longevity in a *dhs-26* mutant background? (4) If *dhs-26* is required for longevity in neuronal knockdown of *raga-1::AID*, does supplementation of Δ7-DA rescue the observed phenotype?

Mammalian DHRS1 shows not just expression in neuronal tissues, but was also detected in liver and adrenals, suggesting that it is expressed in more diverse tissues than its *C. elegans* homologue (Zemanova, Navratilova et al. 2019). However, also in mice, neuronal DHRS1 seems to have a specific role in the context of neuronal mTOR signaling response as mRNA levels of *Dhrs1* in the brain were increased in long-lived mice treated with low-dose rapamycin, whereas *Dhrs1* levels in their kidney were unchanged (Siegmund, Yang et al.

2017). We observe a similar increase of *dhs-26* mRNA in long-lived *raga-1* animals, suggesting that **DHS-26/DHRS1 expression in response to altered mTOR activity is conserved throughout evolution.** The hypothesis of DHRS1 to have an important neurological function is supported by a publicly available CRISPR mouse line lacking *Dhrs1* (The Jackson Laboratory GBC). Male *Dhrs1*$^{-/-}$ animals display tremors hinting towards an underlying neurological disorder as a response to loss of DHRS1.

In contrast to *dhs-26* mRNA levels, I found DHS-26 protein levels to be unchanged in *C. elegans'* CAN, as measured using the DHS-26::Scarlet reporter, and globally measured by single worm proteomics comparing *raga-1* mutants and *wt*. It is known that mRNA levels do not always reflect endogenous protein levels (Liu, Beyer et al. 2016), therefore it is possible that physiological DHS-26 might indeed be unchanged. In case the measured, unchanged DHS-26 protein levels do reflect the true physiological conditions, an increase of *dhs-26* mRNA levels in *raga-1* mutants could be explained by a potential feedback loop regulating dhs-26 mRNA levels. A feedback loop induced by DHS-26 substrate levels could work similarly to other steroid biosynthetic genes such as *dhs-16* and *daf-9* regulation (Lee and Schroeder 2012). However, since DHS-26 was correctly identified as a gene required for longevity induced by a decrease in mTOR activity based on reversed regulation of its mRNA levels between *raga-1;daf-12* and *raga-1* mutants, it is more likely that we did not detect altered DHS-26 levels due to experimental limitations. Only quantifying DHS-26 expression in one tissue, the CAN, did not allow me to pick up on potential changes observed in other tissues that were reported to show *dhs-26* expression, such as neurons and glia localized in the *C. elegans* nerve ring (Lorenzo, Onizuka et al. 2020). Unfortunately, fast bleaching of the reporter as well as high exposure times to compensate for the reporter's low expression levels were challenging parameters that had to be considered in the experimental design. These challenges were potentially due to low *dhs-26* gene expression being limited to only a few cell types, which could also reflect in extremely low *dhs-26* read counts in our transcriptomics data (80 reads per million).

Interestingly, *DHRS1* mRNA and protein changes were also strongly changed upon decreased mTOR signaling in mammalian cell culture (C. Demetriades, data unpublished). This supports our findings and underlines an evolutionarily conserved pathway in which mTOR regulates

DHS-26/DHRS1. However, the detailed mechanism in which DHRS1 is regulated by mTOR seems to be more complex than initially assumed as RagA/B double knock out cells showed a strong down regulation and thereby opposite regulation compared to our work, while HEK cells treated with rapamycin induced an increase in *DHRS1* mRNA (C. Demetriades, data unpublished). Therefore, it seems that DHRS1 expression might be tissue specific or dependent on the severity and timing of reduced mTOR activity.

Mechanistically, loss of the GTPases RagA and RagB decreases mTOR function constitutively via reduced activation of the TORC1 complex (Schreiber, Pierce-Shimomura et al. 2010), while treatment with rapamycin specifically and acutely inhibits TORC1 via rapamycin/ immunophilin complex binding to TORC1 (Schreiber 1991, Li, Kim et al. 2014). It is possible that transient and acute decrease of mTOR activity increases *DHRS-1* mRNA expression, whereas chronic reduction of mTOR in RagA/B knockout cells causes decreased levels of *DHRS-1*. It was previously reported that mTOR activity can have different mechanistic effects dependent on an acute or chronic mTOR treatment. Sin1 KO HEK293T cells that display a chronic loss of TORC2 activity, showed reduced activity of the renal outer medullary K+ channel (ROMK) when assessed via whole cell patch clamp, whereas acute inhibition of mTOR via AZD8055 treatment did not affect ROMK currents. These findings provide insight that acute pharmacological inhibition and chronic inhibition of mTOR can have opposite effects, potentially also oppositely regulating *DHRS-1* expression. Furthermore, there might be tissue specific regulations of *dhs-26/DHRS-1* which might present an additional limitation in comparing my work, measuring full body expression including neuronal *dhs-26*, and work conducted utilizing human kidney cells. The hypothesis of a tissue specific regulation of DHS-26/DHRS1 in mammals is further supported as RNA seq data of chronic rapamycin fed mice displayed significantly elevated *Dhrs1* mRNA levels in brain, but not in liver tissue (Siegmund, Yang et al. 2017). It becomes evident that **DHS-26/DHRS1 regulation by mTOR is a conserved and fine-tuned mechanism** that requires further investigation.

5. DHS-26 regulates a diverse set of downstream pathways to mediate longevity

Next, I aimed to understand which downstream pathways are regulated by *dhs-26* that might be required for mTOR longevity. Proteomics analysis revealed a complex downstream

regulatory network of *dhs-26* that gets dysregulated upon *dhs-26* loss in the *raga-1* mutant background. Mitochondria function as well as lysosomal proteins and metabolism of xenobiotics are dysregulated in *raga-1;dhs-26* mutants compared to long-lived *raga-1* mutant animals. These pathways are not shared targets of DAF-12 and DHS-26, but instead unique to DHS-26. These KEGG pathway enrichments go in line with known and predicted DHRS1 functions. The mammalian orthologue DHRS1 was predicted to be expressed in mitochondria, however, staining experiments in HeLa cells could not show mitochondrial expression (Zemanova, Navratilova et al. 2019). Our proteomics data suggests a clear connection between the *C. elegans* orthologue *dhs-26* and mitochondrial function. A *dhs-26*/mitochondrial link would explain why mitochondrial functions such as oxidative phosphorylation are differentially regulated upon loss of *dhs-26*. To assess *dhs-26* mutants' mitochondrial function the seahorse mitochondrial stress test could be utilized (Leung and Chu 2018). During the test, the oxygen consumption rate and maximal respiration is measured as an indicator for mitochondrial respiration. Significantly reduced or increased mitochondrial respiration in *dhs-26* mutants would suggest that DHS-26 is a regulator of mitochondrial function. Besides a potential implication of *dhs-26* in mitochondrial metabolism, my data showed decreased levels of proteins involved in metabolism of xenobiotics in response to loss of *dhs-26*. In line with this observation also mammalian DHRS1 was shown to be involved in the metabolism of xenobiotics (Zemanova, Navratilova et al. 2019) suggesting a conserved mechanism.

My data also suggests DHS-26 to be involved in peroxisomal homeostasis. ZK550.6, and C15B12.1, both genes predicted to be involved in peroxisomal function (Kishore, Arnaboldi et al. 2020), were able to abolish the longevity of *raga-1* mutants upon RNAi knockdown in my functional genomics screen. TSC proteins and Rheb, both components of TORC1 signaling have been shown to localize to the lysosome as well as to the peroxisome to regulate TORC1 activity (Benjamin and Hall 2013, Zhang, Kim et al. 2013). Whether peroxisomal function requires the presence of mTOR related genes is not yet understood. It also remains unknown if other lysosomal mTOR components localize to peroxisomes. The consistent differential regulation of peroxisomal genes and proteins in *daf-12, dhs-26*, and *raga-1* mutants, in addition to the observed lifespan effects after knockdown of peroxisomal genes on *raga-1* mutants' lifespan, hint towards an angle of peroxisome signaling in longevity induced by

decreased mTOR signaling that might be regulated by steroid signaling and DHS-26. Evidence suggests that AMPK and DR preserve youthful mitochondrial morphology to extend lifespan, but this effect is lost when peroxisomal function is impaired (Weir, Yao et al. 2017). However, the role of mTOR in this process remains unexplored. This study indicates that peroxisomal function contributes to AMPK- and potentially mTOR mediated longevity in *C. elegans*, given the close functional link between these two nutrient-sensing pathways.

My work establishes *dhs-26* as a potential DAF-12 target gene that acts in the same regulatory pathway to induce the observed effects on mTOR longevity. As such, it is not surprising, that my proteomics data shows a strong overlap between proteins regulated by DAF-12 and DHS-26. Nevertheless, both, loss of function mutants of *daf-12* and *dhs-26*, also regulate unique pathways. A potential explanation might be that loss of DAF-12 abolishes the positive, DA activated, as well as the negative, DIN-1S bound regulatory arm of DAF-12 activity (Antebi, Yeh et al. 2000, Ludewig, Kober-Eisermann et al. 2004). Whereas loss of DHS-26 results in the decrease of DA levels and thereby inhibits only the positive regulatory arm of DAF-12 activity, and may activate the negative arm. Inhibition of the positive arm of DAF-12 activity potentially allows more frequent DIN-1S binding to DAF-12. The DIN-1S/DAF-12 complex serves as a molecular switch orchestrating target gene expression during periods of diminished steroid hormone signals (Ludewig, Kober-Eisermann et al. 2004), which goes in line with decreased Δ7-DA levels observed in *dhs-26* mutants, potentially promoting DIN-1S binding to DAF-12.

The overlapping regulated proteins between DAF-12 and DHS-26 showed common regulation of lysosomal factors and proteins involved in lipid transport. While lysosomes do not play a direct role in bile acid conjugation, they are believed to assist in the intracellular transport of bile acids in mouse hematopoietic precursor cells (Persaud, Nair et al. 2021). Disruptions in lysosomal homeostasis by loss of DAF-12 or DHS-26 could thereby indirectly influence bile acid biosynthesis and levels of lysosomal cholesterol, which in turn could potentially disrupt proper recruitment of the Ragulator-TORC1 complex to the lysosome. It remains an open question if the lysosomal regulation of TORC1 might, in addition to cholesterol, also be mediated through recruitment by other steroids such as DAs or DA intermediates. A similar approach as conducted by the initial work describing that lysosomal cholesterol is sufficient to activate mTORC1 (Castellano, Thelen et al. 2017) could be utilized. In more detail, HEK cells

depleted of sterols by treatment with 50 µM MCD (methyl-β cyclodextrin) could be reintroduced to dafachronic acid or other DA intermediates. If indeed TORC1 recruitment to the lysosomal surface is promoted by bile acids besides cholesterol, an increased colocalization of a lysosomal marker with mTOR should be measurable.

6. Functional genomics screen reveals additional angles involved in mTOR longevity

To find downstream modulators of the mTOR/steroid signaling axis, I performed transcriptomics analysis revealing various KEGG pathway enrichments and differentially regulated genes to be potential mediators of longevity. To investigate this, we tested the effect of RNAi mediated gene knockdown on *raga-1* mutants' longevity in a functional genomics screen. The analysis of the preliminary screen hits sheds light onto the diversity of pathways that were able to regulate aging in *raga-1* mutants. Some RNAi clones displayed additive effects to *raga-1* and further increased *raga-1* mutants' lifespan. This suggests that such genes, the top three being F38B6.4/GART, *sams-1*/MAT1.2A, and H41C03.1, might work in parallel pathways to mTOR to regulate aging. For SAMS-1 (S-adenosyl methionine synthetase-1), the best characterized protein of the three, a potential mechanism might involve the regulation of the mTOR targets HLH-30/TFEB (Martina, Chen et al. 2012) and PHA-4/FoxA (Sheaffer, Updike et al. 2008). SAMS-1 was linked to DR induced longevity in *C. elegans* by regulating autophagy related genes, as *sams-1* RNAi significantly upregulated *hlh-30* and *pha-4* mRNA expression (Lim, Lin et al. 2023). Longevity induced by *sams-1* mutants was abolished upon RNAi mediated knockout of *hlh-30* and *pha-4* (Lim, Lin et al. 2023) linking longevity of *sams-1* mutants to decreased autophagy. Regulation of HLH-30 and PHA-4 via mTOR in addition to *sams-1* signaling could induce the observed additive lifespan effects.

Many genes were able to significantly decrease *raga-1* mutant longevity upon targeted RNAi knockdown. The knockdown of most significantly changed genes reduced *raga-1* mutant lifespan further than *raga-1;daf-12* mutant mean lifespan. This could be explained by an RNAi induced knockdown that exceeds the endogenous mRNA regulation in *raga-1;daf-12* mutants. It would be interesting to compare endogenous mRNA levels in *raga-1;daf-12* with mRNA levels after RNAi mediated knockdown. This could be achieved by measuring mRNA levels via qPCR.

The gene knockdown that showed the strongest decrease of *raga-1* longevity was *fat-5*. FAT-5 is one of three ∆9 fatty acid desaturases, which is regulated by NHR-49 (Van Gilst, Hadjivassiliou et al. 2005). Mutation of the *fat-5(tm420)* allele was shown to result in a reduction of *wt* lifespan highlighting the relevance of fat metabolism in aging (Imanikia, Hylands et al. 2015). Indeed, long lived germline less mutants display elevated levels of *fat-5* (Ackerman and Gems 2012). Another gene involved in lipid metabolism, the cytochrome P450 family member *cyp-35a2,* was not just one of the regulators of *raga-1* longevity, but I also found CYP-35A2 to be one of the 20 commonly regulated proteins between DAF-12 and DHS-26. This could indicate a potential connectivity of CYP-35A2 and the investigated steroid pathway. Supportive of this is that members of the cytochrome P450 family, to which DAF-12 belongs as well (Gerisch and Antebi 2004), are involved in the biosynthesis and metabolism of sterols, steroid hormones, lipids, or other xenobiotic substrates (Furge and Guengerich 2006). Surprisingly, a previous study showed that double mutants of *fat-5* and *cyp-35A2* display an increase in lifespan even though the two respective single mutants showed lifespan decrease (Imanikia, Hylands et al. 2015). Several factors are involved in the regulation of *C. elegans* fat stores. Fat can be stored as triacylglycerols in intestinal lysosome-related organelles (Schroeder, Kremer et al. 2007) or in lipid droplets (Mullaney and Ashrafi 2009). Lipids can either directly act as signaling molecules or can be utilized as energy sources through β-oxidation occurring in the peroxisomes and mitochondria (Zhang, Box et al. 2010). The effect of mutants in fatty acid metabolism on lifespan highlights the complexity with which metabolic pathways regulate lipid metabolism in aging.

Besides specific metabolic pathways, my results also indicate lysosomal genes to be potential mediators of mTOR/steroid longevity. TORC1 recruitment to the lysosomal surface is an important step in regulating TORC1 activity (Menon, Dibble et al. 2014). Even though I did not observe a change of TORC1 activity in *daf-12* mutants, DAF-12 and its potential target gene DHS-26 both seem to be involved in the regulation of the lysosomal proteins ASP-4 and CPR-6 as they were amongst the proteins differentially downregulated in *raga-1;daf-12* and *raga-1;dhs-26* mutants compared to *raga-1* mutants. RNAi mediated knockdown of the aspartyl protease *asp-4* was not tested; however, *cpr-6* (cysteine protease related) was found to be required for longevity observed in *raga-1* mutants. *cpr-6* (Kishore, Arnaboldi et al. 2020) is the *C. elegans* orthologue of human cathepsin B (CTSB) which is a lysosomal protease that is

involved in many lysosomal functions such as protein turnover, degradation and metabolism. The *C. elegans* orthologue might be involved in similar biological functions as its human orthologue suggesting that loss of *cpr-6* could influence lysosomal metabolism and amino acid availability which in turn affects TORC1 recruitment to the lysosome (Menon, Dibble et al. 2014). To test if loss of *cpr-6* abolishes *raga-1* mutant's longevity by increasing or further decreasing TORC1 activity, HLH-30 nuclear localization or AMPK phosphorylation could be assessed as readouts of mTOR signaling. Potentially there is a yet unexplored connection between steroid/DAF-12 nuclear hormone signaling and mTOR involving the regulation of lysosomal function.

Further analysis of my transcriptomics data revealed the top two enriched pathways to be lysine degradation as well as arginine and proline metabolism. Therefore, we aimed to test the effects of lysine degradation and arginine and proline metabolism genes on longevity induced by decreased mTOR signaling. Indeed, the knockdown of the arginine and proline metabolism genes *alh-1, alh-5, alh-9, oatr-1,* and *F46H5.3* decreased *raga-1* longevity significantly, suggesting that proper balance of this pathway is required to maintain mTOR mediated lifespan extension. It is known that a defect in arginine metabolism impairs mitochondrial homeostasis in *C. elegans* since mutation of the arginase *argn-1* leads to mitochondrial enlargement and reduced ATP production (Tang, Wang et al. 2020). Assessing if our knockdown conditions alter mitochondrial function might give us insights if the genes tested in my screen induced *raga-1* lifespan shortening through mitochondrial dysregulation. To maintain normative function, health mitochondria constantly adjust to metabolic changes by fusion and fission events. Fragmentation is induced during low energy demands whereas a high fusion rate of mitochondria occurs in metabolically active cells as interconnected mitochondria are efficient in OXPHOS (Westermann 2012). Imaging mitochondrial morphology can give insight if mitochondria are maintaining their normal equilibrium between fusion/fission or if we see higher rates of fission events upon RNAi mediated knockdown of *alh-1, alh-5, alh-9, oatr-1,* and *F46H5.3*. Higher rates of circular mitochondria could hint towards damaged mitochondrial function whereas a balanced network of mitochondria would suggest unchanged function. Mitochondrial function could be more directly assessed using the seahorse mitochondrial stress test (Leung and Chu 2018). Altered

mitochondrial respiration in response to *alh-1, alh-5, alh-9, oatr-1,* and *F46H5.3* knockdown would suggest that mitochondrial dysregulation might induce the observed lifespan effects.

A second angle that might be responsible for the observed reduction in *raga-1* lifespan by arginine and proline metabolism genes is the formation of ornithine as an intermediate in the production of proline from dietary arginine (Jones 1985). My screen candidate *oatr-1* (ornithine amino transferase related) is the orthologue of the mammalian ornithine δ-aminotransferase (OAT) which catalyzes the transfer of the δ-amino group from ornithine to α-ketoglutarate (Ginguay, Cynober et al. 2017). Ornithine is a non-essential amino acid that has been linked to various metabolic diseases (Sivashanmugam, J et al. 2017). Recent work showed a potential connection between ornithine and aging. It was found that ornithine levels as well as spermidine biosynthesis are decreased in short lived vitamin B12 deficient *C. elegans* (Bito, Okamoto et al. 2019). Supplementation of spermidine was partially able to rescue the lifespan of vitamin B12 deficient worms (Bito, Okamoto et al. 2019). Whether downregulation of *oatr-1* causes a similar decrease of *de novo* spermidine biosynthesis from ornithine in long lived *raga-1* mutants remains elusive.

The lists of genes included in the pathway enrichments arginine and proline metabolism, and lysine degradation showed an overlap of the genes *alh-1, alh-5,* and *alh-9*. These genes classify as aldehyde dehydrogenases and are conserved in humans (Kishore, Arnaboldi et al. 2020). It is known that mTOR activity is regulated by lysosomal amino acid levels (Bar-Peled and Sabatini 2014). Lysosomal amino acid homeostasis is mainly regulated by the lysosomal lysine/arginine transporter LAAT-1 (Liu, Du et al. 2012). Loss of *laat-1* accumulates lysine and arginine in the lysosome, which renders lysosomes degradation deficient (Liu, Du et al. 2012). It is possible that loss of genes involved in the catabolic pathway of arginine and lysine via RNAi treatment in *raga-1* mutants induces similar effects.

The integration of my transcriptomics and metabolomics data revealed that loss of *raga-1* indeed induces significant changes of genes and metabolites throughout the lysine degradation pathway, including elevated levels of L-lysine, saccharopine, and the final product acetyl-CoA (Figure IX-4). Lysine can be catabolized through two pathways (Leandro and Houten 2020). The mitochondrial saccharopine pathway is the primary catabolic

pathway. Lysine degradation through the less well understood pipecolate pathway, however, is also possible (Leandro and Houten 2020). Upon loss of *raga-1* I observed elevated levels of the lysine degradation intermediate saccharopine compared to *wt* animals. This is surprising as abnormal accumulation of saccharopine was reported to be detrimental as it results in defective mitochondria in *C. elegans* and mice (Leandro and Houten 2019). However, the impact of elevated saccharopine levels on organismal aging was not yet investigated. My data shows that RNAi knockdown of genes in both pathway arms were able to decrease *raga-1* lifespan. To further pursue the angle of lysine degradation in the context of mTOR/steroid signaling in age it would be interesting to supplement lysine, saccharopine, and pipecolate and assess *C. elegans* lifespan of *raga-1* mutants. Besides exploring DHS-26, the potential involvement of the lysine degradation pathway in mTOR mediated longevity was my most promising angle resulting from my screen. I prioritized the characterization of *dhs-26* as the main focus of my work as it provided more consistent and strong results.

Overall, my work demonstrates the diversity of pathways that are involved in mediating longevity effects observed in the mTOR mutant *raga-1* that are regulated by DAF-12/steroid signaling. **This highlights the complexity with which mTOR and steroid signaling regulate downstream pathways involved in aging.** These are including but not limited to balancing the levels of bile acid variants, balancing arginine and lysine catabolism, and regulating the functions of organelles such as peroxisomes, lysosomes and mitochondria.

7. Scientific contribution and limitations of this study

My work focuses on the connection between mTOR and steroid signaling in the context of organismal aging. I show that the positive regulatory arm of steroid hormone signaling is essential to benefit from mTOR mediated lifespan extension. Additionally, the maintenance of a fine balance between various DA hormone variants seems to be required. **I propose a yet undescribed mechanism in which ligand bound DAF-12 drives the neuronal expression of a novel dehydrogenase DHS-26 required to maintain endogenous DA levels. This strengthens the hypothesis that mTOR might act through an endocrine, cell non-autonomous signaling pathway.** We showed that loss of DHS-26 induces a disbalance of oxidative phosphorylation,

lysosomal function and ribosomal biogenesis, hinting to a complex network of downstream targets, which is regulated by steroid signaling.

C. elegans is a well-suited model organism for the presented study: *C. elegans* utilizes a bile acid-like signaling mechanism and is a powerful model to study aging. The identification of DHS-26 as an enzyme involved in steroid signaling hints towards a conserved mechanism as DHS-26 shows high sequence similarities to its human orthologue DHRS1. Future work should focus on the evolutionary conservation of an mTOR/steroid signaling axis in vertebrates. **Understanding the respective connection between these pathways in higher organisms would allow the development of a druggable steroidal target to regulate mTOR induce aging benefits.**

While we took advantage of the simplicity of *C. elegans* and decided to utilize it for this work, it also has its downside in regard to direct translatability to mammalian systems. Mammalian systems tend to be tighter interconnected than pathways in *C. elegans*. This is nicely exemplified by DAF-12, the *C. elegans* ancestral protein to the mammalian NHRs LXR, FXR, and VDR (Mooijaart, Brandt et al. 2005). Evolutionary specialization of these receptors allows the formation of a more complex regulatory network of bile acid signaling and homeostasis.

Due to experimental limitations, we chose to perform targeted steroidomics instead of measuring overall organismal steroid levels. Although we were able to measure the compound levels of cholesterol, lathosterol, and Δ7-DA, the question of how DA variants outside of the main biosynthetic pathway are regulated remains unanswered. We hypothesize that DHS-26 might support the synthesis of an alternative ligand that can rescue dauer phenotypes but not lifespan. To further understand the DHS-26 point of action, filling in the missing DA intermediate as well as DA isoform levels is essential. Additionally, our data suggests a role of DHS-26 in ascaroside biosynthesis which could be experimentally assessed in the future by investigating ascaroside levels.

Recent work shows a neuronal cell non-autonomous mTOR signaling mechanism (Smith, Lanjuin et al. 2023). This evidence in combination with my work suggests a role of DHS-26 in this signaling pathway. To fully unravel the role of DHS-26 in neuronal mTOR mediated longevity it would be required to induce *raga-1* and *dhs-26* knockdown under neuron specific

promoters. This would allow us to pinpoint the exact neuronal network involved in inducing mTOR longevity.

VII. Future Perspectives

Investigating the role of an mTOR/steroid signaling axis in *C. elegans* aging revealed the highly conserved dehydrogenase *dhs-26*/DHRS1 as a potential novel player in steroid metabolism, regulating longevity induced by loss of *raga-1*. Even though the presented work describes an initial characterization of *dhs-26*, further questions remain unanswered: (1) *dhs-26* shows significant elevation of mRNA levels in *raga-1* mutants. Does the mammalian orthologue DHRS1 display similar change upon decrease mTOR activity? (2) What is the physiological DHS-26 enzymatic function and what can DHS-26 utilize as a substrate? (3) My work shows upregulation of *dhs-26* mRNA upon loss of *raga-1*, but experiments investigating DHS-26 protein levels did not display the same changes. Are DHS-26 levels indeed unaffected by decrease in mTOR activity, or is there a regulation in other, not yet tested tissues? (4) Do the lifespan benefits induced by a decrease in neuronal *raga-1* converge on DHS-26? (5) What are the physiological effects of a *dhs-26* over expressor? (6) Is *dhs-26* indeed a DAF-12 target gene? These questions are close to the main direction of this work. However, my screen also revealed potential other angles that might be of interest such as: (7) What is the role of the lysine degradation pathway to mediate longevity induced by a decrease in mTOR activity.

1. Evolutionary conservation of DHS-26 regulation by mTOR

DHS-26/DHRS1 is highly conserved throughout evolution. A structural conservation has been shown with a sequence similarity of 41%; however, it remains an open question if this evolutionary conservation also translates to DHS-26/DHRS1 regulation and function. In this work I performed RNA sequencing and report significantly elevated levels of *dhs-26* mRNA in *raga-1* knockout worms. A significant regulation of *DHRS-1* mRNA was confirmed in RNA sequencing experiments performed in HEK293T cells even though these analyses revealed elevation of *DHRS1* mRNA in rapamycin treated cells whereas RagA/B KO cells showed a decrease (C. Demetriades, unpublished). Disregarding the directionality of change, this data shows strong regulation of *DHRS1* mRNA in response to decreased mTOR signaling. Yet another set of RNA seq data describes mRNA levels in rapamycin fed Tk2KI knock-in mice in

which *Dhrs1* is significantly elevated in brain, but not in liver tissue (**Figure VII-1**) (Siegmund, Yang et al. 2017).

Figure VII-1: Rapamycin regulates DHRS1 expression in mice. Transcriptomics analysis by Siegmund *et al*. Tk2KI (mitochondrial nucleotide salvage enzyme thymidine kinase 2) knock-in mice were treated with a low dose of rapamycin by feeding rapamycin supplemented water. Transcriptomics analysis was performed on (A) brain and (B) liver. Tissues were collected from 15-days old female pups and age- and treatment matched litter mate controls. Rapamycin was supplemented into drinking water with final concentrations of 8 µg/ml during dam pregnancy and 40 µg/ml after delivery. The water of the control group was administered with EtOH vehicle control in matched concentrations (Siegmund, Yang et al. 2017). (3 biological replicates, bars represent mean ± SD, statistical significance was calculated with *t*-test, ns $p<0.05$, * $p<0.05$)

Our next focus is the validation of these results to establish *dhs-26*/DHRS1 as a conserved target of mTOR signaling. To do so, we would collaborate with a lab within the Max-Planck Institute of Biology of Ageing that has frozen tissue samples harvested from *wt* mice treated with rapamycin. Measuring *Dhrs1* mRNA levels in these animals as well as assessing SDS PAGE followed by western blotting against DHRS1 could give us insight if the observed changes in DHRS1 mRNA of Tk2KI knock-in mice treated with rapamycin also translate to DHRS1 mRNA and protein levels in *wt* animals. Antibodies against DHRS1 are publicly available but require previous testing to not waste precious mouse material. I would focus on brain and liver tissues to allow the comparison between my data set and the published work on *Dhrs1* mRNA levels (Siegmund, Yang et al. 2017). If we observe the same upregulation of DHRS1 protein levels upon rapamycin feeding in *wt* mice as it was reported for the mRNA in Tk2KI knock-in mice would show that the mechanism involving DHRS1 is also involved in normative, *wt* responses to the pharmacological regulation of mTOR. It is possible that mouse and *C. elegans* responses to a decrease in mTOR activity are wired differently despite the high conservation of DHS-26/DHRS1. In this case we could expect an opposite phenotype in response to mTOR inhibition.

For *C. elegans* we hypothesize that neuronal mTOR inhibition might act through DHS-26 to induce beneficial physiological effects. If we can show mammalian DHRS1 to be one of the

main responsive elements to mTOR inhibition, our hypothesized interplay between mTOR and DHS-26/DHRS1 might be conserved and could also be involved in mammalian benefits following decreased mTOR activity. To follow up in this direction it would be important to first understand if mammalian mTOR also acts through neuronal signaling to promote longevity effects. To test this, it would be possible to compare the lifespan of hypomorphic $RagC^{Q119L/+}$ mice which were shown to be long lived (Ortega-Molina, Lebrero-Fernandez et al. 2021) with the lifespan of mice with knockdown of Rag GTPases exclusively in neuronal tissues. Longevity effects after exclusively neuronal mTOR inhibition would suggest a similar cell non-autonomous signaling mechanism in mammals which could be dependent on neuronal DHRS1.

2. Exploring DHS-26 enzymatic function in DA and ascaroside biosynthesis

As part of my work, we collaborated with the institute's metabolomics core facility to directly measure levels of steroid intermediates in the Δ7-DA biosynthetic pathway in *C. elegans*. Since Δ7-DA was significantly downregulated in *dhs-26* knockout animals, this revealed a potential role of DHS-26 as a DA biosynthetic enzyme. The human DHS-26 orthologue DHRS1 was shown to catalyze the *in vitro* reduction of the steroids estrone, androstene-3,17-dione, and cortisone. We hypothesize DHS-26, as a predicted short-chain dehydrogenase, to have similar enzymatic functions as reported for DHRS1. So far, the precise DHS-26 enzymatic function and how it is involved in regulating DA levels remains elusive. Generating a more complete picture of differentially regulated DA precursors and variants would give more detailed insight into DHS-26 function. Unfortunately, DAs are present in low physiological concentrations (Motola, Cummins et al. 2006). This makes it challenging to measure a broad spectrum of DAs. A new collaboration with the lab of Frank Schröder might enable us to explore the levels of more labile DAs in *C. elegans*. We have successfully shipped the strains of interest, N2, *raga-1(ok701), dhs-26(syb8968),* and *raga-1;dhs-26* to the Schröder lab. Additionally, we have successfully grown worms with an alternative culturing method in liquid culture that allows us to increase worm numbers for sample preparation. Higher worm counts are required to measure the desired DA variants due to low extraction efficiency and DA instability.

Differentially regulated compound levels in *dhs-26* mutants would hint towards an enzymatic reaction that is potentially catalyzed by DHS-26. However, this data would still provide only a correlative link. To establish a causative connection between DHS-26 function and compound levels, a direct connection between substrate usage and *dhs-26* mutation needs to be explored. To do so, *C. elegans* could be grown under cholesterol deprivation to deplete them of DHS-26 substrate and therefore a loss of DHS-26 product. If re-introducing the substrate increases compound levels measured by mass spectrometry of the DHS-26 product in *wt* but not a *dhs-26* mutants would be clear evidence for the precise enzymatic function of DHS-26.

Frank Schröder and his colleagues are not only experts in measuring the levels of DA variants, but played a key role in the investigation of dauer pheromone (Butcher, Fujita et al. 2007). The same samples harvested for DA measurements can also be utilized to quantify ascaroside composition and levels. These measurements could shed light into the speculation that DHS-26 as a short-chain dehydrogenase might be involved in both, Δ7-DA formation and ascaroside biosynthesis. My proteomics work shows ascaroside biosynthetic proteins to be differentially expressed, which gives further evidence of a potential implication of DHS-26 in dauer pheromone production. In combination with the loss of Δ7-DA in *dhs-26* mutants this might suggest that DHS-26 coordinates ascaroside and DA biosynthesis in response to anabolic and catabolic organismal cues. This result could link the ascaroside and DA biosynthesis pathways closer together than so far described.

3. Validating DHS-26 protein changes upon decrease mTOR pathway activity

We see a positive regulation of *dhs-26* mRNA in RNA sequencing analysis comparing *wt* and *raga-1(ok701)* mutant *C. elegans.* This was the foundation on which *dhs-26* was selected as a candidate gene for the functional genomics screen and resulted in the strongest hit showing interesting effects on steroid signaling and lifespan. To validate this finding on protein level, I designed the endogenous fusion protein reporter *dhs-26::FLAG::Scarlet.* Surprisingly, crossing the reporter to *raga-1(ok701)* mutants, microscopy imaging, and analysis of fluorescence intensities comparing *wt* and *raga-1* did not result in significant DHS-26 protein changes in the CAN. However, there are several possible reasons for this discrepancy that will be

addressed in the future. DHS-26 protein levels under mTOR deficient conditions will be measured under different conditions:

(1) Knockout of *raga-1* results in only mild downregulation of TORC1 pathway activity compared to loss of the core protein *let-363*/TOR itself. Rather than using *raga-1* mutants, RNAi mediated knockdown of *let-363* might result in a stronger regulation of *dhs-26* translation that could possibly be captured. Preliminary work comparing *dhs-26::FLAG::Scarlet* expression under *let-363* RNAi treatment compared to luci control showed an increase in CAN tissue. This finding needs to be repeated and quantified.

(2) Potentially, DHS-26 protein regulation in response to *raga-1* is tissue specific. My measurements exclusively in the CAN could thereby have missed protein regulation happening in other cell types that were shown to express *dhs-26* mRNA such as the amphid sheath cells, cephalic socket cells, and NA sheath glia (Lorenzo, Onizuka et al. 2020). These cells are located in the head and expression can be detected using my designed *dhs-26::FLAG::Scarlet* reporter strain (**Figure IX-2)**. Fluorescent imaging by confocal microscope could allow us to detect smaller changes in fluorescence intensity and could aid with the challenge of reporter bleaching. Fluorescence imaging with a higher resolution could also provide additional information on potential subcellular localization of DHS-26 that could be utilized to understand its place of action in more detail. (3) The *dhs-26::FLAG::Scarlet* reporter strain can also be utilized to measure protein levels via western blot due to the included FLAG tag. This would allow us to draw conclusions on DHS-26 expression in the whole body that are more sensitive to small changes and allow stronger amplification of the signal intensity than the performed proteomics measurements. Single worm proteomics did detect DHS-26 but did not show significant changes in DHS-26 levels in *raga-1* animals, possible due to low expression rates.

Findings validating unchanged DHS-26 protein levels in *raga-1* mutants, might suggest that instead of altered DHS-26 protein levels, DHS-26 enzymatic activity might be regulated upon decreased mTOR activity. Once we identified the enzymatic reaction catalyzed by DHS-26, we could utilize this knowledge and measure enzyme activity upon decrease of mTOR.

4. Role of DHS-26 in neuronal mTOR induced cell non-autonomous signaling

Our data suggests that DHS-26 expression particularly in neuronal tissue might be a novel regulator of steroid biosynthesis required for mTOR mediated longevity. Data from other labs shows that decrease of neuronal *raga-1* is sufficient to induce longevity in *C. elegans* suggesting cell non-autonomous, potentially an endocrine signaling mechanism (Smith, Lanjuin et al. 2023). We hypothesize that benefits from AID mediated *raga-1* knockdown in neurons are working through neurons that display DHS-26 expression. To further investigate which cells are involved we will utilize AID mediated *raga-1* knockdown under specific promotors expressed in the CAN, amphid sheath cells, cephalic socket cells, and NA sheath glia. Whether *raga-1* knockdown in these specific cell types is sufficient for lifespan extension will be assessed by aging experiments in *C. elegans*. To do so, we aim to induce a neuronal knockdown of *dhs-26.* An established method for gene knockdown is via RNA interference, which was extensively utilized in the presented functional genomics screen. RNAi effectiveness highly depends on the cell type and target tissue (Asikainen, Vartiainen et al. 2005). Unfortunately, neuronal knockdown of genes in *C. elegans* is inherently difficult as the dsRNA transporter SID-1 is absent in neurons. Alternatively, neuronal knockdown can be induced making use of a novel AID induced mechanism. We aim to generate a *dhs-26::AID*^{Neuronal} *C. elegans* mutant expressing a tissue specific TIR1 under the neuronal *rab-3* promotor. TIR1 is a plant enzyme that can interact with *C. elegans* proteins. In the presence of auxin, TIR1 binds and ubiquitinates AID-tagged proteins, which in turn get degraded by the proteasome machinery (Zhang, Ward et al. 2015). We hypothesize that AID induced neuronal double knockdown of *dhs-26::AID*^{Neuronal} and *raga-1::AID*^{Neuronal} might reduce *raga-1* mutants' longevity compared to *raga-1::AID*^{Neuronal} animals that express endogenous *dhs-26* levels. This would provide strong evidence that neuronal mTOR signaling might act through DHS-26 to induce longevity.

A variable to consider is targeting *let-363/TOR* instead of *raga-1* for AID mediated knockdown. Similarly to neuronal *raga-1*, also neuronal *let-363* was shown to be sufficient to induce an increase in *C. elegans* lifespan (Smith, Lanjuin et al. 2023). In case my efforts measuring DHS-26 protein levels result in the conclusion that DHS-26 levels are unchanged in *raga-1* mutants,

but changed upon *let-363* RNAi, *let-363* it would be a better suited target in addition to *dhs-26::AID*^{Neuronal} knockdown.

Besides measuring the lifespan of animals with a double knockdown via *dhs-26::AID*^{Neuronal} and *raga-1::AID*^{Neuronal}, it would be important to include a link to steroid levels. To do so, steroid levels of DA variants and DA precursors could be assessed upon *dhs-26::AID*^{Neuronal} and *raga-1::AID*^{Neuronal} conditions. **These experiments would expand our understanding of a potential neuronal pathway that utilizes steroid hormone signaling to induce longevity.**

5. Effects of a *dhs-26* over expressor

The presented work shows that loss of DHS-26 results in strong effects such as abolishment of *raga-1* mediated longevity, dramatic decrease of Δ7-DA levels and regulation of downstream pathways assessed by proteomics. To further understand the biological function of DHS-26 we will utilize a *dhs-26* over expressor. The over expressor will be generated by microinjection of a vector carrying the *dhs-26p::dhs-26::FLAG::Scarlet* sequence. This sequence has been previously used for generating the endogenous reporter construct that was used in this work. The reporter protein appeared to be functional, as *C. elegans raga-1* mutants with endogenously tagged *dhs-26::FLAG::Scarlet* did not display any growth defects compared to *raga-1* mutants, while *raga-1;dhs-26* mutants showed delayed growth and reduced body size (preliminary data not shown). The co-injection of a fluorescent marker gene will be added to the microinjection to allow easy lineage tracing. To enable physiological regulation of *dhs-26* transcription and translation, non-coding regulatory elements (5 kb of the upstream promoter and intronic regions of the *dhs-26* genome) will be included in the construct. Successful over expression will be validated by fluorescent imaging of worms carrying copies of the *dhs-26p::dhs-26::FLAG::Scarlet* vector. The effects of increased DHS-26 activity will be investigated regarding different physiological properties:

(1) Measurement of DA variants. *dhs-26* mutants displayed decreased levels of Δ7-DA, suggesting DHS-26 to be a positive regulator of DA biosynthesis. Therefore, we hypothesize that over expression of DHS-26 might result in increased levels of Δ7-DA and potentially other DA variants. A direct correlation between DA levels and *dhs-26* expression would solidify the

role of DHS-26 as an enzyme which is (directly or indirectly) regulating DA biosynthesis, and close existing gaps in our knowledge regarding DA hormone biosynthesis.

(2) Does *dhs-26* over expression influence *wt* lifespan or does it further prolong *raga-1* longevity? There is evidence that longevity interventions such as *glp-1* mutation (Shen, Wollam et al. 2012) and DR (Thondamal, Witting et al. 2014) display similarly elevated Δ7-DA levels as we report for *raga-1* mutants. However, increased DA levels alone do not seem to be sufficient to induce lifespan extension as supplementation of Δ7-DA or 4-DA did not or only slightly result in further increase of lifespan of wt (data not shown), *raga-1* and *glp-1* mutants (Gerisch, Rottiers et al. 2007) compared to EtOH vehicle control. It rather appears that endogenous steroid hormone signaling levels are sufficient to allow for lifespan extension via the mentioned interventions. The possibility of *dhs-26* over expression further increasing *raga-1* mutants' longevity might suggest the presence of an alternative, less stable but more potent DA variant than Δ7-DA or 4-DA. Overexpression of *dhs-26* could drive the biosynthesis of such a variant or could further stabilize it to increase its availability. It would also be possible that we observe decreased *raga-1* mutants' lifespan upon overexpression of *dhs-26.* In case a fine-tuned balance of steroid signaling is indeed required for optimal physiological responses such as longer life, increased hormone production and over activation of hormone signaling could also induce detrimental effects. Understanding the effects of reduced and over activated steroid signaling could give us insight into the balance required for organismal health. Especially with the perspective of utilizing steroid hormone signaling pharmacologically it is important to understand the consequences of too high and too low steroid signaling.

6. Solidifying DHS-26 as a DAF-12 target gene

My transcriptomics data shows *dhs-26* mRNA to be strongly downregulated upon mutation of the DAF-12 ligand and DNA binding domain. Furthermore, DAF-12 motif analysis predicted multiple significant potential DAF-12 binding sites on the *dhs-26* genomic region that could not be fully validated by DAF-12 ChIP seq data (Wormbase) possibly due to *dhs-26* expression levels below the detection limit. Therefore, a direct regulatory connection between DAF-12 and DHS-26 remains to be shown. We aim to perform chromatin immunoprecipitation assay

(ChIP) followed by qPCR that allows detection and quantification of DNA-protein interactions (Cecere and Grishok 2014). We will generate a *C. elegans* line harboring an endogenous DAF-12 fused to a FLAG epitope. A non-FLAG tagged DAF-12 strain will be included as a control. FLAG tagged DAF-12 can be targeted via an antibody-mediated pull down, followed by qPCR analysis with primers targeting *dhs-26*.

Alternatively, it would be possible to use an *in vitro* luciferase assay: HEK293T cells transfected with a vector encoding for the promotor region of *dhs-26* fused to luciferase should show increased luminescence when co-transfected with a vector encoding for the full-length DAF-12, but only if DAF-12 indeed transcriptionally regulates the expression of the *dhs-26* promotor region. A similar experiment was performed to establish DAF-12 target genes such as *mir-84* (Mahanti, Bose et al. 2014). The *mir-84* promotor fused to luciferase that increases luminescence activity will be included in my approach as a positive control (Mahanti, Bose et al. 2014).

In case we can show that *dhs-26* is a DAF-12 target gene it would be interesting to identify the exact binding site. My work suggests predicted binding sites on the *dhs-26* genomic region. The systematical mutation of these predicted DAF-12 binding motifs should abolish the signal once the true binding site is targeted. This approach would expand our knowledge of DAF-12 target genes and would present a positive regulatory feedback loop with which DAF-12 could regulate its ligand binding through DHS-26.

If *dhs-26* is not a direct target of DAF-12, we could aim to identify other transcription factors regulating *dhs-26* expression. To do so, we could utilize a promotor-pull down assay that was developed to identify unknown DNA-binding proteins that are interacting with a particular promotor (Chaparian and van Kessel 2021). In this approach we would utilize the *dhs-26* promotor as DNA-bait to capture DNA-binding proteins from *C. elegans* lysate followed by proteomics analysis to identify transcription factors regulating *dhs-26* expression.

7. Validating the role of lysine degradation in the mTOR/steroid signaling axis

Screening for downstream players of the mTOR/steroid signaling axis mediating lifespan revealed genes involved in lysine degradation to be required for longevity observed in *raga-*

1 mutants. However, further exploring the role of lysine degradation was outside the scope of my presented work. Nevertheless, my work offers interesting insights into the regulation of lysine degradation by mTOR which could be used as a base to explore this angle in the future.

Canonical lysine degradation is divided into two arms, the main ε-deamination pathway producing saccharopine and the side α-deamination pathway resulting in the formation of pipecolic acid (Leandro and Houten 2020). (1) I could show that lysine degradation pathway genes are differentially regulated in *raga-1* mutants compared to *wt* in both pathway arms. (2) Metabolomic analysis revealed accumulation of lysine and saccharopine upon loss of *raga-1* compared to *wt*. (3) RNAi mediated downregulation of various lysine degradation pathway genes in *raga-1* mutants abolished longevity effects.

To solidify my findings that the lysine degradation genes *C15B12.1, alh-9, ech-1.1, hacd-1, T02G5.7,* and *kat-1* are required for the lifespan increase of *raga-1* mutants, the longevity experiments need to be repeated and validated. To do so, *raga-1* animals will be fed with RNAi expressing bacteria to induce the knockdown of the respective target genes. *raga-1* and *raga-1;daf-12* mutant animals fed with a *luci* vector will be included as controls. Genes that show consistent lifespan effects upon knockdown should be considered potential targets for further investigations.

Assuming that downregulation of lysine degradation genes disturbs lysine degradation and potentially results in the accumulation of lysine, pipecolate, and saccharopine, the supplementing of these compounds could mimic the observed reduction in *raga-1* mutants' longevity. The metabolites could be directly supplemented into the culture plates' agar to ensure even distribution and minimize potential crystallization of the compounds on the plates' surface. To ensure that the bacteria seeded onto the plates do not metabolize the compounds, heat or UV killed bacteria could be utilized. It is to note, that UV killed bacteria was shown to extend *C. elegans* lifespan (Win, Yamamoto et al. 2013). Therefore, it is of particular importance to include vehicle controls on plates seeded with killed bacteria.

Lysine degradation is subcellularly compartmentalized, including reactions in the cytosol, mitochondria, and peroxisomes (Leandro and Houten 2020). The subcellular localization of

lysine degradation genes that were successfully validated to be required in decreased mTOR mediated longevity could give insight into future directions of the project. Lifespan effects of pipecolic acid supplementation and RNAi mediated knockdown of C15B12.1 would suggest an angle impinging on peroxisomal function, whereas effects of saccharopine supplementation, normally synthesized in mitochondria, would rather hint in the direction of mitochondrial function. A potential role of the lysine degradation pathway would open up yet unknown angles of downstream pathways regulated by steroid signaling that are required for organismal benefits induced by a decrease of mTOR signaling.

VIII. Material and Methods

1. *C. elegans* husbandry

1.1. Worm growth, maintenance, and synchronization

Nematode growth medium (NGM) plates seeded with *E. coli* OP50 as the food source were used to grow and maintain *C. elegans* strains (**Table** VIII-1). To ensure optimal growth conditions, worms were cultured at 20°C if not stated otherwise. All strains used for this work (**Table** VIII-4) as well as an extensive list of buffers and media compositions (**Table** VIII-6) can be found below.

Table VIII-1: Overview of pouring and seeding volumes for NGM plates.

NGM plate diameter	Agar volume	OP50 volume
3 cm	3 ml	100 µl
6 cm	10 ml	150 µl
10 cm	25 ml	400 µl

In case of microbial contaminations, the plates were bleached. If not stated otherwise, bleached worm colonies were maintained for two generations before using them for experiments to not have generational effects of the bleaching stress. For bleaching, worms were collected in M9 buffer. A 1:1 ratio of cold bleaching solution to M9 buffer was added. The samples were vortexed until only eggs were visible, then the bleaching solution was removed and the eggs were washed three times with M9 buffer. Eggs were then transferred to new NGM maintenance plates.

To synchronize worms, eggs from a mixed work population were transferred to fresh NGM plates. These eggs were grown until day 1 of adulthood. These Day 1 adults were used to perform egg lays to yield a synchronized population in the next generation.

1.2. RNAi treatment

To perform RNAi feeding, regular NGM medium was infused with 1 mM Isopropyl β-1-D-thiogalactopyranoside (IPTG) and Ampicillin (100 µg/mL) prior to pouring the plates. The plates were seeded with the respective RNAi-expressing *E. coli* strains HT115 or iOP50. The utilized control was matched with the respective *E. coli* strain used. These RNAi-expressing strains use an IPTG-inducible promotor to express the siRNA of the L4440 vector. The appropriate siRNA expressing bacterial clones were either selected from the Ahringer and Vidal libraries (Rual, Ceron et al. 2004, Boutros and Ahringer 2008), or were specifically cloned for this project. All clones were verified by Sanger sequencing prior to use. As a control, bacteria harboring the luciferase RNAi in the L4440 vector were used. Worms were grown on RNAi plates egg on if not stated otherwise.

1.3. Genotyping

Worms were collected in single worm lysis buffer (10 mM Tris pH 8.3, 50 mM KCl, 2.5 mM MgCl2, 0.45 % Tween 20, 0.45 % Triton X-100 (all v/v), 1 mg/ml proteinase K (NEB)) and incubated for 60 min at 60 °C, followed by 15 min at 95 °C. 2 µl of the lysate was used for PCR amplification using DreamTaq DNA Polymerase (ThermoFisher Scientific) according to the manufacturer's instructions. Annealing temperatures were determined using the T_m Calculator by ThermoFisher Scientific (Allawi and SantaLucia 1997). The primers used for PCR amplification are listed below (**Table** VIII-5). PCR products were analyzed by agarose gel electrophoresis or sequencing. Sequencing was performed by using the Mix2Seq Kit from Eurofins Genomics (Germany) with primer used for PCA amplification.

1.4. Genome editing

Outsourced genome editing

Genome editing using CRISPR/Cas9 was performed by SunyBiotech (China). Correct mutagenesis was verified by sequencing using the Mix2Seq Kit from Eurofins Genomics (Germany) as outlined above.

In-house genome editing

The two genes *fln-2* and *daf-12* are located closely together on the same chromosome. Therefore, it was not possible to generate a *fln-2(ot611);daf-12(rh61rh411)* by crossing. Instead, in-house genome editing was utilized to induce the desired SNP for *fln-2* into the *daf-12* mutant. As a readout for successful genome editing, *dpy-10* mutation was induced to screen for dpy body phenotype.

CRISPR guideRNAs were designed using the online platforms http::://crispr.mit.edu/guides and NeBio sgRNA designer and were ordered from Merck. Two guides were designed per target gene. Guides were stored at -80°C until injection.

Repair templates harboring the SNP site were designed using SeqBuilder (DNASTAR) targeting the desired gene and location of interest and were ordered from Merck. To change PAM sequences and to prevent further cutting by the Cas9, synonymous mutations were included. The injection mix contained 2 µl Cas9 EnGen (NEB), sgRNAs for *dpy-10* (0.6 µl) and *fln-2* (0.6 µl), repair templates for *dpy-10* (1 µl) and *fln-2* (1 µl), 0.25 µl KCl, 0.375 µl HEPES pH 7.4, and 3.875 µl water. L4 *daf-12(rh61rh411)* animals were used for the microinjections. Worms were placed in a drop of halocarbon oil (Sigma) on a 2% agarose pad. Injections were performed into both gonad arms using a Carl Zeiss imager Z1 microscope, which was installed with a manual micromanipulator connected to a microinjector (Femtojet4). The F1 generation was monitored for a dpy phenotype and singled out for *fln-2* SNP genotyping via PCR.

1.5. Lifespan analysis

Worm populations were synchronized as described above. Lifespan assays were performed at 20°C egg on. 20-30 worms per 6 cm plate were used to avoid overly dense populations. Worms were transferred to fresh plates daily for the first three days, then every other day until they stopped being reproductive. Worms were scored for survival every other day. Animals with internal hatching or vulval protrusion phenotypes were removed from the plates and censored from the analysis. All lifespans were blinded for genotypes and RNAi treatment.

1.6. Steroid supplementation

Worms were supplemented with steroids egg on. To do so, NGM plates were prepared and seeded with OP50 *E. coli* bacteria. Ready to use plates were infused with steroids the day of use by pipetting 50 µl Δ7-Dafachronic acid in EtOH on top of the bacterial lawn of a ∅ 6 cm plate. Control plates were infused with EtOH vehicle only. The final steroid concentration was determined considering the total agar volume.

1.7. Dauer formation assay

Worms were synchronized as described above to yield around 100 worms on each 3 cm plate. Eggs were grown at 27°C and scored for dauer-arrest phenotypes after 72 hours. A small, long and thin body shape was used as dauer characteristic.

1.8. Gonad migration phenotype assessment

To induce a gonad migration phenotype (mig), worms were grown under cholesterol depleted conditions. To achieve this, no cholesterol was added to NGM prior to pouring plates and OP50 bacteria were washed 4-5 times in 40 ml M9 buffer before seeding. Worms were synchronized as described above to yield around 50 eggs on each 6 cm plate. Worms were grown at 20°C until reaching adulthood. Gonad migration was determined by assessing the gonadal turn of both gonad arms (using a Zeiss Axio Imager Z1 microscope (DIC, 63x magnification)). Worms that displayed no turning or turning of just one gonad arm were considered mig.

2. Microscopy

2.1. Worm microscopy

Brightfield and fluorescent images were acquired using a Zeiss Axio Imager Z1 Fluorescence Microscope equipped with the Digital Microscope Camera Axio Cam Mono 506 and the IcC5 true color camera. For fluorescence microscopy, the microscope used a 120 Colibri 7 LED Light Source and the filters sets GFP (Set 38 HE), TR (Set 45), and TL. The software used was Zeiss Zen v2.3.69.1017.

Brightfield and fluorescent images were also acquired with the Leica stereo microscope MDG41 equipped with Leica DFC3000G monochrome camera. The microscope was equipped with the Leica EL6000 external light source. The software used was the Leica Application Suite X v3.7.5.24914.

For imaging purposes worms were treated with 50 mM sodium azide and imaged once they were anesthetized.

2.2. Reporter protein measurement

HLH-30::NeonGreen nuclear localization was analyzed in the seam cells of L4 larval-staged animals. Worms were anesthetized with 50 mM sodium azide for 1 minute and imaged for HLH-30::NeonGreen nuclear localization for another 3 minutes (DIC and GFP (Set 38 HE)). After a total of 4 minutes the slides were discarded to minimalize stress induced HLH-30 translocation. Localization was scored as cytosolic or nuclear.

Intensity of DAF-36::GFP, DAF-9::GFP, DAF-12::GFP, DAF-40::GFP, DHS-16::GFP, and DHS-26::Scarlet was quantified in age matched worms comparing treated and control conditions. Fiji image analysis software was used for the quantification of the fluorescence by manually selecting the region of interest and background signal. Mean fluorescence intensity of the selected regions of interest was quantified. Worm fluorescence intensity was corrected by background subtraction.

2.3. Nucleolar size measurement

Nucleolar size was assessed in day 1 adults. The nuclei and nucleoli of the hypodermal cells in the head were visualized using differential interference contrast (DIC) microscopy with a 100x magnification. Worms were anesthetized using 50 mM sodium azide. Worms were imaged once they stopped moving. The freehand tool of Fiji was used to manually analyze the area of nuclei and nucleoli. 3-4 nucleoli were measured for each worm, 10 worms were measured for each condition.

3. Molecular biology

3.1. RNA extraction

Worms were synchronized by egg lay of day 1 adults and were collected at early day 1 stage. Worms were collected in 15 mL M9 buffer and washed three times with M9 to remove bacterial contaminations. Washed worms were resuspended in 700 µl QIAzol lysis reagent (Qiagen), snap-frozen in liquid nitrogen, and stored at -80°C until extraction. To lyse the worms, 200 µL of 0.1 mm Zirconia/Silica beads (FisherScientific) were added to the thawed worm suspension and transferred to the TissueLyser LT (Qiagen) for 15 min, full speed at 4°C. RNA extraction and purification were performed using the RNeasy Mini Kit (Qiagen) and the miRNeasy Mini Kit (Qiagen) according to the manufacturers' protocol. RNA was eluted in 50 µl RNase-free water. RNA purity and concentration were assessed using the NanoPhotometer NP80 spectrophotometer (Implen). RNA was stored at -80°C.

3.2. RNA sequencing

RNA was extracted as described above. The RNA libraries were prepared by the Cologne Center for Genomics (CCG). The removal of ribosomal RNA was conducted using the RiboZero rRNA removal kit (Illumina). Sequencing was performed on Illumina HiSeq4000 sequencing system (25 million reads per sample) using a paired-end 2 x 100-nt sequencing protocol.

Sequencing analysis was performed by the bioinformatics core facility. In brief, Ensembl Caenorhabditis elegans release 105/ce11 was used as the reference sequence, rRNA transcripts were removed from the annotation file and reads were pseudo aligned to the reference transcriptome and were quantified using kallisto/0.46.1 (https://www.nature.com/articles/nbt.3519). Read counts were normalized by making use of the standard median-ratio for estimation of size factors and pair-wise differential gene expression was calculated using DEAes/1.24.0 (https://genomebiology.biomedcentral.com/articles/10.1186/s13059-014-0550-8). Genes with fewer than ten overall reads were removed and overall log2 changes were shrank using approximate posterior estimation for GLM coefficients.

The KEGG pathway analysis of significant genes was performed using the DAVID bioinformatics resource database.

4. Biochemistry

4.1. Protein extraction and western blot analysis

Day 1 worms were harvested from a synchronized population achieved by egg lay. The worm pellet was snap-frozen in liquid nitrogen and stored at -80°C until extraction. The pellet was resuspended in lysis buffer supplemented with 1 unit for 10 ml cOmplete ULTRA EDTA-free protease inhibitors (Roche) and 1 unit for 10 ml PhosSTOP phosphatase inhibitors (Roche) and was sonicated with Bioruptor Plus (Diagenode S.A.) coupled to Minichiller 300 (Huber) for 15 cycles of 30 sec sonication, 30 sec rest at 4 °C. The total protein extract was cleared by spinning down at 13,000 g for 10 min at 4 °C. Supernatant was transferred to a new tube, and protein was quantified using Pierce BCA Protein Assay Kit (ThermoFisher Scientific) according to the manufacturer's instructions. Reagents and samples were incubated at 37!C for 30 mins before measurement.

Equal amounts of protein were mixed with 4X loading buffer containing 50 mM DTT and boiled at 95°C for 10 min. Samples were loaded onto an SDS-PAGE PERCENTAGE gel (BioRad), and proteins were then transferred onto a nitrocellulose membrane (BioRad) using the Trans-Blot Turbo Transfer System (BioRad). Membranes were blocked for 1 h at RT with 5% milk in TBST. Primary and secondary antibodies (**Table** VIII-2) were diluted in 5% skim milk in TBST and incubated for 5-18 h at 4°C. The membranes were washed three times with TBST for 10 min at RT after primary and secondary antibody incubation. The signals were detected using Western Lightning Plus-ECL, Enhanced Chemiluminescence Substrate (PerkinElmer), and imaged in the ChemiDoc MP Imaging System with Image Lab software (BioRad).

Table VIII-2: List of antibodies.

Antibody	Vendor	Cat. Number	Dilution
Anti-beta Actin antibody	Abcam	Ab8224	1:2,000
Phospho-AMPKa (Thr172) (40H9)	CST	2535	1:1,000
Anti-alpha Tubulin antibody	Abcam	Ab4074	1:2,000
Anti-rabbit IgG (H+L)	Invitrogen	G21234	1:10,000
Anti-mouse IgG	Invitrogen	G21040	1:10,000

4.2. Single worm proteomics

4.2.1. Single worm proteomics – Sample preparation

4 µL lysis buffer (0.25% DDM, 125 mM TEAB, 10 mM TCEP (Tris(2-carboxyethyl) phosphine), 20 mM CAA (chloroacetamide)) were added to each PCR tube on ice. A single worm was added to each tube, and the tubes were immediately frozen in liquid nitrogen until ready for further processing. 8 single worms were used for each condition.

The tubes with a single worm each were thawed simultaneously in a water bath at RT, and the samples were frozen and thawed two additional times to ensure proper cell lysis. The samples were then sonicated with Bioruptor Plus (Diagenode S.A.) coupled to Minichiller 300 (Huber) (20 cycles, 30 seconds on, 30 seconds off) while maintaining a temperature of 4°C.

While the Bioruptor was running, Trypsin/LysC protease (1 µg/µl Trypsin and 0.5 µg/µl LysC in 50mM acetic acid) was diluted 10-fold in LCMS water to create the "DiluteProtease" solution. After the Bioruptor treatment, 5 µL of cold PBS (“Invitrogen 10x PBS” diluted 10-fold with LCMS water) was added to each sample, followed by 1 µL of the DiluteProtease. The samples were mixed briefly and spun down. The samples were incubated at 37°C overnight in a PCR cycler. After the incubation, the samples are ready for loading into EvoTips for further analysis.

4.2.2. Single worm proteomics – Measurement and analysis

The digested single worm lysis was loaded to the EvoTip Pure according to manufacturer’s instruction.

The Evosep One liquid chromatography system (Bache, Geyer et al. 2018) was used for analyzing the samples with the predefined 30 samples per day (30SPD) method. The analytical column used was an ReproSil-Pur column, 15 cm x 150 µm, with 1.9 µm C18 beads (EV1106 Endurance Column, Evosep). The mobile phases A and B were 0.1 % formic acid in water and 0.1% formic acid in 100% ACN, respectively.

Peptides were analyzed on a hybrid TIMS quadrupole TOF mass spectrometer (timsTOF Pro 2, Bruker) in a data-independent acquisition parallel accumulation, serial fragmentation (diaPASEF) mode. The mass spectra range was set to 100-1700 m/z and TIMS ion accumulation and ramp times were set to 100 ms and total cycle time was 2.0 s. The ion mobility range was set to 1/K0 = 0.8-1.25 V s/cm^2. Isolation windows in the m/z versus ion mobility plane were defined to cover the region of highest precursor ion density with an m/z slice width of 26 Th. Collision energy was applied linearly with ion mobility from 0.6 to 2.0 V s/cm^2, and collision energy from 20 to 59 eV.

Raw data was analyzed using Spectronaut version 19.3.24 (Biognosys) using the default parameters against the one-protein-per-gene reference proteome for *C. elegans*, UP000001940, downloaded August, 2022. Methionine oxidation and protein N-terminal acetylation were set as variable modifications; cysteine carbamidomethylation was set as fixed modification. The digestion parameters were set to “specific” and “Trypsin/P,” with two missed cleavages permitted. Protein groups were filtered for at least two valid values in at least one comparison group and missing values were imputed from a normal distribution with a down-shift of 1.8 and standard deviation of 0.3. Differential expression analysis was performed using limma, version 3.60.6 (Ritchie, Phipson et al. 2015), in R, version 4.4.0 (Ritchie, Phipson et al. 2015).

4.3. Metabolomics

Semi-targeted Metabolomics – AEX-MS

To analyze the whole metabolome semi-targeted metabolomics was performed. Day 1 adult worms were collected in five biological replicates, using NGM plates that were supplemented with cholesterol of high purity (Sigma, ≥99%). Samples were collected in single tubes and washed three times in M9 buffer, before being snap-frozen and stored at -80°C until analysis. 500 µl extraction buffer and 250 µl zirconium beads were added to the samples and samples were lysed at 4°C for 30 min with 50 Hz. The supernatant after 10 min centrifugation at 21,000 rpm was transferred into two vials, 450 µl for LC-MS analysis and 450 µl for AEX-GC-MS analysis. The worm pellet was re-extracted by treatment with 1 ml MeOH. Re-extracted samples were centrifuged for 10 min at 21,000 rpm and again 450 µl again supernatant was

added to the previous vials already containing 450 µl, resulting in 900 µl extract for each MS analysis.

Extracted metabolites were re-suspended in 150 µl of UPLC/MS grade water (Biosolve), of which 100 µl were transferred to polypropylene autosampler vials (Chromatography Accessories Trott, Germany) before AEX-MS analysis.

The samples were analyzed using a Dionex ionchromatography system (Integrion Thermo Fisher Scientific) (Schwaiger, Rampler et al. 2017). In brief, 5 µL of polar metabolite extract were injected in push partial mode, using an overfill factor of 1, onto a Dionex IonPac AS11-HC column (2 mm × 250 mm, 4 µm particle size, Thermo Fisher Scientific) equipped with a Dionex IonPac AG11-HC guard column (2 mm × 50 mm, 4 µm, Thermo Fisher Scientific). The column temperature was held at 30°C, while the auto sampler was set to 6°C. A potassium hydroxide gradient was generated using a potassium hydroxide cartridge (Eluent Generator, Thermo Scientific), which was supplied with deionized water (Millipore). The metabolite separation was carried at a flow rate of 380 µL/min, applying the following gradient conditions: 0-3 min, 10 mM KOH; 3-12 min, 10−50 mM KOH; 12-19 min, 50-100 mM KOH; 19-22 min, 100 mM KOH, 22-23 min, 100-10 mM KOH. The column was re-equilibrated at 10 mM for 3 min.

For the analysis of metabolic pool sizes the eluting compounds were detected in negative ion mode using full scan measurements in the mass range m/z 77 – 770 on a Q-Exactive HF high resolution MS (Thermo Fisher Scientific). The heated electrospray ionization (HESI) source settings of the mass spectrometer were: Spray voltage 3.2 kV, capillary temperature was set to 300°C, sheath gas flow 50 AU, aux gas flow 20 AU at a temperature of 330°C and a sweep gas flow of 2 AU. The S-lens was set to a value of 60.

The semi-targeted MS data analysis was performed using the TraceFinder software (Version 5.1, Thermo Fisher Scientific). The identity of each compound was validated by authentic reference compounds, which were measured at the beginning and the end of the sequence. For data analysis the area of the deprotonated $[M\text{-}H+]^{-1}$ or doubly deprotonated $[M\text{-}2H]^{-2}$ monoisotopologue mass peaks of every required compound were extracted and integrated using a mass accuracy <3 ppm and a retention time (RT) tolerance of <0.05 min as compared

to the independently measured reference compounds. These areas were then normalized to the internal standards, which were added to the extraction buffer, followed by a normalization to the fresh weight of the analyzed sample.

Semi-targeted Metabolomics – LC-HRSMS

For metabolomics measurement of compounds containing amines, LC-HRMS analysis was performed (Bonekamp, Peter et al. 2020). Samples were extracted as described previously.

50 µL of the available 400 µL of the above mentioned (AEX-MS) polar phase were mixed with 25 µl of 100 mM sodium carbonate (Sigma), followed by the addition of 25 µl 2% [v/v] benzoylchloride (Sigma) in acetonitrile (UPC/MS-grade, Biosove). Derivatized samples were thoroughly mixed and kept at 20°C until analysis.

For the LC-HRMS analysis, 2 µl of the derivatized sample was injected onto a 100 x 2.1 mm HSS T3 UPLC column (Waters). The flow rate was set to 400 µl/min using a binary buffer system consisting of buffer A (10 mM ammonium formate (Sigma), 0.15% [v/v] formic acid (Sigma) in UPC-MS-grade water (Biosolve, Valkenswaard, Netherlands). Buffer B consisted of acetonitrile (IPC-MS grade, Biosolve, Valkenswaard, Netherlands). The column temperature was set to 40°C, while the LC gradient was: 0% B at 0 min, 0-15% B 0- 4.1min; 15-17% B 4.1 – 4.5 min; 17-55% B 4.5-11 min; 55-70% B 11 – 11.5 min, 70-100% B 11.5 - 13 min; B 100% 13 - 14 min; 100-0% B 14 -14.1 min; 0% B 14.1-19 min; 0% B. The mass spectrometer (Q-Exactive Plus, Thermo Fisher Scientific) was operating in positive ionization mode recording the mass range m/z 100-1000. The heated ESI source settings of the mass spectrometer were: Spray voltage 3.5 kV, capillary temperature 300°C, sheath gas flow 60 AU, aux gas flow 20 AU at 330°C and the sweep gas was set to 2 AU. The RF-lens was set to a value of 60.

Semi-targeted data analysis for the samples was performed using the TraceFinder software (Version 5.1, Thermo Fisher Scientific). The identity of each compound was validated by authentic reference compounds, which were run before and after every sequence. Peak areas of $[M + nBz + H]^+$ ions were extracted using a mass accuracy (<3 ppm) and a retention time tolerance of <0.05 min. Areas of the cellular pool sizes were calculated as described in the AEX-MS method.

Steroidomics – Sample preparation

Day 1 adult worms were collected in four or five biological replicates, using NGM plates that were supplemented with cholesterol of high purity (Sigma, ≥99%). For synchronization, staged day 1 adults were bleached and eggs cultured on 30x10 cm plates per condition for a total of ~20,000 worms. Day 1 adults were harvested in M9 buffer and centrifuged at 300xg for 2 min to remove the supernatant. Pellets were snap-frozen and stored at -80°C until extraction. Worm harvest was performed within 4 minutes per condition to minimize changes in metabolome.

Samples were taken from -80°C freezer and stored on dry ice. Sequentially, 200 µl zirconium beads (1mm) and 1 ml of extraction buffer (50 ml MeOH, 20 µl Cholesterol D7) were added to the sample and stored on dry ice. Samples were taken from dry ice and immediately lysed in a tissue lyser for 30 min with 50 Hz at 4°C. Samples were transferred to 5 ml tubes and 3 ml of methanol was added. To fully homogenized worms, the samples were further sonicated with Bioruptor Plus (Diagenode S.A.) coupled to Minichiller 300 (Huber) (20 cycles, 30 seconds on, 30 seconds off) in a water bath filled with ice and with the zirconium beads still in the sample. From the total volume of 4 ml an aliquot of 200 µl from the homogenized and mixed samples was transferred to a fresh 1.5 ml Eppendorf tube and centrifuged with 21000 rpm at 4°C for 10 min to get a protein pellet for quantification. To get a cleared extract, 5 ml tubes were centrifuged at 4°C with 21000 rpm for 10 min and supernatant was transferred and aliquoted in 1700 µl for LC-MS analysis, 1700 µl for GC-MS analysis and 200 µl for metabolomics analysis.

All samples were dried in a speed vac and stored at -80 °C until analysis.

Steroidomics – GC-MS analysis of small molecules

Cholesterol, 7-ketocholesterol, 7-beta-hydroxycholesterol, 7-alpha-hydroxycholesterol, 7-Dehydrocholesterol, and Lathosterol were measured using GC-MS (Gas Chromatography coupled to a Q-Exactive-Orbitrap mass spectrometer, Thermo Fisher Scientific). For this purpose, metabolites were derivatized using a two-step procedure starting with an methoxyamination (methoxyamine hydrochlorid, Sigma) followed by a trimethyl-silylation

using N-Methyl-N-trimethylsilyl-trifluoracetamid (MSTFA, Macherey-Nagel). Analysis was performed as described previously with slight modifications.

Dried samples were methoxyaminated by re-suspending them in 10 µL of a freshly prepared (40 mg/mL) solution of methoxyamine in pyridine (Sigma). The samples were incubated for 45 min at 40°C on an orbital shaker (VWR) at 1500 rpm. In the second step 90 µL of MSTFA spiked with C8 - C40 Alkane standard (40147-U, Sigma Aldrich) to a concentration of 1 µg/ml was added and the samples were incubated for additional 45 min at 40°C and 1500 rpm. At the end of the derivatization the samples were centrifuged for 2 min at 21100x g and the clear supernatant was transferred to fresh auto sampler vials with conical glass inserts (300 µl, Chromatographie Zubehoer Trott). For the GC-MS analysis 0.5 µL of each sample was injected using a TriPlus RSH autosampler system (Thermo Fisher Scientifc) using a Split/SplitLess (SSL) injector at 250°C in splitless mode. The carrier gas flow (helium) was set to 1 ml/min using a 30m MEGA-5 MS capillary column (0.250 mm diameter and 0.25 µm film thickness, MEGA). The GC temperature program was: 1 min at 70°C, followed by a 9°C per min ramp to 350°C. At the end of the gradient the temperature is held for additional 5 min at 350°C. The transfer line and source temperature are both set to 280°C. The filament, which was operating at 70 eV, was switched on 4.5 min after the sample was injected. During the whole gradient period the MS was operated in full scan mode covering a mass range m/z 70 and 700 with a resolution of 60.000.

The GC-MS data analysis was performed using the open-source software El Maven (Agrawal, Kumar et al. 2019) (Version 0.12.0). For this purpose, Thermo raw mass spectra files were converted to mzML format using MSConvert (Chambers, Maclean et al. 2012) (Version 3.0.22060, Proteowizard). The identity of each compound was validated by authentic reference compounds, which were measured at the beginning or at the end of the sequence, furthermore, a compound's identity was matched to EI spectra and the retention index (RI).

For data analysis the peak areas of extracted ion chromatograms from selected fragment ions were determined with El Maven; only in rare cases peaks were manually re-integrated. Extracted ion chromatograms were generated with a mass accuracy of <5 ppm and a retention time (RT) tolerance of <0.05 min as compared to the independently measured reference compounds. These areas were then normalized to the internal standards, which

were added to the extraction buffer, followed by a normalization to the the protein content of the analyzed samples.

Steroidomics – LC-MS analysis of dafachronic acids

Δ-7-DA was measured using LC-MS. Dried samples were reconstituted in 100 µl 80% MeOH for 10 min on a shaker with 1500 rpm at 4°C. Samples were centrifuged at 21000 rpm for 10 min at 4°C and supernatant was transferred to glass LC Autosampler Vials with 300 µl glass inserts. Of the sample 20 µl were injected and analyzed in a Vanquish horizon UHPLC coupled to a QExactive plus HRMS (Thermo Fisher Scientific).

Separation on the UHPLC system was done on a HSS T3, 2.1 x 150 mm column with precolumn and a gradient elution with buffer A 85% MeOH and buffer B 100 % MeOH both with 5 mM Ammonium acetate. The column was kept at 30°C and the flow rate was 300 µl/min and the gradient as follows: 0-2 min, 0% B; 2-15 min 0-100% B, 15-25 min, 100%B and 25.1-27.5, 0% B. The MS was running in negative mode from 0-15 min and in positive mode from 15-27.5 min. Cholestenones and dafachronic acids were analyzed with a t-SIM scan and identity was validated by running pure reference compounds. Data was extracted using TraceFinder (v. 5.1, Thermo Fisher Scientific) software by integrating the respective peaks in the t-SIM scans of the [M-H]- and [M+H]+ adduct mass traces, respectively, with a mass accuracy of <5 ppm and a retention time (RT) tolerance of <0.05 min as compared to the independently measured reference compounds.

5. Bioinformatical target gene prediction

DAF-12 binding motif prediction on the *dhs-26* genomic region was done by utilizing the online platform https://meme-suite.org/meme/. The area used as the *dhs-26* genomic region included 5,000 bp upstream of the start codon, as well as 5,000 bp downstream of the ATG start site. The genomic region was compared to DAF-12 binding motifs published in the open-access database of transcription factor binding profiles by Wassermann *et al*. (**Figure VIII-1, Table** VIII-3) (Mathelier, Zhao et al. 2014), which is based on DAF-12 ChiP-seq data. DAF-12 binding site occurrence on the *dhs-26* genomic region was determined with a *p* value cutoff set to 0.001.

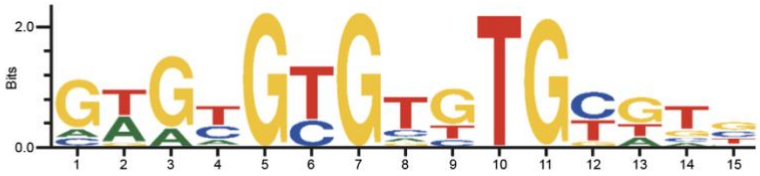

Figure VIII-1: Consensus sequence of the DAF-12 motif M2332_1.02. Motif occurrence of DAF-12 binding sites was determined using open-access database of transcription factor binding profiles by Wassermann *et al.* (Mathelier, Zhao et al. 2014). Probability matrix is listed below (Table VIII 2).

Table VIII-3: Letter probability matrix of DAF-12 binding motif M2332_1.02.

Position/Nucleotide	A	C	G	T
1	0.141026	0.128205	0.724359	0.006410
2	0.455128	0.000000	0.083333	0.461538
3	0.211538	0.000000	0.788462	0.000000
4	0.147436	0.333333	0.038462	0.480769
5	0.000000	0.000000	1	0.000000
6	0.000000	0.333333	0.000000	0.666667
7	0.000000	0.000000	1	0.000000
8	0.096154	0.160256	0.089744	0.653846
9	0.000000	0.128205	0.621795	0.250000
10	0.006410	0.000000	0.000000	0.993590
11	0.000000	0.006410	0.987179	0.006410
12	0.000000	0.506410	0.102564	0.391026
13	0.205128	0.000000	0.538462	0.256410
14	0.108974	0.128205	0.179487	0.583333
15	0.108974	0.275641	0.358974	0.256410

6. Statistical analysis

The results are presented as mean ± standard deviation (SD). The number of biological replicates is shown in the figure legends. For normally distributed data, unpaired *t*-test with Welch's correction or one-way ANOVA with Brown-Forsythe and Welch's correction were calculated in GraphPad Prism 9 (GraphPad software). For lifespan analysis, *p*-values were calculated using Log-rank (Mantel-Cox) test. Statistical data from all the lifespans except for RNAi screen lifespan data can be found below (**Table** IX-1). RNAi screen lifespan data of significant RNAi hits can be found below (**Table** IX-2 **and Table** IX-3). For RNAseq data, KEGG and GO terms enrichment analysis was performed using Fisher's test. Genes included in KEGG

and GO enrichment terms are listed below (**Table** IX-4 **and Table** IX-5). Significance levels are: not significant (ns) $p>0.05$, * $p<0.05$. ** $p<0.01$, *** $p<0.001$, **** $p<0.0001$.

7. Software

Image analysis was performed using Fiji. Graphs were generated using GraphPad Prism 9. Images were designed using Adobe Illustrator.

Table VIII-4: Worm strains used for this work.

Name	Genotype	Short Name	Source
	N2 (Bristol)	*N2/wild type*	CGC
AA5288	*nhr-8(hd117)IV;fln-2(ot611)X*	*nhr-8*	This work
AA5286	*daf-36(k114)V;fln-2(ot611)X*	*daf-36*	This work
AA1052	*dhs-16(tm1890)V*	*dhs-16*	J. Wollam
AA5287	*daf-9(rh50) fln-2(ot611)X*	*daf-9*	This work
AA1053	*daf-40(hd100)II*	*daf-40*	J. Wollam
AA5291	*daf-12(rh61rh411)X;fln-2(ot611)X*	*daf-12*	This work
AA408	*din-1(dh127)II*	*din-1*	A. Antebi
PHX8968	*dhs-26(syb8968)X*	*dhs-26*	This work
VC533	*raga-1(ok701)II*	*raga-1*	CGC
AA5297	*raga-1(ok701)II;nhr-8(hd117)IV*	*raga-1;nhr-8*	This work
AA5295	*raga-1(ok701)II;daf-36(k114)V*	*raga-1;daf-36*	This work
AA5447	*raga-1(ok701)II;dhs-16(tm1890)V*	*raga-1;dhs-16*	This work
AA5294	*raga-1(ok701)II;daf-9(rh50)X*	*raga-1;daf-9*	This work
AA5446	*raga-1(ok701) daf-40(hd100)II*	*raga-1;daf-40*	This work
AA5293	*raga-1(ok701)II;daf-12(rh61rh411)X*	*raga-1;daf-12*	This work
PHX809	*raga-1(ok701) din-1(dh127)II*	*raga-1 din-1*	This work
AA5841	*raga-1(ok701)II;dhs-26(syb8968)X*	*raga-1;dhs-26*	This work
PHX809	*hlh-30(syb809)*	*hlh-30::NG*	A. Antebi
AA5301	*hlh-30(syb809) nhr-8(hd117)IV*	*hlh-30::NG; nhr-8*	This work
AA5300	*hlh-30(syb809)IV;daf-36(k114)V*	*hlh-30::NG; daf-36*	This work
AA5299	*hlh-30(syb809)IV;daf-9(rh50)X*	*hlh-30::NG; daf-9*	This work
AA5298	*hlh-30(syb809)IV;daf-12(rh61rh411)X*	*hlh-30::NG; daf-12*	This work
AA5587	*din-1(dh127)II;hlh-30(syb809)IV*	*din-1;hlh-30::NG*	This work
AA5197	*raga-1(ok701)II;hlh-30(syb809)IV*	*raga-1;hlh-30::NG*	This work
AA5302	*raga-1(ok701)II;hlh-30(syb809)IV;daf-36(k114)V*	*raga-1;daf-36;hlh-30::NG*	This work
AA5586	*raga-1(ok701) din-1(dh127)II;hlh-30(syb809)IV*	*raga-1 din-1, hlh-30::NG*	This work
AA752	*dhEx320(Pdaf-36::daf-36::gfp)*	*daf-36::GFP*	V. Rottiers
AA2591	*dhs-16(tm1890)V; dhEx396(Pdhs-16::dhs-16::gfp; lin-15(+))*	*dhs-16 dhs-16::GFP*	J. Wollam
AA2646	*dhIs64(Pdaf-9::daf-9::GFP; lin-15[+])*	*daf-9::GFP*	J. Wollam
AA1087	*dhs-16(tm1890)X;dhIs64(Pdaf-9::daf-9::GFP; lin-15[+])*	*dhs-16 daf-9::GFP*	J. Wollam
AA120	*dhIs26(daf-12A::GFP, lin-15(+))I*	*daf-12::GFP*	CKE
AA1055	*dhEx460(Pdaf-40::daf-40::gfp; coel::rfp)*	*daf-40::GFP*	J. Wollam
AA5244	*raga-1(ok701)II;dhEx320(Pdaf-36::daf-36::gfp)*	*raga-1;daf-36::GFP*	This work

AA5448	*raga-1(ok701)II;dhEx396(Pdhs-16::dhs-16::gfp; lin-15(+))*	*raga-1;dhs-16::GFP*	This work
AA5261	*raga-1(ok701)II;dhIs64(Pdaf-9::daf-9::GFP;lin-15(+))*	*raga-1;daf-9::GFP*	This work
AA5449	*raga-1(ok701)II;dhEx460(Pdaf-40::daf-40::gfp; coel::rfp)*	*raga-1;daf-40::GFP*	This work
AA5199	*dhIs26(daf-12A::GFP; lin-15(+))I;raga-1(ok701)II*	*raga-1;daf-12::GFP*	This work
AA5271	*raga-1(ok701)II;dhEx151(din-1::GFP; rol-6+)*	*raga-1;din-1::GFP*	This work
AA5839	*daf-36(k114)V;dhs-26(syb8968)X*	*daf-36;dhs-26::FLAG::Scarlet*	This work
AA5875	*daf-12(rh61rh411) dhs-26::FLAG::Scarlet(syb8359)X*	*daf-12;dhs-26::FLAG::Scarlet*	This work
PHX8359	*dhs-26(syb8359)X*	*dhs-26::FLAG::Scarlet*	This work
AA5840	*raga-1(ok701)II;dhs-26(syb8359)X*	*raga-1;dhs-26::FLAG::Scarlet*	This work
AA1355	*dhIs500(mir-84p::gfp,ttx-3::rfp))*	*mir-84p::GFP*	A. Riezenman
AA1294	*dhEx458(mir-241pFL::4xNLS::gfp::unc-54UTR; coel::rfp)*	*mir-241p::GFP*	A. Bethke
AA5490	*raga-1(ok701)II;dhIs501(mir-84p::gfp, ttx-3::rfp))*	*raga-1;mir-84p::GFP*	This work
AA5489	*raga-1(ok701)II;dhEx458(mir-241pFL::4xNLS::gfp::unc-54UTR; coel::rfp)*	*raga-1;mir-241p::GFP*	This work
AA1205	*dhIs26(daf-12A::GFP, lin-15(+))I;mir-48mir-241(nDf51)V;mir-84(n4037)X*	*mir-48 mir-241;mir-84;daf-12::GFP*	A. Antebi
LIU1	*ldrIs1[dhs-3p::dhs-3::GFP + unc-76(+)]*	*dhs-3::GFP*	CGC
AA5874	*ldrIs1[dhs-3p::dhs-3::GFP + unc-76(+)];dhs-26::FLAG::Scarlet(syb8359)X*	*dhs-3::GFP;dhs-26::FLAG::Scarlet*	This work
WBM1177	*wbmIs81[eft-3p::3XFLAG::GFP::SKL::unc-54 3'UTR, *wbmIs65]*	*eft-3p::GFP::SKL*	CGC
NL2099	*rrf-3(pk1426)II*	*rrf-3*	CGC
YY166	*ergo-1(gg98)V*	*ergo-1*	CGC
GR1373	*eri-1(mg366)IV*	*eri-1*	CGC

Table VIII-5: Oligonucleotides used for this work.

Name	Sequence	Used for
nhr-8(dh117) F	CGTGAATCACAGTTAACTATGCG	genotyping
nhr-8(dh117) R	CCATTCACTGTTCATTCCAAC	genotyping
daf-36(k114) F	CCGGAATTTCCCATTCTGGT	genotyping
daf-36(k114) R	CAGGTAGTACGTGACAATTGCA	genotyping
dhs-16(tm1890) F	GATCACTGTCAACTTATCGG	genotyping
dhs-16(tm1890) R	GGCTAGTTACATCGAGTTG	genotyping
daf-9(rh50) F	AGCAGGAACAATTCAGGTAAGA	genotyping
daf-9(rh50) R	CTCACATACGGCGTCTGATT	genotyping
daf-40(hd100) F	CTACCAAGAATACACCATGG	genotyping
daf-40(hd100) R	CTAGTCTTATTTCCTGTCTC	genotyping
daf-12(rh61) F	GTGAGGTATCTCAGGAAGGAAAG	genotyping
daf-12(rh61) R	CTCGTCGAAGAAACCGAAGAA	genotyping
daf-12(rh411) F	GATCATGCGACGGGCTATAA	genotyping
daf-12(rh411) R	CATACCAACTGTGAAGCATTTCC	genotyping
din-1(dh127) F	GGTAGGAATTGCAAACCCGC	genotyping
din-1(dh127) R	GCACAACGCTGAATAGAGAC	genotyping
dhs-26(syb8968) F	TTTGCCCAGAAGTTTCCAGT	genotyping
dhs-26(syb8968) R	ACTGGGGCAATGTTTCTCTA	genotyping
dhs-26::Scarlet F	GCTTCAAAGTTGTGGATCGC	genotyping
dhs-26::Scarlet R	GTAGAGCAGCAGCTTGTGTG	genotyping
raga-1 F	GTGGTTATTGAAATTCAATTATT	genotyping
raga-1 R	CTCCACCGATGTCTTTATC	genotyping
PHX7281 F	ATGCTCATGTCAAGTAAGGG	genotyping
PHX7281 R	CGGCTCACAATATCTCTTGG	genotyping
hlh-30::NG F	CGCTCATCCATCACCACACT	genotyping
hlh-30::NG R	ACTTGGGAACGGGCAAATGTA	genotyping
fln-2(ot611) F	CATTCACTCCGGACGGCGCTGGTGAATT	genotyping
fln-2(ot611) R	AACGGATGCTGATCTCAAGTTC	genotyping
fln-2(ot611) F	GGCTTAGTTAACAAGTGTCG	sequencing
fln-2(ot611) R	GTTGAACAGGAGACTTGGAC	sequencing
fln-2 guide RNA 1	TTCTAATACGACTCACTATAGCAAGTTTCATTCACTCCGG AGTTTTAGAGCTAGA	CRISPR
fln-2 guide RNA 2	TTCTAATACGACTCACTATAGTCATTCACTCCGGACGGCG CGTTTTAGAGCTAGA	CRISPR
fln-2 repair template	CAAGTTTCGTTCACACCGGACGGAGCTGGTCAATAAAAA ATCCACGTTCTTTTTAACAGAATGGAAATTAA	CRISPR
dpy-10 guide RNA	TTCTAATACGACTCACTATAGCTACCATAGGCACCACGAG GTTTTAGAGCTAGA	CRISPR
dpy-10 repair template	CACTTGAACTTCAATACGGCAAGATGAGAATGACTGGAA ACCGTACCGCATGCGGTGCCTATGGTAGCGGAGCTTCAC ATGGCTTCAGACCAACAGCCTAT	CRISPR

Table VIII-6: Media, Buffers, and Solutions.

Nematode Growth Media (NGM)	
NaCl	0.3% (w/v) (51.3 mM)
Bacto Peptone	0.25% (w/v)
Bacto Agar	1.7% (w/v)
KPO_4 (Stock 1 M)	25 mM
Cholesterol (Stock 5 mg/mL)	5 µg/mL
$MgSO_4$ (Stock 1 M)	1 mM
$CaCl_2$ (Stock 1 M)	1 mM
Dissolve in ddH_2O and autoclave. Add cholesterol, $MgSO_4$, and CaCl after autoclaving.	

Luria-Bertani (LBH) media	
NaCl	0.5% (w/v) (85.55 mM)
Bacto Yeast Extract	0.5% (w/v)
Tryptone	1% (w/v)
Dissolve in ddH_2O and autoclave.	

Luria-Bertani (LBH) media plates with ampicillin	
NaCl	0.5% (w/v) (85.55 mM)
Bacto Yeast Extract	0.5% (w/v)
Tryptone	1% (w/v)
Bacto Agar	1.5% (w/v)
NaOH (Stock 1 M)	1 mM
Ampicillin (Stock 50 mg/mL)	100 µg/mL
Dissolve in ddH_2O and autoclave. Add ampicillin after autoclaving.	

M9 buffer	
NaCl	0.5% (w/v) (85.55 mM)
Na_2HPO_4	42.26 mM
KH_2PO_4	22.04 mM
$MgSO_4$ (Stock 1 M)	1 mM
Dissolve in ddH_2O and autoclave. Add the $MgSO_4$ after autoclaving.	

Bleaching solution	
NaClO (Stock 6%)	1.8%
KOH (Stock 5 M)	0.75 M
Dissolve in ddH_2O and keep at 4°C in an amber bottle.	

Single worm lysis buffer	
Tris pH 8.3	10 mM
KCl	50 mM
$MgCl_2$	2.5 mM

Tween-20	0.45% (v/v)
Triton X-100	0.45% (v/v)
Proteinase K (NEB)	1 mg/mL
Dissolve in ddH_2O.	

TBST buffer	
Tris base	24.77 mM
NaCl	137 mM
KCl	2.68 mM
Tween-20	0.05%
Dissolve in ddH_2O and adjust the pH to 7.4.	

Lysis buffer (for protein extraction)	
Tris/HCl, pH 7.4	50 mM
NaCl	150 mM
EDTA	1 mM
NP-40	0.5% (v/v)
Dissolve in ddH_2O and store at 4°C. Add protease and phosphatase inhibitors before using.	

SDS-PAGE running buffer	
Tris base	24.77 mM
Glycine	192 mM
SDS	3.47 mM
Dissolve in ddH_2O.	

Transfer buffer	
Trans-Blot Turbo 5x Transfer Buffer (BioRad)	200 mL
Ethanol	200 mL
ddH_2O	600 mL

IX. Supplementary data

Table IX-1: Lifespan analysis.

Genotype	Mean ± SD	No. of exps	*P* value	Compared to
N2 (wild type)	23 ± 1	3		
daf-36(k114)	21 ± 1	3	ns	to N2
raga-1(ok701)	29 ± 1	3	<0.00001	to N2
raga-1;daf-36	24 ± 1	3	0.00017	to *raga-1*
N2 (wild type)	21 ± 1	3		
daf-9(rh50)	20 ± 1	3	ns	to N2
raga-1(ok701)	28 ± 1	3	<0.00001	to N2
raga-1;daf-9	18 ± 1	3	<0.00001	to *raga-1*
N2 (wild type)	22 ± 1	3		
daf-40(dh100)	23 ± 1	3	ns	to N2
raga-1(ok701)	30 ± 2	3	<0.00001	to N2
raga-1;daf-40	24 ± 1	3	<0.00001	to *raga-1*
N2 (wild type)	24 ± 0	3		
daf-12(rh61rh411)	20 ± 1	3	0.00012	to N2
raga-1(ok701)	29 ± 2	3	<0.00001	to N2
raga-1;daf-12	22 ± 1	3	<0.00001	to *raga-1*
N2 (wild type)	22 ± 2	3		
nhr-8(hd117)	19 ± 1	3	0.00228	to N2
raga-1(ok701)	28 ± 2	3	<0.00001	to N2
raga-1;nhr-8	27 ± 3	3	ns	to *raga-1*
N2 (wild type)	23 ± 0	3		
din-1(dh127))	23 ± 1	3	ns	to N2
raga-1(ok701)	27 ± 1	3	<0.00001	to N2
raga-1 din-1	30 ± 3	3	ns	to *raga-1*
raga-1(ok701) + EtOH	30	1		
raga-1;daf-9 + EtOH	23	1	<0.00001	to *raga-1* + EtOH
raga-1(ok701) + 1 µM D7-DA	33	1	0.00593	to *raga-1* + EtOH
raga-1;daf-9 + 1 µM D7-DA	28	1	<0.00001	to *raga-1;daf-9* + EtOH
N2 + luci	22 ± 1	3		
daf-12(rh61rh411) + luci	17 ± 1	3	<0.00001	to N2 + luci
N2 + *let-363i*	28 ± 2	3	<0.00001	to N2 + luci
daf-12(rh61rh411) + *let-363i*	19 ± 0	3	<0.00001	to N2 + *let-363i*
N2 + luci	22 ± 1	2		
N2 + *dhs-26i*	22 ± 1	2	ns	to N2 + luci

raga-1(ok701) + luci	25 ± 0	3	<0.00001	to N2 + luci
raga-1(ok701) + *dhs-26i*	23 ± 1	3	0.00372	to *raga-1* + luci
N2	24 ± 3	3		
dhs-26(syb8968)	23 ± 1	3	ns	to N2
raga-1(ok701)	30 ± 2	3	<0.00001	to N2
raga-1;dhs-26	22 ± 2	3	0.00026	to *raga-1*
raga-1(ok701) + EtOH	34	1		
raga-1;dhs-26 + EtOH	26	1	<0.00001	to *raga-1* + EtOH
raga-1(ok701) + 0.5 µM D7-DA	34	1	ns	to *raga-1* + EtOH
raga-1;dhs-26 + 0.5 µM D7-DA	31	1	0.000386	to *raga-1;dhs-26* + EtOH

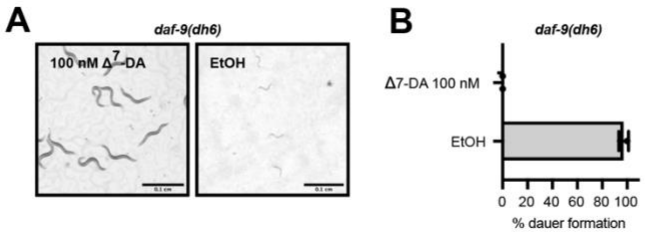

Figure IX-1: Dafachronic acid rescues *daf-9(dh6)* dauer phenotype. (A) 100 nM D7-dafachronic acid but not EtOH vehicle control rescues *daf-9(dh6)* Daf-c phenotype when grown egg on. (B) Quantification of dauer penetrance.

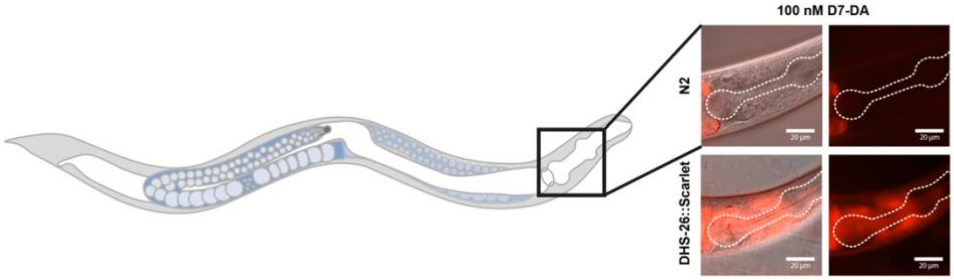

Figure IX-2: DHS-26::Scarlet is expressed in head neurons and glial cells. Microscopy imaging of the DHS-26::FLAG::Scarlet reporter reveals expression in the head region. Representative images of non fluorescent N2 worms to assess background fluorescent intensity and the *dhs-26::FLAG::Scarlet* reporter strain. To increase reporter expression, animals were treated with 100 nM D7-DA egg on (day 1 animals, scale bars represent 20 µm).

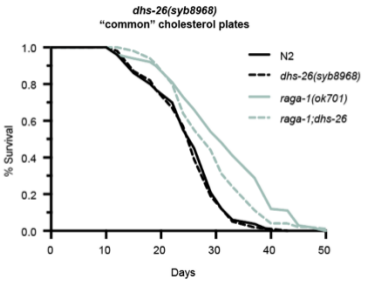

Figure IX-3: *dhs-26(syb8968)* partially abolished *raga-1* longevity on common cholesterol plates. Lifespan analysis of *dhs-26(syb8968)* full knockout mutants shows partial abolishment of *raga-1* longevity (2 biological replicates, >100 worms per lifespan).

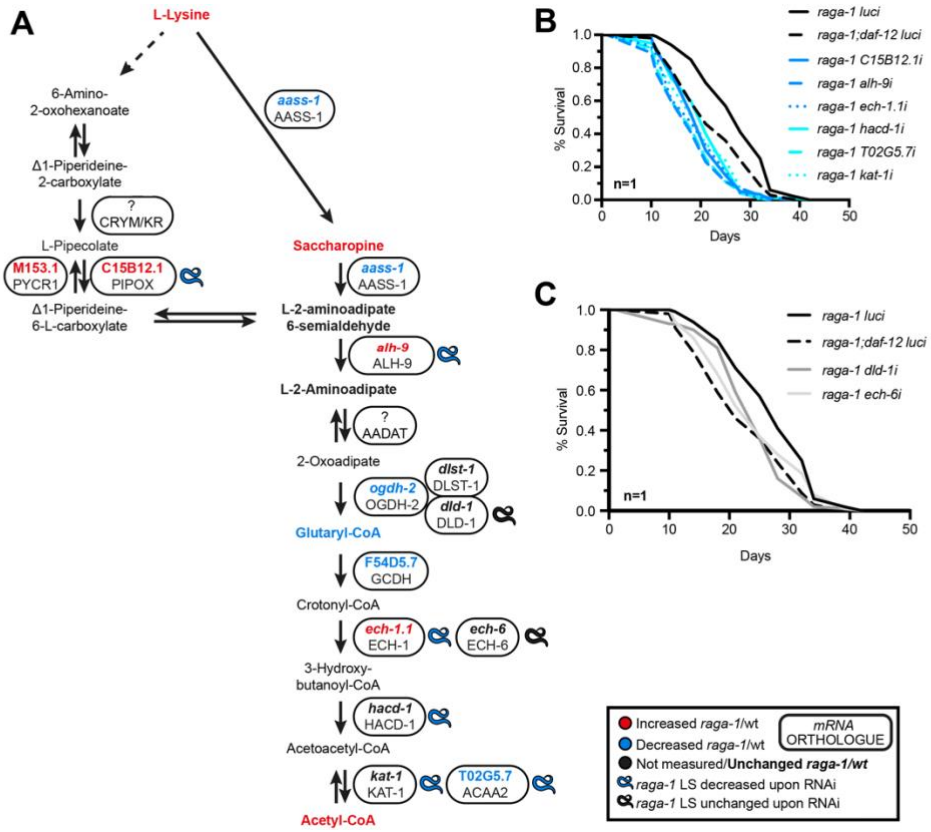

Figure IX-4: Genes of the lysine degradation patwhay are regulated by the mTOR/steroid signaling axis. (A) Schematic overview of the lysine degradation pathway. Displayed are the involved genes in *C. elegans*, their orthologues in humans, as well as their effect on *raga-1(ok701)* longevity upon RNAi treatment of the respective gene (worm icon). (B) Lifespan analysis of *raga-1* worms on lysine degradation pathway gene and control (luci) RNAi. Egg on treatment of worms showed significant decrease in *raga-1* lifespan. (C) Lifespan analysis of *raga-1* worms on lysine degradation pathway gene and control (luci) RNAi. Egg on treatment of worms showed no significant changes in *raga-1* lifespan. (1 biological replicate, > 100 worms per lifespan, Mantel-Cox Log rank test).

Table IX-2: Overview of RNAi clones significantly changing the lifespan in the functional genomics abolishment screen. RNAi mediated knockdown in long-lived *raga-1(ok701)* induced significant changes of lifespan in 83 clones comparing *raga-1 luci* vector control to the respective RNAi treatment, including relative mean lifespan and *p*-value based on Mantel-Cox Log rank test.

RNAi KD in *raga-1*	Relative mean lifespan	*p*-value
fat-5	0.79	0.0001
alh-9	0.79	0.0001
T02G5.7	0.8	0.0001
alh-1	0.8	0.0001
F22B8.7	0.81	0.0001
gst-42	0.81	0.0001
T04A11.4	0.81	0.0004
pccb-1	0.81	0.0001
B0272.3	0.89	0.0105
scrm-4	0.89	0.0027
asm-3	0.89	0.0012
acox-1.4	0.89	0.0316
catp-3	0.89	0.016
B0272.4	0.89	0.0405
ZK550.2	0.89	0.0001
ucr-2.2	0.9	0.0137

hacd-1	0.82	0.0008	*dhs-7*	0.9	0.0146
coh-1	0.82	0.0001	*abts-2*	0.9	0.0314
			raga-1;daf-12 luci	**0.9**	
chil-12	0.82	0.0001			
acox-1.2	0.83	0.0291	*vps-52*	0.91	0.0362
vit-5	0,83	0.0001	*oac-32*	0.91	0.0498
ech-1.1	0.83	0.0001	*mgl-2*	0.91	0.0213
PDB1.1	0.84	0.0001	*pgph-3*	0.91	0.0212
col-184	0.84	0.0005	*T22B7.7*	0.92	0.0001
dhs-2	0.84	0.0017	*smp-2*	0.92	0.0449
oatr-1	0.85	0.0001	*tps-2*	0.92	0.0338
F46H5.3	0.85	0.0001	*T05E7.1*	0.92	0.0376
cdk-11.2	0.85	0.0004	*cyp-33C4*	0.92	0.0374
ZK287.4	0.85	0.0004	*aat-1*	0.92	0.0125
alh-5	0.85	0.0001	*gcp-2.1*	0.92	0.0081
kat-1	0.85	0.0001	*gpdh-1*	0.93	0.0474
pho-11	0.86	0.0016	*F20G2.2*	0.93	0.0442
hrg-6	0.86	0.0001	*F26C11.1*	0.94	0.0002
ZK550.6	0.86	0.0133	*rbc-1*	0.94	0.0302
mai-1	0.86	0.0014	*odc-1*	0.94	0.0029
dhs-4	0.87	0.0014	*F22B7.9*	0.95	0.042
cyp-35A2	0.87	0.001	*R11F4.1*	0.95	0.0051
C15B12.1	0.87	0.0001	*lipl-2*	0.96	0.0291
Zc328.3	0.87	0.0001	*hpo-15*	0.97	0.0001
F09B12.3	0.88	0.0106	*F37C4.6*	1.0	0.0469
glt-6	0.88	0.002	***raga-1***	**1.0**	
hmit-1.1	0.88	0.0037	*R04B5.5*	1.09	0.0459
ets-9	0.88	0.0362	*ivns-1*	1.13	0.009
cpr-6	0.88	0.0092	*suca-1*	1.14	0.0034
dhs-26	0.88	0.0002	*cpz-1*	1.17	0.0079
cpl-1	0.88	0.0022	*T28F4.5*	1.18	0.001
gem-1	0.88	0.0022	*H41C03.1*	1.20	0.0045
scl-2	0.88	0.0005	*sams-1*	1.23	0.0001
F23F12.13	0.88	0.0007	*F38B6.4*	1.34	0.0001
pcp-2	0.88	0.0001			

Table IX-3: Overview of RNAi clones significantly changing the lifespan in the functional genomics rescue screen. RNAi mediated knockdown in short-lived *raga-1(ok701);daf-12(rh61rh411)* induced significant lifespan changes using 7 clones when comparing *raga-1;daf-12 luci* vector control to RNAi treatment. Table includes mean lifespan and *p*-value based on Mantel-Cox Log rank test.

RNAi KD in *raga-1;daf-12*	Relative mean lifespan	*p*-value
raga-1;daf-12 luci	**1.00**	
cls-3	1.90	0.0172
cyp-33C8	1.09	0.0432
ctsa-2	1.09	0.0452
oac-54	1.11	0.0381
cpr-1	1.11	0.0319
R05D7.5	1.12	0.037
rom-1	1.18	0.0001
raga-1 luci	**1.30**	

Table IX-4: KEGG pathway enrichment gene list. Summary of the genes considered in the KEGG pathway enrichments of the generated transcriptomics data displayed in Figure V-10.

KEGG: Up in *raga-1;daf-12* vs *raga-1*	
Axon regeneration	*sek-6, kgb-1, kgb-2, pmk-3, faah-1, mlk-1, cebp-1, fos-1, aak-1*
Lysosome	*ncr-1, haf-7, T28H10.3, cpr-2, cpr-1, W07B8.4, lipl-1, cln-3.3, cpr-3, ctsa-2*
Hippo signaling pathway	*mob-2, egl-44, nfm-1, sav-1, yap-1*
Longevity regulating pathway	*gst-20, kgb-1, fard-1, kgb-2, pmk-3, dve-1, gst-24, gst-38, kri-1, hsp-16.11, ins-7*
KEGG: Down in *raga-1;daf-12* vs *raga-1*	
Fatty acid degradation	*alh-5, alh-9, ech-1.1, acox-1.1, acox-1.2, acox-1.3, acox-1.4, alh-1, alh-12, acdh-12, T02G5.7, ech-6, B0272.3, acdh-7, kat-1, acaa-2, ech-4, acdh-1, cpt-2, hacd-1*
Biosynthesis of amino acids	*pah-1, gpd-2, gpd-3, sams-1, alh-13, W07E11.1, asns-2, aldo-2, cysl-3, ipgm-1, C32F10.8, pgk-1, mel-32, pyc-1, idh-2, tpi-1, tkt-1, R151.2, pyk-1, enol-1, metr-1, got-2.2*
Biosynthesis of unsaturated fatty acids	*fat-5, fat-6, acox-1.2, acox-1.3, acox-1.4, daf-22, hpo-8, dhs-28, fat-7, art-1, elo-6, let-767, acox-1.1*
Peroxisome	*ctl-2, sod-3, B0395.3, acox-1.2, acox-1.3, acox-1.4, daf-22, ZK550.6, C15B12.1, F41E6.5, ddo-2,*

	Y25C1A.13, dhs-28, sod-1, ctl-1, idh-2, prdx-2, pmp-5, ech-4, B0334.3, acox-1.1, daao-1
Biosynthesis of cofactors	*alh-5, dhs-3, sams-1, ugt-6, ugt-46, C05C8.7, kynu-1, alh-1, C31H2.4, gcs-1, F57B9.1, lias-1, cat-4, mel-32, dhs-19, K07E3.4, rml-1, dld-1, F38B2.4, nadk-2, ugt-62, dao-3, ugt-61*
Glutathione metabolism	*gst-4, gst-10, gst-39, odc-1, Y7A9A.1, gcs-1, Y38F2AR.12, gst-36, idh-2, gsr-1, gst-33, gpx-2, T25B9.9, C02D5.4, gpx-7*
One carbon pool by folate	*atic-1, F38B6.4, mthf-1, mel-32, dao-3, gcst-1, metr-1, K07E3.4*
Citrate cycle	*suca-1, dld-1, pck-1, pdhb-1, pck-2, pyc-1, acly-1, sucl-1, idh-2, mdh-1, dlat-2*
Arginine and proline metabolism	*alh-5, alh-9, odc-1, alh-13, alh-1, alh-12, daao-1, oatr-1, F46H5.3, got-2.2*
Lysine degradation	*alh-5, alh-9, ech-1.1, C15B12.1, alh-1, alh-12, ogdh-2 (TCA), T02G5.7, ech-6, B0272.3, kat-1, dld-1, hacd-1*

Table IX-5: KEGG pathway enrichment analysis gene list: Summary of the genes considered in the KEGG pathway enrichments of the generated single worm proteomics data displayed in Figure V-18.

KEGG: Up in *dhs-26*/N2	
RNA degradation	*skih-2, ntl-3, lsm-4, lsm-1, dcap-1, mtr-4, panl-3, ntl-9, gld-4, lsm-8, let-711*
mRNA surveillance pathway	*swd-2.2, erfa-1, ddx-19, aly-2, paa-1, cel-1, tag-72, nxf-1, C05C10.2, let-92, sur-6, smg-2, fipp-1, acin-1, T20G5.9*
ATP-dependent chromatin remodeling	*phf-10, hda-1, let-418, swsn-2.2, isw-1, swsn-4, swsn-1, lin-53, mrg-1, ubh-4, swsn-7, ruvb-1, trr-1, ekl-4, pbrm-1*
Spliceosome	*Y108G3AL.2, snr-6, syf-3, teg-4, aly-2, eftu-2, rsp-1, isy-1, emb-4, usp-39, bud-31, uaf-1, wbp-11, lsm-4, prp-8, acin-1, thoc-1, mog-2, hrpk-1, lsm-8, snrp-200*
Base excision repair	*rfc-4, pole-1, F10C2.4, ung-1, exo-3, rfc-1, pcn-1, lig-1, rfc-2*
Mismatch repair	*rfc-4, F10C2.4, rfc-1, msh-6, rpa-1, rpa-2, pcn-1, lig-1, rfc-2*
Proteasome	*F56F11.4, rpn-13, rpn-1, rpt-2, rpt-1, rpt-5, rpt-4, pbs-7, rpt-3, rpn-3, C14C10.5, rpn-9, rpn-8, rpn-6.1*
DNA replication	*rfc-1, mcm-7, mcm-6, mcm-5, div-1, pcn-1, lig-1, rfc-2, rfc-4, pole-1, F10C2.4, pola-1, mcm-4, mcm-3, mcm-2, rpa-1, rpa-2, pri-2*
Nucleocytoplasmic transport	*ddx-19, aly-2, npp-10, npp-9, npp-22, nxf-1, npp-13, xpo-1, imb-1, imb-2, acin-1, T20G5.9, npp-18, thoc-5, rae-1, npp-1, xpo-2, npp-16, npp-15, npp-14, npp-3, C05C10.2, npp-8, npp-6, smg-2, npp-5, thoc-1*

Oxidative phosphorylation	*C34B2.8, ucr-11, nuo-5, nuo-1, nuo-2, F45H10.2, T20H4.5, nduf-9, D2030.4, lpd-5, cox-5B, C33A12.1, F45H10.3, C18E9.4, nuo-6, T02H6.11, C16A3.5, R07E4.3, cox-7C, F59C6.5, Y51H1A.3, Y71H2AM.4, ZK809.3, gas-1, nduf-5, cox-6A, F42G8.10, isp-1, F44G4.2, F53F4.10, nduf-2.2, C25H3.9, F31D4.9, cox-4, nduf-7, cox-5A, ucr-2.1, cox-6B*

KEGG: Down in *dhs-26*/N2	
Arginine and proline metabolism	*got-1.2, alh-1, alh-12, ZK1307.1, alh-5, alh-4, argk-1, alh-6, W10C8.5, phy-2, alh-13, daao-1, pycr-1, oatr-1, F46H5.3*
Pyruvate metabolism	*alh-1, alh-12, pck-1, pyk-2, sodh-1, alh-5, alh-4, pyc-1, fum-1, dlat-2, mdh-2, dld-1, ldh-1, pck-2, dlat-1, pdha-1*
Glycine, serine and threonine metabolism	*R102.4, ipgm-1, Y37E3.17, gldc-1, C31C9.2, mel-32, gcsh-2, cth-2, K01C8.1, dld-1, F26H9.5, cth-1, gcsh-1, daao-1, gcst-1*
Biosynthesis of cofactors	*alh-1, nfs-1, dhs-3, C05C8.7, nprt-1, mel-32, Y47D9A.1, coq-3, coq-6, coq-5, adss-1, dao-3, ugt-62, ugt-61, fecl-1, clk-1, flad-1, tdo-2, alh-5, alh-4, K07E3.4, bcat-1, cox-15, dld-1, F26H9.5, F38B2.4, Y65B4A.8, ZK673.2, ugt-50, Y71H2AM.6*
Valine, leucine and isoleucine degradation	*alh-1, alh-12, alh-5, alh-4, bckd-1B, gta-1, ech-7, mce-1, B0272.3, bcat-1, mccc-1, bckd-1A, ard-1, dld-1, ech-5, mmcm-1, acdh-8, pccb-1, Y71G12B.10, B0303.3, pcca-1*
Glycolysis / Gluconeogenesis	*alh-1, alh-12, ipgm-1, pgk-1, pck-1, pyk-2, pfk-1.1, sodh-1, alh-5, gpd-3, alh-4, C01B4.6, tpi-1, dlat-2, Y43F4B.5, dld-1, ldh-1, pck-2, aldo-1, dlat-1, enol-1, pdha-1*
Citrate cycle	*cts-1, pck-1, idhg-2, pyc-1, suca-1, sdha-1, fum-1, dlat-2, ogdh-1, mdh-2, sdhb-1, dld-1, aco-2, aco-1, idha-1, pck-2, idhg-1, sucl-1, dlat-1, pdha-1, idh-1*
Biosynthesis of amino acids	*ipgm-1, pfk-1.1, tald-1, C31C9.2, mel-32, tpi-1, tkt-1, cth-2, alh-13, idha-1, cth-1, aldo-1, idhg-1, pycr-1, metr-1, got-1.2, cts-1, R102.4, gln-3, pgk-1, pyk-2, idhg-2, gpd-3, pyc-1, F08F8.7, bcat-1, cysl-1, K01C8.1, aco-2, aco-1, F26H9.5, enol-1, idh-1*
Carbon metabolism	*gdh-1, pfk-1.1, C31C9.2, acox-3, suca-1, mdh-2, sdhb-1, idha-1, mmcm-1, got-1.2, cts-1, C45E5.1, pgk-1, idhg-2, gldc-1, pyk-2, gpd-3, ctl-1, F08F8.7, dlat-2, ctl-2, acox-1.4, dld-1, aco-2, aco-1, F26H9.5, pcca-1, T25B9.9, sucl-1, enol-1, idh-1, ipgm-1, tald-1, mel-32, gcsh-2, ech-7, tpi-1, tkt-1, ogdh-1, gcsh-1, aldo-1, idhg-1, pccb-1, pdha-1, dlat-1, W02H5.8, pyc-1, fum-1, mce-1, sdha-1, acox-1.6, cysl-1, K01C8.1, gcst-1*
Metabolic pathways	*dhs-3, rml-3, pfk-1.1, dhp-1, C44B7.7, adss-1, stdh-1, idha-1, tir-1, mmcm-1, glna-1, WBGene00045322, mboa-2, fecl-1, cts-1, R102.4, Y38F2AR.12, Y69A2AR.18, ctl-1, F08F8.7, vps-34, ctl-2, C01G10.9, acox-1.4, aco-2, aco-1, F38B2.4, mecr-1, T25B9.9, sucl-1, Y45G12B.3, pho-14, elo-1, vha-11, Y43F4B.5, dlat-1, metr-1, klo-1, bgal-1, flad-1, R53.4, mce-1, tatn-1, acs-17,*

	T05C3.6, gdh-1, cyc-2.1, apy-1, F54D5.7, WBGene00044040, F54D5.24, eppl-1, alh-13, dao-3, ugt-61, got-1.2, bas-1, alh-12, Y37E3.17, sptl-1, rml-4, idhg-2, gldc-1, gpd-3, alh-5, alh-4, alh-7, alh-6, pld-1, ttx-7, F26H9.5, tag-96, acdh-8, vha-16, C50D2.9, adk-1, atp-2, alh-1, alh-3, F52C9.3, gta-1, tkt-1, atp-3, cth-1, pck-2, aldo-1, ZC262.5, W02H5.8, asg-2, gst-36, pyc-1, WBGene00050970, C01B4.6, sdha-1, gst-39, cysl-1, phy-2, gst-42, lin-56, ZK673.2, asb-2, nfs-1, ddo-2, fah-1, acox-3, haly-1, suca-1, mdh-2, sdhb-1, pycr-1, oatr-1, gst-20, dpyd-1, pgk-1, vha-15, gna-1, semo-1, 21ur-787, B0303.3, ugt-50, T27E9.2, gst-10, Y94H6A.7, pck-1, tald-1, dhs-12, gst-4, gcsh-2, gst-5, gst-6, ucr-2.2, ugt-62, clk-1, tdo-2, bckd-1B, fum-1, acox-1.6, K01C8.1, Y65B4A.8, Y71G12B.10, gcst-1, acl-2, C05C8.7, daf-22, C31C9.2, Y47D9A.1, coq-3, coq-6, coq-5, aass-1, ckc-1, gln-3, gana-1, C45E5.1, paf-2, pyk-2, art-1, hgo-1, K07E3.4, dlat-2, aagr-1, ads-1, cox-15, cchl-1, gyg-1, dld-1, ldh-1, vha-13, pcca-1, F52H2.5, dhcr-24, enol-1, C02D5.4, idh-1, tyr-4, Y71H2AM.6, cyc-1, ipgm-1, pcyt-2.2, nprt-1, sodh-1, mel-32, ech-7, T19B4.3, tpi-1, cth-2, ogdh-1, mccc-1, gcsh-1, pccb-1, idhg-1, pdha-1, dhs-13

Table IX-6: Pathway enrichment analysis gene list: Summary of the genes considered in the KEGG and GO pathway enrichments of the generated single worm proteomics data displayed in Figure V-19.

KEGG: Down in *raga-1;dhs-26/raga-1* and up in *raga-1*/N2	
Retinol metabolism	*ugt-46, dhs-3, ugt-23, ugt-50, adh-5*
Pentose and glucuronate interconversions	*ugt-46, ugt-23, ugt-50, F08F8.7, Y39G8B.1*
Glutathione metabolism	*gss-1, C44B7.7, gstk-1, gst-10, gst-36, odc-1, gst-39, gst-28*
Drug metabolism - cytochrome P450	*ugt-46, gstk-1, gst-10, ugt-23, gst-36, ugt-50, adh-5, gst-39, gst-28*
Drug metabolism - other enzymes	*ugt-46, upb-1, gst-10, ugt-23, gst-36, ugt-50, gst-39, gst-28, C29F7.3, ges-1*
Metabolism of xenobiotics by cytochrome P450	*ugt-46, gstk-1, gst-10, ugt-23, gst-36, ugt-50, adh-5, gst-39, gst-28*
Phagosome	*vha-19, vha-10, vha-14, act-5, vha-16, vha-15, vha-6, vha-11, vha-12, vha-2, cpl-1*
Lysosome	*nuc-1, haf-4, asp-4, cpz-2, vha-19, haf-9, vha-15, vha-6, cpr-6, cpz-1, vha-2, cpl-1, cpr-9, pho-11, vha-16, Y16B4A.2*
Oxidative phosphorylation	*vha-19, vha-10, vha-14, cox-6A, vha-15, vha-6, vha-11, vha-12, vha-2, cox-5B, F26E4.14, F26E4.16, C25H3.9, cox-4, cox-5A, vha-16, cox-6B*

Metabolic pathways	*ugt-46, T05C3.6, upb-1, gstk-1, dhs-3, C15B12.1, daf-22, vha-14, gst-28, C44B7.7, cox-5B, alh-13, F58H1.3, asns-2, ckc-1, bas-1, ptps-1, vha-19, R102.4, dpm-1, pyk-2, pcyt-2.1, alh-5, vha-15, F08F8.7, R151.2, ads-1, acox-1.2, acox-1.1, ampd-1, vha-16, ugt-50, cox-6B, gst-10, hpd-1, gta-1, F07A11.5, F42F12.4, adh-5, vha-11, vha-12, C29F7.3, gss-1, Y43F4B.5, serr-1, Y62E10A.13, T03F6.3, cox-7C, Y39G8B.1, vha-10, adah-1, gst-36, vha-6, cox-6A, odc-1, T24C12.3, vha-2, gst-39, C06A6.4, uda-1, spl-1, C50B6.7, pho-11, ugt-23, C25H3.9, cox-4, cox-5A, T13G4.4, cox-6C*

GO BP: Down in *raga-1;dhs-26/raga-1* and up in *raga-1*/N2

vacuolar acidification	*vha-14, vha-16, vha-6, vha-12*
organonitrogen compound metabolic process	*Y43F8C.13, gss-1, upb-1, serr-1*
proton transmembrane transport	*vha-10, vha-14, vha-16, vha-15, vha-6, vha-11, vha-12, vha-2*
glutathione metabolic process	*gstk-1, gst-10, gst-36, gst-26, gst-13, gst-27, gst-39, gst-28*
ascaroside biosynthetic process	*acox-1.2, daf-22, acox-1.1, cest-9.2, acs-7*
oxidative phosphorylation	*cox-4, cox-5A, cox-6A, cox-7C*
proteolysis involved in protein catabolic process	*cpr-9, Y40H7A.10, cpz-2, app-1, R07E3.1, cpr-6, cpz-1, cpl-1*
mitochondrial electron transport, cytochrome c to oxygen	*cox-5B, cox-4, cox-5A, cox-6A, cox-7C*
lipid transport	*vit-3, daf-22, vit-4, vit-5, vit-1, vit-2, vit-6, obr-1*
proteolysis	*asp-5, asp-4, cpz-2, K12C11.1, pcp-3, dnpp-1, pcp-2, F56F10.1, Y71H2AM.11, atg-4.1, C26B9.5, app-1, cpr-6, pcp-1, nep-17, cpz-1, cpl-1, nep-22, cpr-9, Y40H7A.10, T16G12.1, R07E3.1, Y16B4A.2, ctsa-3.1*

KEGG: Up in *raga-1;dhs-26/raga-1* and down in *raga-1*/N2

RNA degradation	*exos-1, hsp-6, mtr-4, crn-3, xrn-2*
Biosynthesis of cofactors	*adss-1, ZK632.4, sams-4, Y65B4A.8, nmat-2, ugt-61, sams-3, bcat-1*
Cysteine and methionine metabolism	*got-2.1, sams-4, mpst-1, sams-3, tatn-1, bcat-1*
Ribosome biogenesis in eukaryotes	*snu-13, C53H9.2, K01G5.5, nola-3, ZC434.4, F55F10.1, nxf-2, xrn-2*

Work contributions

This work had the support of multiple people and core facilities at different stages of the project, including conceptualization, training and assistance, analysis, and conducting experiments. The conceptualization of the experiments and initial training was supported by Dr. Adam Antebi and Dr. Birgit Gerisch. The sequencing of the RNAi clones was performed by Nadine Hochhard. Anna Löhrke, Christian Latza, Luca Jeromin, and Tim Droth, gave technical assistance in multiple experiments presented here.

The RNAseq was conducted by the Cologne Center for Genomics, and was analyzed by the Bioinformatics Core Facility of the Max Planck Institute for Biology of Ageing. Metabolomics analysis and measurement of steroid compounds was conducted by the Metabolomics Core Facility of the Max Planck Institute for Biology of Ageing. Proteomics Core Facility of the MPI AGE performed single worm sequencing analyses.

Dafachronic acids for supplementation experiments were kindly provided by Hans-Joachim Knölker from Technische Universität Dresden, Germany.

Outsourced CRISPR mediated gene editing to generate new *C. elegans* strains was performed by SunyBiotech.

XIV. References

Abbott, A. L., E. Alvarez-Saavedra, E. A. Miska, N. C. Lau, D. P. Bartel, H. R. Horvitz and V. Ambros (2005). "The let-7 MicroRNA family members mir-48, mir-84, and mir-241 function together to regulate developmental timing in Caenorhabditis elegans." Dev Cell **9**(3): 403-414.

Ackerman, D. and D. Gems (2012). "The mystery of C. elegans aging: an emerging role for fat. Distant parallels between C. elegans aging and metabolic syndrome?" Bioessays **34**(6): 466-471.

Aghayeva, U., A. Bhattacharya, S. Sural, E. Jaeger, M. Churgin, C. Fang-Yen and O. Hobert (2021). "DAF-16/FoxO and DAF-12/VDR control cellular plasticity both cell-autonomously and via interorgan signaling." PLoS Biol **19**(4): e3001204.

Agrawal, S., S. Kumar, R. Sehgal, S. George, R. Gupta, S. Poddar, A. Jha and S. Pathak (2019). "El-MAVEN: A Fast, Robust, and User-Friendly Mass Spectrometry Data Processing Engine for Metabolomics." Methods Mol Biol **1978**: 301-321.

Aguilaniu, H., P. Fabrizio and M. Witting (2016). "The Role of Dafachronic Acid Signaling in Development and Longevity in Caenorhabditis elegans: Digging Deeper Using Cutting-Edge Analytical Chemistry." Front Endocrinol (Lausanne) **7**: 12.

Ailion, M. and J. H. Thomas (2000). "Dauer formation induced by high temperatures in Caenorhabditis elegans." Genetics **156**(3): 1047-1067.

Albert, P. S., S. J. Brown and D. L. Riddle (1981). "Sensory control of dauer larva formation in Caenorhabditis elegans." J Comp Neurol **198**(3): 435-451.

Albert, P. S. and D. L. Riddle (1988). "Mutants of Caenorhabditis elegans that form dauer-like larvae." Dev Biol **126**(2): 270-293.

Aldridge, S. and S. A. Teichmann (2020). "Single cell transcriptomics comes of age." Nat Commun **11**(1): 4307.

Allawi, H. T. and J. SantaLucia, Jr. (1997). "Thermodynamics and NMR of internal G.T mismatches in DNA." Biochemistry **36**(34): 10581-10594.

Angel, A. and J. Farkas (1974). "Regulation of cholesterol storage in adipose tissue." J Lipid Res **15**(5): 491-499.

Antebi, A., W. H. Yeh, D. Tait, E. M. Hedgecock and D. L. Riddle (2000). "daf-12 encodes a nuclear receptor that regulates the dauer diapause and developmental age in C. elegans." Genes Dev **14**(12): 1512-1527.

Apfeld, J. and C. Kenyon (1998). "Cell nonautonomy of C. elegans daf-2 function in the regulation of diapause and life span." Cell **95**(2): 199-210.

Apfeld, J., G. O'Connor, T. McDonagh, P. S. DiStefano and R. Curtis (2004). "The AMP-activated protein kinase AAK-2 links energy levels and insulin-like signals to lifespan in C. elegans." Genes Dev **18**(24): 3004-3009.

Arantes-Oliveira, N., J. Apfeld, A. Dillin and C. Kenyon (2002). "Regulation of life-span by germ-line stem cells in Caenorhabditis elegans." Science **295**(5554): 502-505.

Asikainen, S., S. Vartiainen, M. Lakso, R. Nass and G. Wong (2005). "Selective sensitivity of Caenorhabditis elegans neurons to RNA interference." Neuroreport **16**(18): 1995-1999.

Avery, L. (1993). "The genetics of feeding in Caenorhabditis elegans." Genetics **133**(4): 897-917.

Avruch, J., K. Hara, Y. Lin, M. Liu, X. Long, S. Ortiz-Vega and K. Yonezawa (2006). "Insulin and amino-acid regulation of mTOR signaling and kinase activity through the Rheb GTPase." Oncogene **25**(48): 6361-6372.

Bache, N., P. E. Geyer, D. B. Bekker-Jensen, O. Hoerning, L. Falkenby, P. V. Treit, S. Doll, I. Paron, J. B. Muller, F. Meier, J. V. Olsen, O. Vorm and M. Mann (2018). "A Novel LC System Embeds Analytes in Pre-formed Gradients for Rapid, Ultra-robust Proteomics." Mol Cell Proteomics **17**(11): 2284-2296.

Bar-Peled, L., L. Chantranupong, A. D. Cherniack, W. W. Chen, K. A. Ottina, B. C. Grabiner, E. D. Spear, S. L. Carter, M. Meyerson and D. M. Sabatini (2013). "A Tumor suppressor complex with GAP activity for the Rag GTPases that signal amino acid sufficiency to mTORC1." Science **340**(6136): 1100-1106.

Bar-Peled, L. and D. M. Sabatini (2014). "Regulation of mTORC1 by amino acids." Trends Cell Biol **24**(7): 400-406.

Bar-Ziv, R., N. Dutta, A. Hruby, E. Sukarto, M. Averbukh, A. Alcala, H. R. Henderson, J. Durieux, S. U. Tronnes, Q. Ahmad, T. Bolas, J. Perez, J. G. Dishart, M. Vega, G. Garcia, R. Higuchi-Sanabria and A. Dillin (2023). "Glial-derived mitochondrial signals affect neuronal proteostasis and aging." Sci Adv **9**(41): eadi1411.

Bargmann, C. I. and H. R. Horvitz (1991). "Control of larval development by chemosensory neurons in Caenorhabditis elegans." Science **251**(4998): 1243-1246.

Baudry, M., Y. Yao, D. Simmons, J. Liu and X. Bi (2003). "Postnatal development of inflammation in a murine model of Niemann-Pick type C disease: immunohistochemical observations of microglia and astroglia." Exp Neurol **184**(2): 887-903.

Baugh, L. R. and P. J. Hu (2020). "Starvation Responses Throughout the Caenorhabditiselegans Life Cycle." Genetics **216**(4): 837-878.

Bayele, H. K. (2019). "A conserved mechanism of sirtuin signalling through steroid hormone receptors." Biosci Rep **39**(12).

Beato, M. and J. Klug (2000). "Steroid hormone receptors: an update." Hum Reprod Update **6**(3): 225-236.

Beckstead, R. B. and C. S. Thummel (2006). "Indicted: worms caught using steroids." Cell **124**(6): 1137-1140.

Benjamin, D. and M. N. Hall (2013). "TSC on the peroxisome controls mTORC1." Nat Cell Biol **15**(10): 1135-1136.

Berman, J. R. and C. Kenyon (2006). "Germ-cell loss extends C. elegans life span through regulation of DAF-16 by kri-1 and lipophilic-hormone signaling." Cell **124**(5): 1055-1068.

Bethke, A., N. Fielenbach, Z. Wang, D. J. Mangelsdorf and A. Antebi (2009). "Nuclear hormone receptor regulation of microRNAs controls developmental progression." Science **324**(5923): 95-98.

Birnby, D. A., E. M. Link, J. J. Vowels, H. Tian, P. L. Colacurcio and J. H. Thomas (2000). "A transmembrane guanylyl cyclase (DAF-11) and Hsp90 (DAF-21) regulate a common set of chemosensory behaviors in caenorhabditis elegans." Genetics **155**(1): 85-104.

Bito, T., N. Okamoto, K. Otsuka, Y. Yabuta, J. Arima, T. Kawano and F. Watanabe (2019). "Involvement of Spermidine in the Reduced Lifespan of Caenorhabditis elegans During Vitamin B(12) Deficiency." Metabolites **9**(9).

Bjedov, I., J. M. Toivonen, F. Kerr, C. Slack, J. Jacobson, A. Foley and L. Partridge (2010). "Mechanisms of life span extension by rapamycin in the fruit fly Drosophila melanogaster." Cell Metab **11**(1): 35-46.

Blackwell, T. K., A. K. Sewell, Z. Wu and M. Han (2019). "TOR Signaling in Caenorhabditis elegans Development, Metabolism, and Aging." Genetics **213**(2): 329-360.

Blagosklonny, M. V. (2008). "Aging: ROS or TOR." Cell Cycle **7**(21): 3344-3354.

Bonekamp, N. A., B. Peter, H. S. Hillen, A. Felser, T. Bergbrede, A. Choidas, M. Horn, A. Unger, R. Di Lucrezia, I. Atanassov, X. Li, U. Koch, S. Menninger, J. Boros, P. Habenberger, P. Giavalisco, P. Cramer, M. S. Denzel, P. Nussbaumer, B. Klebl, M. Falkenberg, C. M. Gustafsson and N. G. Larsson (2020). "Small-molecule inhibitors of human mitochondrial DNA transcription." Nature **588**(7839): 712-716.

Boutros, M. and J. Ahringer (2008). "The art and design of genetic screens: RNA interference." Nat Rev Genet **9**(7): 554-566.

Brown, M. S. and J. L. Goldstein (1986). "A receptor-mediated pathway for cholesterol homeostasis." Science **232**(4746): 34-47.

Buerger, C., B. DeVries and V. Stambolic (2006). "Localization of Rheb to the endomembrane is critical for its signaling function." Biochem Biophys Res Commun **344**(3): 869-880.

Burkewitz, K., Y. Zhang and W. B. Mair (2014). "AMPK at the nexus of energetics and aging." Cell Metab **20**(1): 10-25.

Butcher, R. A. (2017). "Small-molecule pheromones and hormones controlling nematode development." Nat Chem Biol **13**(6): 577-586.

Butcher, R. A., M. Fujita, F. C. Schroeder and J. Clardy (2007). "Small-molecule pheromones that control dauer development in Caenorhabditis elegans." Nat Chem Biol **3**(7): 420-422.

Butcher, R. A., J. R. Ragains, W. Li, G. Ruvkun, J. Clardy and H. Y. Mak (2009). "Biosynthesis of the Caenorhabditis elegans dauer pheromone." Proc Natl Acad Sci U S A **106**(6): 1875-1879.

Carstea, E. D., J. A. Morris, K. G. Coleman, S. K. Loftus, D. Zhang, C. Cummings, J. Gu, M. A. Rosenfeld, W. J. Pavan, D. B. Krizman, J. Nagle, M. H. Polymeropoulos, S. L. Sturley, Y. A. Ioannou, M. E. Higgins, M. Comly, A. Cooney, A. Brown, C. R. Kaneski, E. J. Blanchette-Mackie, N. K. Dwyer, E. B. Neufeld, T. Y. Chang, L. Liscum, J. F. Strauss, 3rd, K. Ohno, M. Zeigler, R. Carmi, J. Sokol, D. Markie, R. R. O'Neill, O. P. van Diggelen, M. Elleder, M. C. Patterson, R. O. Brady, M. T. Vanier, P. G. Pentchev and D. A. Tagle (1997). "Niemann-Pick C1 disease gene: homology to mediators of cholesterol homeostasis." Science **277**(5323): 228-231.

Carstensen, H. R., R. M. Villalon, N. Banerjee, E. A. Hallem and R. L. Hong (2021). "Steroid hormone pathways coordinate developmental diapause and olfactory remodeling in Pristionchus pacificus." Genetics **218**(2).

Cassada, R. C. and R. L. Russell (1975). "The dauerlarva, a post-embryonic developmental variant of the nematode Caenorhabditis elegans." Dev Biol **46**(2): 326-342.

Castellano, B. M., A. M. Thelen, O. Moldavski, M. Feltes, R. E. van der Welle, L. Mydock-McGrane, X. Jiang, R. J. van Eijkeren, O. B. Davis, S. M. Louie, R. M. Perera, D. F. Covey, D. K. Nomura, D. S. Ory and R. Zoncu (2017). "Lysosomal cholesterol activates mTORC1 via an SLC38A9-Niemann-Pick C1 signaling complex." Science **355**(6331): 1306-1311.

Cecere, G. and A. Grishok (2014). "RNA Chromatin Immunoprecipitation (RNA-ChIP) in Caenorhabditis elegans." Bio Protoc **4**(24).

Chambers, M. C., B. Maclean, R. Burke, D. Amodei, D. L. Ruderman, S. Neumann, L. Gatto, B. Fischer, B. Pratt, J. Egertson, K. Hoff, D. Kessner, N. Tasman, N. Shulman, B. Frewen, T. A. Baker, M. Y. Brusniak, C. Paulse, D. Creasy, L. Flashner, K. Kani, C. Moulding, S. L. Seymour, L. M. Nuwaysir, B. Lefebvre, F. Kuhlmann, J. Roark, P. Rainer, S. Detlev, T. Hemenway, A. Huhmer, J. Langridge, B. Connolly, T. Chadick, K. Holly, J. Eckels, E. W. Deutsch, R. L. Moritz, J. E. Katz, D. B. Agus, M. MacCoss, D. L. Tabb and P. Mallick (2012). "A cross-platform toolkit for mass spectrometry and proteomics." Nat Biotechnol **30**(10): 918-920.

Chaparian, R. R. and J. C. van Kessel (2021). "Promoter Pull-Down Assay: A Biochemical Screen for DNA-Binding Proteins." Methods Mol Biol **2346**: 165-172.

Chiang, J. Y., R. Kimmel and D. Stroup (2001). "Regulation of cholesterol 7alpha-hydroxylase gene (CYP7A1) transcription by the liver orphan receptor (LXRalpha)." Gene **262**(1-2): 257-265.

Chitwood, D. J. (1999). "Biochemistry and function of nematode steroids." Crit Rev Biochem Mol Biol **34**(4): 273-284.

Chu, B. B., Y. C. Liao, W. Qi, C. Xie, X. Du, J. Wang, H. Yang, H. H. Miao, B. L. Li and B. L. Song (2015). "Cholesterol transport through lysosome-peroxisome membrane contacts." Cell **161**(2): 291-306.

Cole, T. J., K. L. Short and S. B. Hooper (2019). "The science of steroids." Semin Fetal Neonatal Med **24**(3): 170-175.

Conrad, K. S., T. W. Cheng, D. Ysselstein, S. Heybrock, L. R. Hoth, B. A. Chrunyk, C. W. Am Ende, D. Krainc, M. Schwake, P. Saftig, S. Liu, X. Qiu and M. D. Ehlers (2017). "Lysosomal integral membrane protein-2 as a phospholipid receptor revealed by biophysical and cellular studies." Nat Commun **8**(1): 1908.

Cota, D., K. Proulx, K. A. Smith, S. C. Kozma, G. Thomas, S. C. Woods and R. J. Seeley (2006). "Hypothalamic mTOR signaling regulates food intake." Science **312**(5775): 927-930.

da Graca, L. S., K. K. Zimmerman, M. C. Mitchell, M. Kozhan-Gorodetska, K. Sekiewicz, Y. Morales and G. I. Patterson (2004). "DAF-5 is a Ski oncoprotein homolog that functions in a neuronal TGF beta pathway to regulate C. elegans dauer development." Development **131**(2): 435-446.

Dagon, Y., E. Hur, B. Zheng, K. Wellenstein, L. C. Cantley and B. B. Kahn (2012). "p70S6 kinase phosphorylates AMPK on serine 491 to mediate leptin's effect on food intake." Cell Metab **16**(1): 104-112.

Dai, Y., P. C. Wensink and R. H. Abeles (1999). "One protein, two enzymes." J Biol Chem **274**(3): 1193-1195.

Daniels, T. F., K. M. Killinger, J. J. Michal, R. W. Wright, Jr. and Z. Jiang (2009). "Lipoproteins, cholesterol homeostasis and cardiac health." Int J Biol Sci **5**(5): 474-488.

Davis, O. B., H. R. Shin, C. Y. Lim, E. Y. Wu, M. Kukurugya, C. F. Maher, R. M. Perera, M. P. Ordonez and R. Zoncu (2021). "NPC1-mTORC1 Signaling Couples Cholesterol Sensing to Organelle Homeostasis and Is a Targetable Pathway in Niemann-Pick Type C." Dev Cell **56**(3): 260-276 e267.

de Falco, B., F. Giannino, F. Carteni, S. Mazzoleni and D. H. Kim (2022). "Metabolic flux analysis: a comprehensive review on sample preparation, analytical techniques, data analysis, computational modelling, and main application areas." RSC Adv **12**(39): 25528-25548.

Dibble, C. C. and B. D. Manning (2013). "Signal integration by mTORC1 coordinates nutrient input with biosynthetic output." Nat Cell Biol **15**(6): 555-564.

Dumas, K. J., C. Guo, H. J. Shih and P. J. Hu (2013). "Influence of steroid hormone signaling on life span control by Caenorhabditis elegans insulin-like signaling." G3 (Bethesda) **3**(5): 841-850.

Duvel, K., J. L. Yecies, S. Menon, P. Raman, A. I. Lipovsky, A. L. Souza, E. Triantafellow, Q. Ma, R. Gorski, S. Cleaver, M. G. Vander Heiden, J. P. MacKeigan, P. M. Finan, C. B. Clish, L. O. Murphy and B. D. Manning (2010). "Activation of a metabolic gene regulatory network downstream of mTOR complex 1." Mol Cell **39**(2): 171-183.

Elliott, W. H. and P. M. Hyde (1971). "Metabolic pathways of bile acid synthesis." Am J Med **51**(5): 568-579.

Esquela-Kerscher, A., S. M. Johnson, L. Bai, K. Saito, J. Partridge, K. L. Reinert and F. J. Slack (2005). "Post-embryonic expression of C. elegans microRNAs belonging to the lin-4 and let-7 families in the hypodermis and the reproductive system." Dev Dyn **234**(4): 868-877.

Estevez, M., L. Attisano, J. L. Wrana, P. S. Albert, J. Massague and D. L. Riddle (1993). "The daf-4 gene encodes a bone morphogenetic protein receptor controlling C. elegans dauer larva development." Nature **365**(6447): 644-649.

Ferdinandusse, S., S. Denis, P. L. Faust and R. J. Wanders (2009). "Bile acids: the role of peroxisomes." J Lipid Res **50**(11): 2139-2147.

Fernandes, S. A., D. D. Angelidaki, J. Nuchel, J. Pan, P. Gollwitzer, Y. Elkis, F. Artoni, S. Wilhelm, M. Kovacevic-Sarmiento and C. Demetriades (2024). "Spatial and functional separation of mTORC1 signalling in response to different amino acid sources." Nat Cell Biol **26**(11): 1918-1933.

Fiamoncini, J., M. J. Rist, L. Frommherz, P. Giesbertz, B. Pfrang, W. Kremer, F. Huber, G. Kastenmuller, T. Skurk, H. Hauner, K. Suhre, H. Daniel and S. E. Kulling (2022). "Dynamics and determinants of human plasma bile acid profiles during dietary challenges." Front Nutr **9**: 932937.

Fielenbach, N. and A. Antebi (2008). "C. elegans dauer formation and the molecular basis of plasticity." Genes Dev **22**(16): 2149-2165.

Fonseca, B. D., E. M. Smith, N. Yelle, T. Alain, M. Bushell and A. Pause (2014). "The ever-evolving role of mTOR in translation." Semin Cell Dev Biol **36**: 102-112.

Forrester, W. C. and G. Garriga (1997). "Genes necessary for C. elegans cell and growth cone migrations." Development **124**(9): 1831-1843.

Forrester, W. C., E. Perens, J. A. Zallen and G. Garriga (1998). "Identification of Caenorhabditis elegans genes required for neuronal differentiation and migration." Genetics **148**(1): 151-165.

Franzosa, E. A., T. Hsu, A. Sirota-Madi, A. Shafquat, G. Abu-Ali, X. C. Morgan and C. Huttenhower (2015). "Sequencing and beyond: integrating molecular 'omics' for microbial community profiling." Nat Rev Microbiol **13**(6): 360-372.

Friedman, D. B. and T. E. Johnson (1988). "A mutation in the age-1 gene in Caenorhabditis elegans lengthens life and reduces hermaphrodite fertility." Genetics **118**(1): 75-86.

Fuller, P. J., Y. Yao, J. Yang and M. J. Young (2012). "Mechanisms of ligand specificity of the mineralocorticoid receptor." J Endocrinol **213**(1): 15-24.

Furge, L. L. and F. P. Guengerich (2006). "Cytochrome P450 enzymes in drug metabolism and chemical toxicology: An introduction." Biochem Mol Biol Educ **34**(2): 66-74.

Galilea, A., V. J. Santillan, S. L. Acebedo, M. Virginia Dansey, L. D. Alvarez, G. I. Mazaira, M. D. Galigniana, O. A. Castro, G. F. Gola and J. A. Ramirez (2024). "Expanding the Repertoire of ceDAF-12 Ligands for Modulation of the Steroid Endocrine System in C. Elegans." Chembiochem **25**(21): e202400018.

Garcia-Rodriguez, J. L., L. Barbier-Torres, S. Fernandez-Alvarez, V. Gutierrez-de Juan, M. J. Monte, E. Halilbasic, D. Herranz, L. Alvarez, P. Aspichueta, J. J. Marin, M. Trauner, J. M. Mato, M. Serrano, N. Beraza and M. L. Martinez-Chantar (2014). "SIRT1 controls liver regeneration by regulating bile acid metabolism through farnesoid X receptor and mammalian target of rapamycin signaling." Hepatology **59**(5): 1972-1983.

Gems, D. and L. Partridge (2013). "Genetics of longevity in model organisms: debates and paradigm shifts." Annu Rev Physiol **75**: 621-644.

Georgi, L. L., P. S. Albert and D. L. Riddle (1990). "daf-1, a C. elegans gene controlling dauer larva development, encodes a novel receptor protein kinase." Cell **61**(4): 635-645.

Gerisch, B. and A. Antebi (2004). "Hormonal signals produced by DAF-9/cytochrome P450 regulate C. elegans dauer diapause in response to environmental cues." Development **131**(8): 1765-1776.

Gerisch, B., V. Rottiers, D. Li, D. L. Motola, C. L. Cummins, H. Lehrach, D. J. Mangelsdorf and A. Antebi (2007). "A bile acid-like steroid modulates Caenorhabditis elegans lifespan through nuclear receptor signaling." Proc Natl Acad Sci U S A **104**(12): 5014-5019.

Gerisch, B., C. Weitzel, C. Kober-Eisermann, V. Rottiers and A. Antebi (2001). "A hormonal signaling pathway influencing C. elegans metabolism, reproductive development, and life span." Dev Cell **1**(6): 841-851.

Gerstein, M. B., Z. J. Lu, E. L. Van Nostrand, C. Cheng, B. I. Arshinoff, T. Liu, K. Y. Yip, R. Robilotto, A. Rechtsteiner, K. Ikegami, P. Alves, A. Chateigner, M. Perry, M. Morris, R. K. Auerbach, X. Feng, J. Leng, A. Vielle, W. Niu, K. Rhrissorrakrai, A. Agarwal, R. P. Alexander, G. Barber, C. M. Brdlik, J. Brennan, J. J. Brouillet, A. Carr, M. S. Cheung, H. Clawson, S. Contrino, L. O. Dannenberg, A. F. Dernburg, A. Desai, L. Dick, A. C. Dose, J. Du, T. Egelhofer, S. Ercan, G. Euskirchen, B. Ewing, E. A. Feingold, R. Gassmann, P. J. Good, P. Green, F. Gullier, M. Gutwein, M. S. Guyer, L. Habegger, T. Han, J. G. Henikoff, S. R. Henz, A. Hinrichs, H. Holster, T. Hyman, A. L.

Iniguez, J. Janette, M. Jensen, M. Kato, W. J. Kent, E. Kephart, V. Khivansara, E. Khurana, J. K. Kim, P. Kolasinska-Zwierz, E. C. Lai, I. Latorre, A. Leahey, S. Lewis, P. Lloyd, L. Lochovsky, R. F. Lowdon, Y. Lubling, R. Lyne, M. MacCoss, S. D. Mackowiak, M. Mangone, S. McKay, D. Mecenas, G. Merrihew, D. M. Miller, 3rd, A. Muroyama, J. I. Murray, S. L. Ooi, H. Pham, T. Phippen, E. A. Preston, N. Rajewsky, G. Ratsch, H. Rosenbaum, J. Rozowsky, K. Rutherford, P. Ruzanov, M. Sarov, R. Sasidharan, A. Sboner, P. Scheid, E. Segal, H. Shin, C. Shou, F. J. Slack, C. Slightam, R. Smith, W. C. Spencer, E. O. Stinson, S. Taing, T. Takasaki, D. Vafeados, K. Voronina, G. Wang, N. L. Washington, C. M. Whittle, B. Wu, K. K. Yan, G. Zeller, Z. Zha, M. Zhong, X. Zhou, E. C. mod, J. Ahringer, S. Strome, K. C. Gunsalus, G. Micklem, X. S. Liu, V. Reinke, S. K. Kim, L. W. Hillier, S. Henikoff, F. Piano, M. Snyder, L. Stein, J. D. Lieb and R. H. Waterston (2010). "Integrative analysis of the Caenorhabditis elegans genome by the modENCODE project." Science **330**(6012): 1775-1787.

Ginguay, A., L. Cynober, E. Curis and I. Nicolis (2017). "Ornithine Aminotransferase, an Important Glutamate-Metabolizing Enzyme at the Crossroads of Multiple Metabolic Pathways." Biology (Basel) **6**(1).

Ginsberg, H. N. (1998). "Lipoprotein physiology." Endocrinol Metab Clin North Am **27**(3): 503-519.

Golden, J. W. and D. L. Riddle (1982). "A pheromone influences larval development in the nematode Caenorhabditis elegans." Science **218**(4572): 578-580.

Golden, J. W. and D. L. Riddle (1985). "A gene affecting production of the Caenorhabditis elegans dauer-inducing pheromone." Mol Gen Genet **198**(3): 534-536.

Goodrick, C. L., D. K. Ingram, M. A. Reynolds, J. R. Freeman and N. Cider (1990). "Effects of intermittent feeding upon body weight and lifespan in inbred mice: interaction of genotype and age." Mech Ageing Dev **55**(1): 69-87.

Graham, P. and L. Pick (2017). "Drosophila as a Model for Diabetes and Diseases of Insulin Resistance." Curr Top Dev Biol **121**: 397-419.

Green, C. L., D. W. Lamming and L. Fontana (2022). "Molecular mechanisms of dietary restriction promoting health and longevity." Nat Rev Mol Cell Biol **23**(1): 56-73.

Greer, E. L. and A. Brunet (2009). "Different dietary restriction regimens extend lifespan by both independent and overlapping genetic pathways in C. elegans." Aging Cell **8**(2): 113-127.

Greer, E. L., D. Dowlatshahi, M. R. Banko, J. Villen, K. Hoang, D. Blanchard, S. P. Gygi and A. Brunet (2007). "An AMPK-FOXO pathway mediates longevity induced by a novel method of dietary restriction in C. elegans." Curr Biol **17**(19): 1646-1656.

Gu, X., J. M. Orozco, R. A. Saxton, K. J. Condon, G. Y. Liu, P. A. Krawczyk, S. M. Scaria, J. W. Harper, S. P. Gygi and D. M. Sabatini (2017). "SAMTOR is an S-adenosylmethionine sensor for the mTORC1 pathway." Science **358**(6364): 813-818.

Gudibanda, P. R. (2019). "A framework of steroid metabolism and nuclear receptor interactions in nematodes." PhD Thesis.

Gwinn, D. M., D. B. Shackelford, D. F. Egan, M. M. Mihaylova, A. Mery, D. S. Vasquez, B. E. Turk and R. J. Shaw (2008). "AMPK phosphorylation of raptor mediates a metabolic checkpoint." Mol Cell **30**(2): 214-226.

Han, H., U. Braunschweig, T. Gonatopoulos-Pournatzis, R. J. Weatheritt, C. L. Hirsch, K. C. H. Ha, E. Radovani, S. Nabeel-Shah, T. Sterne-Weiler, J. Wang, D. O'Hanlon, Q. Pan, D. Ray, H. Zheng, F. Vizeacoumar, A. Datti, L. Magomedova, C. L. Cummins, T. R. Hughes, J. F. Greenblatt, J. L. Wrana, J. Moffat and B. J. Blencowe (2017). "Multilayered Control of Alternative Splicing Regulatory Networks by Transcription Factors." Mol Cell **65**(3): 539-553 e537.

Han, S. and J. Y. Chiang (2009). "Mechanism of vitamin D receptor inhibition of cholesterol 7alpha-hydroxylase gene transcription in human hepatocytes." Drug Metab Dispos **37**(3): 469-478.

Han, S., T. Li, E. Ellis, S. Strom and J. Y. Chiang (2010). "A novel bile acid-activated vitamin D receptor signaling in human hepatocytes." Mol Endocrinol **24**(6): 1151-1164.

Hannich, J. T., E. V. Entchev, F. Mende, H. Boytchev, R. Martin, V. Zagoriy, G. Theumer, I. Riezman, H. Riezman, H. J. Knolker and T. V. Kurzchalia (2009). "Methylation of the sterol nucleus by STRM-1 regulates dauer larva formation in Caenorhabditis elegans." Dev Cell **16**(6): 833-843.

Hansen, M., S. Taubert, D. Crawford, N. Libina, S. J. Lee and C. Kenyon (2007). "Lifespan extension by conditions that inhibit translation in Caenorhabditis elegans." Aging Cell **6**(1): 95-110.

Hara, K., Y. Maruki, X. Long, K. Yoshino, N. Oshiro, S. Hidayat, C. Tokunaga, J. Avruch and K. Yonezawa (2002). "Raptor, a binding partner of target of rapamycin (TOR), mediates TOR action." Cell **110**(2): 177-189.

Harrison, D. E., R. Strong, Z. D. Sharp, J. F. Nelson, C. M. Astle, K. Flurkey, N. L. Nadon, J. E. Wilkinson, K. Frenkel, C. S. Carter, M. Pahor, M. A. Javors, E. Fernandez and R. A. Miller (2009). "Rapamycin fed late in life extends lifespan in genetically heterogeneous mice." Nature **460**(7253): 392-395.

Haussler, M. R. and A. W. Norman (1969). "Chromosomal receptor for a vitamin D metabolite." Proc Natl Acad Sci U S A **62**(1): 155-162.

Heitman, J., N. R. Movva and M. N. Hall (1991). "Targets for cell cycle arrest by the immunosuppressant rapamycin in yeast." Science **253**(5022): 905-909.

Heybrock, S., K. Kanerva, Y. Meng, C. Ing, A. Liang, Z. J. Xiong, X. Weng, Y. Ah Kim, R. Collins, W. Trimble, R. Pomes, G. G. Prive, W. Annaert, M. Schwake, J. Heeren, R. Lullmann-Rauch, S. Grinstein, E. Ikonen, P. Saftig and D. Neculai (2019). "Lysosomal integral membrane protein-2 (LIMP-2/SCARB2) is involved in lysosomal cholesterol export." Nat Commun **10**(1): 3521.

Hieb, W. F. and M. Rothstein (1968). "Sterol requirement for reproduction of a free-living nematode." Science **160**(3829): 778-780.

Hochbaum, D., Y. Zhang, C. Stuckenholz, P. Labhart, V. Alexiadis, R. Martin, H. J. Knolker and A. L. Fisher (2011). "DAF-12 regulates a connected network of genes to ensure robust developmental decisions." PLoS Genet **7**(7): e1002179.

Hofmann, A. F. and L. R. Hagey (2014). "Key discoveries in bile acid chemistry and biology and their clinical applications: history of the last eight decades." J Lipid Res **55**(8): 1553-1595.

Hoglinger, D., T. Burgoyne, E. Sanchez-Heras, P. Hartwig, A. Colaco, J. Newton, C. E. Futter, S. Spiegel, F. M. Platt and E. R. Eden (2019). "NPC1 regulates ER contacts with endocytic organelles to mediate cholesterol egress." Nat Commun **10**(1): 4276.

Holz, M. K., B. A. Ballif, S. P. Gygi and J. Blenis (2005). "mTOR and S6K1 mediate assembly of the translation preinitiation complex through dynamic protein interchange and ordered phosphorylation events." Cell **123**(4): 569-580.

Honjo, Y., S. Sasaki, Y. Kobayashi, H. Misawa and H. Nakamura (2006). "1,25-dihydroxyvitamin D3 and its receptor inhibit the chenodeoxycholic acid-dependent transactivation by farnesoid X receptor." J Endocrinol **188**(3): 635-643.

Horvath, S. (2013). "DNA methylation age of human tissues and cell types." Genome Biol **14**(10): R115.

Houtkooper, R. H., E. Pirinen and J. Auwerx (2012). "Sirtuins as regulators of metabolism and healthspan." Nat Rev Mol Cell Biol **13**(4): 225-238.

Hsin, H. and C. Kenyon (1999). "Signals from the reproductive system regulate the lifespan of C. elegans." Nature **399**(6734): 362-366.

Hu, P. J. (2007). "Dauer." WormBook: 1-19.

Hua, Q. X., S. H. Nakagawa, J. Wilken, R. R. Ramos, W. Jia, J. Bass and M. A. Weiss (2003). "A divergent INS protein in Caenorhabditis elegans structurally resembles human insulin and activates the human insulin receptor." Genes Dev **17**(7): 826-831.

Hunt-Newbury, R., R. Viveiros, R. Johnsen, A. Mah, D. Anastas, L. Fang, E. Halfnight, D. Lee, J. Lin, A. Lorch, S. McKay, H. M. Okada, J. Pan, A. K. Schulz, D. Tu, K. Wong, Z. Zhao, A. Alexeyenko, T. Burglin, E. Sonnhammer, R. Schnabel, S. J. Jones, M. A. Marra, D. L. Baillie and D. G. Moerman (2007). "High-throughput in vivo analysis of gene expression in Caenorhabditis elegans." PLoS Biol **5**(9): e237.

Imanikia, S., P. Hylands and S. R. Sturzenbaum (2015). "The double mutation of cytochrome P450's and fatty acid desaturases affect lipid regulation and longevity in C. elegans." Biochem Biophys Rep **2**: 172-178.

Inoue, T. and J. H. Thomas (2000). "Targets of TGF-beta signaling in Caenorhabditis elegans dauer formation." Dev Biol **217**(1): 192-204.

Izrayelit, Y., S. L. Robinette, N. Bose, S. H. von Reuss and F. C. Schroeder (2013). "2D NMR-based metabolomics uncovers interactions between conserved biochemical pathways in the model organism Caenorhabditis elegans." ACS Chem Biol **8**(2): 314-319.

Janowski, B. A., M. J. Grogan, S. A. Jones, G. B. Wisely, S. A. Kliewer, E. J. Corey and D. J. Mangelsdorf (1999). "Structural requirements of ligands for the oxysterol liver X receptors LXRalpha and LXRbeta." Proc Natl Acad Sci U S A **96**(1): 266-271.

Janowski, B. A., P. J. Willy, T. R. Devi, J. R. Falck and D. J. Mangelsdorf (1996). "An oxysterol signalling pathway mediated by the nuclear receptor LXR alpha." Nature **383**(6602): 728-731.

Jeong, P. Y., M. Jung, Y. H. Yim, H. Kim, M. Park, E. Hong, W. Lee, Y. H. Kim, K. Kim and Y. K. Paik (2005). "Chemical structure and biological activity of the Caenorhabditis elegans dauer-inducing pheromone." Nature **433**(7025): 541-545.

Jia, K., P. S. Albert and D. L. Riddle (2002). "DAF-9, a cytochrome P450 regulating C. elegans larval development and adult longevity." Development **129**(1): 221-231.

Jia, K., D. Chen and D. L. Riddle (2004). "The TOR pathway interacts with the insulin signaling pathway to regulate C. elegans larval development, metabolism and life span." Development **131**(16): 3897-3906.

Jiang, W., T. Miyamoto, T. Kakizawa, S. I. Nishio, A. Oiwa, T. Takeda, S. Suzuki and K. Hashizume (2006). "Inhibition of LXRalpha signaling by vitamin D receptor: possible role of VDR in bile acid synthesis." Biochem Biophys Res Commun **351**(1): 176-184.

Johnson, S. C., P. S. Rabinovitch and M. Kaeberlein (2013). "mTOR is a key modulator of ageing and age-related disease." Nature **493**(7432): 338-345.

Jones, M. E. (1985). "Conversion of glutamate to ornithine and proline: pyrroline-5-carboxylate, a possible modulator of arginine requirements." J Nutr **115**(4): 509-515.

Jurevics, H. and P. Morell (1995). "Cholesterol for synthesis of myelin is made locally, not imported into brain." J Neurochem **64**(2): 895-901.

Kaeberlein, M., R. W. Powers, 3rd, K. K. Steffen, E. A. Westman, D. Hu, N. Dang, E. O. Kerr, K. T. Kirkland, S. Fields and B. K. Kennedy (2005). "Regulation of yeast replicative life span by TOR and Sch9 in response to nutrients." Science **310**(5751): 1193-1196.

Kapahi, P., B. M. Zid, T. Harper, D. Koslover, V. Sapin and S. Benzer (2004). "Regulation of lifespan in Drosophila by modulation of genes in the TOR signaling pathway." Curr Biol **14**(10): 885-890.

Keitel, V., R. Kubitz and D. Haussinger (2008). "Endocrine and paracrine role of bile acids." World J Gastroenterol **14**(37): 5620-5629.

Kennedy, E. P. and F. H. Westheimer (1964). "Nobel Laureates: Bloch and Lynen Win Prize in Medicine and Physiology." Science **146**(3643): 504-506.

Kenyon, C., J. Chang, E. Gensch, A. Rudner and R. Tabtiang (1993). "A C. elegans mutant that lives twice as long as wild type." Nature **366**(6454): 461-464.

Kim, E., P. Goraksha-Hicks, L. Li, T. P. Neufeld and K. L. Guan (2008). "Regulation of TORC1 by Rag GTPases in nutrient response." Nat Cell Biol **10**(8): 935-945.

Kim, J., M. Kundu, B. Viollet and K. L. Guan (2011). "AMPK and mTOR regulate autophagy through direct phosphorylation of Ulk1." Nat Cell Biol **13**(2): 132-141.

Kim, K., K. Sato, M. Shibuya, D. M. Zeiger, R. A. Butcher, J. R. Ragains, J. Clardy, K. Touhara and P. Sengupta (2009). "Two chemoreceptors mediate developmental effects of dauer pheromone in C. elegans." Science **326**(5955): 994-998.

Kimura, K. D., D. L. Riddle and G. Ruvkun (2011). "The C. elegans DAF-2 insulin-like receptor is abundantly expressed in the nervous system and regulated by nutritional status." Cold Spring Harb Symp Quant Biol **76**: 113-120.

Kimura, K. D., H. A. Tissenbaum, Y. Liu and G. Ruvkun (1997). "daf-2, an insulin receptor-like gene that regulates longevity and diapause in Caenorhabditis elegans." Science **277**(5328): 942-946.

Kiriyama, Y. and H. Nochi (2019). "The Biosynthesis, Signaling, and Neurological Functions of Bile Acids." Biomolecules **9**(6).

Kishore, R., V. Arnaboldi, C. E. Van Slyke, J. Chan, R. S. Nash, J. M. Urbano, M. E. Dolan, S. R. Engel, M. Shimoyama, P. W. Sternberg and T. A. O. Genome Resources (2020). "Automated generation of gene summaries at the Alliance of Genome Resources." Database (Oxford) **2020**.

Klass, M. and D. Hirsh (1976). "Non-ageing developmental variant of Caenorhabditis elegans." Nature **260**(5551): 523-525.

Kunz, J., R. Henriquez, U. Schneider, M. Deuter-Reinhard, N. R. Movva and M. N. Hall (1993). "Target of rapamycin in yeast, TOR2, is an essential phosphatidylinositol kinase homolog required for G1 progression." Cell **73**(3): 585-596.

Lapierre, L. R., C. D. De Magalhaes Filho, P. R. McQuary, C. C. Chu, O. Visvikis, J. T. Chang, S. Gelino, B. Ong, A. E. Davis, J. E. Irazoqui, A. Dillin and M. Hansen (2013). "The TFEB orthologue HLH-30 regulates autophagy and modulates longevity in Caenorhabditis elegans." Nat Commun **4**: 2267.

Lapierre, L. R., S. Gelino, A. Melendez and M. Hansen (2011). "Autophagy and lipid metabolism coordinately modulate life span in germline-less C. elegans." Curr Biol **21**(18): 1507-1514.

Laplante, M. and D. M. Sabatini (2009). "mTOR signaling at a glance." J Cell Sci **122**(Pt 20): 3589-3594.

Lathe, R. and Y. Kotelevtsev (2014). "Steroid signaling: ligand-binding promiscuity, molecular symmetry, and the need for gating." Steroids **82**: 14-22.

Lawrence, R. E. and R. Zoncu (2019). "The lysosome as a cellular centre for signalling, metabolism and quality control." Nat Cell Biol **21**(2): 133-142.

Leandro, J. and S. M. Houten (2019). "Saccharopine, a lysine degradation intermediate, is a mitochondrial toxin." J Cell Biol **218**(2): 391-392.

Leandro, J. and S. M. Houten (2020). "The lysine degradation pathway: Subcellular compartmentalization and enzyme deficiencies." Mol Genet Metab **131**(1-2): 14-22.

Lee, S. S., S. Kennedy, A. C. Tolonen and G. Ruvkun (2003). "DAF-16 target genes that control C. elegans life-span and metabolism." Science **300**(5619): 644-647.

Lee, S. S. and F. C. Schroeder (2012). "Steroids as central regulators of organismal development and lifespan." PLoS Biol **10**(4): e1001307.

Leung, D. T. H. and S. Chu (2018). "Measurement of Oxidative Stress: Mitochondrial Function Using the Seahorse System." Methods Mol Biol **1710**: 285-293.

Lewis, C. A., B. Griffiths, C. R. Santos, M. Pende and A. Schulze (2011). "Regulation of the SREBP transcription factors by mTORC1." Biochem Soc Trans **39**(2): 495-499.

Li, J., G. Brown, M. Ailion, S. Lee and J. H. Thomas (2004). "NCR-1 and NCR-2, the C. elegans homologs of the human Niemann-Pick type C1 disease protein, function upstream of DAF-9 in the dauer formation pathways." Development **131**(22): 5741-5752.

Li, J., S. G. Kim and J. Blenis (2014). "Rapamycin: one drug, many effects." Cell Metab **19**(3): 373-379.

Li, N., B. Hua, Q. Chen, F. Teng, M. Ruan, M. Zhu, L. Zhang, Y. Huo, H. Liu, M. Zhuang, H. Shen and H. Zhu (2022). "A sphingolipid-mTORC1 nutrient-sensing pathway regulates animal development by an intestinal peroxisome relocation-based gut-brain crosstalk." Cell Rep **40**(4): 111140.

Li, T. M., J. Chen, X. Li, X. J. Ding, Y. Wu, L. F. Zhao, S. Chen, X. Lei and M. Q. Dong (2013). "Absolute quantification of a steroid hormone that regulates development in Caenorhabditis elegans." Anal Chem **85**(19): 9281-9287.

Li, T. M., W. Liu, S. Lu, Y. P. Zhang, L. M. Jia, J. Chen, X. Li, X. Lei and M. Q. Dong (2015). "No Significant Increase in the Delta4- and Delta7-Dafachronic Acid Concentration in the Long-Lived glp-1 Mutant, nor in the Mutants Defective in Dauer Formation." G3 (Bethesda) **5**(7): 1473-1479.

Li, W., L. R. DeBella, T. Guven-Ozkan, R. Lin and L. S. Rose (2009). "An eIF4E-binding protein regulates katanin protein levels in C. elegans embryos." J Cell Biol **187**(1): 33-42.

Libina, N., J. R. Berman and C. Kenyon (2003). "Tissue-specific activities of C. elegans DAF-16 in the regulation of lifespan." Cell **115**(4): 489-502.

Lijun Zhang, J. Y., Xiaoyan Gao, Yingxuan Yan, Xinyi Wang, Hang Shi, Minglv Fang, Ying Liu, Young-Bum Kim, Huanhu Zhu, Xiaojun Wu, Cheng Huang, Shengjie Fan (2025). "Targeting farnesoid X receptor as aging intervention therapy." Acta Pharmaceutica Sinica B.

Lim, C. Y., O. B. Davis, H. R. Shin, J. Zhang, C. A. Berdan, X. Jiang, J. L. Counihan, D. S. Ory, D. K. Nomura and R. Zoncu (2019). "ER-lysosome contacts enable cholesterol sensing by mTORC1 and drive aberrant growth signalling in Niemann-Pick type C." Nat Cell Biol **21**(10): 1206-1218.

Lim, C. Y., H. T. Lin, C. Kumsta, T. C. Lu, F. Y. Wang, Y. H. Kang, M. Hansen, T. T. Ching and A. L. Hsu (2023). "SAMS-1 coordinates HLH-30/TFEB and PHA-4/FOXA activities through histone methylation to mediate dietary restriction-induced autophagy and longevity." Autophagy **19**(1): 224-240.

Lin, K., J. B. Dorman, A. Rodan and C. Kenyon (1997). "daf-16: An HNF-3/forkhead family member that can function to double the life-span of Caenorhabditis elegans." Science **278**(5341): 1319-1322.

Lin, K., H. Hsin, N. Libina and C. Kenyon (2001). "Regulation of the Caenorhabditis elegans longevity protein DAF-16 by insulin/IGF-1 and germline signaling." Nat Genet **28**(2): 139-145.

Liu, B., H. Du, R. Rutkowski, A. Gartner and X. Wang (2012). "LAAT-1 is the lysosomal lysine/arginine transporter that maintains amino acid homeostasis." Science **337**(6092): 351-354.

Liu, G. Y. and D. M. Sabatini (2020). "mTOR at the nexus of nutrition, growth, ageing and disease." Nat Rev Mol Cell Biol **21**(4): 183-203.

Liu, Y., A. Beyer and R. Aebersold (2016). "On the Dependency of Cellular Protein Levels on mRNA Abundance." Cell **165**(3): 535-550.

Lopez-Otin, C., M. A. Blasco, L. Partridge, M. Serrano and G. Kroemer (2013). "The hallmarks of aging." Cell **153**(6): 1194-1217.

Lopez-Otin, C., M. A. Blasco, L. Partridge, M. Serrano and G. Kroemer (2023). "Hallmarks of aging: An expanding universe." Cell **186**(2): 243-278.

Lopez-Otin, C. and G. Kroemer (2021). "Hallmarks of health." Cell **184**(7): 1929-1939.

Lorenzo, R., M. Onizuka, M. Defrance and P. Laurent (2020). "Combining single-cell RNA-sequencing with a molecular atlas unveils new markers for Caenorhabditis elegans neuron classes." Nucleic Acids Res **48**(13): 7119-7134.

Luciani, G. M., L. Magomedova, R. Puckrin, M. L. Urbanus, I. M. Wallace, G. Giaever, C. Nislow, C. L. Cummins and P. J. Roy (2011). "Dafadine inhibits DAF-9 to promote dauer formation and longevity of Caenorhabditis elegans." Nat Chem Biol **7**(12): 891-893.

Ludewig, A. H., C. Kober-Eisermann, C. Weitzel, A. Bethke, K. Neubert, B. Gerisch, H. Hutter and A. Antebi (2004). "A novel nuclear receptor/coregulator complex controls C. elegans lipid metabolism, larval development, and aging." Genes Dev **18**(17): 2120-2133.

Ludewig, A. H. and F. C. Schroeder (2013). "Ascaroside signaling in C. elegans." WormBook: 1-22.

Magner, D. B., J. Wollam, Y. Shen, C. Hoppe, D. Li, C. Latza, V. Rottiers, H. Hutter and A. Antebi (2013). "The NHR-8 nuclear receptor regulates cholesterol and bile acid homeostasis in C. elegans." Cell Metab **18**(2): 212-224.

Mahanti, P., N. Bose, A. Bethke, J. C. Judkins, J. Wollam, K. J. Dumas, A. M. Zimmerman, S. L. Campbell, P. J. Hu, A. Antebi and F. C. Schroeder (2014). "Comparative metabolomics reveals endogenous ligands of DAF-12, a nuclear hormone receptor, regulating C. elegans development and lifespan." Cell Metab **19**(1): 73-83.

Mair, W., I. Morantte, A. P. Rodrigues, G. Manning, M. Montminy, R. J. Shaw and A. Dillin (2011). "Lifespan extension induced by AMPK and calcineurin is mediated by CRTC-1 and CREB." Nature **470**(7334): 404-408.

Mak, H. Y. and G. Ruvkun (2004). "Intercellular signaling of reproductive development by the C. elegans DAF-9 cytochrome P450." Development **131**(8): 1777-1786.

Makishima, M., A. Y. Okamoto, J. J. Repa, H. Tu, R. M. Learned, A. Luk, M. V. Hull, K. D. Lustig, D. J. Mangelsdorf and B. Shan (1999). "Identification of a nuclear receptor for bile acids." Science **284**(5418): 1362-1365.

Mancino, V., G. Ceccarelli, A. Carotti, L. Goracci, R. Sardella, D. Passeri, R. Pellicciari and A. Gioiello (2021). "Synthesis and biological activity of cyclopropyl Delta7-dafachronic acids as DAF-12 receptor ligands." Org Biomol Chem **19**(24): 5403-5412.

Mannick, J. B. and D. W. Lamming (2023). "Targeting the biology of aging with mTOR inhibitors." Nat Aging **3**(6): 642-660.

Martina, J. A., Y. Chen, M. Gucek and R. Puertollano (2012). "MTORC1 functions as a transcriptional regulator of autophagy by preventing nuclear transport of TFEB." Autophagy **8**(6): 903-914.

Martinez-Reyes, I. and N. S. Chandel (2020). "Mitochondrial TCA cycle metabolites control physiology and disease." Nat Commun **11**(1): 102.

Mathelier, A., X. Zhao, A. W. Zhang, F. Parcy, R. Worsley-Hunt, D. J. Arenillas, S. Buchman, C. Y. Chen, A. Chou, H. Ienasescu, J. Lim, C. Shyr, G. Tan, M. Zhou, B. Lenhard, A. Sandelin and W. W. Wasserman (2014). "JASPAR 2014: an extensively expanded and updated open-access database of transcription factor binding profiles." Nucleic Acids Res **42**(Database issue): D142-147.

Mattison, J. A., G. S. Roth, T. M. Beasley, E. M. Tilmont, A. M. Handy, R. L. Herbert, D. L. Longo, D. B. Allison, J. E. Young, M. Bryant, D. Barnard, W. F. Ward, W. Qi, D.

K. Ingram and R. de Cabo (2012). "Impact of caloric restriction on health and survival in rhesus monkeys from the NIA study." Nature **489**(7415): 318-321.

Mayer, M. G., C. Rodelsperger, H. Witte, M. Riebesell and R. J. Sommer (2015). "The Orphan Gene dauerless Regulates Dauer Development and Intraspecific Competition in Nematodes by Copy Number Variation." PLoS Genet **11**(6): e1005146.

McCormick, M., K. Chen, P. Ramaswamy and C. Kenyon (2012). "New genes that extend Caenorhabditis elegans' lifespan in response to reproductive signals." Aging Cell **11**(2): 192-202.

McGrath, P. T., Y. Xu, M. Ailion, J. L. Garrison, R. A. Butcher and C. I. Bargmann (2011). "Parallel evolution of domesticated Caenorhabditis species targets pheromone receptor genes." Nature **477**(7364): 321-325.

Mehrmohamadi, M., M. H. Sepehri, N. Nazer and M. R. Norouzi (2021). "A Comparative Overview of Epigenomic Profiling Methods." Front Cell Dev Biol **9**: 714687.

Meng, Y., S. Heybrock, D. Neculai and P. Saftig (2020). "Cholesterol Handling in Lysosomes and Beyond." Trends Cell Biol **30**(6): 452-466.

Menon, S., C. C. Dibble, G. Talbott, G. Hoxhaj, A. J. Valvezan, H. Takahashi, L. C. Cantley and B. D. Manning (2014). "Spatial control of the TSC complex integrates insulin and nutrient regulation of mTORC1 at the lysosome." Cell **156**(4): 771-785.

Menon, S. and B. D. Manning (2013). "Cell signalling: nutrient sensing lost in cancer." Nature **498**(7455): 444-445.

Miller, R. A., D. E. Harrison, C. M. Astle, E. Fernandez, K. Flurkey, M. Han, M. A. Javors, X. Li, N. L. Nadon, J. F. Nelson, S. Pletcher, A. B. Salmon, Z. D. Sharp, S. Van Roekel, L. Winkleman and R. Strong (2014). "Rapamycin-mediated lifespan increase in mice is dose and sex dependent and metabolically distinct from dietary restriction." Aging Cell **13**(3): 468-477.

Miller, W. L. and R. J. Auchus (2011). "The molecular biology, biochemistry, and physiology of human steroidogenesis and its disorders." Endocr Rev **32**(1): 81-151.

Mizwicki, M. T., D. Keidel, C. M. Bula, J. E. Bishop, L. P. Zanello, J. M. Wurtz, D. Moras and A. W. Norman (2004). "Identification of an alternative ligand-binding pocket in the nuclear vitamin D receptor and its functional importance in 1alpha,25(OH)2-vitamin D3 signaling." Proc Natl Acad Sci U S A **101**(35): 12876-12881.

Mooijaart, S. P., B. W. Brandt, E. A. Baldal, J. Pijpe, M. Kuningas, M. Beekman, B. J. Zwaan, P. E. Slagboom, R. G. Westendorp and D. van Heemst (2005). "C. elegans DAF-12, Nuclear Hormone Receptors and human longevity and disease at old age." Ageing Res Rev **4**(3): 351-371.

Morita, S. Y., Y. Ikeda, T. Tsuji and T. Terada (2019). "Molecular Mechanisms for Protection of Hepatocytes against Bile Salt Cytotoxicity." Chem Pharm Bull (Tokyo) **67**(4): 333-340.

Motola, D. L., C. L. Cummins, V. Rottiers, K. K. Sharma, T. Li, Y. Li, K. Suino-Powell, H. E. Xu, R. J. Auchus, A. Antebi and D. J. Mangelsdorf (2006). "Identification of ligands for DAF-12 that govern dauer formation and reproduction in C. elegans." Cell **124**(6): 1209-1223.

Mullaney, B. C. and K. Ashrafi (2009). "C. elegans fat storage and metabolic regulation." Biochim Biophys Acta **1791**(6): 474-478.

Narasimhan, S. D., K. Yen, A. Bansal, E. S. Kwon, S. Padmanabhan and H. A. Tissenbaum (2011). "PDP-1 links the TGF-beta and IIS pathways to regulate longevity, development, and metabolism." PLoS Genet **7**(4): e1001377.

O'Donnell, M. P., P. H. Chao, J. E. Kammenga and P. Sengupta (2018). "Rictor/TORC2 mediates gut-to-brain signaling in the regulation of phenotypic plasticity in C. elegans." PLoS Genet **14**(2): e1007213.

Ogg, S., S. Paradis, S. Gottlieb, G. I. Patterson, L. Lee, H. A. Tissenbaum and G. Ruvkun (1997). "The Fork head transcription factor DAF-16 transduces insulin-like metabolic and longevity signals in C. elegans." Nature **389**(6654): 994-999.

Ojasoo, T., J. C. Dore, J. Gilbert and J. P. Raynaud (1988). "Binding of steroids to the progestin and glucocorticoid receptors analyzed by correspondence analysis." J Med Chem **31**(6): 1160-1169.

Ortega-Molina, A., C. Lebrero-Fernandez, A. Sanz, N. Deleyto-Seldas, A. B. Plata-Gomez, C. Menendez, O. Grana-Castro, E. Caleiras and A. Efeyan (2021). "Inhibition of Rag GTPase signaling in mice suppresses B cell responses and lymphomagenesis with minimal detrimental trade-offs." Cell Rep **36**(2): 109372.

Panzitt, K. and M. Wagner (2021). "FXR in liver physiology: Multiple faces to regulate liver metabolism." Biochim Biophys Acta Mol Basis Dis **1867**(7): 166133.

Park, D., I. O'Doherty, R. K. Somvanshi, A. Bethke, F. C. Schroeder, U. Kumar and D. L. Riddle (2012). "Interaction of structure-specific and promiscuous G-protein-coupled receptors mediates small-molecule signaling in Caenorhabditis elegans." Proc Natl Acad Sci U S A **109**(25): 9917-9922.

Parks, D. J., S. G. Blanchard, R. K. Bledsoe, G. Chandra, T. G. Consler, S. A. Kliewer, J. B. Stimmel, T. M. Willson, A. M. Zavacki, D. D. Moore and J. M. Lehmann (1999). "Bile acids: natural ligands for an orphan nuclear receptor." Science **284**(5418): 1365-1368.

Patel, D. S., L. L. Fang, D. K. Svy, G. Ruvkun and W. Li (2008). "Genetic identification of HSD-1, a conserved steroidogenic enzyme that directs larval development in Caenorhabditis elegans." Development **135**(13): 2239-2249.

Patterson, G. I., A. Koweek, A. Wong, Y. Liu and G. Ruvkun (1997). "The DAF-3 Smad protein antagonizes TGF-beta-related receptor signaling in the Caenorhabditis elegans dauer pathway." Genes Dev **11**(20): 2679-2690.

Patterson, G. I. and R. W. Padgett (2000). "TGF beta-related pathways. Roles in Caenorhabditis elegans development." Trends Genet **16**(1): 27-33.

Persaud, A. K., S. Nair, M. F. Rahman, R. Raj, B. Weadick, D. Nayak, C. McElroy, M. Shanmugam, S. Knoblaugh, X. Cheng and R. Govindarajan (2021). "Facilitative lysosomal transport of bile acids alleviates ER stress in mouse hematopoietic precursors." Nat Commun **12**(1): 1248.

Peterson, T. R., S. S. Sengupta, T. E. Harris, A. E. Carmack, S. A. Kang, E. Balderas, D. A. Guertin, K. L. Madden, A. E. Carpenter, B. N. Finck and D. M. Sabatini (2011). "mTOR complex 1 regulates lipin 1 localization to control the SREBP pathway." Cell **146**(3): 408-420.

Porstmann, T., C. R. Santos, B. Griffiths, M. Cully, M. Wu, S. Leevers, J. R. Griffiths, Y. L. Chung and A. Schulze (2008). "SREBP activity is regulated by mTORC1 and contributes to Akt-dependent cell growth." Cell Metab **8**(3): 224-236.

Qu, Q., Y. Chen, Y. Wang, S. Long, W. Wang, H. Y. Yang, M. Li, X. Tian, X. Wei, Y. H. Liu, S. Xu, C. Zhang, M. Zhu, S. M. Lam, J. Wu, C. Yun, J. Chen, S. Xue, B. Zhang, Z. Z. Zheng, H. L. Piao, C. Jiang, H. Guo, G. Shui, X. Deng, C. S. Zhang and S. C. Lin (2024). "Lithocholic acid phenocopies anti-ageing effects of calorie restriction." Nature.

Qu, Q., Y. Chen, Y. Wang, W. Wang, S. Long, H. Y. Yang, J. Wu, M. Li, X. Tian, X. Wei, Y. H. Liu, S. Xu, J. Xiong, C. Yang, Z. Wu, X. Huang, C. Xie, Y. Wu, Z. Xu, C. Zhang, B. Zhang, J. W. Feng, J. Chen, Y. Feng, H. Fang, L. Lin, Z. K. Xie, B. Sun, H. Tian, Y. Yu, H. L. Piao, X. S. Xie, X. Deng, C. S. Zhang and S. C. Lin (2024). "Lithocholic acid binds TULP3 to activate sirtuins and AMPK to slow down ageing." Nature.

Raymond Laboy, M. N., Maximilian Vonolfen, Eugen Ballhysa, Shamsh Tabrez Syed, Tim Droth, Klara Schilling, Anna Löhrke, Ilian Atanassov, Adam Antebi (2023). "Hexokinase regulates Mondo-mediated longevity via the PPP and organellar dynamics." eLife **12:RP89225**.

Ren, P., C. S. Lim, R. Johnsen, P. S. Albert, D. Pilgrim and D. L. Riddle (1996). "Control of C. elegans larval development by neuronal expression of a TGF-beta homolog." Science **274**(5291): 1389-1391.

Riddle, D. L., M. M. Swanson and P. S. Albert (1981). "Interacting genes in nematode dauer larva formation." Nature **290**(5808): 668-671.

Ritchie, M. E., B. Phipson, D. Wu, Y. Hu, C. W. Law, W. Shi and G. K. Smyth (2015). "limma powers differential expression analyses for RNA-sequencing and microarray studies." Nucleic Acids Res **43**(7): e47.

Robida-Stubbs, S., K. Glover-Cutter, D. W. Lamming, M. Mizunuma, S. D. Narasimhan, E. Neumann-Haefelin, D. M. Sabatini and T. K. Blackwell (2012). "TOR signaling and rapamycin influence longevity by regulating SKN-1/Nrf and DAF-16/FoxO." Cell Metab **15**(5): 713-724.

Roczniak-Ferguson, A., C. S. Petit, F. Froehlich, S. Qian, J. Ky, B. Angarola, T. C. Walther and S. M. Ferguson (2012). "The transcription factor TFEB links mTORC1 signaling to transcriptional control of lysosome homeostasis." Sci Signal **5**(228): ra42.

Rog, T., M. Pasenkiewicz-Gierula, I. Vattulainen and M. Karttunen (2009). "Ordering effects of cholesterol and its analogues." Biochim Biophys Acta **1788**(1): 97-121.

Rottiers, V., D. L. Motola, B. Gerisch, C. L. Cummins, K. Nishiwaki, D. J. Mangelsdorf and A. Antebi (2006). "Hormonal control of C. elegans dauer formation and life span by a Rieske-like oxygenase." Dev Cell **10**(4): 473-482.

Rual, J. F., J. Ceron, J. Koreth, T. Hao, A. S. Nicot, T. Hirozane-Kishikawa, J. Vandenhaute, S. H. Orkin, D. E. Hill, S. van den Heuvel and M. Vidal (2004). "Toward improving Caenorhabditis elegans phenome mapping with an ORFeome-based RNAi library." Genome Res **14**(10B): 2162-2168.

Russell, D. W. (2003). "The enzymes, regulation, and genetics of bile acid synthesis." Annu Rev Biochem **72**: 137-174.

Russell, D. W. (2009). "Fifty years of advances in bile acid synthesis and metabolism." J Lipid Res **50 Suppl**(Suppl): S120-125.

Saltiel, A. R. (2021). "Insulin signaling in health and disease." J Clin Invest **131**(1).

Sancak, Y., L. Bar-Peled, R. Zoncu, A. L. Markhard, S. Nada and D. M. Sabatini (2010). "Ragulator-Rag complex targets mTORC1 to the lysosomal surface and is necessary for its activation by amino acids." Cell **141**(2): 290-303.

Sancak, Y., T. R. Peterson, Y. D. Shaul, R. A. Lindquist, C. C. Thoreen, L. Bar-Peled and D. M. Sabatini (2008). "The Rag GTPases bind raptor and mediate amino acid signaling to mTORC1." Science **320**(5882): 1496-1501.

Sarbassov, D. D., S. M. Ali, D. H. Kim, D. A. Guertin, R. R. Latek, H. Erdjument-Bromage, P. Tempst and D. M. Sabatini (2004). "Rictor, a novel binding partner of mTOR, defines a rapamycin-insensitive and raptor-independent pathway that regulates the cytoskeleton." Curr Biol **14**(14): 1296-1302.

Sarbassov, D. D., S. M. Ali, S. Sengupta, J. H. Sheen, P. P. Hsu, A. F. Bagley, A. L. Markhard and D. M. Sabatini (2006). "Prolonged rapamycin treatment inhibits mTORC2 assembly and Akt/PKB." Mol Cell **22**(2): 159-168.

Satoh, A., S. I. Imai and L. Guarente (2017). "The brain, sirtuins, and ageing." Nat Rev Neurosci **18**(6): 362-374.

Saxton, R. A. and D. M. Sabatini (2017). "mTOR Signaling in Growth, Metabolism, and Disease." Cell **169**(2): 361-371.

Saxton, R. A. and D. M. Sabatini (2017). "mTOR Signaling in Growth, Metabolism, and Disease." Cell **168**(6): 960-976.

Schackwitz, W. S., T. Inoue and J. H. Thomas (1996). "Chemosensory neurons function in parallel to mediate a pheromone response in C. elegans." Neuron **17**(4): 719-728.

Schreiber, M. A., J. T. Pierce-Shimomura, S. Chan, D. Parry and S. L. McIntire (2010). "Manipulation of behavioral decline in Caenorhabditis elegans with the Rag GTPase raga-1." PLoS Genet **6**(5): e1000972.

Schreiber, S. L. (1991). "Chemistry and biology of the immunophilins and their immunosuppressive ligands." Science **251**(4991): 283-287.

Schroeder, L. K., S. Kremer, M. J. Kramer, E. Currie, E. Kwan, J. L. Watts, A. L. Lawrenson and G. J. Hermann (2007). "Function of the Caenorhabditis elegans ABC transporter PGP-2 in the biogenesis of a lysosome-related fat storage organelle." Mol Biol Cell **18**(3): 995-1008.

Schulz, T. J., K. Zarse, A. Voigt, N. Urban, M. Birringer and M. Ristow (2007). "Glucose restriction extends Caenorhabditis elegans life span by inducing mitochondrial respiration and increasing oxidative stress." Cell Metab **6**(4): 280-293.

Schwaiger, M., E. Rampler, G. Hermann, W. Miklos, W. Berger and G. Koellensperger (2017). "Anion-Exchange Chromatography Coupled to High-Resolution Mass Spectrometry: A Powerful Tool for Merging Targeted and Non-targeted Metabolomics." Anal Chem **89**(14): 7667-7674.

Segatto, M., L. Leboffe, L. Trapani and V. Pallottini (2014). "Cholesterol homeostasis failure in the brain: implications for synaptic dysfunction and cognitive decline." Curr Med Chem **21**(24): 2788-2802.

Seo, K., E. Choi, D. Lee, D. E. Jeong, S. K. Jang and S. J. Lee (2013). "Heat shock factor 1 mediates the longevity conferred by inhibition of TOR and insulin/IGF-1 signaling pathways in C. elegans." Aging Cell **12**(6): 1073-1081.

Settembre, C., C. Di Malta, V. A. Polito, M. Garcia Arencibia, F. Vetrini, S. Erdin, S. U. Erdin, T. Huynh, D. Medina, P. Colella, M. Sardiello, D. C. Rubinsztein and A. Ballabio (2011). "TFEB links autophagy to lysosomal biogenesis." Science **332**(6036): 1429-1433.

Sewell, A. K., Z. C. Poss, C. C. Ebmeier, J. R. Jacobsen, W. M. Old and M. Han (2022). "The TORC1 phosphoproteome in C. elegans reveals roles in transcription and autophagy." iScience **25**(5): 104186.

Shamsuzzama, R. Lebedev, B. Trabelcy, I. Langier Goncalves, Y. Gerchman and A. Sapir (2020). "Metabolic Reconfiguration in C. elegans Suggests a Pathway for Widespread Sterol Auxotrophy in the Animal Kingdom." Curr Biol **30**(15): 3031-3038 e3037.

Sharma, K. K., Z. Wang, D. L. Motola, C. L. Cummins, D. J. Mangelsdorf and R. J. Auchus (2009). "Synthesis and activity of dafachronic acid ligands for the C. elegans DAF-12 nuclear hormone receptor." Mol Endocrinol **23**(5): 640-648.

Shaw, W. M., S. Luo, J. Landis, J. Ashraf and C. T. Murphy (2007). "The C. elegans TGF-beta Dauer pathway regulates longevity via insulin signaling." Curr Biol **17**(19): 1635-1645.

Sheaffer, K. L., D. L. Updike and S. E. Mango (2008). "The Target of Rapamycin pathway antagonizes pha-4/FoxA to control development and aging." Curr Biol **18**(18): 1355-1364.

Shen, Y., J. Wollam, D. Magner, O. Karalay and A. Antebi (2012). "A steroid receptor-microRNA switch regulates life span in response to signals from the gonad." Science **338**(6113): 1472-1476.

Siegmund, S. E., H. Yang, R. Sharma, M. Javors, O. Skinner, V. Mootha, M. Hirano and E. A. Schon (2017). "Low-dose rapamycin extends lifespan in a mouse model of mtDNA depletion syndrome." Hum Mol Genet **26**(23): 4588-4605.

Sivashanmugam, M., J. J, U. V and N. S. K (2017). "Ornithine and its role in metabolic diseases: An appraisal." Biomed Pharmacother **86**: 185-194.

Smith, H. J., A. Lanjuin, A. Sharma, A. Prabhakar, E. Nowak, P. G. Stine, R. Sehgal, K. Stojanovski, B. D. Towbin and W. B. Mair (2023). "Neuronal mTORC1 inhibition promotes longevity without suppressing anabolic growth and reproduction in C. elegans." PLoS Genet **19**(9): e1010938.

Solaas, K., A. Ulvestad, O. Soreide and B. F. Kase (2000). "Subcellular organization of bile acid amidation in human liver: a key issue in regulating the biosynthesis of bile salts." J Lipid Res **41**(7): 1154-1162.

Srinivasan, J., F. Kaplan, R. Ajredini, C. Zachariah, H. T. Alborn, P. E. Teal, R. U. Malik, A. S. Edison, P. W. Sternberg and F. C. Schroeder (2008). "A blend of small molecules regulates both mating and development in Caenorhabditis elegans." Nature **454**(7208): 1115-1118.

Stamm, S. (2008). "Regulation of alternative splicing by reversible protein phosphorylation." J Biol Chem **283**(3): 1223-1227.

Stenesen, D., J. M. Suh, J. Seo, K. Yu, K. S. Lee, J. S. Kim, K. J. Min and J. M. Graff (2013). "Adenosine nucleotide biosynthesis and AMPK regulate adult life span and mediate the longevity benefit of caloric restriction in flies." Cell Metab **17**(1): 101-112.

Strautnieks, S. S., L. N. Bull, A. S. Knisely, S. A. Kocoshis, N. Dahl, H. Arnell, E. Sokal, K. Dahan, S. Childs, V. Ling, M. S. Tanner, A. F. Kagalwalla, A. Nemeth, J. Pawlowska, A. Baker, G. Mieli-Vergani, N. B. Freimer, R. M. Gardiner and R. J. Thompson (1998). "A gene encoding a liver-specific ABC transporter is mutated in progressive familial intrahepatic cholestasis." Nat Genet **20**(3): 233-238.

Sun, X., W. D. Chen and Y. D. Wang (2017). "DAF-16/FOXO Transcription Factor in Aging and Longevity." Front Pharmacol **8**: 548.

Sym, M., M. Basson and C. Johnson (2000). "A model for niemann-pick type C disease in the nematode Caenorhabditis elegans." Curr Biol **10**(9): 527-530.

Tang, R., X. Wang, J. Zhou, F. Zhang, S. Zhao, Q. Gan, L. Zhao, F. Wang, Q. Zhang, J. Zhang, G. Wang and C. Yang (2020). "Defective arginine metabolism impairs mitochondrial homeostasis in Caenorhabditiselegans." J Genet Genomics **47**(3): 145-156.

Temburni, M. K. and M. H. Jacob (2001). "New functions for glia in the brain." Proc Natl Acad Sci U S A **98**(7): 3631-3632.

Thomas, J. H., D. A. Birnby and J. J. Vowels (1993). "Evidence for parallel processing of sensory information controlling dauer formation in Caenorhabditis elegans." Genetics **134**(4): 1105-1117.

Thondamal, M., M. Witting, P. Schmitt-Kopplin and H. Aguilaniu (2014). "Steroid hormone signalling links reproduction to lifespan in dietary-restricted Caenorhabditis elegans." Nat Commun **5**: 4879.

Tiku, V., C. Jain, Y. Raz, S. Nakamura, B. Heestand, W. Liu, M. Spath, H. E. D. Suchiman, R. U. Muller, P. E. Slagboom, L. Partridge and A. Antebi (2017). "Small nucleoli are a cellular hallmark of longevity." Nat Commun **8**: 16083.

Tsun, Z. Y., L. Bar-Peled, L. Chantranupong, R. Zoncu, T. Wang, C. Kim, E. Spooner and D. M. Sabatini (2013). "The folliculin tumor suppressor is a GAP for the RagC/D GTPases that signal amino acid levels to mTORC1." Mol Cell **52**(4): 495-505.

Umetani, M. and P. W. Shaul (2011). "27-Hydroxycholesterol: the first identified endogenous SERM." Trends Endocrinol Metab **22**(4): 130-135.

Van Gilst, M. R., H. Hadjivassiliou, A. Jolly and K. R. Yamamoto (2005). "Nuclear hormone receptor NHR-49 controls fat consumption and fatty acid composition in C. elegans." PLoS Biol **3**(2): e53.

Vance, J. E. (2012). "Dysregulation of cholesterol balance in the brain: contribution to neurodegenerative diseases." Dis Model Mech **5**(6): 746-755.

Vellai, T., K. Takacs-Vellai, Y. Zhang, A. L. Kovacs, L. Orosz and F. Muller (2003). "Genetics: influence of TOR kinase on lifespan in C. elegans." Nature **426**(6967): 620.

Vivar, O. I., X. Zhao, E. F. Saunier, C. Griffin, O. S. Mayba, M. Tagliaferri, I. Cohen, T. P. Speed and D. C. Leitman (2010). "Estrogen receptor beta binds to and regulates three distinct classes of target genes." J Biol Chem **285**(29): 22059-22066.

Vowels, J. J. and J. H. Thomas (1992). "Genetic analysis of chemosensory control of dauer formation in Caenorhabditis elegans." Genetics **130**(1): 105-123.

Wang, Z., X. E. Zhou, D. L. Motola, X. Gao, K. Suino-Powell, A. Conneely, C. Ogata, K. K. Sharma, R. J. Auchus, J. B. Lok, J. M. Hawdon, S. A. Kliewer, H. E. Xu and D. J. Mangelsdorf (2009). "Identification of the nuclear receptor DAF-12 as a therapeutic target in parasitic nematodes." Proc Natl Acad Sci U S A **106**(23): 9138-9143.

Waterham, H. R., F. A. Wijburg, R. C. Hennekam, P. Vreken, B. T. Poll-The, L. Dorland, M. Duran, P. E. Jira, J. A. Smeitink, R. A. Wevers and R. J. Wanders (1998).

"Smith-Lemli-Opitz syndrome is caused by mutations in the 7-dehydrocholesterol reductase gene." Am J Hum Genet **63**(2): 329-338.

Weber, L. W., M. Boll and A. Stampfl (2004). "Maintaining cholesterol homeostasis: sterol regulatory element-binding proteins." World J Gastroenterol **10**(21): 3081-3087.

Weindruch, R., R. L. Walford, S. Fligiel and D. Guthrie (1986). "The retardation of aging in mice by dietary restriction: longevity, cancer, immunity and lifetime energy intake." J Nutr **116**(4): 641-654.

Weir, H. J., P. Yao, F. K. Huynh, C. C. Escoubas, R. L. Goncalves, K. Burkewitz, R. Laboy, M. D. Hirschey and W. B. Mair (2017). "Dietary Restriction and AMPK Increase Lifespan via Mitochondrial Network and Peroxisome Remodeling." Cell Metab **26**(6): 884-896 e885.

Westermann, B. (2012). "Bioenergetic role of mitochondrial fusion and fission." Biochim Biophys Acta **1817**(10): 1833-1838.

Win, M. T., Y. Yamamoto, S. Munesue, D. Han, S. Harada and H. Yamamoto (2013). "Validated Liquid Culture Monitoring System for Lifespan Extension of Caenorhabditis elegans through Genetic and Dietary Manipulations." Aging Dis **4**(4): 178-185.

Winkler, M. B. L., R. T. Kidmose, M. Szomek, K. Thaysen, S. Rawson, S. P. Muench, D. Wustner and B. P. Pedersen (2019). "Structural Insight into Eukaryotic Sterol Transport through Niemann-Pick Type C Proteins." Cell **179**(2): 485-497 e418.

Wolkow, C. A., K. D. Kimura, M. S. Lee and G. Ruvkun (2000). "Regulation of C. elegans life-span by insulinlike signaling in the nervous system." Science **290**(5489): 147-150.

Wollam, J. (2011). "A bile acid synthetic pathway that modulates reproductive development and lifespan in *C. elegans.*" PhD Thesis.

Wollam, J. and A. Antebi (2011). "Sterol regulation of metabolism, homeostasis, and development." Annu Rev Biochem **80**: 885-916.

Wollam, J., D. B. Magner, L. Magomedova, E. Rass, Y. Shen, V. Rottiers, B. Habermann, C. L. Cummins and A. Antebi (2012). "A novel 3-hydroxysteroid dehydrogenase that regulates reproductive development and longevity." PLoS Biol **10**(4): e1001305.

Wollam, J., L. Magomedova, D. B. Magner, Y. Shen, V. Rottiers, D. L. Motola, D. J. Mangelsdorf, C. L. Cummins and A. Antebi (2011). "The Rieske oxygenase DAF-36 functions as a cholesterol 7-desaturase in steroidogenic pathways governing longevity." Aging Cell **10**(5): 879-884.

Wu, Q., M. Xu, C. Cheng, Z. Zhou, Y. Huang, W. Zhao, L. Zeng, J. Xu, X. Fu, K. Ying, Y. Xie and Y. Mao (2001). "Molecular cloning and characterization of a novel Dehydrogenase/reductase (SDR family) member 1 genea from human fetal brain." Mol Biol Rep **28**(4): 193-198.

Xie, G., R. Jiang, X. Wang, P. Liu, A. Zhao, Y. Wu, F. Huang, Z. Liu, C. Rajani, X. Zheng, J. Qiu, X. Zhang, S. Zhao, H. Bian, X. Gao, B. Sun and W. Jia (2021). "Conjugated secondary 12alpha-hydroxylated bile acids promote liver fibrogenesis." EBioMedicine **66**: 103290.

Yamawaki, T. M., J. R. Berman, M. Suchanek-Kavipurapu, M. McCormick, M. M. Gaglia, S. J. Lee and C. Kenyon (2010). "The somatic reproductive tissues of C. elegans promote longevity through steroid hormone signaling." PLoS Biol **8**(8).

Yang, Q., K. Inoki, T. Ikenoue and K. L. Guan (2006). "Identification of Sin1 as an essential TORC2 component required for complex formation and kinase activity." Genes Dev **20**(20): 2820-2832.

Yasuda, M., Y. Tanaka, S. Kume, Y. Morita, M. Chin-Kanasaki, H. Araki, K. Isshiki, S. Araki, D. Koya, M. Haneda, A. Kashiwagi, H. Maegawa and T. Uzu (2014). "Fatty acids are novel nutrient factors to regulate mTORC1 lysosomal localization and apoptosis in podocytes." Biochim Biophys Acta **1842**(7): 1097-1108.

Zaufel, A. (2022). "The role of bile acids in lipid and energy metabolism in health and disease." PhD Thesis.

Zemanova, L., H. Navratilova, R. Andrys, K. Sperkova, J. Andrejs, K. Kozakova, M. Meier, G. Moller, E. Novotna, M. Safr, J. Adamski and V. Wsol (2019). "Initial characterization of human DHRS1 (SDR19C1), a member of the short-chain dehydrogenase/reductase superfamily." J Steroid Biochem Mol Biol **185**: 80-89.

Zhang, J., J. Kim, A. Alexander, S. Cai, D. N. Tripathi, R. Dere, A. R. Tee, J. Tait-Mulder, A. Di Nardo, J. M. Han, E. Kwiatkowski, E. A. Dunlop, K. M. Dodd, R. D. Folkerth, P. L. Faust, M. B. Kastan, M. Sahin and C. L. Walker (2013). "A tuberous sclerosis complex signalling node at the peroxisome regulates mTORC1 and autophagy in response to ROS." Nat Cell Biol **15**(10): 1186-1196.

Zhang, L., J. D. Ward, Z. Cheng and A. F. Dernburg (2015). "The auxin-inducible degradation (AID) system enables versatile conditional protein depletion in C. elegans." Development **142**(24): 4374-4384.

Zhang, S. O., A. C. Box, N. Xu, J. Le Men, J. Yu, F. Guo, R. Trimble and H. Y. Mak (2010). "Genetic and dietary regulation of lipid droplet expansion in Caenorhabditis elegans." Proc Natl Acad Sci U S A **107**(10): 4640-4645.

Zhang, Y., A. Lanjuin, S. R. Chowdhury, M. Mistry, C. G. Silva-Garcia, H. J. Weir, C. L. Lee, C. C. Escoubas, E. Tabakovic and W. B. Mair (2019). "Neuronal TORC1 modulates longevity via AMPK and cell nonautonomous regulation of mitochondrial dynamics in C. elegans." Elife **8**.

Zhang, Y. P., W. H. Zhang, P. Zhang, Q. Li, Y. Sun, J. W. Wang, S. O. Zhang, T. Cai, C. Zhan and M. Q. Dong (2022). "Intestine-specific removal of DAF-2 nearly doubles lifespan in Caenorhabditis elegans with little fitness cost." Nat Commun **13**(1): 6339.

Zhao, C. and K. Dahlman-Wright (2010). "Liver X receptor in cholesterol metabolism." J Endocrinol **204**(3): 233-240.

Zhu, H., H. Shen, A. K. Sewell, M. Kniazeva and M. Han (2013). "A novel sphingolipid-TORC1 pathway critically promotes postembryonic development in Caenorhabditis elegans." Elife **2**: e00429.

Zwaal, R. R., J. E. Mendel, P. W. Sternberg and R. H. Plasterk (1997). "Two neuronal G proteins are involved in chemosensation of the Caenorhabditis elegans Dauer-inducing pheromone." Genetics **145**(3): 715-727.